

MULTIFUNCTIONAL MONOMERIC AND POLYMERIC  
PHOTOINITIATORS FOR FREE RADICAL PHOTOPOLYMERIZATION

by

Türkan Gençođlu

B.S., Chemistry, Bođaziçi University, 2016

M.S., Chemistry, Bođaziçi University, 2017

Submitted to the Institute for Graduate Studies in  
Science and Engineering in partial fulfillment of  
the requirements for the degree of  
Doctor of Philosophy

Graduate Program in Chemistry

Bođaziçi University

2022

## ACKNOWLEDGEMENTS

First and foremost, I would like to express my gratitude to my supervisor Prof. Duygu Avcı Semiz for her invaluable advice, support, encouragement, and patience during the course of my PhD study. It was a great pleasure to do academic research under her guidance.

I want to acknowledge Prof. Jacques Lalevée for welcoming me in the Institut of Materials Science of Mulhouse – National Center for Scientific Research (IS2M - CNRS) for the collaboration with the support of the French Embassy Fellowship.

I wish to express my appreciation to my committee members Prof. İlknur Doğan, Assoc. Prof. Muhammet Kahveci, Prof. Turgut Nugay and Prof. Binnur Aydoğan Temel for taking their treasured time for reviewing this thesis and for their insightful comments.

I would like to thank to my labmates Seçkin, Melek, Tuğçe, Betül, Burcu, Neslihan and Simay for their support, precious friendship and for the warm working environment they created.

I would like to acknowledge Dr. Ayla Türkecul Bıyık for structural characterization of my samples through NMR. I wish to thank Prof. Neren Ökte, Duygu Tuncel and Assist. Prof. Fırat İlker for their assistance in UV-vis absorption analyses. I would also like to thank all members of Chemistry Department for their help.

My sincere thanks also goes to my family for their unlimited love and support throughout my entire life.

Finally, I would like to acknowledge The Scientific and Technological Research Council of Turkey (TÜBİTAK) [117Z622 & 102Z729].

## ABSTRACT

### MULTIFUNCTIONAL MONOMERIC AND POLYMERIC PHOTOINITIATORS FOR FREE RADICAL PHOTOPOLYMERIZATION

In this study, novel polymerizable, polymeric and branched photoinitiators (PIs) were synthesized to attain high polymerization efficiency, migration stability, visible light absorption and water solubility to address environmental concerns. The photochemical and photophysical properties and photoinitiation mechanisms were investigated by electron-spin resonance, laser flash photolysis and steady-state photolysis techniques, as well as theoretical calculations. The performance of the photoinitiators was demonstrated for (photo)polymerizations of commercial monomers such as poly(ethylene glycol) diacrylate and 2-hydroxyethyl methacrylate. The first part of this thesis describes synthesis of novel thioxanthone and (bis)phosphonate functionalized poly(ethylene imine)s (PEI,  $M_w = 1800$  g/mol) which can take part in dual curing process; in the first stage as the nucleophile and base for an aza-Michael reaction with acrylates, in the second stage as a photoinitiator in conjunction with iodonium salt (Iod). Also, charge transfer complexes (CTCs) formed between amines (PEI) and Iod can lead to free radical polymerization with or without irradiation in both stages. The second part describes two oligomeric photoinitiators prepared by integrating benzophenone (BP) alone or BP and phosphonate functionalities onto the oligo(amido amine) backbone. These PIs can generate radicals by CTC formation and by Type II photoinitiation at the same time under visible irradiation. The third part reports synthesis of a both polymeric and polymerizable PI, the first poly( $\beta$ -amino ester)-based PI, by the aza-Michael reaction of poly(ethylene glycol) diacrylate and 2-(2-aminoethoxy)-9H-thioxanthen-9-one. In the last part of this thesis, a cyclopolymerizable photoinitiator containing two Irgacure 2959 groups was synthesized by esterification reaction between 2,2'-(oxybis(methylene))diacrylic acid and Irgacure 2959. Its cyclic copolymer with di(tert-butyl) 2,2'-[oxybis(methylene)]bis(2-propenoate) was prepared by thermal polymerization.

## ÖZET

# SERBEST RADİKAL FOTOPOLİMERİZASYONU İÇİN ÇOK FONKSİYONLU MONOMERİK VE POLİMERİK FOTOBAŞLATICILAR

Bu çalışmada çevresel endişeleri gidermek amacıyla yüksek polimerizasyon verimi, migrasyon kararlılığı, görünür ışık altında çalışabilme ve suda çözünebilme özelliği olabilecek yeni polimerik, dallanmış polimerik ve polimerleşebilen fotobaşlatıcılar sentezlenmiştir. Sentezlenen fotobaşlatıcıların fotofiziksel ve fotokimyasal özellikleri ile fotobaşlatma mekanizmaları elektron-spin rezonans, fotoliz, lazer flaş fotoliz yöntemleriyle ve teorik hesaplamalarla analiz edilmiştir. Poli(etilen glikol) diakrilat ve 2-hidroksietil metakrilat gibi ticari monomerlerin fotopolimerleşmesiyle, fotobaşlatıcıların performansları gösterilmiştir. Bu tezin ilk bölümünde çift kütleme işlemine katılabilen, tiyokzanton ve (bis)fosfonat fonksiyonları olan yeni poli(etilen imin)'lerin (PEI,  $M_w = 1800$  g/mol) sentezi tanımlanmıştır. Bu başlatıcılar çift kütleme işleminin ilk aşamasında akrilatlarla aza-Michael reaksiyonuna katılarak nükleofil ve baz olarak davranmaktadır, ikinci aşamasında ise iyodonyum tuzu (Iod) ile birleştirilerek fotobaşlatıcı olarak kullanılmıştır. Ayrıca, aminlerle (PEI) Iod arasında oluşan yük aktarım kompleksi (CTC), iki aşamadada ışık tutularak ya da ışık tutulmadan serbest radikal polimerizasyonuna öncülük etmektedir. İkinci bölümde, oligo(amido amin)'e sadece benzofenon (BP) ya da BP ve fosfonat fonksiyonlarının entegre edilmesiyle hazırlanan iki tane oligomerik fotobaşlatıcı tanımlanmıştır. Bu fotobaşlatıcılar, aynı anda CTC oluşumu ve tip II fotobaşlatımı ile görünür ışık altında radikal üretmektedir. Üçüncü bölümde, poli(etilen glikol) diakrilat ve 2-(2-aminoetoksi)-9H-tiyokzanten-9-on'un aza-Michael reaksiyonuyla elde edilen, hem polimerik hem de polimerize olabilen, ilk poli( $\beta$ -amino ester) bazlı fotobaşlatıcının sentezi rapor edilmiştir. Bu tezin son bölümünde, Irgacure 2959 ile 2,2'-(oksibis(metilen))diakrilik asit'in esterifikasyon reaksiyonu sonucu elde edilen, siklopolymerleşen ve iki tane Irgacure 2959 içeren fotobaşlatıcı sentezlenmiştir. Bu fotobaşlatıcının di(tert-butil) 2,2'-[oksibis(metilen)]bis(2-propenoat) ile siklik kopolimeri, termal polimerizasyonla hazırlanmıştır.

## TABLE OF CONTENTS

ACKNOWLEDGEMENTS .....	iii
ABSTRACT.....	iv
ÖZET .....	v
TABLE OF CONTENTS.....	vi
LIST OF FIGURES .....	xi
LIST OF TABLES.....	xxii
LIST OF SYMBOLS .....	xxiv
LIST OF ACRONYMS/ABBREVIATIONS .....	xxvi
1. INTRODUCTION .....	1
1.1. Photoinduced Polymerization .....	3
1.2. Free Radical Photoinitiators .....	4
1.3. Visible Light Photoinitiators .....	8
1.4. Water-Soluble Photoinitiators .....	10
1.5. Polymerizable and Macromolecular Photoinitiators .....	13
1.6. Anti-Oxygen Inhibition Photoinitiators .....	17
1.7. Monomers .....	20
1.8. Irradiation Sources .....	21
2. OBJECTIVES AND SCOPE.....	24
3. PHOTOINITIATING SYSTEMS BASED ON POLY(ETHYLENE IMINE) FOR MICHAEL ADDITION AND FREE RADICAL PHOTOPOLYMERIZATION.....	25
3.1. Introduction .....	25
3.2. Experimental Section .....	26
3.2.1. Materials .....	26
3.2.2. Methods .....	26
3.2.3. Synthesis of the Photoinitiators .....	27
3.2.3.1. Synthesis of PDT-2 and PDT-5. ....	27

3.2.3.2. Synthesis of PBT-2 and PBT-5.....	27
3.2.4. Photochemical Analysis .....	28
3.2.4.1. UV-vis Spectroscopy Experiments.....	28
3.2.4.2. Fluorescence Experiments.....	28
3.2.4.3. Laser Flash Photolysis (LFP) Experiments. ....	29
3.2.4.4. ESR Spin Trapping (ESR-ST) Experiments.....	29
3.2.5. Photopolymerization.....	29
3.2.5.1. RT-FTIR Spectroscopy.....	29
3.2.5.2. Photo-DSC.....	29
3.3. Results and Discussion.....	30
3.3.1. Synthesis and Characterization of Photoinitiators.....	30
3.3.2. Light Absorption and Emission Properties.....	33
3.3.3. Photochemical Mechanisms .....	34
3.3.4. Michael Addition and Polymerization Results.....	38
3.3.5. Radical Formation Mechanism.....	46
3.3.6. Thermal Properties of Polymers .....	46
3.4. Conclusion.....	48
4. BENZOPHENONE-FUNCTIONALIZED OLIGO (AMIDO AMINE)/IODONIUM SALT SYSTEMS AS VISIBLE LIGHT PHOTOINITIATORS .....	50
4.1. Introduction .....	50
4.2. Experimental Section .....	51
4.2.1. Materials .....	51
4.2.2. Characterization.....	51
4.2.3. Synthesis of the Photoinitiators .....	51
4.2.3.1. Synthesis of Oligo(amido amine) (OAA).....	51
4.2.3.2. Synthesis of OAA-B. ....	51
4.2.3.3. Synthesis of OAA-BP.....	52

4.2.4. Photochemical Analysis .....	52
4.2.4.1. UV-vis Spectroscopy Experiments.....	52
4.2.4.2. Laser Flash Photolysis (LFP) Experiments. ....	52
4.2.4.3. ESR Spin Trapping (ESR-ST) Experiments.....	53
4.2.5. Photopolymerization.....	53
4.2.5.1. Real-Time Fourier Transform Infrared (RT-FTIR) Spectroscopy. ....	53
4.2.5.2. Photo-DSC.....	53
4.2.6. Computational Procedure .....	54
4.3. Results and Discussion.....	54
4.3.1. Synthesis and Characterization of Photoinitiators.....	54
4.3.2. Light Absorption and Emission Properties.....	58
4.3.3. Photochemical Mechanisms .....	60
4.3.4. Polymerization Results .....	63
4.3.5. Molecular Modeling Studies .....	68
4.3.6. Radical Formation Mechanism.....	69
4.4. Conclusion.....	70
5. A WATER SOLUBLE, LOW MIGRATION, AND VISIBLE LIGHT PHOTOINITIATOR BY THIOXANTHONE-FUNCTIONALIZATION OF POLY(ETHYLENE GLYCOL)-CONTAINING POLY( $\beta$ -AMINO ESTER) .....	71
5.1. Introduction .....	71
5.2. Experimental Section .....	72
5.2.1. Materials .....	72
5.2.2. Characterization.....	72
5.2.3. Synthesis of p(PEGDA575-TX).....	72
5.2.4. Photochemical Analysis .....	73
5.2.4.1. UV-vis Spectroscopy Experiments. ....	73
5.2.4.2. LFP Experiments. ....	73

5.2.5. Photopolymerization.....	73
5.2.5.1. RT-FTIR Spectroscopy.....	73
5.2.5.2. Photo-DSC.....	74
5.2.5.3. Photoreactor.....	74
5.2.6. Migration Study.....	74
5.3. Results and Discussion.....	75
5.3.1. Synthesis and Characterization of Photoinitiator .....	75
5.3.2. Light Absorption Properties .....	78
5.3.3. Photochemical Mechanisms .....	79
5.3.4. Photopolymerization Results.....	81
5.3.5. Radical Formation Mechanism.....	85
5.3.6. Migration Stability.....	85
5.4. Conclusion.....	87
6. CYCLOPOLYMERIZABLE AND POLY-CYCLIC IRGACURE 2959 DERIVATIVES .....	88
6.1. Introduction .....	88
6.2. Experimental Section .....	89
6.2.1. Materials .....	89
6.2.2. Characterization.....	89
6.2.3. Synthesis of the Photoinitiators .....	89
6.2.3.1. Synthesis of CTI. ....	89
6.2.3.2. Synthesis of P-CTI.....	90
6.2.4. UV-vis Spectroscopy Experiments.....	90
6.2.5. Photopolymerization.....	90
6.2.6. Migration Study.....	91
6.3. Results and Discussion.....	91
6.3.1. Synthesis and Characterization of Photoinitiators.....	91

6.3.2. Light Absorption Properties .....	96
6.3.3. Photopolymerization Results.....	98
6.3.4. Migration Results .....	102
6.4. Conclusion.....	103
7. CONCLUDING REMARKS.....	104
REFERENCES .....	106
APPENDIX A: COPYRIGHT LICENCES.....	135

## LIST OF FIGURES

Figure 1.1.	Representation of possible photophysical and photochemical processes upon irradiation by light [2].....	2
Figure 1.2.	Typical absorption spectrum of a benzoyl-containing molecule. Reproduced with permission from [7] John Wiley and Sons, Copyright (2012), (Figure A.1). .....	2
Figure 1.3.	General pathway for photopolymerization. Reproduced with permission from [23] American Chemical Society, Copyright (2010), (Figure A.2). ...	3
Figure 1.4.	General representation for type I photoinitiation. Reproduced with permission from [27] Elsevier, Copyright (2019), (Figure A.4). .....	6
Figure 1.5.	Radical formation mechanism by type II photoinitiators. Reproduced with permission from [31] Royal Society of Chemistry, Copyright (2015), (Figure A.5). .....	6
Figure 1.6.	Photosensitization of diaryliodonium salt by acridinedione. Reproduced with permission from [33] Elsevier, Copyright (2001), (Figure A.6). .....	7
Figure 1.7.	Requirements for photoinitiators. Reproduced with permission from [35] licensed under CC BY 4.0, (Figure A.7). .....	8
Figure 1.8.	(a) Absorption spectra of 4,N,N-TMA, Iod salt and CTC (upper plot), (b) Iod, CTC and 4,N,N-TMA solutions (from left to right). Reproduced with permission from [85] American Chemical Society, Copyright (2016), (Figure A.8). .....	10

- Figure 1.9. Structures of the (1) I2959 and (2) LAP. Reproduced with permission from [105] Elsevier, Copyright (2009), (Figure A.9)..... 11
- Figure 1.10. Complexation of MMA with  $\beta$ -CD, proposed radical generation mechanism and photopolymerization process. Reproduced with permission from [121] Springer Nature, Copyright (2010), (Figure A.10). ..... 12
- Figure 1.11. (a) Photoinitiator structures, (b) Conversion of alkyne groups during photopolymerization (red: 1c, black: 1d), (c) Results of migration studies of PIs from polymeric network. Reproduced with permission from [154] Elsevier, Copyright (2017), (Figure A.11). ..... 14
- Figure 1.12. Structures of photoinitiators (left), Butyl acrylate/PI/EDB formulations (right) (a) before irradiation, (b) after irradiation by 405 nm LED, (c) after irradiation, the bottles were inverted and left to stand 10 min, Ac: C3POAC and PO: C3PO. Reproduced with permission from [149] Elsevier, Copyright (2022), (Figure A.12)..... 15
- Figure 1.13. Synthesis of PVA-TX. Reproduced with permission from [163] John Wiley and Sons, Copyright (2015), (Figure A.13)..... 16
- Figure 1.14. (a) Photopolymerization of HEA, TPGDA and TMPTA in the presence of  $\text{NP}_5\text{OCH}_3$  under 365 nm LED, (b) The migration rate of BP+EDB, TPO and  $\text{NP}_5\text{OCH}_3$ , (c) The cell viability under the treatment of  $\text{NP}_5\text{OCH}_3$  before and after 365 nm LED irradiation, (d) EPR spectra of  $\text{NP}_5\text{OCH}_3$  during 365 nm LED irradiation. Reproduced with permission from [185] John Wiley and Sons, Copyright (2021), (Figure A.14)..... 17
- Figure 1.15. Interaction between peroxy radical and hydrogen donor, and radical reinitiation. Reproduced with permission from [192] Elsevier, Copyright (2014), (Figure A.15)..... 18

Figure 1.16.	Double-bond conversion values of TMPTMA (a) in the presence of TX and various hydrogen donors at fixed weight ratios under air, (b) in the presence of TX/TEOA (1/2 wt %) under air, (c) different compositions of TX/TEOA at (1/2, 1.5/1.5, 2/1 wt%) under air, (d) different compositions of TX/TEOA (1/2, 1.5/1.5 wt%) under N <sub>2</sub> or air. Reproduced with permission from [200] Springer Nature, Copyright (2020), (Figure A.16).....	19
Figure 1.17.	Photoinitiator structures (top figure), (a) Photopolymerization profiles of HDDA in the presence of ND-O-EA, ND-N-EA, and BAPO upon LED at 405 nm exposure and CQ/MDEA upon LED at 470 nm exposure under air, (b) the cured HDDA and PUA polymers upon LED at 405 nm exposure under air. Reproduced with permission from [196] John Wiley and Sons, Copyright (2018), (Figure A.17).....	20
Figure 1.18.	Emission spectra of (a) Hg-Xe lamp, (b) Xe lamp, (c) a: fluorescent bulb, b: blue LED bulb, c: white LED bulb, (d) Laser diodes can perform, e.g., at 405, 457, 473, 532, 635 and 808 nm [209]......	23
Figure 3.1.	The synthesis pathway of PIs.....	31
Figure 3.2.	<sup>1</sup> H-NMR spectrum of PBT-2. ....	32
Figure 3.3.	FTIR spectra of PIs. ....	33
Figure 3.4.	(a) UV–vis absorption of PDT-2, PBT-2, PDT-5, PBT-5 (3.5 × 10 <sup>-5</sup> M, 4.1 × 10 <sup>-5</sup> M, 1.3 × 10 <sup>-5</sup> M, 1.7 × 10 <sup>-5</sup> M); E <sub>S1</sub> determination for (b) PBT-5 and (c) PDT-5. Solvent: MeOH.....	34
Figure 3.5.	Fluorescence lifetime measurements of (a) PBT-5 and (b) PDT-5. ....	34

- Figure 3.6. Photolysis of PIs in MeOH (a) PBT-5 ( $4.8 \times 10^{-5}$  M), (b) PBT-5/EDB ( $4.8 \times 10^{-5}$  M/ $1 \times 10^{-3}$  M), (c) PBT-5/Iod ( $4.8 \times 10^{-5}$  M/ $1 \times 10^{-3}$  M) by LED at 385 nm; (d) PBT-2/Iod ( $3.5 \times 10^{-5}$  M/ $3.5 \times 10^{-3}$  M) by LED at 375 nm...35
- Figure 3.7. The CTC formation of (a) PDT-2/Iod ( $4.7 \times 10^{-4}$  M/ $2.1 \times 10^{-3}$  M) in  $\text{CHCl}_3$ :toluene (10:90 v:v) and its photolysis (light source: 375 nm LED), (b) PDT-5/Iod ( $4.7 \times 10^{-4}$  M/ $2.1 \times 10^{-3}$  M) in  $\text{CHCl}_3$ ..... 36
- Figure 3.8. Fluorescence quenching of PBT-5 ( $1.4 \times 10^{-5}$  M) in MeOH with additives at different concentrations ( $\lambda_{\text{exc}} = 403$  nm). (a) EDB, (b) Iod, (c) Stern-Volmer plots (blue line: PBT-5/Iod, red line: PBT-5/EDB)..... 37
- Figure 3.9. LFP results of (a) PBT-5 and (b) PDT-5 excitation at 355 nm. The laser excitation (nanosecond pulse) arrived for  $t = 20$   $\mu\text{s}$ .....38
- Figure 3.10. ESR-spin trapping spectrum of PDT-2/Iod ( $2.8 \times 10^{-4}$  M/ $2.1 \times 10^{-3}$  M) in  $\text{CHCl}_3$ :toluene (10:90 v/v) under nitrogen in the presence of PBN (as a spin trap) (a) before irradiation and (b) after 40 s irradiation by LED at 420 nm. ....38
- Figure 3.11. (a) Polymerization profiles of formulation 1 with and without Iod under air; thickness =1.4 mm and (b) Double bond peak area for formulation 1 (with Iod) before and after reaction.....40
- Figure 3.12. (a) Polymerization profiles of formulation 2 with and without Iod under air; thickness = 1.4 mm and (b) Double bond peak area for formulation 2 (with Iod) before and after reaction.....40
- Figure 3.13. Photopolymerization profiles of formulations under air upon exposure to LED@405 nm; thickness =1.4 mm: (a) (meth)acrylate conversion for

	formulation 1 (dual curing vs one-step), (b) (meth)acrylate conversion for formulation 2 (dual curing vs one-step), (c) Double bond peak area for formulation 2 (dual curing) before and after irradiation. Light was switched on at 10 s. ....	41
Figure 3.14.	Network formation by one-step and dual curing processes. ....	42
Figure 3.15.	Photopolymerization profiles of formulations 1 and 5 in laminate, 20 min without light followed by 10 min upon exposure to light at 320-500 nm. ....	43
Figure 3.16.	Photo-DSC results of PI/Iod/HEMA/PEGDA (1/2/60/40 wt%) formulations under nitrogen, irradiated by 320-500 nm. (a) Rate of polymerization and (b) Conversion plot. [TX]: $5 \times 10^{-2}$ M. ....	44
Figure 3.17.	Photopolymerization profiles of formulations 3 (a) and 4 (b): 10 min without light (red) and 10 min with exposure to LED@405 nm (black) under air; thickness =1.4 mm. Light was switched on at 10 s. ....	45
Figure 3.18.	Photopolymerization profiles of formulations 6, 6a and 6b with and without exposure to LED@405 nm under air; thickness =1.4 mm. ....	46
Figure 3.19.	TGA analysis of the materials. ....	48
Figure 4.1.	The synthesis pathway of PIs. ....	55
Figure 4.2.	$^1\text{H-NMR}$ spectra of OAA and OAA-B. ....	56
Figure 4.3.	$^1\text{H-NMR}$ spectrum of OAA-BP. ....	56

Figure 4.4.	$^{13}\text{C}$ -NMR spectrum of OAA-BP.....	57
Figure 4.5.	FTIR spectra of the synthesized PIs. ....	58
Figure 4.6.	UV-vis absorption spectra of (a) OAA-B and OAA-BP ( $0.6 \times 10^{-4}$ M) in MeOH and $\text{H}_2\text{O}$ , (b) OAA-B and OAA-BP ( $2.1 \times 10^{-4}$ M) with and without Iod ( $4 \times 10^{-3}$ M) in MeOH, (c) Iod ( $3.5 \times 10^{-3}$ M), BP and OAA-BP ( $1.7 \times 10^{-3}$ M) with and without Iod ( $3.5 \times 10^{-3}$ M) in $\text{CHCl}_3$ :toluene (10:90 v/v), (d) Frontier orbitals (HOMO-LUMO) calculated at the UB3LYP/6-31G* level for OAA-BP.....	59
Figure 4.7.	UV-vis absorption spectra of OAA-B with and without Iod in $\text{CHCl}_3$ :toluene (10:90 v/v). OAA-B ( $1.7 \times 10^{-3}$ M) and Iod ( $3.5 \times 10^{-3}$ M).60	60
Figure 4.8.	LFP results of (a) OAA-B and (b) OAA-BP [PI] = $1.5 \times 10^{-4}$ M in MeOH. ....	61
Figure 4.9.	Photolysis of (a) OAA-B/Iod mixture by LED at 375 nm, OAA-B ( $1.9 \times 10^{-3}$ M) and Iod ( $3.6 \times 10^{-3}$ M) in $\text{CHCl}_3$ :toluene (10:90 v/v) (b) CTC formation between OAA-B and Iod (c) UV-vis absorption spectra of OAA-B and OAA-B/Iod in HEMA (OAA-B=0.12 wt% wrt BP moiety, Iod=0.48 wt%). ....	61
Figure 4.10.	(a) Photolysis of OAA-BP ( $1.7 \times 10^{-3}$ M) and Iod ( $3.5 \times 10^{-3}$ M) in $\text{CHCl}_3$ :toluene (10:90 v/v), (b) CTC formation between OAA-BP and Iod. ....	62
Figure 4.11.	ESR-spin trapping spectra of OAA-B/Iod under nitrogen in the presence of PBN (as a spin trap) (a) spectra at different times by LED at 420 nm and (b) experimental and simulated spectra after 60 s irradiation by LED at 420 nm. ....	62

Figure 4.12.	Experimental and simulated ESR-spin trapping spectra of OAA-BP/Iod under nitrogen in the presence of PBN (as a spin trap) after 60 s irradiation by LED at 420 nm.....	63
Figure 4.13.	(Meth)acrylate conversions (from FTIR experiments) of formulations under air at room temperature upon exposure to LED@405 nm; thickness=1.4 mm: (a) formulation BP-1 and BP-2, (b) formulation 1-4 and (c) formulation 2-P-4-P. Light was turned on at 10 s.....	65
Figure 4.14.	(Meth)acrylate conversions (from FTIR experiments) of formulations 4 and 4-P in air and in laminate at room temperature upon exposure to 320 - 500 nm; Light was turned on at 10 s.....	65
Figure 4.15.	Rate of polymerization vs. time and conversion vs. time plots for the photopolymerization of formulations 3, 3-P, 5, 6 and 7 under nitrogen at 30 °C upon exposure to light at (a), (c) 400-500 nm and (b), (d) 320-500 nm. ....	67
Figure 4.16.	Photopolymerization heat flow curves of formulations 4-P (with Iod) and 5-P (no additives) under nitrogen at 30 °C upon exposure to light at 320-500 nm. ....	68
Figure 4.17.	Proposed mechanism for the photoinitiation. ....	70
Figure 5.1.	Synthesis of TXOCH <sub>2</sub> CH <sub>2</sub> NH <sub>2</sub> and p(PEGDA575-TX).....	75
Figure 5.2.	<sup>1</sup> H-NMR spectrum of p(PEGDA575-TX).....	76
Figure 5.3.	<sup>1</sup> H NMR spectrum of p(PEGDA575-TX) synthesized in the absence of DBU.....	77

Figure 5.4.	FTIR spectrum of p(PEGDA575-TX).....	78
Figure 5.5.	UV–vis absorption of p(PEGDA575-TX) (n = 8) and TX in methanol, chloroform and water [p(PEGDA575-TX)] = $1 \times 10^{-5}$ M, [TX] = $8 \times 10^{-5}$ M.....	79
Figure 5.6.	Triplet state decay traces observed after laser excitation of p(PEGDA575-TX) (n= 4) in chloroform at 355 nm, kinetic traces recorded at 600 nm under N <sub>2</sub> : (a) without coinitiator, (b) with Iod, (c) with EDB.....	80
Figure 5.7.	(a) UV–vis absorption spectrum of p(PEGDA575-TX) (n = 4), photolysis of p(PEGDA575-TX) alone (b), in the presence of (c) EDB ( $1 \times 10^{-3}$ M) and (d) Iod ( $1 \times 10^{-3}$ M) using a 385 nm LED. Solvent: chloroform, [PI]: $4 \times 10^{-5}$ M.....	81
Figure 5.8.	Rate of polymerization and double bond conversion graphs of (a) TMPTA and (b) HEMA and TEGDMA in the absence of coinitiators at 30 °C under nitrogen irradiated by 400–500 nm. PI = 0.8 wt% wrt TX moiety.....	82
Figure 5.9.	(a) Rate of polymerization and (b) double bond conversion graphs of TEGDMA and TMPTA in the presence of coinitiators at 30 °C under nitrogen irradiated by visible light (400–500 nm). PI = 0.8 wt% wrt TX moiety, Iod and EDB = 2 wt%.....	83
Figure 5.10.	Methacrylate conversions of PI/Iod/HEMA and PI/Iod/TEGDMA formulations at 30 °C under nonlaminated conditions irradiated by UV–vis light (320–500 nm). PI = 0.8 wt% wrt TX moiety, Iod = 2 wt%. Irradiation starts at t = 10 s.....	84
Figure 5.11.	(a) Rate of polymerization and (b) double bond conversion graphs of HEMA and PEGDA in the absence and presence of Iod (2 wt%) with (10 wt%) and	

	without water at 30 °C under nitrogen irradiated by 400–500 nm. PI: 0.8 wt% wrt TX moiety.....	85
Figure 5.12.	Proposed radical formation mechanism.....	86
Figure 5.13.	UV–vis absorption spectra of TX and p(PEGDA575-TX) extracted with chloroform from the TX/EDB/TMPTA and p(PEGDA575-TX)/EDB/TMPTA (0.8–2–100 wt%) formulations.....	86
Figure 6.1.	Synthesis of TBEED, TBEED-COOH, CTI, P-CTI and minor products...	92
Figure 6.2.	<sup>1</sup> H-NMR spectrum of CTI in MeOD. ....	93
Figure 6.3.	<sup>13</sup> C-NMR spectrum of CTI. ....	94
Figure 6.4.	<sup>1</sup> H-NMR spectrum of P-CTI.....	95
Figure 6.5.	FTIR spectra of TBEED-COOH (black spectrum), I2959 (blue spectrum), CTI (purple spectrum) and P-CTI (green spectrum). ....	95
Figure 6.6.	UV-vis absorption spectra of CTI, P-CTI and I2959 in CHCl <sub>3</sub> and MeOH. [CTI], [I2959] = 2.6 x 10 <sup>-5</sup> M, [P-CTI] = 3.2 x 10 <sup>-5</sup> M wrt CTI moiety....	96
Figure 6.7.	Photolysis of (a) CTI (2.5 x 10 <sup>-5</sup> M) and (b) P-CTI (3.2 x 10 <sup>-5</sup> M wrt CTI moiety) under 320-500 nm light illumination.....	97
Figure 6.8.	Rate of polymerization (a, c) and double bond conversion graphs (b, d) of HEMA and TMPTA in the presence of CTI or I2959 at 30 °C under nitrogen irradiated by 320-500 nm.....	100

Figure 6.9.	(a) Rate of polymerization and (b) double bond conversion graphs of CTI alone (100 wt%), TEGDMA and TBEED in the presence of CTI at 30 °C under nitrogen irradiated by 320-500 nm. ....	101
Figure 6.10.	(a) Rate of polymerization and (b) double bond conversion graphs of TEGDMA in the presence of CTI and P-CTI (0.3 wt% wrt CTI moiety) at 30 °C under nitrogen irradiated by 320-500 nm. ....	102
Figure 6.11.	UV–vis absorption spectra of I2959 and CTI extracted with chloroform from the PI/TEGDMA (0.3–99.7 wt%) formulations.....	103
Figure A.1.	Permission from [7] John Wiley and Sons, Copyright (2012). ....	135
Figure A.2.	Permission from [23] American Chemical Society, Copyright (2010). ..	135
Figure A.3.	Permission from [26] Elsevier, Copyright (2016). ....	136
Figure A.4.	Permission from [27] Elsevier, Copyright (2019). ....	136
Figure A.5.	Permission from [31] Royal Society of Chemistry, Copyright (2015)....	137
Figure A.6.	Permission from [33] Elsevier, Copyright (2001). ....	138
Figure A.7.	Permission from [35] ( <a href="https://www.ncbi.nlm.nih.gov/pmc/articles/PMC7285382/">https://www.ncbi.nlm.nih.gov/pmc/articles/PMC7285382/</a> ), licensed under CC BY 4.0 ( <a href="https://creativecommons.org/licenses/by/4.0/">https://creativecommons.org/licenses/by/4.0/</a> ). ....	138
Figure A.8.	Permission from [85] American Chemical Society, Copyright (2016). ..	139

Figure A.9.	Permission from [105] Elsevier, Copyright (2009). .....	139
Figure A.10.	Permission from [121] Springer Nature, Copyright (2010). .....	140
Figure A.11.	Permission from [154] Elsevier, Copyright (2017). .....	140
Figure A.12.	Permission from [149] Elsevier, Copyright (2022). .....	141
Figure A.13.	Permission from [163] John Wiley and Sons, Copyright (2015). .....	141
Figure A.14.	Permission from [185] John Wiley and Sons, Copyright (2021). .....	142
Figure A.15.	Permission from [192] Elsevier, Copyright (2014). .....	142
Figure A.16.	Permission from [200] Springer Nature, Copyright (2020). .....	143
Figure A.17.	Permission from [196] John Wiley and Sons, Copyright (2018). .....	143
Figure A.18.	Permission from “Benzophenone-Functionalized Oligo(Amido Amine)/Iodonium Salt Systems as Visible Light Photoinitiators”, John Wiley and Sons, Copyright (2021). .....	144
Figure A.19.	Permission from “A Water Soluble, Low Migration, and Visible Light Photoinitiator by Thioxanthone-Functionalization of Poly(ethylene glycol)-Containing Poly( $\beta$ -amino ester)”, John Wiley and Sons, Copyright (2022). .....	144

## LIST OF TABLES

Table 1.1.	Structures and absorption wavelengths of commercially available free radical photoinitiators. Reproduced with permission from [26] Elsevier, Copyright (2016), (Figure A.3).....	5
Table 3.1.	Compositions of the PIs, <sup>a</sup> Calculated from <sup>1</sup> H NMR spectra. ....	31
Table 3.2.	Photopolymerization formulations, PI = 1 wt% with respect to TX moiety and Iod = 2 wt% in the formulations. <sup>1</sup> PI = 8 wt%, no Iod, <sup>2</sup> PI = 8 wt%, Iod = 2 wt%.....	39
Table 3.3.	Total conversion, T <sub>g</sub> and thermal degradation characteristics of the materials.....	47
Table 4.1.	Absorption characteristics of PIs in methanol and water.....	59
Table 4.2.	Photopolymerization formulations. PI = 0.5 wt% with respect to BP moiety and EDB, Iod = 2 wt% in the formulation. [a] OAA = 3 wt%, [b] OAA = 3 wt%, BP = 0.5 wt%, [c] BP = 1 wt%.....	64
Table 4.3.	Frontier molecular orbital properties of Iod, OAA-B and the CTC optimized structure ([OAA-B-Iod]CTC) and their respective calculated UV-vis spectra (F = oscillator strength).....	69
Table 5.1.	Absorption characteristics of p(PEGDA575-TX) and TX in different solvents. ....	79

Table 6.1.	Absorption characteristics of CTI and I2959. ....	97
Table 6.2.	Formulation contents, $R_{pmax}$ , $t_{max}$ and conversion values. ....	98

## LIST OF SYMBOLS

$a_H$	Hyperfine splitting constant for hydrogen
$a_N$	Hyperfine splitting constant for nitrogen
$Ar_2I^+X^-$	Diaryliodonium salt
$CHCl_3$	Chloroform
$CDCl_3$	Deuterated chloroform
$E_{S1}$	First singlet excited-state energy
$I_0$	Fluorescence intensity of photoinitiator in the absence of quencher
$I_Q$	Fluorescence intensity of photoinitiator in the presence of quencher
$k_q$	Quenching rate
$K_{sv}$	Stern-Volmer constant
$m$	Mass of monomer
$M$	Molar mass of monomer
$M_n$	The number average molecular weight
$n$	Number of double bonds per monomer molecule
$Na_2SO_4$	Sodium sulfate
$NP_5OCH_3$	Prism[5]arene
$Q/s$	Heat flow per second
$R_{pmax}$	Maximum polymerization rate
$S_0$	Ground state
$S_n$	Singlet excited states
$t_{max}$	Time at maximum polymerization rate
$T_1$	Triplet excited state

$T_g$	Glass transition temperature
$\text{TXOCH}_2\text{CH}_2\text{NH}_2$	2-(2-aminoethoxy)-9H-thioxanthen-9-one
$\Delta H_p$	Heat of reaction evolved
$\varepsilon$	Extinction coefficient
$\lambda_{\text{max}}$	Maximum absorption wavelength
$\tau_0$	Singlet excited state lifetime of photoinitiator

## LIST OF ACRONYMS/ABBREVIATIONS

$\beta$ -CD	$\beta$ -cyclodextrin
4,N,N-TMA	4,N,N-trimethylaniline
AAm	Acrylamide
ADD	Acridinedione
ATX	2-acryloyloxy thioxanthone
BAPO	Phenylbis(2,4,6-trimethylbenzoyl)phosphine oxide
Bis-GMA	Bisphenol A-glycidyl methacrylate
BP	Benzophenone
C3PO	(1E,4E)-1,5-bis(4-methoxyphenyl)penta-1,4-dien-3-one
C3POAC	(((1E,4E)-3-oxopenta-1,4-diene-1,5-diyl)bis(4,1-phenylene))bis (oxy))bis(ethane-2,1-diyl) diacrylate
CQ	Camphorquinone
CTC	Charge transfer complex
CTI	Cyclopolymerizable di(tert-butyl) 2,2'-[oxybis(methylene)]bis(2-propenoate and Irgacure 2959 derivative
DABCO	1,4-diazabicyclo[2.2.2]octane
DBU	1,8-diazabicyclo[5.4.0]undec-7-ene
DH	Hydrogen donor
DMF	N,N-dimethylformamide
DMPA	2,2-dimethoxy-2-phenylacetophenone
DSC	Differential scanning calorimetry
DVP	Diethyl vinylphosphonate

EDB	Ethyl 4-(dimethylamino)benzoate
EPR/ESR-ST	Electron paramagnetic resonance/Electron spin resonance-spin trapping
FRP	Free radical photopolymerization
FTIR	Fourier transform infrared spectroscopy
GPC	Gel permeation chromatography
HDDA	1,6-hexanediol diacrylate
HEA	2-hydroxyethyl acrylate
HEMA	2-hydroxyethyl methacrylate
HOMO	Highest occupied molecular orbital
I2959	2-hydroxy-4'-(2-hydroxyethoxy)-2-methylpropiophenone
IC	Internal conversion
Iod	Bis-(4-tert-butylphenyl)-iodonium hexafluorophosphate
IPN	Interpenetrating network
ISC	Intersystem crossing
ITX	Isopropyl thioxanthone
LAP	Lithium acylphosphinate salt
LED	Light emitting diode
LFP	Laser flash photolysis
LUMO	Lowest occupied molecular orbital
MBA	N,N-methylenebisacrylamide
MDEA	N-methyldiethanolamine
MeOH	Methanol
MeOD	Deuterated methanol

MMA	Methyl methacrylate
MO	Molecular orbital
<i>n</i> -PDEA	N-phenyldiethanolamine
ND-N-EA	2-((2-(1,3-dioxo-6-(piperidin-1-yl)-1H-benzo[de]isoquinolin-2(3H)-yl)ethyl)(methyl)-amino)ethyl acrylate
ND-O-EA	2-(2-(1,3-dioxo-6-(piperidin-1-yl)-1H-benzo[de]-isoquinolin-2(3H)-yl)ethoxy)ethyl acrylate
NPG	N-phenylglycine
NMR	Nuclear magnetic resonance spectroscopy
OAA-B	Benzophenone functionalized oligo(amido amine)
OAA-BP	Benzophenone and phosphonate functionalized oligo(amido amine)
P	Phosphonate
p(PEGDA575-TX)	Thioxanthone and poly(ethylene glycol) functionalized poly( $\beta$ -amino ester)
P-CTI	Poly-cyclic di(tert-butyl) 2,2'-[oxybis(methylene)]bis(2-propenoate)/Irgacure 2959 derivative
<i>p</i> -TDEA	2,2'-(4-methylphenylimino)diethanol
PBAE	Poly( $\beta$ -amino ester)
PBN	N-tert-butyl- $\alpha$ -phenylnitron
PBT-2	Bisphosphonate and thioxanthone functionalized poly(ethylene imine) at the ratio of 2:2:1
PBT-5	Bisphosphonate and thioxanthone functionalized poly(ethylene imine) at the ratio of 5:5:1
PDI	Polydispersity index
PDT-2	Phosphonate and thioxanthone functionalized poly(ethylene imine) at the ratio of 2:2:1

PDT-5	Phosphonate and thioxanthone functionalized poly(ethylene imine) at the ratio of 5:5:1
PEI	Poly(ethylene imine)
PEG	Poly(ethylene glycol)
PEGDA	Poly(ethylene glycol) diacrylate
PI	Photoinitiator
PIS	Photoinitiating system
PUA	Polyurethane acrylate
PVA-TX	Poly(vinyl alcohol)–thioxanthone
TBEED	Di(tert-butyl) 2,2'-[oxybis(methylene)]bis(2-propenoate)
TBEED-COOH	2,2'-(oxybis(methylene))diacrylic acid
TEA	Triethylamine
TEGDMA	Triethylene glycol dimethacrylate
TEOA	Triethanolamine
TEVBP	Tetraethyl vinylidene bisphosphonate
TFA	Trifluoroacetic acid
TGA	Thermogravimetric analysis
THF	Tetrahydrofuran
TMPTA	Trimethylolpropane triacrylate
TMPTMA	Trimethylolpropane trimethacrylate
TPGDA	Tripropylene glycol diacrylate
TPO	Diphenyl(2,4,6-trimethylbenzoyl)phosphine oxide
TX	Thioxanthone
TX-Ct	Thioxanthone-catechol-O,O'-diacetic acid

UV	Ultraviolet light
VA-086	2,2'-azobis (2-methyl-N-(2-hydroxyethyl)propionamide)

## 1. INTRODUCTION

Sunlight is essential for life on planet earth, providing the energy input that life requires. Furthermore, it induces many processes associated with, or even critical for, life. Foremost among these is the production of oxygen, which almost all of known life needs. As is well-known, this production, photosynthesis, is a light-induced process. Our vision ability is triggered by cis-trans photoisomerization of 11-cis-retinal in our eyes, also a light-induced process [1]. Formation of ozone layer, synthesis of vitamin D and many more processes are dependent on sunlight. These transformations can be explained by photochemistry, photobiology and photophysics. Absorption of photons can result in excitation to singlet excited states ( $S_n$ ) from ground state ( $S_0$ ), followed by nonradiative or radiative deactivation steps. After excitation to  $S_2$ , it might relax to singlet excited state ( $S_1$ ) via nonradiative process, namely internal conversion (IC) by passing through a conical intersection (Figure 1.1) [2]. From  $S_1$ , three pathways can be pursued: (i) fluorescence which is a radiative relaxation, (ii) nonradiative relaxation to  $S_0$  by going through intersections, and (iii) a photoproduct can form. Besides  $S_1$ ,  $S_2$  excited state may transition to triplet excited state ( $T_1$ ) via intersystem crossing (ISC) which is accomplished by singlet-triplet crossing. ISC is affected by the spin-orbit coupling and the overlap between vibrational levels of singlet and triplet states [2-4]. Similar to  $S_1$ , three routes can be followed after reaching to  $T_1$ : (i) phosphorescence which is a radiative decay, (ii) nonradiative transition to  $S_0$ , and (iii) formation of a photoproduct.

Transitions can be characterized as  $n - \pi^*$  and  $\pi - \pi^*$  transitions in which  $n$ ,  $\pi$  and  $\pi^*$  correspond to nonbonding, bonding and antibonding molecular orbitals (MO) respectively [5,6]. An electron passes to an empty MO (excited state) from a filled MO (ground state) upon absorbing a photon. As a result of this transition, an absorption spectrum is obtained which can be in the ultraviolet (UV) and visible region of electromagnetic spectrum (Figure 1.2) [7]. Molecular structure, chemical environment and light source play important roles in the aforementioned transitions. First of all, emission spectrum of light source must overlap with absorption spectrum of a molecule in order to obtain transitions between the aforementioned states. Excited states with higher energies can be reached by altering irradiation wavelength, and light intensity can be changed to alter the photon

amounts [8]. Characteristics of deactivation steps and excited state lifetimes are determined by the structure of the molecule and the solvent polarity, which affects the electronic environment of the molecule [8-10].

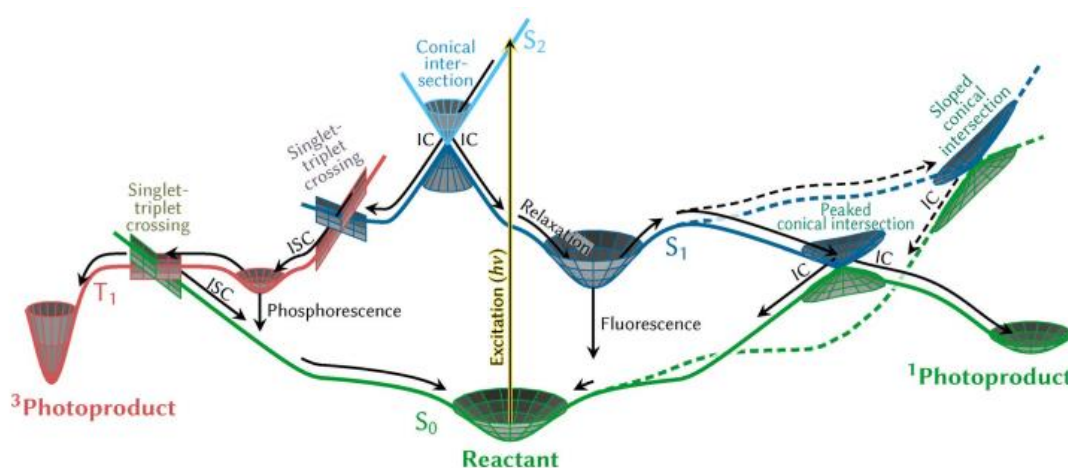


Figure 1.1. Representation of possible photophysical and photochemical processes upon irradiation by light [2].

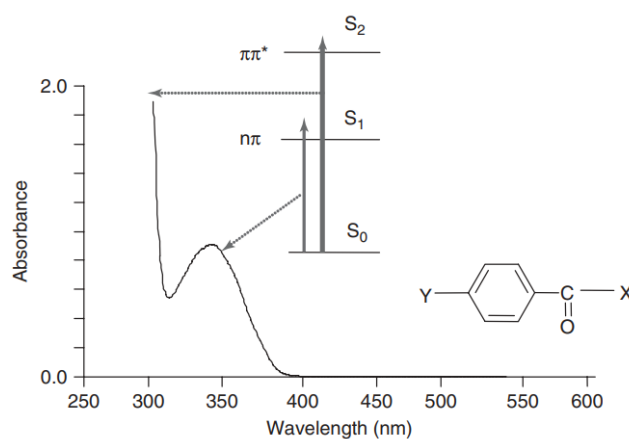


Figure 1.2. Typical absorption spectrum of a benzoyl-containing molecule. Reproduced with permission from [7] John Wiley and Sons, Copyright (2012), (Figure A.1).

## 1.1. Photoinduced Polymerization

Photochemistry is the examination of chemical transformations induced by photoexcitation. Photoexcitation does not necessarily result in photochemical changes but can also lead to emission of light (fluorescence and phosphorescence) and nonradiative decay such as vibrational relaxation. Photochemical transformations are observed when reactive chemical intermediates (free radicals and ionic species) are generated. These intermediates can be utilized to initiate photopolymerization reactions [11]. Photopolymerization is a type of reaction in which a liquid formulation is converted into a solid material upon exposure to UV or visible light. As a polymerization technology, light curing has gained attention due to its advantageous and relatively environmentally friendly properties such as high rate of polymerization at ambient temperatures, less energy consumption, solvent-free formulations and low cost. Photoinduced polymerization reaction is energetically more favorable at room temperature than thermal polymerization. A photon in the range of 250 – 370 nm delivers 130 – 190 times more energy than the thermal energy per molecule accessible to activate a reaction at 25 °C [12]. These beneficial properties enables photopolymerization to be applied in variety of fields such as lithography, coatings, optoelectronics, solar cells, medicine and dental adhesives [13-21]. In a photoinitiating system (PIS), a polymerizable formulation and an irradiation source are necessary for photoinitiated polymerization as depicted in Figure 1.3 [22,23].

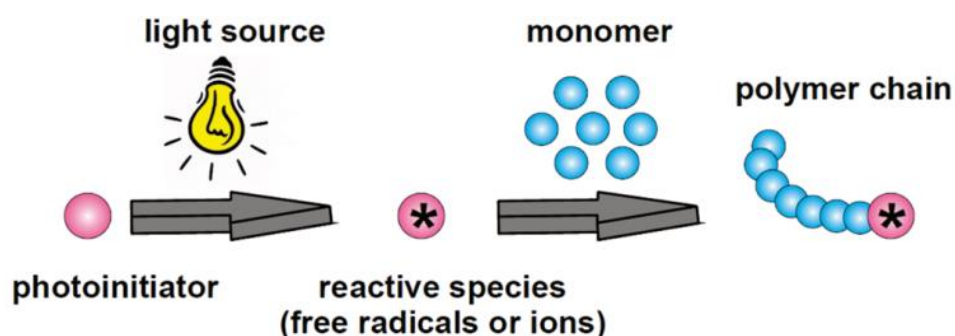


Figure 1.3. General pathway for photopolymerization. Reproduced with permission from [23] American Chemical Society, Copyright (2010), (Figure A.2).

## 1.2. Free Radical Photoinitiators

A photoinitiator (PI) or PIS is specified as a single molecule or mixture of molecules producing reactive species which can initiate light-mediated polymerization when photoexcited [24]. PIs are the most important part of the photopolymerization, they regulate the initiation rate [25]. Free radical PIs generate radicals which initiate free radical photopolymerization (FRP) upon absorbing light in UV and visible region. These type of PIs are classified into two categories: unimolecular bond scission (type I) and bimolecular, H-abstraction type (type II) initiators [23]. Commercially available type I and type II photoinitiators are depicted in Table 1.1 [26].

As illustrated in Figure 1.4, type I PIs form two types of radicals through homolytic  $\alpha$ -cleavage (major) or  $\beta$ -cleavage (minor) in triplet excited state [27]. Both radicals are capable of inducing polymerization. Type I PIs generally possess benzoyl moiety as a chromophore, including benzoin ethers, benzil ketals, acetophenones and acylphosphine oxides [28-30].

Type II photoinitiation proceeds via heteroatoms, unlike type I photoinitiation. They require a coinitiator for generation of radicals via photoinduced electron transfer or hydrogen abstraction in triplet state. In type II photoinitiation, coinitiators act as an electron/H donors and PIs act as an electron/H acceptors. Radical anion - radical cation excited state complex (exciplex) is formed following electron transfer between PI and coinitiator, then hydrogen is abstracted from the coinitiator resulting in generation of ketyl radical and radical on the coinitiator (Figure 1.5) [31]. Ketyl radicals are not reactive at initiating polymerization, rather contribute to chain termination in polymerization or dimerization [32]. Coinitiator radicals are initiating species. Thiols and ethers can be utilized as coinitiators, although amines are used widely. As depicted in Table 1.1, type II PIs are generally benzophenone, thioxanthone, coumarin or camphorquinone derivatives.

Table 1.1. Structures and absorption wavelengths of commercially available free radical photoinitiators. Reproduced with permission from [26] Elsevier, Copyright (2016), (Figure A.3).

Compounds	Type	Structure	$\lambda_{max}$ (nm)
Benzoin and benzoin ethers	Unimolecular		323
Benzil ketals	Unimolecular		365
Oxime esters	Unimolecular		335
Acetophenones	Unimolecular		340
Aminoalkyl phenones	Unimolecular		320
Acylophosphine oxides	Unimolecular		380
Benzophenones	Bimolecular		335
Thioxanthenes	Bimolecular		390
Coumarins	Bimolecular		370
Benzils	Bimolecular		340
Camphorquinones	Bimolecular		470

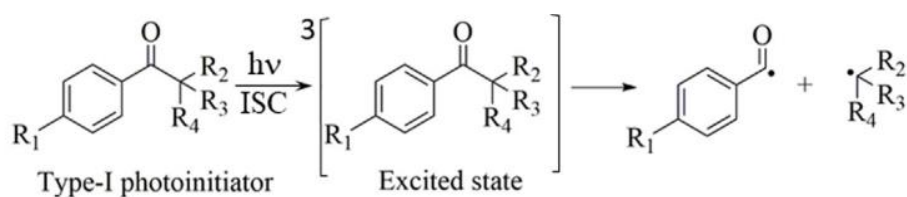


Figure 1.4. General representation for type I photoinitiation. Reproduced with permission from [27] Elsevier, Copyright (2019), (Figure A.4).

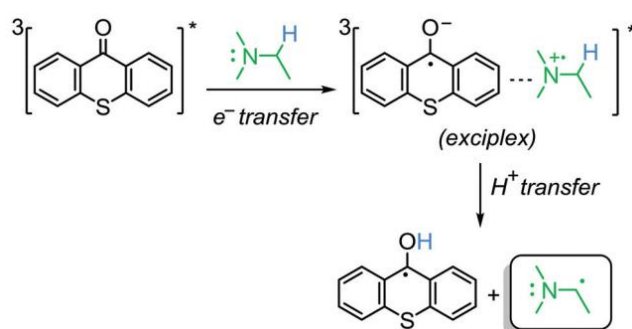


Figure 1.5. Radical formation mechanism by type II photoinitiators. Reproduced with permission from [31] Royal Society of Chemistry, Copyright (2015), (Figure A.5).

Onium salts can also be used as coinitiators in combination with type II PIs (also called photosensitizers). An electron is transferred from photoexcited photosensitizer to ground state onium salt followed by cleavage reactions and formation of radicals and/or cations which are capable of inducing polymerization [31]. Selvaraju et al. investigated the excited state reactions between acridinedione (photosensitizer) and different onium salts [33]. Both singlet and triplet photoexcited states of acridinedione (ADD) are involved in the electron transfer to diaryliodonium salt ( $\text{Ar}_2\text{I}^+\text{X}^-$ ). Figure 1.6 illustrates that after electron is transferred to  $\text{Ar}_2\text{I}$  from ADD, radical cation ( $\text{ADD}^{\bullet+}$ ) and diaryliodonine radical ( $\text{Ar}_2\text{I}\cdot$ ) are generated. The radical cation  $\text{ADD}^{\bullet+}$  tautomerizes to enol radical cation  $\text{ADE}^{\bullet+}$ , and  $\text{Ar}_2\text{I}\cdot$  radical decomposes into iodobenzene and phenyl radical.

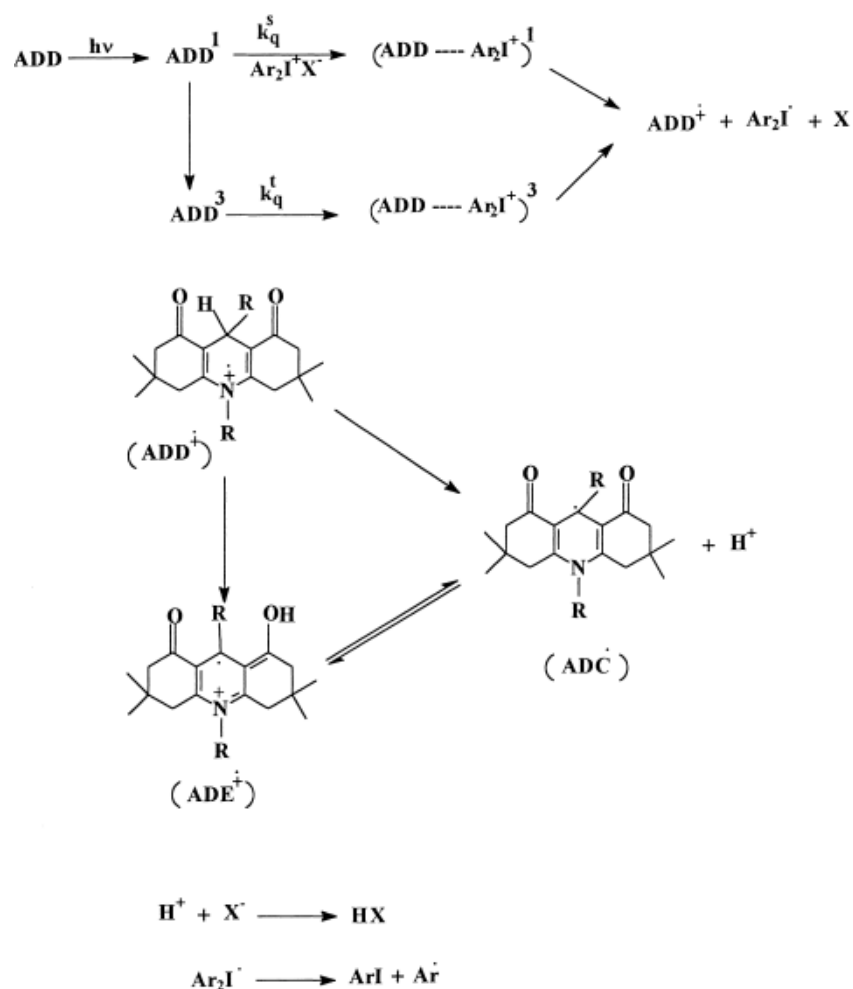


Figure 1.6. Photosensitization of diaryliodonium salt by acridinedione. Reproduced with permission from [33] Elsevier, Copyright (2001), (Figure A.6).

The characteristics of PIs determine the photocuring rate and final properties of photopolymers, so they should have the following features (Figure 1.7): (i) absorptivity in the emission range of the irradiation source, (ii) high quantum efficiency, (iii) sufficient solubility in photocuring formulation and in water, (iv) low cost and no toxicity and (v) low migration of PIs from final polymers in order to eliminate yellowing, odour and toxicity [34,35]. Water solubility of PIs is important for environmental concerns and it is a requirement in biomedical applications. In addition to these features, it is preferable to employ PIs activated by visible light due to the fact that visible light consumes less energy than UV light and is non-carcinogenic. Type I PIs undergo unimolecular photodissociation upon photoexcitation, so visible light may not have the required photon energy for

dissociation. Although there are type I PIs which can function upon visible light irradiation, type II PIs are generally more appropriate for photopolymerization by visible light. The following sections will cover the research in the literature to improve the properties of PIs regarding the aforementioned features.

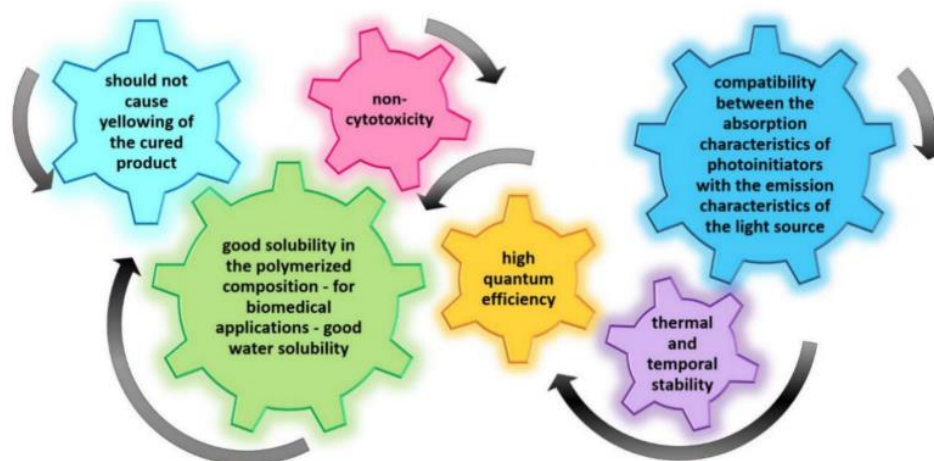


Figure 1.7. Requirements for photoinitiators. Reproduced with permission from [35] licensed under CC BY 4.0, (Figure A.7).

### 1.3. Visible Light Photoinitiators

The light that radiation curing requires has often been UV, which is problematic because it can cause DNA damage and cancer, also the sources are expensive and not as available as those of visible light. Additionally visible light consumes less energy, penetrates deeper and is safer, therefore it is more environmental friendly. Hence, there have been a variety of research efforts to develop type I and type II PI derivatives which are efficiently activated under visible light, such as acylstannane [36], acylgermanium [37-40], acylphosphine oxide [41-46], methyl benzoylformate [47], camphorquinone [48-51], naphthalimide [52-55], carbazole [56-58], phenothiazine [59-61], thioxanthone (TX) [62-69], and benzophenone (BP) [70-74]. He et al. synthesized methyl benzoylformate derivatives which are able to photolyze under 405 nm LED efficiently [47]. Photoinitiating radicals are formed in two steps: the first step is the formation of methyl benzoyl and methoxyacyl radicals via  $\alpha$ -cleavage of the C–C bond between the dicarbonyl and the second step is the

decarboxylation reaction of methoxyacyl radicals to generate carbon dioxide and methyl radicals. Tri-(propylene glycol) diacrylate was irradiated by 405 nm LED for 30 seconds for curing depth experiments, results were compared with phenylbis(2,4,6-trimethylbenzoyl)phosphine oxide (BAPO). The synthesized PIs have a much higher curing depth (5 – 6.5 cm) in comparison to BAPO (< 1 cm). Wang et al. utilized a visible light absorbing TX derivative in surface engineering of individual living cells due to the less toxic nature of visible light over UV light [75]. Firstly they incorporated poly(ethylene imine) on the yeast cell via electrostatic interaction, secondly the TX derivative was assembled with poly(ethylene imine) by electrostatic interaction between carboxyl groups of TX and the amino groups of poly(ethylene imine). Finally, radicals were formed by PI abstracting hydrogen from polymer after photoexcitation by visible light, resulting in photografting of poly(ethylene glycol) diacrylate (PEGDA) onto the yeast cell.

Charge transfer complex (CTC) is a ground state electron donor - electron acceptor complex in which an electronic charge is transferred from donor to acceptor. CTCs can be identified by spectroscopic methods, because bathochromic shift in absorption maxima can be observed with CTC which is characteristics to neither electron donor nor electron acceptor [76]. If bathochromic shift results in visible light absorption, CTCs can initiate photopolymerization under visible light [77-84]. Garra et al. obtained CTCs by combining amine or phosphines (electron donor) with iodonium salt (electron acceptor) [85]. A shift in absorption spectrum, thus yellow color, was observed when colorless 4,N,N-trimethylaniline (4,N,N-TMA) solution was mixed with colorless iodonium salt (Iod) solution, indicating CTC formation between 4,N,N-TMA and Iod salt (Figure 1.8). CTCs were irradiated by 405 nm LED leading to generation of aryl radicals and resulting in polymerization of methacrylate resins.

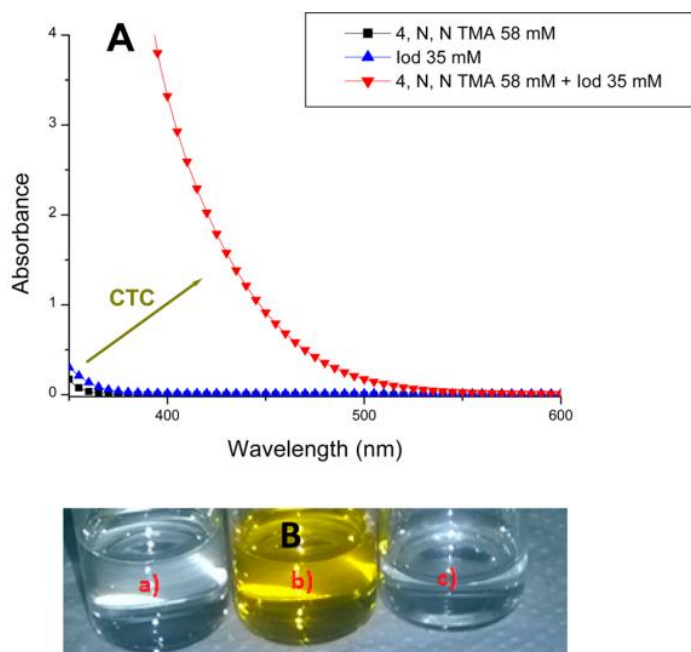


Figure 1.8. (a) Absorption spectra of 4,N,N-TMA, Iod salt and CTC (upper plot), (b) Iod, CTC and 4,N,N-TMA solutions (from left to right). Reproduced with permission from [85] American Chemical Society, Copyright (2016), (Figure A.8).

#### 1.4. Water-Soluble Photoinitiators

Water is more advantageous than volatile organic solvents in terms of toxicity, cost and availability, hence water-borne formulations are more environmental-friendly and are preferable in the paints, coatings and biomedical applications [86,87]. These formulations are in need of water-soluble photoinitiators so that photopolymerization process can be applicable. Riboflavin and xanthene dyes such as eosin Y and erythrosin B are water-soluble type II photoinitiators used in aqueous photopolymerization of 2-hydroxyethyl methacrylate (HEMA), acrylamide or PEGDA [88-96]. 2-hydroxy-4'-(2-hydroxyethoxy)-2-methylpropiophenone (I2959) and 2,2'-azobis (2-methyl-N-(2-hydroxyethyl)propionamide) (VA-086) are water-soluble type I photoinitiators commonly utilized in hydrogel synthesis through photopolymerization for biomedical applications [97-103]. Although I2959 is cytocompatible and is considered water soluble, its solubility in water is actually quite limited. Dissolution of I2959 in water can require considerable stirring and heating, even 5 mg/mL can be prepared only under stirring at 37 °C during 24 h for complete dissolution

[104,105]. Fairbanks et al. synthesized a water-soluble lithium acylphosphinate salt (LAP) to obtain a hydrogel for cell encapsulation, and compared the properties of LAP to those of I2959 (Figure 1.9) [105]. LAP has absorbance stretching to 420 nm with a maximum at approximately 375 nm, and I2959 has absorbance in UV region stretching to 370 nm. Both of the PIs undergo homolytic bond scission upon photoexcitation. LAP is more soluble than I2959 in water, photopolymerization of PEGDA is faster under 365 nm light exposure, and cell survival is 95% or greater with hydrogels prepared with LAP. Furthermore, polymerization is also achieved upon 405 nm visible light irradiation which is not possible with I2959 due to lack of absorbance in visible region.

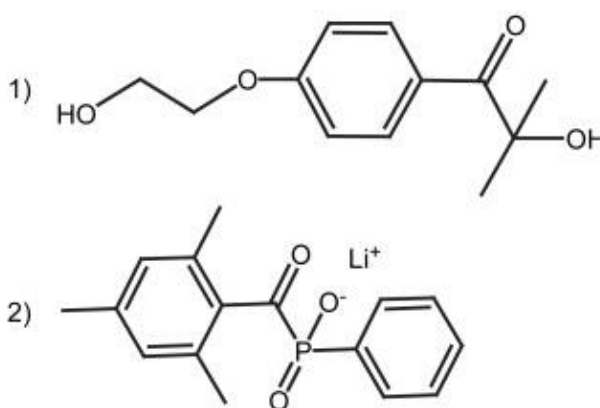


Figure 1.9. Structures of the (1) I2959 and (2) LAP. Reproduced with permission from [105] Elsevier, Copyright (2009), (Figure A.9).

Various water-soluble PIs have been synthesized in the literature by modifying hydrophobic type I (acylphosphine oxides and Irgacure 1173) and type II PIs (thioxanthone, benzophenone, coumarin, naphthalimide and camphorquinone) with hydrophilic moieties such as oxalate [86], alkali metal salts [106-108], carboxylate [109,110], quaternary ammonium [111-114], sulfonate [115-117], imidazolium [119], bisphosphonate [120], carboxylic acid [48], [121], bisphosphonic acid [122], carbohydrate [123]. Host/guest interactions can convert oil-soluble PIs into water-soluble PIs such as supramolecular assembly between cyclodextrin (host) and type I (2,2-dimethoxy-2-phenylacetophenone (DMPA)) and type II PIs (camphorquinone and naphthalimide) or by encapsulating thioxanthone or benzophenone derivatives into hyperbranched poly(ether amine)s [124-

127]. Karasu et al. synthesized a water soluble thioxanthone-based photoinitiator containing di-acetic acid groups (TX-Ct), and studied the aqueous photopolymerization of  $\beta$ -cyclodextrin/methyl methacrylate ( $\beta$ -CD/MMA) complex [121]. As illustrated in Figure 1.10, TX-Ct is a one-component PI in which the radical formation mechanism is based on the intramolecular and intermolecular electron transfer followed by hydrogen abstraction and decarboxylation. The generated alkyl radical induced photopolymerization of  $\beta$ -CD/MMA complex in water.

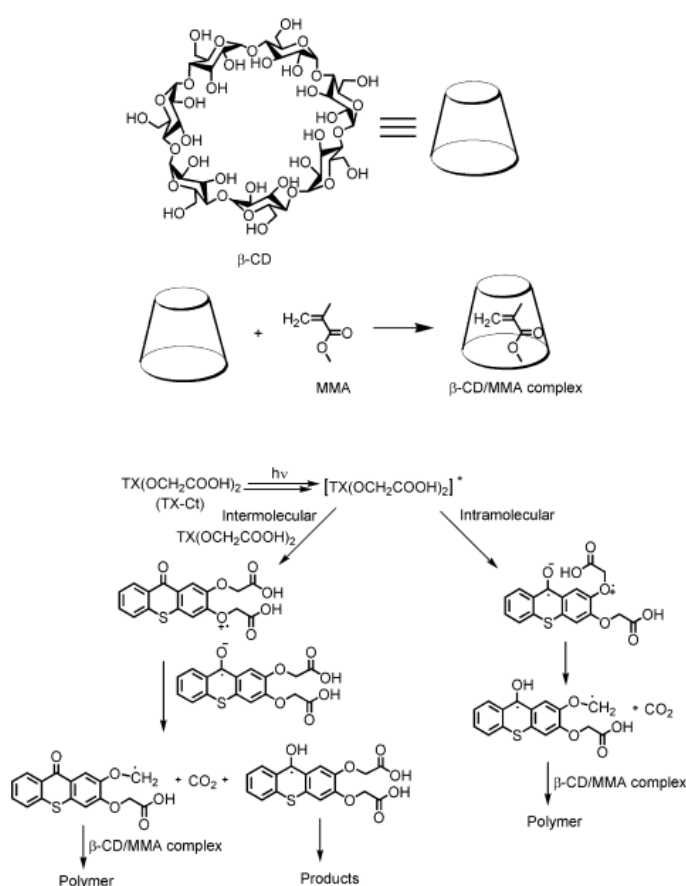


Figure 1.10. Complexation of MMA with  $\beta$ -CD, proposed radical generation mechanism and photopolymerization process. Reproduced with permission from [121] Springer Nature, Copyright (2010), (Figure A.10).

### 1.5. Polymerizable and Macromolecular Photoinitiators

Radiation curing is an effective polymerization method, but it does not ensure the complete consumption of photoinitiators/coinitiators in the polymerization formulation. Unreacted small molecule photoinitiators, their photodissociation products and/or coinitiators can be harmful by migrating out of the light-cured polymeric networks and thereby causing yellowing/discoloration of the final product, odour and toxicity. These problems can limit the use of photopolymerization in any application that can come in contact with food (e.g. packaging and inks used in the labeling of packaging), and all labeling/printing applications. Isopropyl thioxanthone (250  $\mu\text{g/l}$ ) was detected in milk, having migrated from the milk packaging to the milk in 2005 in Italy, consequently 30 million litres of milk were withdrawn from the market because they were found unfit for human use [128].

One way to overcome these disadvantages is the design of polymerizable (monomeric) photoinitiators which bind covalently to the product. Allyl [129,130], maleimide [131-135], methacrylamide [136], meth/acrylate [137-152] and alkyne [153,154] functionalities can be integrated onto type I and type II PIs to obtain polymerizable PIs. Roth et al. synthesized four benzophenone derivatives bearing ethyl ester (1a), vinyl carbonate (1b), but-1-yn-4-yl ester (1c) and propargyl ester (1d) groups (Figure 1.11a) [154]. 1b, 1c and 1d were evaluated as polymerizable PIs in a thiol/vinyl carbonate formulation. Integration of 1c and 1d into thiol/vinyl carbonate network during photopolymerization was determined by monitoring alkyne peak in FT-IR, high polymerization rate and conversion of alkyne groups of the functionalized PIs in the polymerization formulation were obtained (Figure 1.11b). Leaching studies showed that polymerizable PIs (1b-d) migrated less than the non-polymerizable PI (1a) (Figure 1.11c). Reduced migration indicated the immobilization of polymerizable PIs in the growing polymer chain. Xue et al. synthesized a bis-acrylate functionalized enone derivative (C3POAC) serving as a type II PI with reduced yellowing compared to TX and a crosslinker [149]. Crosslinking ability of C3POAC was analyzed by inducing photopolymerization of butyl acrylate, a monofunctional monomer, and the results were compared to isopropyl thioxanthone (ITX) and an analog compound of C3POAC without acrylate group (C3PO) in the presence of ethyl 4-(dimethylamino)benzoate (EDB) as coinitiator. As illustrated in Figure 1.12a,

C3POAC/EDB and C3PO/EDB solutions were yellow and ITX/EDB solution was colorless before illumination by 405 nm LED. After irradiation for 15 minutes, the colors of C3POAC/EDB and C3PO/EDB solutions faded and the color of ITX/EDB solution became yellow (Figure 1.12b). Butyl acrylate polymers obtained by C3PO/EDB and ITX/EDB were fluid and C3POAC/EDB polymer displayed no fluidity suggesting that C3PO and ITX led to linear polymers and C3POAC led to crosslinked polymer due to integration of the PI through its bis-acrylate moiety into polymeric network (Figure 1.12c).

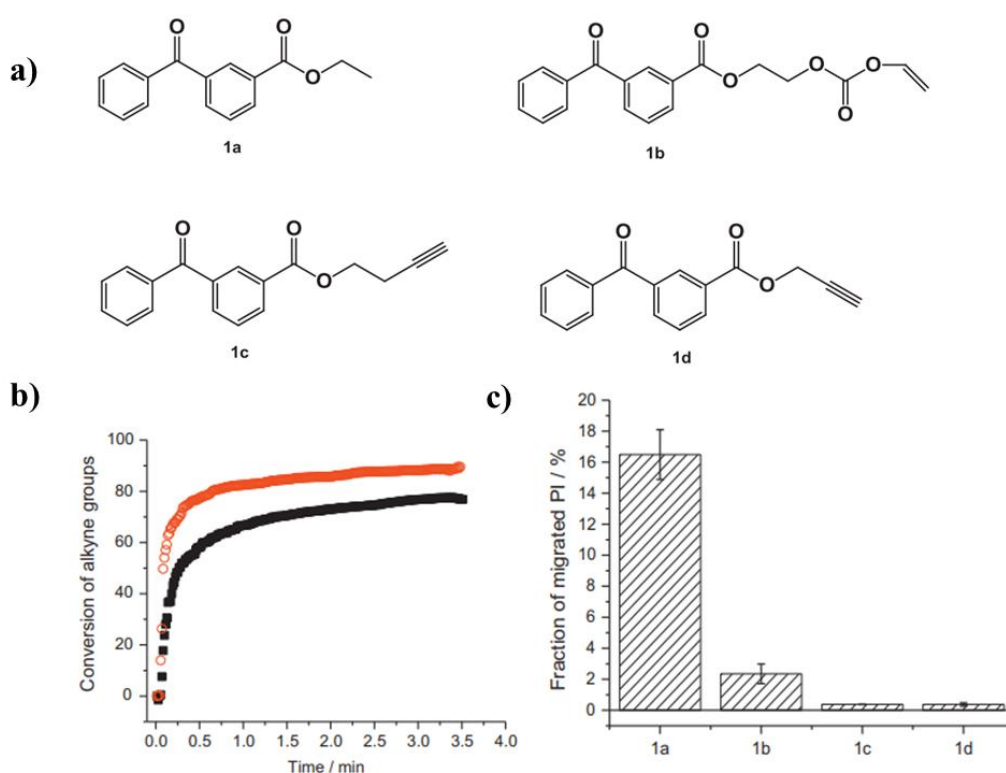


Figure 1.11. (a) Photoinitiator structures, (b) Conversion of alkyne groups during photopolymerization (red: 1c, black: 1d), (c) Results of migration studies of PIs from polymeric network. Reproduced with permission from [154] Elsevier, Copyright (2017), (Figure A.11).

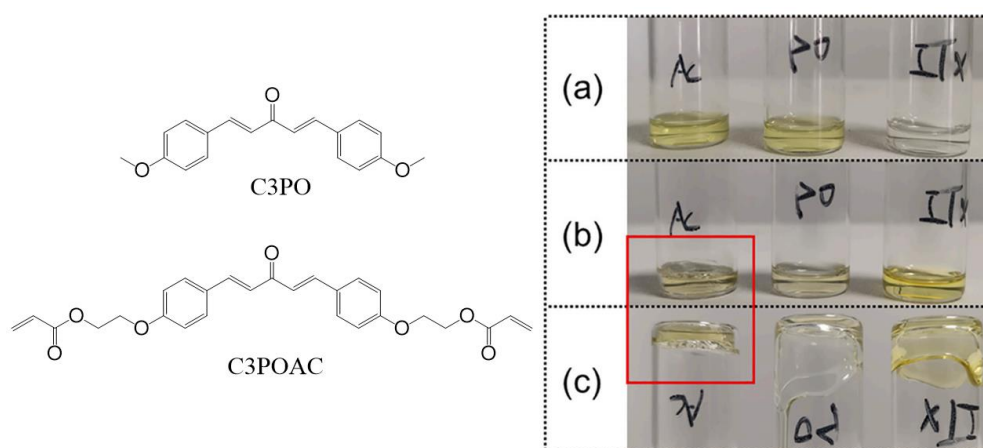


Figure 1.12. Structures of photoinitiators (left), Butyl acrylate/PI/EDB formulations (right) (a) before irradiation, (b) after irradiation by 405 nm LED, (c) after irradiation, the bottles were inverted and left to stand 10 min, Ac: C3POAC and PO: C3PO. Reproduced with permission from [149] Elsevier, Copyright (2022), (Figure A.12).

Design of macromolecular PIs can make progress in solving the leaching problem of low molecular weight PIs. Integration of small molecule PIs onto macromolecular structures can also improve solubility and compatibility of PIs in curable formulations. Polymeric PIs can contain macromolecular groups in their structures such as poly(ethylene glycol) (PEG) or poly(propylene glycol) [155-159], polystyrene [160,161], poly(amido amine) [162], poly(vinyl alcohol) [163], lignin [164], alginate [165], hyperbranched poly(ether amine) [166], hyperbranched poly(ethylene imine) or dendrimeric poly(propylene imine) [167-169], and hyperbranched polyglycerol [170,171]. Polymeric PIs can be synthesized via diverse range of reactions such as phospho-Michael addition [155], aza-Michael addition [162], esterification [156], [171], Diels-Alder reaction [157]. Copolymerization of polymerizable PIs with different monomers is also another method, these monomers can be acrylamide [172,173], siloxy silylester methacrylate [174], and coinitiator amines such as N,N-dimethylaminoethyl methacrylate [175-178] and piperazine [179,180]. Macromolecular PIs can contain polymerizable functionalities such as allyl [181], acrylate [182] or alkene [183,184].

A type II macrophotoinitiator (PVA-TX) was synthesized by incorporating thioxanthone into side chains of poly(vinyl alcohol) through acetalization reaction (Figure

1.13) [163]. PVA–TX is soluble in water and organic solvents, so photopolymerization in both organic and aqueous environment was achieved. PVA-TX contains hydrogen donating sites (hydroxyl and ether) in the polymeric backbone which are required for type II photoinitiation. Hence the synthesized PI is one-component, photopolymerization is induced even in the absence of an additional coinitiator. Polymeric and one-component nature of the PI eliminate the possible shortcomings related to low molar mass photoinitiators.

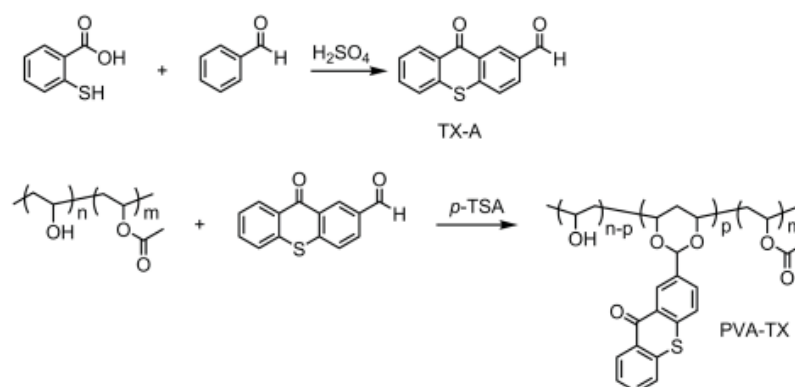


Figure 1.13. Synthesis of PVA-TX. Reproduced with permission from [163] John Wiley and Sons, Copyright (2015), (Figure A.13).

Song et al. developed a naphthalene-based macrocycle prism[5]arene ( $\text{NP}_5\text{OCH}_3$ ) photoinitiator [185]. Photoinitiation efficiency of  $\text{NP}_5\text{OCH}_3$  was analyzed for three monomers under 365 nm LED illumination (hydroxyethyl acrylate, HEA; tripropylene glycol diacrylate, TPGDA and trimethylolpropane triacrylate, TMPTA), the PI induces photopolymerization successfully (Figure 1.14a). The migration rate of  $\text{NP}_5\text{OCH}_3$  was calculated and compared to that of commercial type I (TPO) and type II (BP+EDB) PIs, the rate for  $\text{NP}_5\text{OCH}_3$  was lower than the TPO and BP+EDB due to the size of the PI (Figure 1.14b). Toxicity studies showed no significant cytotoxicity, indicating high safety of  $\text{NP}_5\text{OCH}_3$  (Figure 1.14c). Hyperfine splitting constants for both the nitrogen ( $a_{\text{N}}$ ) and the hydrogen ( $a_{\text{H}}$ ) were found to be  $a_{\text{N}} = 14.0 \text{ G}$ ,  $a_{\text{H}} = 2.17 \text{ G}$  as a result of electron paramagnetic resonance (EPR), showing the radicals are generated via homolytic cleavage (Figure 1.14d).

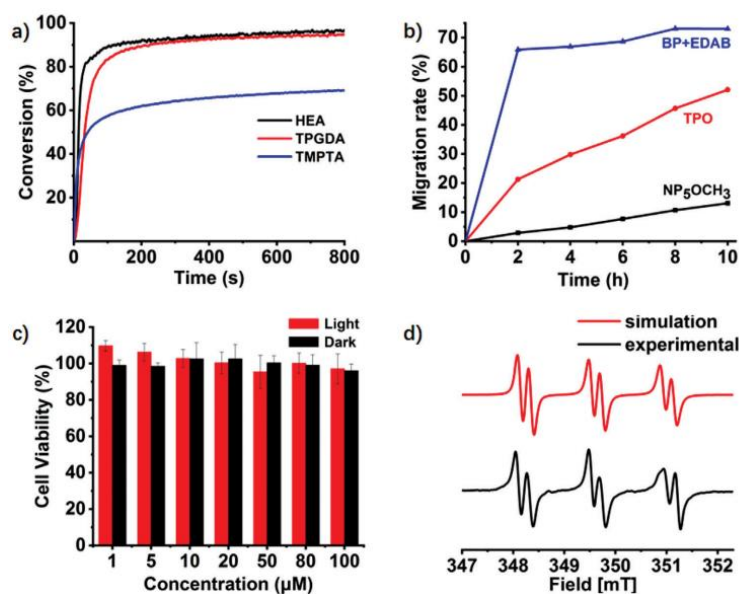


Figure 1.14. (a) Photopolymerization of HEA, TPGDA and TMPTA in the presence of NP<sub>5</sub>OCH<sub>3</sub> under 365 nm LED, (b) The migration rate of BP+EDB, TPO and NP<sub>5</sub>OCH<sub>3</sub>, (c) The cell viability under the treatment of NP<sub>5</sub>OCH<sub>3</sub> before and after 365 nm LED irradiation, (d) EPR spectra of NP<sub>5</sub>OCH<sub>3</sub> during 365 nm LED irradiation. Reproduced with permission from [185] John Wiley and Sons, Copyright (2021), (Figure A.14).

## 1.6. Anti-Oxygen Inhibition Photoinitiators

Molecular oxygen is reactive towards radicals, so oxygen inhibition is an issue for radical-mediated polymerization. Molecular oxygen is able to adopt a triplet biradical structure in its ground state, consuming initiating radicals and growing polymer radicals to produce stable peroxy radicals which are ineffective to propagate the polymerization [186,187]. Polymerization can be hindered severely depending on the oxygen concentration and film thickness. Oxygen diffuses back into the curing sample from the air–monomer interface continuously, and scavenging radicals in thin films, hence critically retarding the polymerization. The top layer in thicker films is the most affected part by the oxygen, resulting in tacky surface and impaired optical and surface properties, the lower depths of the curing formulation polymerize [188]. Oxygen inhibition can be lessened by using high intensity light source, increasing photoinitiator amount, radiation curing under inert atmosphere (e.g. nitrogen, carbon dioxide) [189], and additives [190,191]. Hydrogen donors

(DH) reduce the negative effect of oxygen in photoinitiated polymerization by donating hydrogen to peroxy radical ( $\text{ROO}\cdot$ ), therefore polymerization can be reinitiated by newly generated donor radicals ( $\text{D}\cdot$ ) (Figure 1.15) [192]. Photoinitiators can be also designed to reduce the oxygen inhibition in photoinduced polymerization [181], [193-199].

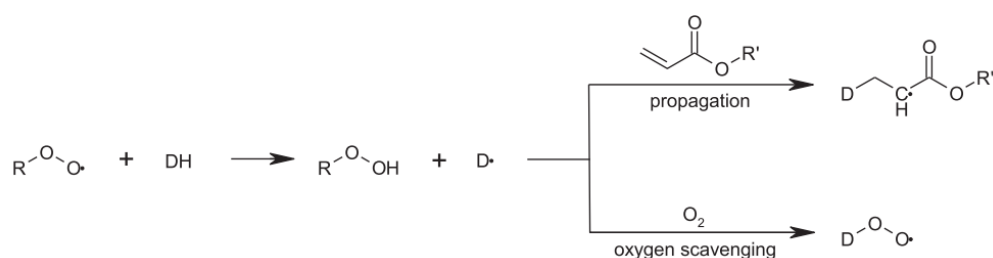


Figure 1.15. Interaction between peroxy radical and hydrogen donor, and radical reinitiation. Reproduced with permission from [192] Elsevier, Copyright (2014), (Figure A.15).

Photopolymerization of trimethylolpropane trimethacrylate (TMPTMA) was examined by type II photoinitiation under aerated media [200]. Five amino-based hydrogen donors were used in combination with TX, namely N-phenylglycine (NPG), triethylamine (TEA), triethanolamine (TEOA), 2,2'-(4-methylphenylimino)diethanol (*p*-TDEA) and N-phenyldiethanolamine (*n*-PDEA). As demonstrated in Figure 1.16a, TMPTMA reached the highest double-bond conversion value in the presence of TX/TEOA (1/2 wt%) mixture, followed by TX/TEA and TX/NPG proving the quenching of oxygen inhibition during light curing. No polymerization was observed with TX/*p*-TDEA and TX/*n*-PDEA. TEOA- and TEA-based formulations showed better conversion values than others, due to the steric hindrance caused by the aromatic groups in *p*-TDEA and *n*-PDEA. Photopolymerization was investigated with different weight ratios of TX/TEOA under air, highest conversion value was obtained with the highest amount of TEOA (2 wt%) (Figure 1.16c). Conversion efficiency of the photocuring reaction under air and nitrogen atmosphere was analyzed with different weight ratios of TX/TEOA, the conversion was affected the most when TEOA was lower in amount and the efficiency between  $\text{N}_2$  and air was insignificant with higher amounts of TEOA (Figure 1.16d).

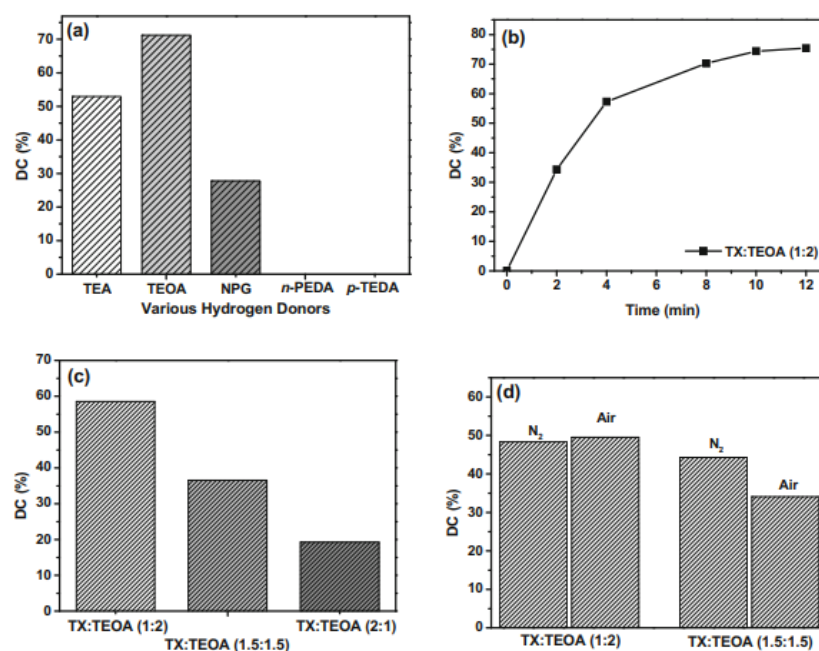


Figure 1.16. Double-bond conversion values of TMPTMA (a) in the presence of TX and various hydrogen donors at fixed weight ratios under air, (b) in the presence of TX/TEOA (1/2 wt %) under air, (c) different compositions of TX/TEOA at (1/2, 1.5/1.5, 2/1 wt%) under air, (d) different compositions of TX/TEOA (1/2, 1.5/1.5 wt%) under N<sub>2</sub> or air. Reproduced with permission from [200] Springer Nature, Copyright (2020), (Figure A.16).

A visible light, polymerizable PI based on naphthalimide and ether (ND-O-EA) was synthesized to diminish the oxygen inhibition in free radical polymerization, results were compared to ND-N-EA, camphorquinone/N-methyldiethanolamine (CQ/MDEA) and BAPO [196]. The polymerization of 1,6-hexanediol diacrylate (HDDA) was examined under air upon exposure to LED at 405 nm to evaluate the PI's ability to overcome the oxygen inhibition (Figure 1.17a). The results depicted that HDDA was successfully polymerized and there is no induction period for ND-O-EA proving its ability to overcome oxygen inhibition without using any additives unlike CQ and BAPO. Polyurethane acrylate (PUA) and HDDA were cured under air in the presence of ND-O-EA, and a fully cured polymer with a tack-free surface was achieved (Figure 1.17b).

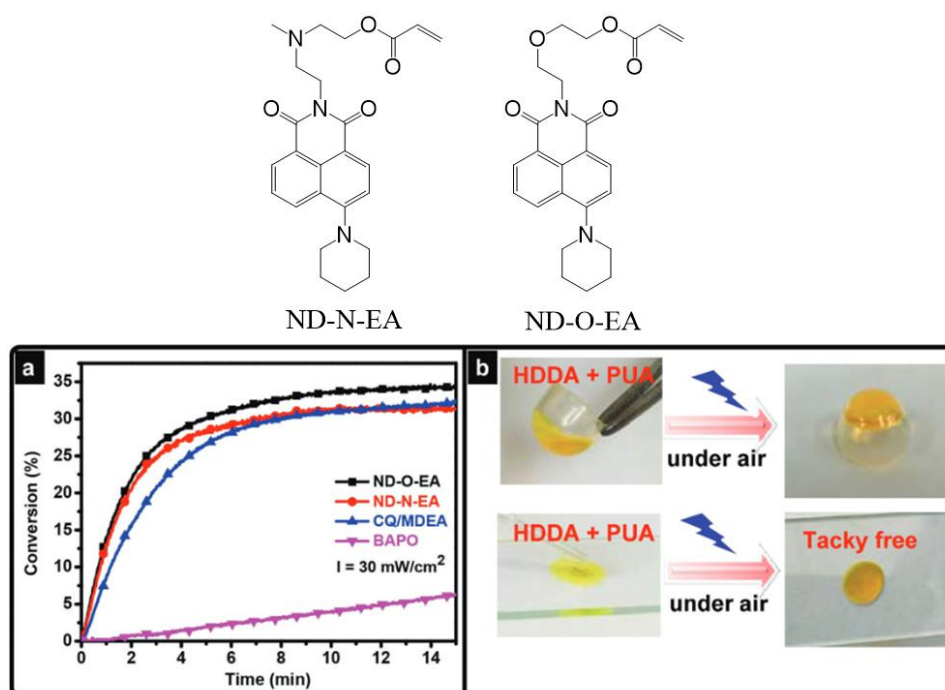


Figure 1.17. Photoinitiator structures (top figure), (a) Photopolymerization profiles of HDDA in the presence of ND-O-EA, ND-N-EA, and BAPO upon LED at 405 nm exposure and CQ/MDEA upon LED at 470 nm exposure under air, (b) the cured HDDA and PUA polymers upon LED at 405 nm exposure under air. Reproduced with permission from [196] John Wiley and Sons, Copyright (2018), (Figure A.17).

## 1.7. Monomers

Free radical photopolymerization can be performed to transform unsaturated monomers, oligomers or prepolymers to linear polymers or crosslinked networks depending on the number of unsaturation. Styrene, vinyl acetate, N-vinylpyrrolidone, vinyl isobutyl ether, meth/acrylates and maleic anhydride are some of the compounds for photocurable monomers [201]. Acrylate-based formulations are the most extensively used light-curable systems due to their high reactivity towards radicals. Higher concentration of functional groups in monomers (greater number of double bonds) raises polymerization rate leading to more dense crosslinks, quicker onset of gelation and vitrification. Freezing of the formulation at the early stages of polymerization decreases the mobility of the monomer and double bond conversion, however it can be prevented by increasing the length of spacer

group between double bonds [202]. Viscosity of the photocurable formulation is also determinant in mobility and diffusion, thus chain termination and propagation reactions are affected. For example, 2,2-bis[4-(2-hydroxymethacryloxypropoxy)phenyl]propane (Bis-GMA) is a very viscous monomer which has a low polymerization rate and conversion stemming from the restricted mobility, so viscosity of the medium is decreased via addition of reactive diluent (triethylene glycol dimethacrylate (TEGDMA)) resulting in increased mobility of the monomers, raised polymerization rate and conversion [203].

Volume shrinkage is encountered in photopolymerization due to the distance reduction between polymerizable units caused by the replacement of Van der Waals forces by shorter covalent bonds. Monomer structure affects volumetric shrinkage which in turn can harm the mechanical properties of the polymers, lower molecular weight monomers leads to greater volumetric shrinkage compared to higher molecular weight monomers [204]. Photopolymerization parameters such as PI concentration, curing time and light intensity impact the mechanical properties of light-cured methacrylate resins [205]. In general, the curing of acrylate systems is more rapid than methacrylates. The structure of monomers plays a critical role in determining the photopolymer properties and their applications. Although acrylates are widely utilized in radiation curing applications, their photopolymers exhibit mediocre mechanical properties such as low toughness and brittleness whereas methacrylate-based photopolymers demonstrate improved tensile strength and stiffness [206].

### **1.8. Irradiation Sources**

“Light” is electromagnetic radiation comprised of ultraviolet (UV), visible, infrared, X-ray, gamma-ray and radio waves [207]. For a photoinduced process to occur, emission spectrum of the light source should overlap with the absorption spectrum of photosensitive reagents. Photoinitiating systems are generally activated by UV light (200–400 nm) and visible light (400–780 nm) illumination owing to their absorption in these regions, and sometimes near-infrared (IR) light (780–1000 nm). UV light is divided into three regions: UVA (315–400 nm), UVB (280–315 nm) and UVC (200–280 nm). The spectrum of sunlight is in the near-UV-visible wavelength range, and it is the first light source of photoinduced polymerization. In 1845, styrene was polymerized upon exposure to sunlight which is one

of the first examples of light-induced polymerization of vinyl monomers [208]. Since then, there has been huge development in artificial light sources such as xenon (Xe) lamps, mercury (Hg) arc lamps, xenon-mercury lamps, microwave lamps, excimer lamps, light emitting diodes (LEDs) and laser sources [7].

Different light intensities with variable wavelengths can be applied based on the light source. High intensity monochromatic irradiation can be delivered by laser sources, and high intensity polychromatic light can be acquired with Xe and Hg lamps. Hg arc lamps emit in the range of 280 – 445 nm and 530 – 600 nm, more intensely at specific wavelengths of 254, 313, 366, 405, 435, 546, and 579 nm (Figure 1.18a) [7]. Low intensity irradiation ( $<10$  mW/cm<sup>2</sup>) can be generated from household light sources such as fluorescent lamps, halogen lamps and household LED bulbs or can be generated from sun, a green light source, in which the intensity is influenced by the weather and location [209]. LEDs emit quasi-monochromatic light (e.g. UV at 365 nm, near-UV at 385 and 395 nm, violet at 405 nm) with a relatively narrow bandwidth (20 – 70 nm) in which the intensity is approximately 10 – 100 mW/cm<sup>-2</sup> [22]. Typical emission spectra of Hg-Xe lamp, Xe lamp, halogen lamps and laser diodes (performing at 405, 457, 473, 532, 635 and 808 nm) are exhibited in Figure 1.18 [209].

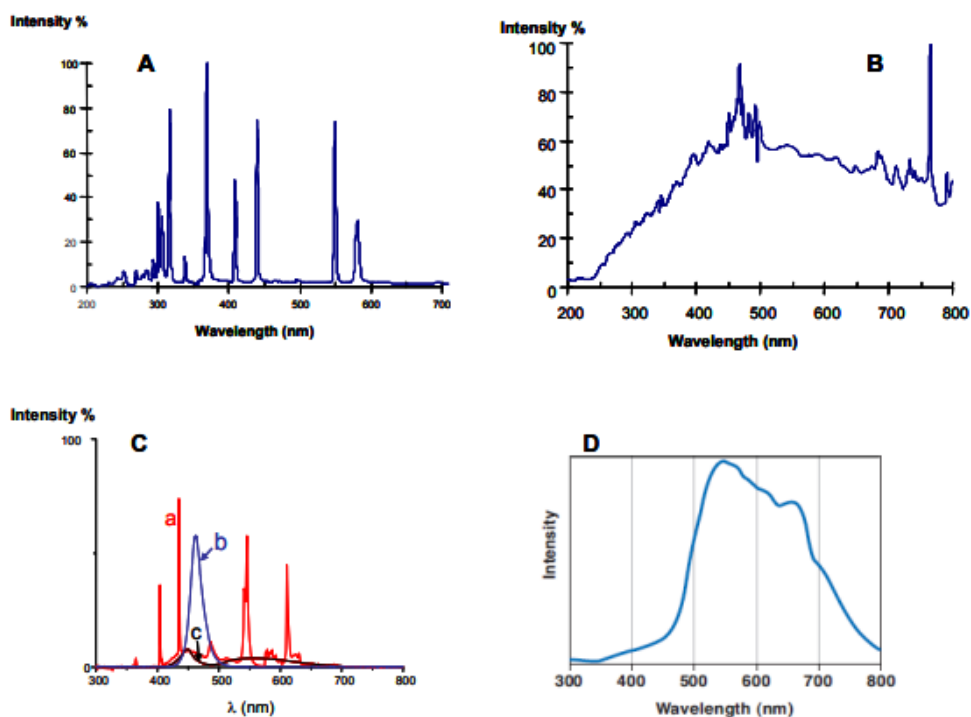


Figure 1.18. Emission spectra of (a) Hg-Xe lamp, (b) Xe lamp, (c) a: fluorescent bulb, b: blue LED bulb, c: white LED bulb, (d) Laser diodes can perform, e.g., at 405, 457, 473, 532, 635 and 808 nm [209].

In photopolymerization, LED is a widely used light source due to its advantageous features which are low energy consumption, low heat release, high lifetimes, no ozone release, less UV emission, easy handling and low cost. LEDs are desirable in biomedical applications in which mild irradiation conditions are necessary. Although more intense illumination can be provided by Hg and Hg-Xe lamps, their intrinsic structures (presence of harmful Hg), more heat generation and presence of comparatively more dangerous UV rays leads to LEDs being preferred.

## 2. OBJECTIVES AND SCOPE

The purpose of this study was to produce and assess novel photoinitiators with desirable features: visible light activity, water solubility, high photoinitiation efficiency, biocompatibility, compatibility with the curable formulation and migration stability. These features will contribute to make photopolymerization processes more environmentally friendly and safer to use. To obtain these beneficial properties, polymerizable and macromolecular photoinitiators for free radical photopolymerization were developed. Macromolecular or polymerizable nature of photoinitiators enable the migration stability, and functional groups on the backbone and at the side chain can provide water solubility, compatibility, biocompatibility and visible light operation. The photochemical and photophysical characteristics of the synthesized photoinitiators were analyzed.

Various polymeric/hyperbranched/oligomeric backbones (poly(ethylene imine), oligo(amido amine) and poly(ethylene glycol)), polymerizable groups (meth/acrylate), functional groups (bis/phosphonate) and commercial photoinitiators (thioxanthone, benzophenone and Irgacure 2959) were combined to obtain the desired properties mentioned above.

In the first part, four hyperbranched and visible light-activated thioxanthone derivatives (PBT-2, PDT-2, PBT-5 and PDT-5) based on bis/phosphonate functionalized poly(ethylene imine) were described. The second part reports synthesis of the two oligomeric, water soluble photoinitiators (OAA-B and OAA-BP) by integration of benzophenone and/or phosphonate functionalities onto oligo(amido amine). These PIs can operate under visible light stemming from their charge transfer complex formation ability through the amines in their structure. In the third part, a water soluble, thioxanthone functionalized and polymerizable poly( $\beta$ -amino ester) based on poly(ethylene glycol), p(PEGDA575-TX), was depicted. In the last part, the syntheses and evaluations of one novel cyclopolymerizable (CTI) and one cyclopolymeric photoinitiators were performed which are based on ether dimer of *tert*-butyl  $\alpha$ -hydroxymethacrylate, combining the high reactivity of Irgacure 2959 with advantageous properties of cyclopolymerizable and/or cyclic structures.

### 3. PHOTOINITIATING SYSTEMS BASED ON POLY(ETHYLENE IMINE) FOR MICHAEL ADDITION AND FREE RADICAL PHOTOPOLYMERIZATION

This chapter is published as: Gencoglu, T., T.N. Eren, J. Lalevée, and D. Avci, “Photoinitiating Systems Based on Poly(ethylene imine) for Michael Addition and Free Radical Photopolymerization”, *Journal of Photochemistry and Photobiology A: Chemistry*, Vol. 404, p. 112959, 2021.

#### 3.1. Introduction

In this chapter, novel multifunctional hyperbranched photoinitiators were synthesized which can achieve FRP by forming CTC with Iod and dual curing by aza-Michael addition and FRP. The synthesized initiators were short chain branched poly(ethylene imine) (PEI,  $M_n = 1800$  g/mol) functionalized with (bis)phosphonate and the photosensitizer group TX. (Bis)phosphonate functionality was integrated to increase the biocompatibility of PIs and to raise the solubility of PIs in the monomers. Amino groups are also beneficial to reduce or eliminate the oxygen inhibition during photopolymerization.

Dual curing process involves two stages in which the usual choices are Michael addition for the first stage and methacrylate photopolymerization for the second. In the Michael addition stage, di- or triacrylates and di- or triamines can be reacted to obtain a polymer. The remaining double bonds are then further polymerized by light-induced curing to increase the crosslink density [210-213]. This approach obviously is quite flexible due to the use of two polymerization steps, and can lead to interpenetrating polymer networks (IPNs) [214,215]. In this work, acrylate/methacrylate systems were designed to demonstrate the potential of the dual curing behavior of the PI systems to obtain interpenetrating networks. The first step of dual curing is aza-Michael addition which takes place between primary and secondary amines on PIs coming from PEI and acrylate monomer, and FRP due to CTC formation from the interaction of PI with Iod without light. The second step is the photopolymerization of remaining methacrylate and acrylate monomers by FRP due to type

II photoinitiation and CTC under visible light. The photochemical properties of the novel photoinitiators were also investigated by electron-spin resonance-spin trapping, fluorescence and steady-state photolysis techniques.

## 3.2. Experimental Section

### 3.2.1. Materials

Branched PEI ( $M_n = 1800$  g/mol) was purchased from Polysciences Inc. 2-acryloyloxy thioxanthone (ATX) and tetraethyl vinylidene bisphosphonate (TEVBP) were synthesized according to the literature procedures [216,217]. Diethyl vinylphosphonate (DVP), ethyl 4-(dimethylamino)benzoate (EDB), 2-hydroxyethyl methacrylate (HEMA), poly(ethylene glycol) diacrylate (PEGDA,  $M_n = 575$  g/mol), bisphenol A glycidyl methacrylate (Bis-GMA), triethylene glycol dimethacrylate (TEGDMA) and the other reagents and solvents were purchased from Sigma-Aldrich or Alfa Aesar and used as received without further purification. Bis-(4-tert-butylphenyl)-iodonium hexafluorophosphate (SpeedCure938 or Iod) was obtained from Lambson Ltd.

### 3.2.2. Methods

$^1\text{H-NMR}$  spectra were recorded on a Varian Gemini (400 MHz) spectrometer with deuterated chloroform ( $\text{CDCl}_3$ ) as a solvent, and tetramethylsilane as an internal standard. A Nicolet 6700 FTIR spectrophotometer was used for recording IR spectra. The UV-vis spectra were obtained using a Carry 3 UV-vis spectrophotometer from Varian. Differential scanning calorimetry (DSC) (TA Instruments Q100) was used to determine the glass transition temperatures ( $T_g$ ) of the polymers. All samples (10-20 mg) were sealed in aluminium pans and heated under nitrogen atmosphere from  $-50$  °C to  $250$  °C with a scanning rate of  $10$  °C  $\text{min}^{-1}$ . Thermogravimetric analyses (TGA) were performed using a Perkin Elmer STA 6000 machine. Samples were heated up to  $700$  °C at a rate of  $10$  °C/min under nitrogen atmosphere.

### 3.2.3. Synthesis of the Photoinitiators

3.2.3.1. Synthesis of PDT-2 and PDT-5. Two TX and phosphonate-functionalized PEIs were prepared by reacting PEI with DVP and ATX at mole ratios PEI:DVP:ATX of 1:2:2 and 1:5:5, denoted as PDT-2 and PDT-5, respectively. For example, for synthesis of PDT-2, PEI (328.1 mg, 0.18 mmol) and DVP (59.8 mg, 0.36 mmol) were dissolved in DMF (1.51 mL) and mixed at room temperature for 24 h. ATX (102.8 mg, 0.36 mmol) and 1.51 mL of DMF were added to the reaction mixture and stirred for 24 h at room temperature. The mixture was filtered and excess DMF was evaporated under vacuum. The residue was precipitated in excess diethyl ether to obtain PDT-2 as an orange viscous liquid in 47% yield. PDT-5 was obtained as an orange viscous liquid in 39% yield.

<sup>1</sup>H-NMR for PDT-2 (400 MHz, CDCl<sub>3</sub>, δ): 1.24 (6H, CH<sub>3</sub>-CH<sub>2</sub>-O), 2.60 (160 H, N-CH<sub>2</sub>-CH<sub>2</sub>-N, NH-CH<sub>2</sub>-CH<sub>2</sub>-C=O), 4.01 (4H, CH<sub>3</sub>-CH<sub>2</sub>-O), 7.05-8.55 (7H, aromatic hydrogens) ppm.

FTIR for PDT-2 (ATR): 960, 1027 (P-O-C), 1261 (P=O), 1585 (N-H), 1653 (C=O), 2828 & 2941 (C-H), 3100-3500 (N-H) cm<sup>-1</sup>.

<sup>1</sup>H-NMR for PDT-5 (400 MHz, CDCl<sub>3</sub>, δ): 1.31 (6H, CH<sub>3</sub>-CH<sub>2</sub>-O), 2.60 (160 H, N-CH<sub>2</sub>-CH<sub>2</sub>-N, NH-CH<sub>2</sub>-CH<sub>2</sub>-C=O), 4.07 (4H, CH<sub>3</sub>-CH<sub>2</sub>-O), 7.05-8.55 (7H, aromatic hydrogens) ppm.

FTIR for PDT-5 (ATR): 966, 1020 (P-O-C), 1243 (P=O), 1590 (N-H), 1632 (C=O), 2823 & 2914 (C-H), 3100-3500 (N-H) cm<sup>-1</sup>.

3.2.3.2. Synthesis of PBT-2 and PBT-5. Two TX and bisphosphonate-functionalized PEIs were prepared by reacting PEI with TEVBP and ATX at mole ratios PEI:TEVBP:ATX of 1:2:2 and 1:5:5, denoted as PBT-2 and PBT-5, respectively. For example, for synthesis of PBT-2, PEI (300.1 mg, 0.17 mmol) and TEVBP (100.1 mg, 0.34 mmol) were dissolved in DMF (1.34 mL) and mixed at room temperature for 24 h. ATX (94.01 mg, 0.34 mmol) and 1.34 mL of DMF were added to the reaction mixture and stirred for 24 h at room temperature. The mixture was filtered and excess DMF was evaporated under vacuum. The residue was precipitated in excess diethyl ether to obtain PBT-2 as an orange viscous liquid in 42% yield. PBT-5 was also obtained as an orange viscous liquid in 35% yield.

$^1\text{H-NMR}$  for PBT-2 (400 MHz,  $\text{CDCl}_3$ ,  $\delta$ ): 1.28 (12H,  $\text{CH}_3\text{-CH}_2\text{-O}$ ), 2.56 (161H,  $\text{N-CH}_2\text{-CH}_2\text{-N}$ ,  $\text{NH-CH}_2\text{-CH}_2\text{-C=O}$ ,  $\text{P-CH-P}$ ), 4.09 (8H,  $\text{CH}_3\text{-CH}_2\text{-O}$ ), 7.10-8.55 (7H, aromatic hydrogens) ppm.

FTIR for PBT-2 (ATR): 969, 1022 (P-O-C), 1240 (P=O), 1559 (N-H), 1652 (C=O), 2825 & 2942 (C-H), 3100-3500 (N-H)  $\text{cm}^{-1}$ .

$^1\text{H-NMR}$  for PBT-5 (400 MHz,  $\text{CDCl}_3$ ,  $\delta$ ): 1.32 (12H,  $\text{CH}_3\text{-CH}_2\text{-O}$ ), 2.57 (161H,  $\text{N-CH}_2\text{-CH}_2\text{-N}$ ,  $\text{NH-CH}_2\text{-CH}_2\text{-C=O}$ ,  $\text{P-CH-P}$ ), 4.16 (8H,  $\text{CH}_3\text{-CH}_2\text{-O}$ ), 7.15-8.55 (7H, aromatic hydrogens) ppm.

FTIR for PBT-5 (ATR): 970, 1021 (P-O-C), 1237 (P=O), 1590 (N-H), 1652 (C=O), 2824 & 2965 (C-H), 3100-3500 (N-H)  $\text{cm}^{-1}$ .

### 3.2.4. Photochemical Analysis

3.2.4.1. UV-vis Spectroscopy Experiments. UV-vis measurements of the PIs were carried out in methanol (MeOH) or chloroform ( $\text{CHCl}_3$ ) using Carry 3 UV-vis spectrophotometer (Varian). For steady state photolysis experiments, PIs were irradiated with LED@375 nm or 385 nm in the presence and absence of additives (Iod or EDB) in methanol and  $\text{CHCl}_3$ :toluene (10:90 v/v) mixture. Their UV-vis spectra were recorded at different irradiation times.

3.2.4.2. Fluorescence Experiments. Fluorescence properties of the PIs were investigated in methanol using a spectrofluorometer (JASCO FP-750). The interaction rate constants between the studied PI and the quencher (Iod, EDB) were derived from the Stern-Volmer equation

$$I_0/I_Q = 1 + k_q\tau_0[\text{quencher}] \quad (3.1)$$

$$k_q = K_{sv}/\tau_0, \quad (3.2)$$

where  $I_0$  and  $I_Q$  symbolize the fluorescence intensity of the photoinitiator in the absence and presence of the quencher, respectively and  $\tau_0$  is the singlet excited state lifetime of the PI in the absence of the quencher.  $k_q$  represents the quenching rate, and  $K_{sv}$  indicates Stern-Volmer constant. The first singlet excited-state energy ( $E_{S1}$ ) was determined from the crossing point of the absorption and fluorescence spectra [218].

3.2.4.3. Laser Flash Photolysis (LFP) Experiments. Nanosecond laser flash photolysis (LFP) experiments were carried out using a Q-switched nanosecond Nd/YAG laser ( $\lambda_{\text{exc}} = 355$  nm, 9 ns pulses; energy reduced down to 10 mJ; minilite Continuum) and the analyzing system (for absorption measurements) consisted of a ceramic xenon lamp, a monochromator, a fast photomultiplier and a transient digitizer (Luzchem LFP 212) [219].

3.2.4.4. ESR Spin Trapping (ESR-ST) Experiments. The ESR-ST experiments were performed using a Bruker EMX-plus spectrometer. The radicals were generated at room temperature upon irradiation by LED at 420 nm under nitrogen in  $\text{CHCl}_3$ :toluene (10:90 v/v) solution in the presence of Iod. The radicals generated were trapped by N-tert-butyl- $\alpha$ -phenylnitron (PBN) according to a procedure described in the literature [220]. The ESR spectra simulations were carried out using the WINSIM software [221].

### **3.2.5. Photopolymerization**

The photosensitive formulations, HEMA/PEGDA/PI/Iod, HEMA/Bis-GMA/PI/Iod and HEMA/TEGDMA/PI/Iod were prepared by first mixing PI (1 wt%, with respect to TX moiety) with the monomers and then adding Iod (2 wt%). The polymerization of the formulations were monitored by real-time Fourier Transform Infrared (RT-FTIR) spectroscopy and photo-DSC.

3.2.5.1. RT-FTIR Spectroscopy. JASCO 4100 RT-FTIR spectrometer was used to follow the (meth)acrylate function conversions versus time for polymerizations of 1.4 mm thick samples. In one step curing process, the formulations were irradiated by LED@405 nm under air for 10 min at room temperature. In the dual-curing process, the aza-Michael addition reaction was allowed to proceed for 10-20 minutes, and then 10 minutes of irradiation by LED@405 nm or 320-500 nm light sources under air or laminated conditions was applied to monitor the photopolymerization reaction at room temperature. The photopolymerizations were monitored by following the (meth)acrylate C=C double bond peaks at around 6170 or 1637  $\text{cm}^{-1}$ .

3.2.5.2. Photo-DSC. TA Instruments DSC 250 differential photocalorimeter using an Omnicure 2000 mercury lamp light source with a 320-500 nm filter was used for

photopolymerization experiments. Formulations (3-4 mg) were exposed to irradiation at 30 °C under nitrogen for 5 min. The heat flow was monitored as a function of time with DSC. The polymerization rate was calculated by using the formula

$$\text{Rate} = \frac{(Q/s)M}{n(\Delta H_p)m}, \quad (3.3)$$

where  $Q/s$  is the heat flow per second,  $M$  the molar mass of the monomer,  $n$  the number of double bonds per monomer molecule,  $\Delta H_p$  the heat of reaction evolved and  $m$  the mass of monomer in the sample. The theoretical heat for the total conversion of an acrylate and methacrylate double bonds are 86 kJ/mol and 55 kJ/mol.

### 3.3. Results and Discussion

#### 3.3.1. Synthesis and Characterization of Photoinitiators

Poly(ethylene imine) (PEI) is a water soluble polymer with linear or branched forms. In this study, a branched PEI ( $M_n = 1800$  g/mol) containing primary, secondary and tertiary amino groups at approximately 10:9:6 ratios was used to prepare novel PIs. Four PEI-based PIs functionalized with TX and phosphonate (P) or bisphosphonate (BP) were synthesized in two steps (Figure 3.1). In the first step, PEI was functionalized with DVP or TEVBP via an aza-Michael addition reaction in DMF at room temperature. Then the product was reacted with acrylate functionalized TX (ATX) through again an aza-Michael addition reaction under the same conditions, yielding a highly soluble PI. (If unfunctionalized PEI is reacted with ATX the product precipitates immediately from DMF. The precipitate is insoluble in organic solvents, and is probably highly-substituted PEI). In general, acrylates are the most reactive in aza-Michael reactions among  $\alpha, \beta$ -unsaturated compounds [222]. Therefore, ATX reacts faster with PEI compared to DVP. Two different initial mol ratios of PEI:DVP/TEVBP:ATX (1:2:2 and 1:5:5) were used for the synthesis of PIs (Table 3.1). Incorporation of TEVBP is more efficient than for DVP, due to TEVBP with its two electron withdrawing phosphonate groups being better Michael acceptor than DVP. The PIs were purified by precipitation into diethyl ether in which DVP, TEVBP and ATX are soluble and the products were obtained as orange oils in 35-47 % yields.

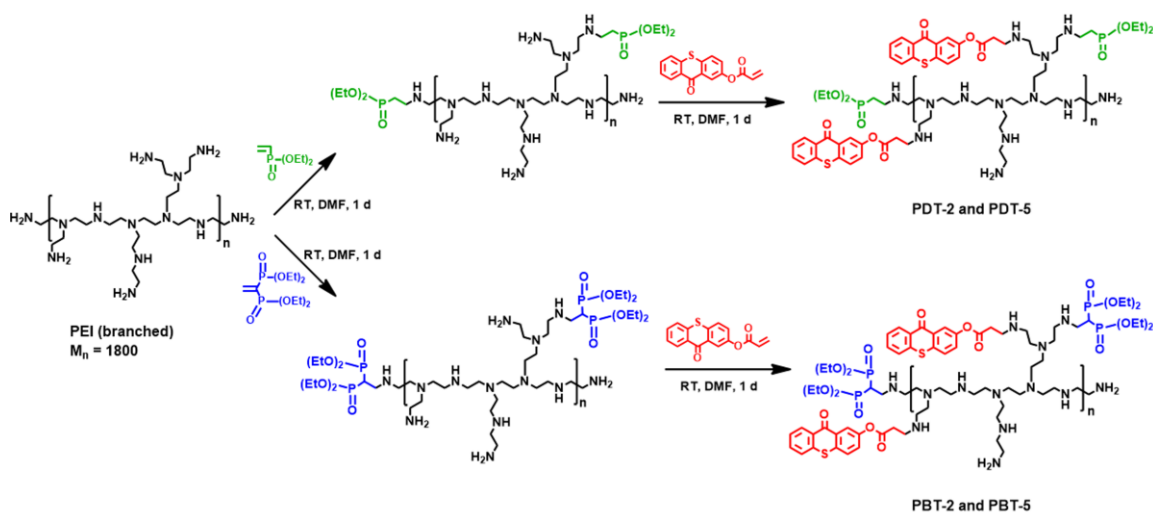


Figure 3.1. The synthesis pathway of PIs.

Table 3.1. Compositions of the PIs, <sup>a</sup>Calculated from <sup>1</sup>H NMR spectra.

PI	PEI:DVP/TEVBP:ATX in feed (mol)	PEI:DVP/TEVBP:ATX in PI <sup>a</sup> (mol)
PDT-2	1:2:2	1:0.64:1.10
PDT-5	1:5:5	1:2.09:3.72
PBT-2	1:2:2	1:1.04:1.07
PBT-5	1:5:5	1:3.05:4.85

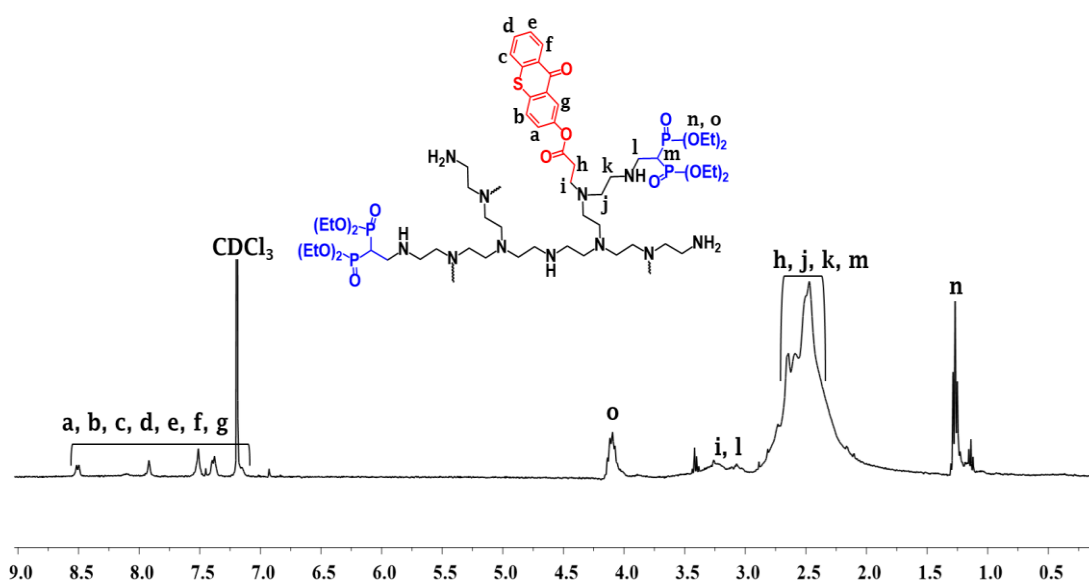


Figure 3.2.  $^1\text{H}$ -NMR spectrum of PBT-2.

The structures of the PIs were confirmed by  $^1\text{H}$ -NMR and FTIR spectroscopies.  $^1\text{H}$  NMR spectra of all PIs show the aromatic protons of TX between 7.1–8.6 ppm (Figure 3.2). The peaks at 1.24/1.28 and 4.01/4.09 ppm are ascribed to the methyl and methylene protons of phosphonate/bisphosphonate groups. The amounts of TX groups of PIs were calculated by integrating aromatic protons with respect to PEI protons at 2.2–2.9 ppm, and (bis)phosphonate amounts by integrating methyl protons with respect to PEI protons (Table 3.1). The FTIR spectra of PIs show strong peaks at around 1650 (C–O), 1230 (P–O), 1020 and 960  $\text{cm}^{-1}$  (P–O–C) corresponding to both TX and phosphonate/bisphosphonate functionalities. The intensities of these peaks are increasing from PBT-2/PDT-2 to PBT-5/PDT-5 with an increase in TX and (bis)phosphonate functionality, as expected (Figure 3.3). Also a lower N–H peak intensity in PBT-5 and PDT-5 compared to PBT-2 and PDT-2 means a higher substitution of the same functionalities.

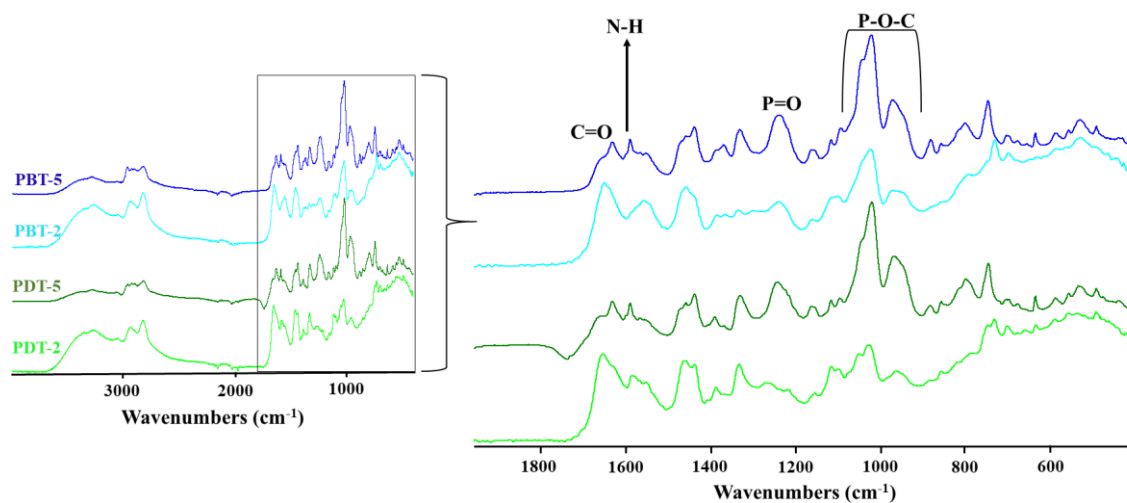


Figure 3.3. FTIR spectra of PIs.

### 3.3.2. Light Absorption and Emission Properties

Absorption characteristics of the synthesized PIs were analyzed by UV–vis spectroscopy (Figure 3.4). All PIs showed similar absorption maxima ( $\lambda_{\max}$ ) at 401 nm ( $n-\pi^*$  transition) hence a strong bathochromic shift of 21 nm compared to the reference TX ( $\lambda_{\max} = 380$  nm). This shift can be explained by the high concentration of electron donating amine groups on PEI. The synthesized PIs are convenient for the near UV light sources or visible LEDs used in this work (e.g., @375 and @405 nm).

Luminescence properties of PDT-5 and PBT-5 were investigated by a spectrofluorometer after excitation with a wavelength of 437 nm. The PIs are found to be fluorescent which is expected due to electron donating amine and electron accepting TX functionalities in their structures. The maximum emission wavelength is around 480 nm (Figure 3.4b, Figure 3.4c). The first singlet excited energies ( $E_{S1}$ ) were calculated as 2.84 eV for both PIs from the crossing point of their absorption and fluorescence spectra. Singlet state lifetimes were found to be 7.7 ns from fluorescence lifetime measurements (Figure 3.5).

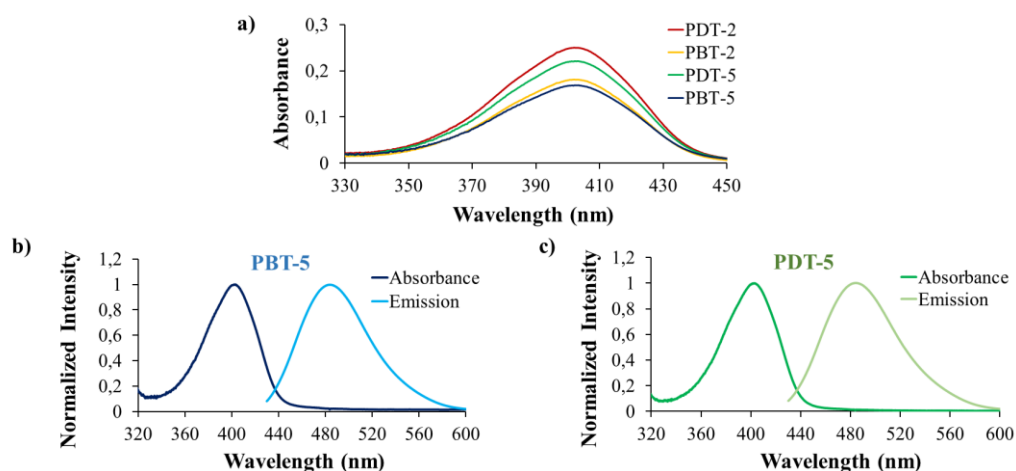


Figure 3.4. (a) UV–vis absorption of PDT-2, PBT-2, PDT-5, PBT-5 ( $3.5 \times 10^{-5}$  M,  $4.1 \times 10^{-5}$  M,  $1.3 \times 10^{-5}$  M,  $1.7 \times 10^{-5}$  M);  $E_{S1}$  determination for (b) PBT-5 and (c) PDT-5.

Solvent: MeOH.

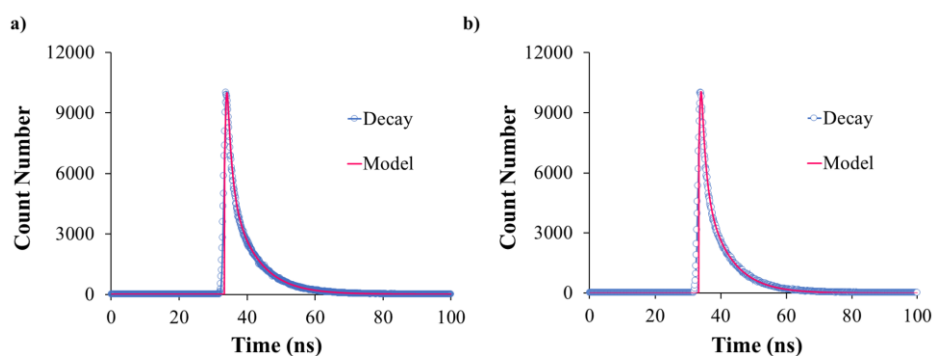


Figure 3.5. Fluorescence lifetime measurements of (a) PBT-5 and (b) PDT-5.

### 3.3.3. Photochemical Mechanisms

In order to understand the photochemical mechanisms of the synthesized PIs steady-state photolysis, fluorescent quenching, laser flash photolysis and ESR experiments were performed. Photolysis studies of the synthesized PIs were performed for PBT's under four different conditions: PBT-5, PBT-5/EDB, PBT-5/Iod, PBT-2/Iod after irradiation by the LED at 375 or 385 nm. UV-vis spectra were used to monitor decay of the absorption at 401 nm (Figure 3.6). It is observed that PBT-5 does not photolyze without additives and with

cointiator amine EDB, however it photolyzes in the presence of Iod. These results indicate that the synthesized PIs do not form complexes with amines in their structures or with EDB, however they form complexes with Iod. These results stem from the fluorescent nature of the PIs and the reactivity of this excited state.

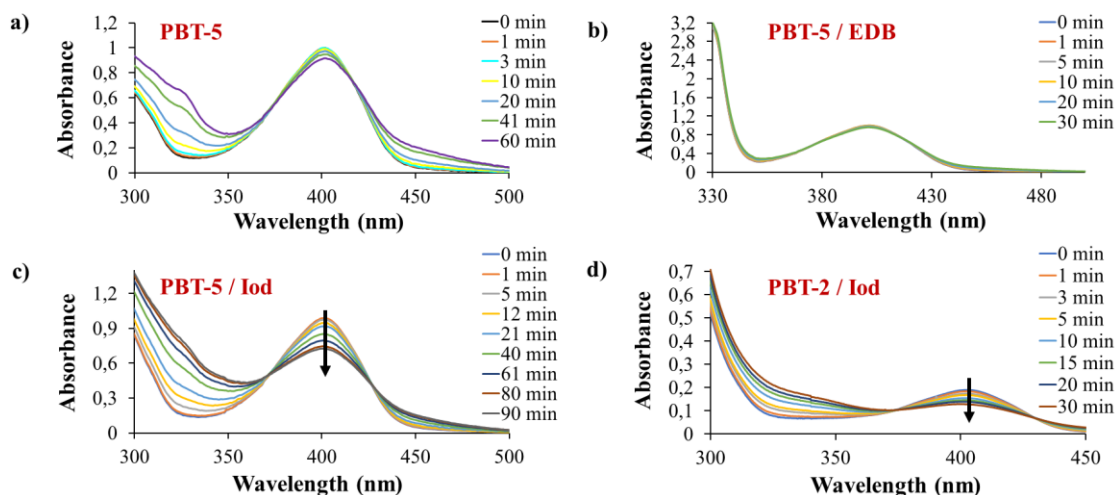


Figure 3.6. Photolysis of PIs in MeOH (a) PBT-5 ( $4.8 \times 10^{-5}$  M), (b) PBT-5/EDB ( $4.8 \times 10^{-5}$  M/ $1 \times 10^{-3}$  M), (c) PBT-5/Iod ( $4.8 \times 10^{-5}$  M/ $1 \times 10^{-3}$  M) by LED at 385 nm; (d) PBT-2/Iod ( $3.5 \times 10^{-5}$  M/ $3.5 \times 10^{-3}$  M) by LED at 375 nm.

Recently, it was observed that amine compounds (donor) and iodonium salt (acceptor) form CTC systems for radical and cationic polymerizations [82], [223]. Therefore, the synthesized PIs with different types (primary, secondary and tertiary) of amine moieties were expected to form CTCs in combination with Iod. However, no change in the absorption features, a shift of the absorption band to the visible range or a new peak, was observed for the mixture of PDT-2/Iod, indicating no formation of CTC in methanol i.e. CTC required low polarity solvent to enhance the interaction between donor and acceptor partners. Therefore, to prove the presence of CTC, photolysis study was also performed in a solvent mixture with a lower polarity ( $\text{CHCl}_3$ :toluene 10:90 v/v) than methanol. As shown in Figure 3.7a, a new peak appeared around 440 nm confirming the interaction between the amines in PI and Iod. Also, color of the solution became brighter yellow when Iod was added to the solution. The photolysis of CTC for different time intervals resulted in a significant decrease of the absorbance at 440 nm upon exposure to light, indicating bleaching of the

CTC. Another example of the CTC formation is indicated for the mixture of PDT-5/Iod in  $\text{CHCl}_3$  (Figure 3.7b). The absorbance is shifted to longer wavelengths, thus covering a greater part of the visible region.

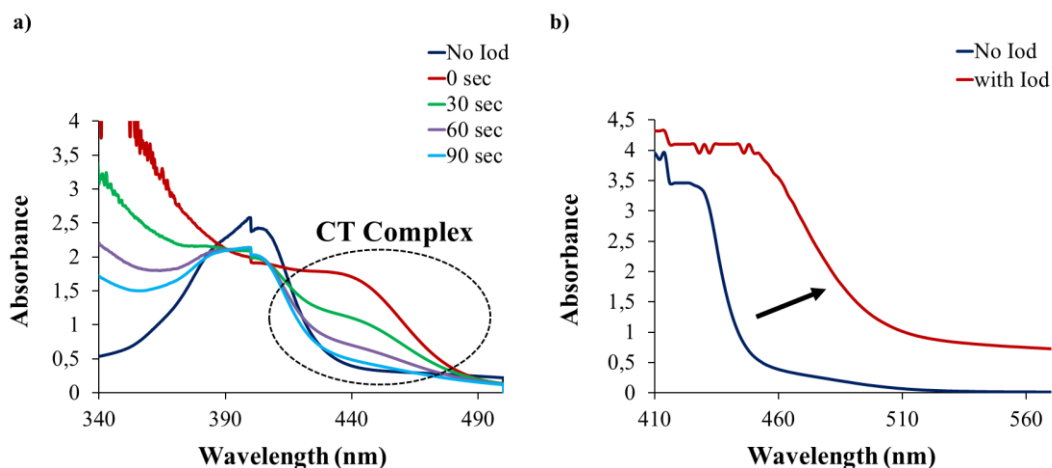


Figure 3.7. The CTC formation of (a) PDT-2/Iod ( $4.7 \times 10^{-4} \text{ M}/2.1 \times 10^{-3} \text{ M}$ ) in  $\text{CHCl}_3$ :toluene (10:90 v:v) and its photolysis (light source: 375 nm LED), (b) PDT-5/Iod ( $4.7 \times 10^{-4} \text{ M}/2.1 \times 10^{-3} \text{ M}$ ) in  $\text{CHCl}_3$ .

Fluorescence is an intramolecular deactivation (quenching) process for a singlet excited state. An intermolecular deactivation process or fluorescence quenching can be performed to investigate the singlet excited state reactivities in which the presence of another chemical species (Iod or EDB) can accelerate the decay rate of the singlet excited state. Fluorescence quenching of PBT-5 was performed with Iod and EDB at an excitation wavelength of 403 nm, and it was observed that both of the quenchers interact with photoinitiators more strongly in higher concentrations (Figure 3.8). Stern-Volmer plots exhibited good linearity ( $R^2 = 0.99$ ). The Stern-Volmer constants,  $K_{sv}$ , calculated from the slope were found to be  $72.28 \text{ M}^{-1}$  and  $32.20 \text{ M}^{-1}$  for PBT-5/EDB and PBT-5/Iod respectively (Figure 3.8c). These results depict that EDB is a more efficient quencher than Iod based on the higher  $K_{sv}$ . Quenching rates,  $k_q$ , were calculated from equation 3.2, and found to be  $9.39 \times 10^9 \text{ s}^{-1} \text{ M}^{-1}$  and  $4.18 \times 10^9 \text{ s}^{-1} \text{ M}^{-1}$  for PBT-5/EDB and PBT-5/Iod respectively.

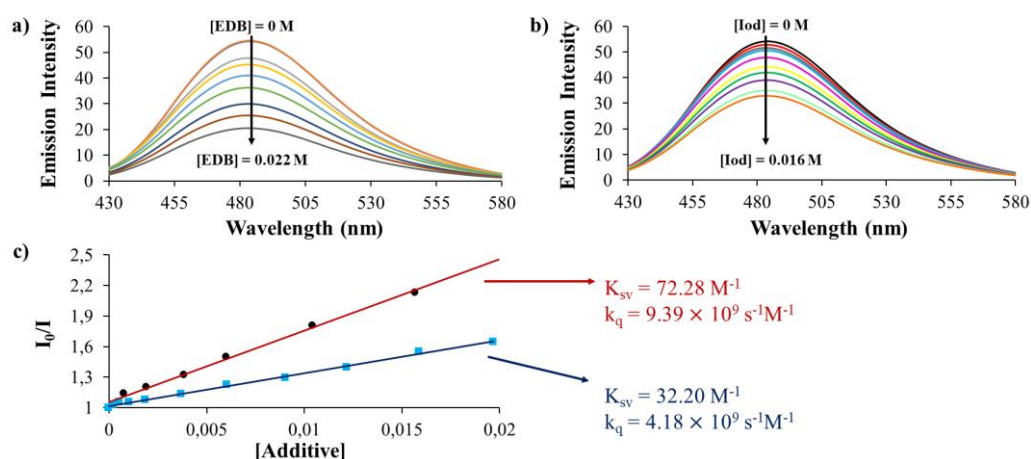


Figure 3.8. Fluorescence quenching of PBT-5 ( $1.4 \times 10^{-5} \text{ M}$ ) in MeOH with additives at different concentrations ( $\lambda_{\text{exc}} = 403 \text{ nm}$ ). (a) EDB, (b) Iod, (c) Stern-Volmer plots (blue line: PBT-5/Iod, red line: PBT-5/EDB).

Generally, type II photoinitiators form complexes with amines in the triplet excited state. The synthesized photoinitiators show very slow bleaching without additives (Figure 3.6a), and don't photolyze in the presence of EDB (Figure 3.6b). However, the PIs show fast photobleaching in the presence of Iod. So LFP analysis was performed to investigate the excited state characteristics. The results (Figure 3.9) show that the PIs have a singlet state, but no triplet state, hence no singlet-triplet intersystem crossing. Hence the PIs cannot undergo photoreduction with amines, but they can undergo photooxidation with Iod. The fluorescence of the PIs is consistent with this result. In order to characterize the radicals formed, ESR-ST measurements were performed for PDT-2/Iod mixture in  $\text{CHCl}_3$ :toluene (10:90 v/v) under nitrogen and in the presence of a spin-trap agent, PBN (Figure 3.10). In the control experiment (no irradiation), formation of an  $\text{Ar}\cdot/\text{PBN}$  radical adduct was detected. The corresponding spectrum was simulated with the hyperfine coupling constants,  $hfc$ , ( $a_N = 13.7 \text{ G}$ ;  $a_H = 1.9 \text{ G}$ ) in full agreement with the reference values [221]. When the analysis was performed under 420 nm LED (40 s irradiation), the formation of phenyl radicals was again detected, confirmed by the  $hfc$  ( $a_N = 13.8 \text{ G}$ ;  $a_H = 1.8 \text{ G}$ ).

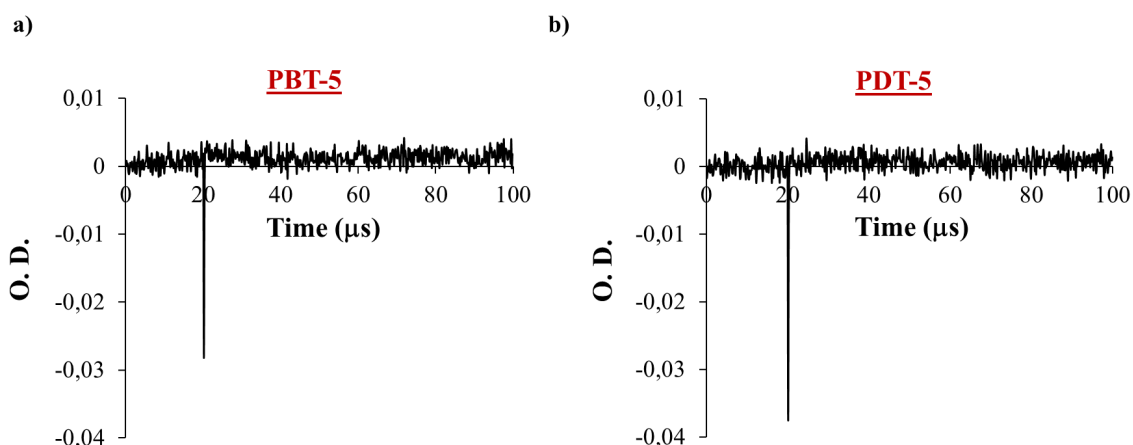


Figure 3.9. LFP results of (a) PBT-5 and (b) PDT-5 excitation at 355 nm. The laser excitation (nanosecond pulse) arrived for  $t = 20 \mu\text{s}$ .

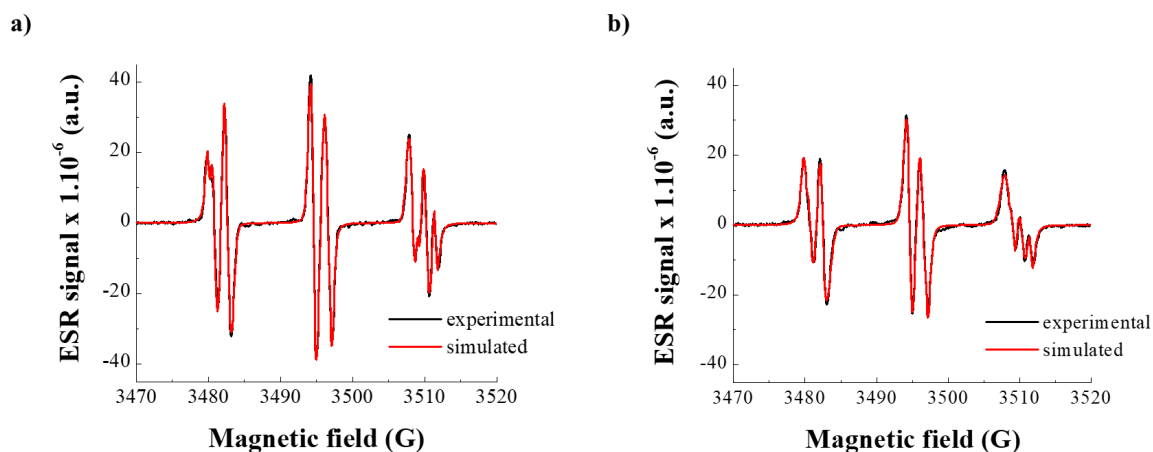


Figure 3.10. ESR-spin trapping spectrum of PDT-2/Iod ( $2.8 \times 10^{-4} \text{ M}/2.1 \times 10^{-3} \text{ M}$ ) in  $\text{CHCl}_3$ :toluene (10:90 v/v) under nitrogen in the presence of PBN (as a spin trap) (a) before irradiation and (b) after 40 s irradiation by LED at 420 nm.

### 3.3.4. Michael Addition and Polymerization Results

The efficiency of the synthesized PIs during one-step and dual-curing reactions was investigated using FTIR. PEGDA ( $M_n = 575 \text{ g/mol}$ ) was used as an acrylate for the aza-Michael addition of our PIs which contain primary and secondary amino groups in their structure and HEMA was chosen as a methacrylate (poor Michael acceptor) for free radical

photopolymerization. HEMA/PEGDA/PI/Iod formulations (Table 3.2) were prepared and their FTIR spectra were collected to monitor the polymerizations. The conversion of HEMA/PEGDA/PI mixture reaches 10 % in 10 min without irradiation proving the aza-Michael addition reaction between the PI and PEGDA (Figure 3.11a). This low conversion can be explained by the steric hindrance of the polymer backbone that reduces the reactivity of the amines and also diffusion of the chains [211]. However, when Iod is present (formulation 1), the conversion reaches to 25 % in 10 min without irradiation. This increase in the conversion stems from the formation of CTC between PI and Iod leading to radical formation without irradiation which is consistent with the ESR data. Similar results were obtained with the formulation 2 (Figure 3.12).

Table 3.2. Photopolymerization formulations, PI = 1 wt% with respect to TX moiety and Iod = 2 wt% in the formulations. <sup>1</sup> PI = 8 wt%, no Iod, <sup>2</sup> PI = 8 wt%, Iod = 2 wt%.

<b>Formulations</b>	<b>PI</b>	<b>HEMA (wt%)</b>	<b>PEGDA (wt%)</b>	<b>Bis-GMA (wt%)</b>	<b>TEGDMA (wt%)</b>
<b>1</b>	PBT-2	60	40	-	-
<b>2</b>	PDT-2	60	40	-	-
<b>3</b>	PDT-2	60	-	-	40
<b>4</b>	PDT-2	60	-	40	-
<b>5</b>	PBT-5	60	40	-	-
<b>6</b>	PEI	60	40	-	-
<b>6a<sup>1</sup></b>	PEI	60	40	-	-
<b>6b<sup>2</sup></b>	PEI	60	40	-	-

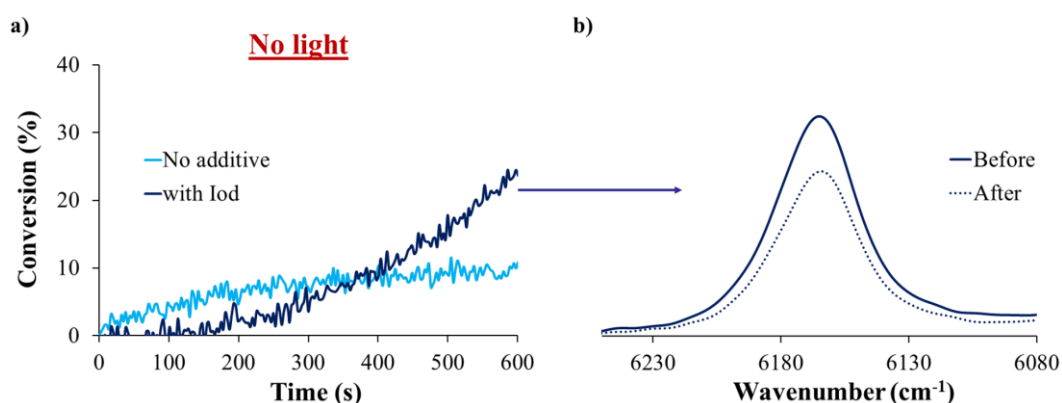


Figure 3.11. (a) Polymerization profiles of formulation 1 with and without Iod under air; thickness = 1.4 mm and (b) Double bond peak area for formulation 1 (with Iod) before and after reaction.

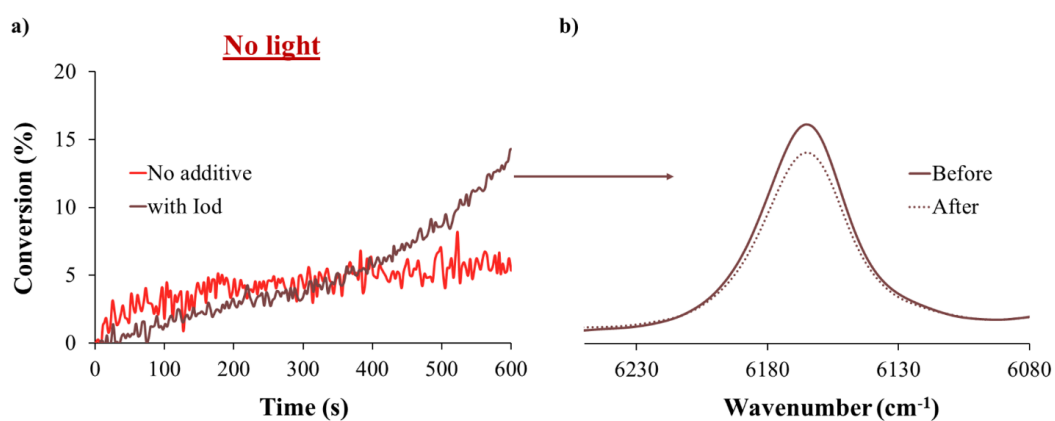


Figure 3.12. (a) Polymerization profiles of formulation 2 with and without Iod under air; thickness = 1.4 mm and (b) Double bond peak area for formulation 2 (with Iod) before and after reaction.

Photopolymerization kinetics (one-step) of the formulations (Table 3.2) were also investigated upon irradiation by LED@405 nm under air. Conversion-time measurements are shown in Figure 3.13. Excellent photopolymerization efficiencies were observed for these systems with final methacrylate conversions around 100 %, indicating that irradiation raises polymerization rate (Figure 3.13). This can be explained by a combined effect of CTC and TX/Iod complex which are both able to generate radicals for free radical polymerization

(Figure 3.14). The effect of Michael addition capability of the PIs on functional group conversions was also investigated. Some of the formulations (1 and 2) were polymerized 10 min at room temperature followed by photopolymerization using LED@ 405 nm for 10 min (dual curing) (Figure 3.13). It was observed that the dual curing method has a positive impact on rate of photopolymerization reaction. In the literature, during dual curing reactions final methacrylate conversions increase due to delay of gel point and vitrification. This was explained by an increase in viscosity of the medium due to the polymer formation via the aza-Michael addition [224]. However, reaction rate decreases due to a decrease in the diffusion rate of radicals to monomers. The faster initial rate of polymerization of our samples after aza-Michael addition can be explained by the formation of radicals even at the first step due to PI-Iod complex formation without light absorption. This process leads to free radical polymerization of the (meth)acrylate in addition to aza-Michael addition. In addition, the photopolymerizations can be performed under air because amines in the PIs prevent oxygen inhibition.

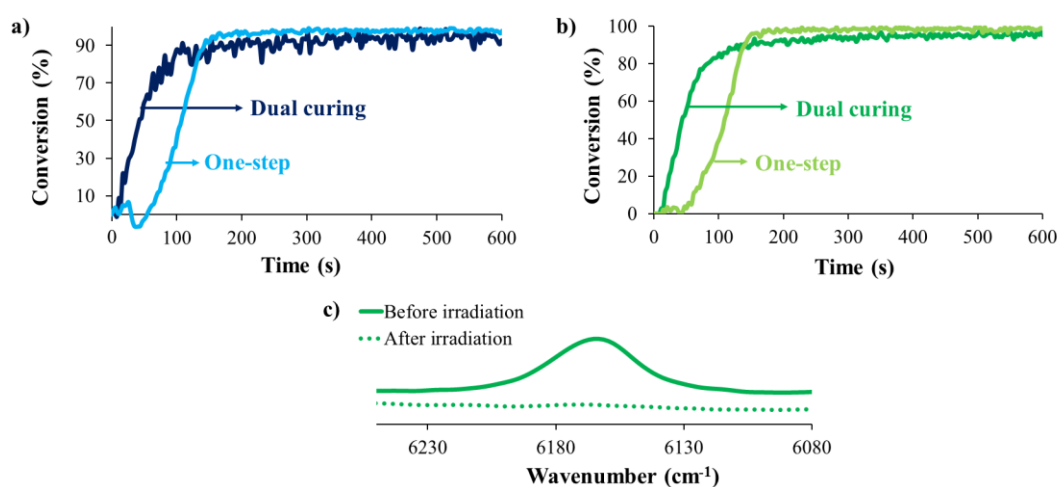


Figure 3.13. Photopolymerization profiles of formulations under air upon exposure to LED@405 nm; thickness = 1.4 mm: (a) (meth)acrylate conversion for formulation 1 (dual curing vs one-step), (b) (meth)acrylate conversion for formulation 2 (dual curing vs one-step), (c) Double bond peak area for formulation 2 (dual curing) before and after irradiation. Light was switched on at 10 s.

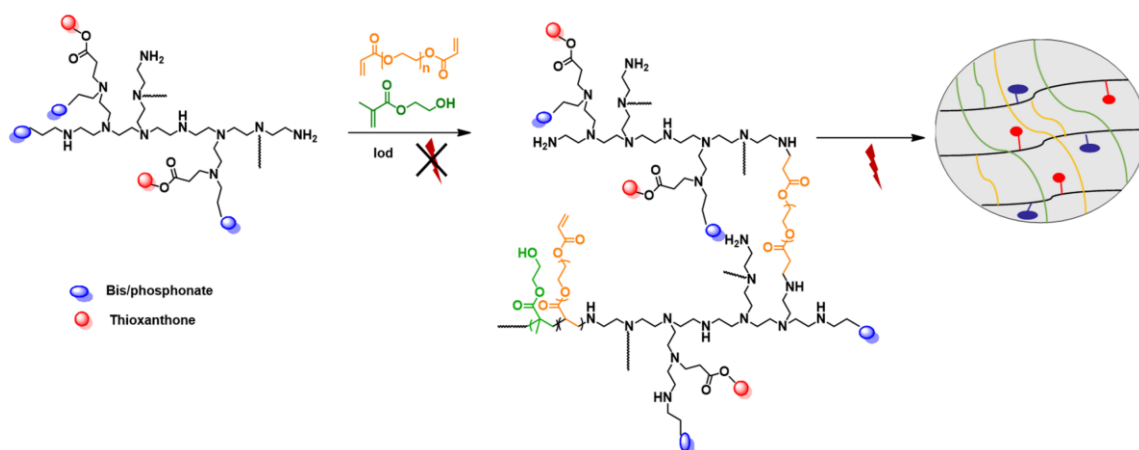


Figure 3.14. Network formation by one-step and dual curing processes.

In order to compare reactivities of PIs containing different amounts of (bis)phosphonate and TX functionalities, polymerizations of formulations 1 (with and without Iod) and 5 (with Iod) were monitored (20 min without light and 10 min with light) (Figure 3.15). The conversions were found to be about 20 and 50 % during the first 20 min for 1 and 1 (with Iod) and no significant polymerization was observed for 5 (with Iod), indicating that PBT-2 is more reactive towards Michael addition and radicalic polymerization compared to PBT-5. This result can be explained by the lower substitution of TX and (bis)phosphonate functionalities on PBT-2, thus higher amounts of reactive amines enhancing both Michael addition and CTC formation. Formulations containing Iod showed a sharp increase in conversion when light was turned on; however the formulation without Iod did not, which was expected from the photolysis results discussed above.

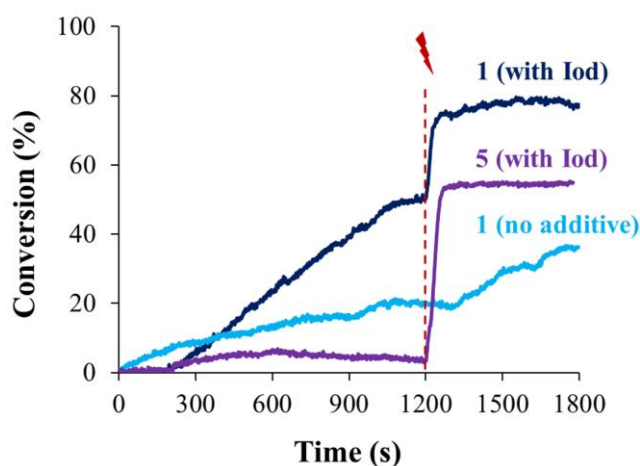


Figure 3.15. Photopolymerization profiles of formulations 1 and 5 in laminate, 20 min without light followed by 10 min upon exposure to light at 320-500 nm.

The effect of CTC on polymerization abilities of the synthesized PIs were analyzed and compared by photo-DSC studies. The formulations contain 1 wt% PI with respect to TX moiety. However PEI concentrations are different:  $4.8 \times 10^{-2}$  M for PBT-2,  $3.5 \times 10^{-2}$  M for PDT-2,  $1.4 \times 10^{-2}$  M for PBT-5, and  $0.8 \times 10^{-2}$  M for PDT-5. As shown in the Figure 3.16, PBT-2 and PDT-2 have higher polymerization rates than PBT-5 and PDT-5. This result indicates that at higher PEI concentrations, CTC is formed more efficiently leading to an enhancement in the rate of polymerization. Higher double bond conversions were obtained for PBT-5 and PDT-5 containing formulations stemming from the slower polymerization compared to PBT-2 and PDT-2.

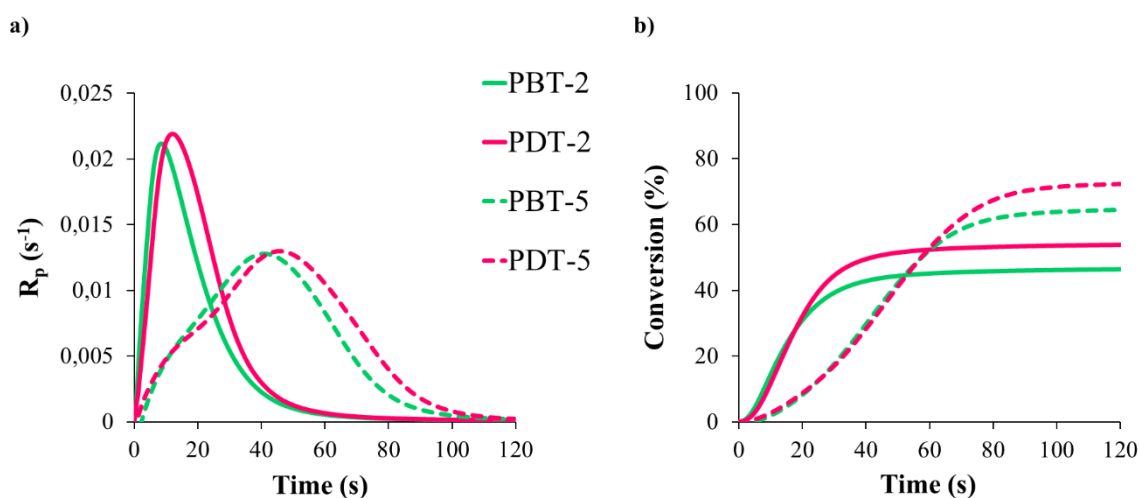


Figure 3.16. Photo-DSC results of PI/Iod/HEMA/PEGDA (1/2/60/40 wt%) formulations under nitrogen, irradiated by 320-500 nm. (a) Rate of polymerization and (b) Conversion plot.  $[TX]: 5 \times 10^{-2}$  M.

Polymerization kinetics of HEMA/Bis-GMA/PI/Iod and HEMA/TEGDMA/PI/Iod mixtures (formulations 3 and 4) were investigated with and without irradiation by LED@405 nm under air. Figure 3.17 shows that formulations reach about 10 % conversion at 10 min without irradiation confirming the ESR data. In the presence of light, the polymerizations are very fast and reach almost 100 % conversions in about 100 s. The formulations containing TEGDMA react faster than those containing Bis-GMA. These results indicate that in the presence of light CTC forms radicals faster, also aryl radicals formed during interaction of TX with Iod contribute to polymerization.

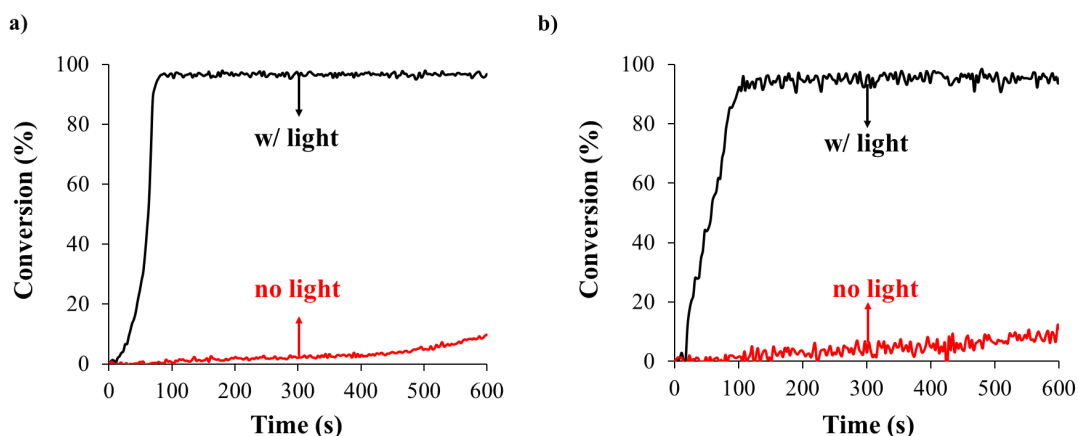


Figure 3.17. Photopolymerization profiles of formulations 3 (a) and 4 (b): 10 min without light (red) and 10 min with exposure to LED@405 nm (black) under air; thickness =1.4 mm. Light was switched on at 10 s.

To analyze the polymerization efficiencies of CTCs by itself, polymerizations of PEI/Iod formulations with and without exposure to LED@405 nm under air were monitored by RT-FTIR (Figure 3.18). The formulation 1 have 1 wt% TX and approximately 8 wt% PEI. Formulations 6, 6a and 6b containing 1 and 8 wt% PEI were monitored for 10 min without irradiation, then for 10 min with irradiation. As shown in Figure 3.18, PEI does not induce polymerization without Iod (formulation 6a), only aza-Michael addition is observed. When Iod is present, polymerization reaches approximately 100 % conversion without irradiation (formulation 6b). When PEI is 1 wt%, polymerization doesn't take place without irradiation. PI containing formulations (formulation 1 and 5) do not reach 100 % conversion without irradiation, because TX and (bis)phosphonate functionalities block the efficient CTC formation to some extent.

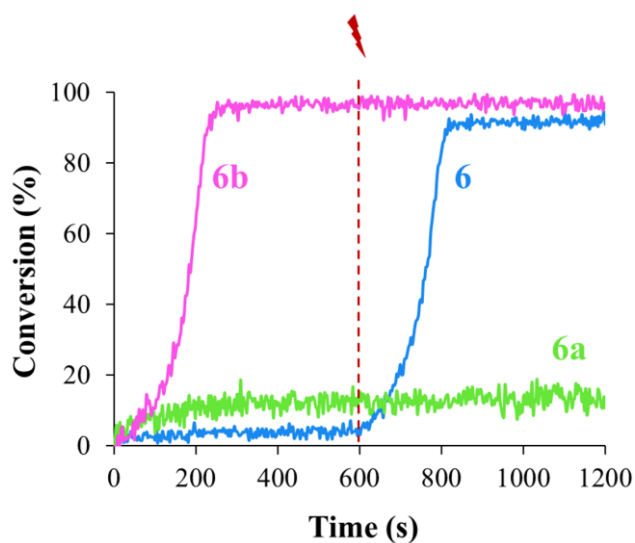


Figure 3.18. Photopolymerization profiles of formulations 6, 6a and 6b with and without exposure to LED@405 nm under air; thickness =1.4 mm.

### 3.3.5. Radical Formation Mechanism

Upon irradiation, TX part of the PI absorbs light and reaches its excited singlet state. This excited state reacts with the iodonium salt to generate aryl radicals (Ar.), capable of initiating the free-radical polymerization of (meth)acrylates. Amine functionality of the PI prevents oxygen inhibition of these radicals. Also amine groups of PI create CTCs with Iod and generate aryl radicals to initiate free-radical polymerization. CTC can undergo degradation and form radicals even without irradiation proving the efficient interaction between the donor and the acceptor.

### 3.3.6. Thermal Properties of Polymers

Polymer properties, glass transition temperature and thermal stability were investigated using DSC and TGA (Table 3.3). The formulations 1, 2, 3 and 4 (Table 3.2) were polymerized with two different methods: dual and one-step curing (both with thickness 1.4 mm) to obtain the polymeric materials, P-1, P-2, P-3 and P-4. In the first step of the dual curing process PIs undergo aza-Michael addition with PEGDA and also initiate polymerization of (meth)acrylates through CTC formation without irradiation, for 10 min.

In the second step, the formulations were irradiated by 405 nm LED for 10 min. In this step, radical formation was faster and higher conversions were reached compared to the first step of the dual curing process. In one-step curing, the formulations were polymerized by 405 nm LED for 10 min.

Table 3.3. Total conversion,  $T_g$  and thermal degradation characteristics of the materials.

Materials	Irradiation	Total conversion (%)	$T_g$ (°C)	Temp. at 10% wt. loss (°C)	Char yield at 550 °C
P-1	One-step	97	10	298	8.1
P-1	Dual curing	93	20	299	9.1
P-2	One-step	100	10	308	7.0
P-2	Dual curing	95	25	312	7.4
P-3	Dual curing	96	119	317	9.9
P-4	Dual curing	94	111	307	15.2

All formulations reach total conversion between 93 and 100 %. As seen in Table 3.3, there is a small difference in  $T_g$  due to the curing method, one-step or dual-curing. For example,  $T_g$  values of P-1 was found to be 10 and 20 °C for one-step and dual-curing systems. The main differences in  $T_g$  mostly depend on the initial monomer composition of the formulations. The formulations based on HEMA/TEGDMA/PDT-2 and HEMA/Bis-GMA/PDT-2 gave higher  $T_g$  (119 and 111 °C) materials compared to HEMA/PEGDA/PDT-2 or PBT-2 systems.

To check for an indication of IPN formation,  $T_g$  of P-1, P-2 and P-3 were studied.  $T_g$ 's of IPNs are known to generally be in between its composing homopolymers and to be broad [225].  $T_g$  for HEMA/PEGDA polymers (P1 and P-2) (10 - 25 °C) was in fact found to be between the homopolymers of HEMA (81 °C [226]) and PEGDA (- 35 °C [227]). Also,  $T_g$  of HEMA/Bis-GMA polymers (P-3) is 111 °C, close to the value (133 °C) given in the literature for the similar composition (HEMA/Bis-GMA, 45:55 wt%) [228]. Thus, we tentatively conclude that some IPN formation has occurred, and this aspect requires further study.

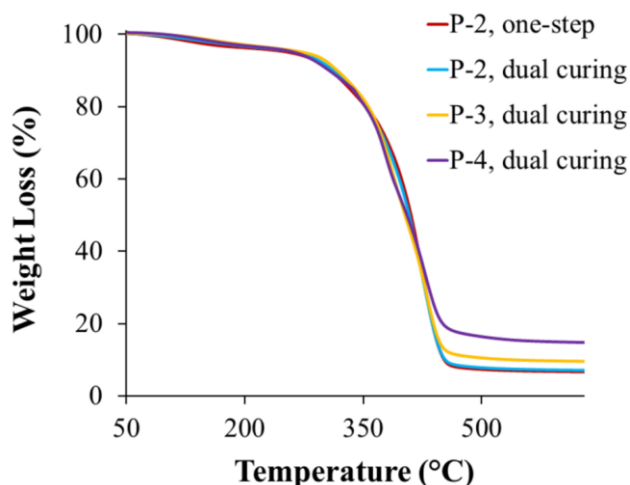


Figure 3.19. TGA analysis of the materials.

As can be seen in Figure 3.19, the curing method did not affect the thermal stability and degradation behavior of the crosslinked polymers. All polymers start to degrade around 300 °C. The fifth column of Table 3.3 shows the temperatures at 10 % weight loss and have similar trend with initial degradation temperatures. It is clear that PI structure can influence char yield of the synthesized materials. The formulations containing the bisphosphonated PIs (P-1) showed slightly higher char yields than those of phosphonated ones (P-2) due to higher phosphorus content (Table 3.3). The highest char yield of 15 % obtained for P-4 is due to contribution of both phosphonate and aromatic structures.

### 3.4. Conclusion

In this study, branched PEI is used as a scaffold for the preparation of four new PIs with controllable amount of TX and (bis)phosphonate functionalities. These PIs absorb light in the visible region. Emission spectra and LFP data indicate that they are fluorescent and have singlet state ( $S_1$ ) lifetimes of 7.7 ns. These PIs can be used as high performance PIs with the ability of aza-Michael addition reaction with acrylates and free radical polymerization with (meth)acrylates in one-step or dual curing processes. CTCs formed between amines (PEI) (donors) and Iod (acceptors) can lead to high conversions without irradiation. The interaction of TX with Iod also generates radicals by photochemical free radical polymerization using LED@405 nm under air. Excellent polymerization initiating

abilities and high final conversions are found for both one-step and dual curing processes, also indicating oxygen inhibition effect of the PIs. PIs with lower substitution of TX and (bis)phosphonate functionalities are found to be more reactive towards Michael addition and radicalic polymerization due to higher amounts of reactive amines enhancing both aza-Michael addition and CTC formation. These new PIs can play a role of a photoinitiator and a monomer by dual curing systems, giving custom-tailorable products for different industrial applications.

## 4. BENZOPHENONE-FUNCTIONALIZED OLIGO (AMIDO AMINE)/IODONIUM SALT SYSTEMS AS VISIBLE LIGHT PHOTOINITIATORS

This chapter is published as: Gencoglu, T., B. Graff, F. Morlet-Savary, J. Lalevée, and D. Avci, “Benzophenone-Functionalized Oligo (Amido Amine)/Iodonium Salt Systems as Visible Light Photoinitiators”, *ChemistrySelect*, Vol. 6, No. 23, pp. 5743-5751, 2021. This copyrighted article was reproduced with permission from John Wiley and Sons (Figure A.18).

### 4.1. Introduction

In this chapter, two new water soluble oligomeric photoinitiators, based on a oligomeric poly(amido amine) (OAA), functionalized with BP and both BP and diethyl phosphonate were synthesized. OAA backbone brings water solubility, biodegradability and biocompatibility, so they are suitable for biomedical applications [229,230]. This backbone also plays an important role for additional functionalization through its unmodified amine groups. The amino groups are also utilized to decrease the oxygen inhibition effect during photopolymerization process. The purpose of integrating phosphonate functionality was to enhance the biocompatibility and to show the flexibility of our synthetic approach for further functionalization of PIs. These PIs were intended to initiate FRP of (meth)acrylates by i) photoinitiation through photoreduction process (electron transfer from the amines in OAA backbone to BP) as one-component PI, ii) CTC formation between Iod and amines in OAA and iii) interaction of BP with Iod through photooxidation process (electron transfer from BP to Iod). The photochemical mechanisms of the novel photoinitiators for the initiation of FRP were investigated using electron-spin resonance-spin trapping, laser flash, steady-state photolysis experiments and molecular orbital calculations.

## 4.2. Experimental Section

### 4.2.1. Materials

N,N'-methylenebisacrylamide (MBA), 1,4-diaminobutane, 4-hydroxybenzophenone, acryloyl chloride, diethyl vinylphosphonate (DVP), triethylamine, BP, ethyl 4-(dimethylamino)benzoate (EDB), 2-hydroxyethyl methacrylate (HEMA), poly(ethylene glycol) diacrylate (PEGDA, Mn = 575) were obtained from Sigma-Aldrich and used as received without any further purification. 4-benzoylphenyl acrylate was prepared by the literature method [231]. Bis-(4-tert-butylphenyl)iodonium hexafluorophosphate (Iod or SpeedCure938) was obtained from Lambson Ltd.

### 4.2.2. Characterization

$^1\text{H}$ ,  $^{13}\text{C}$  NMR spectra were recorded on a Varian Gemini (400 MHz) spectrometer with deuterated methanol (MeOD) as a solvent. A Nicolet 6700 FT-IR spectrophotometer was used for recording IR spectra. Mass spectroscopy analysis was performed with AGILENT 6460 Triple Quadrupole System (ESI+Agilent Jet Stream) coupled with AGILENT 1200 Series HPLC at METU Central Laboratory, Ankara, Turkey.

### 4.2.3. Synthesis of the Photoinitiators

4.2.3.1. Synthesis of Oligo(amido amine) (OAA). This oligomer was prepared with a slight modification of the procedure used in reference 162. MBA (279 mg, 1.81 mmol) and 1,4-diaminobutane (180 mg, 2.04 mmol) were dissolved in methanol (1.29 mL) and stirred for 16 hours at 40 °C. The oligomer was isolated by precipitation into excess diethyl ether, filtered and dried under vacuum (white solid-67 % yield).

4.2.3.2. Synthesis of OAA-B. OAA (307 mg, 0.29 mmol) and 4-benzoylphenyl acrylate (77.4 mg, 0.30 mmol) were stirred in methanol (7.5 mL) at 70 °C for 2 days. After removal of excess solvent by rotary evaporation, the solution was precipitated into excess diethyl ether under stirring. The product was obtained as yellow viscous liquid in 65 % yield.

$^1\text{H}$  NMR (400 MHz): 1.5 (4 H, NH-CH<sub>2</sub>-CH<sub>2</sub>-CH<sub>2</sub>), 2.27 - 2.94 (12 H, NH-CH<sub>2</sub>, N-CH<sub>2</sub>, O=C-CH<sub>2</sub>), 4.54 (2 H, NH-CH<sub>2</sub>-NH), 6.80 - 7.73 (aromatic H) ppm.

FTIR: 1533 (N-H), 1636 (C=O), 2848, 2933 (C-H), 3000-3750 (N-H) cm<sup>-1</sup>.

**4.2.3.3. Synthesis of OAA-BP.** OAA (280 mg, 0.27 mmol), 4-benzoylphenyl acrylate (70 mg, 0.28 mmol) and diethyl vinylphosphonate (45.4 mg, 0.28 mmol) were stirred in methanol (7.7 mL) at 70 °C for 2 days. The solution was concentrated by rotary evaporation and the solution was precipitated into excess diethyl ether under stirring. The product was obtained as a yellow viscous liquid in 51 % yield.

$^1\text{H}$  NMR (400 MHz): 1.32 (6 H, P-O-CH<sub>2</sub>-CH<sub>3</sub>), 1.51 (4 H, NH-CH<sub>2</sub>-CH<sub>2</sub>-CH<sub>2</sub>), 2.27 - 2.91 (12 H, NH-CH<sub>2</sub>, N-CH<sub>2</sub>, O=C-CH<sub>2</sub>), 4.09 (4 H, P-O-CH<sub>2</sub>-CH<sub>3</sub>), 4.55 (2 H, NH-CH<sub>2</sub>-NH), 6.76 - 7.74 (aromatic H) ppm.

$^{13}\text{C}$  NMR (400 MHz): 16.4 (CH<sub>3</sub>-CH<sub>2</sub>-O), 26.6 (NH<sub>2</sub>-CH<sub>2</sub>-CH<sub>2</sub>, CH<sub>2</sub>-CH<sub>2</sub>-N), 33.6 (CH<sub>2</sub>-P=O, O=C-CH<sub>2</sub>), 43.7 (CH<sub>2</sub>-CH<sub>2</sub>-P=O, CH<sub>2</sub>-NH, CH<sub>2</sub>-N), 52.8 (O=C-CH<sub>2</sub>-CH<sub>2</sub>-N), 61.9 (CH<sub>3</sub>-CH<sub>2</sub>-O), 115.5 – 139.5 (aromatic carbons), 166.4 (O=C-NH), 173.6 (O-C=O, O=C-NH), 196.2 (O=C-CH=CH) ppm.

FTIR: 962, 1025 (P-O-C), 1216 (P=O), 1532 (N-H), 1640 (C=O), 2852, 2929 (C-H), 3000-3750 (N-H) cm<sup>-1</sup>.

#### 4.2.4. Photochemical Analysis

**4.2.4.1. UV-vis Spectroscopy Experiments.** UV-vis light absorptions of the PIs were measured in methanol on a Varian®Cary 3 spectrometer. For steady-state photolysis experiment solutions of PIs, with Iod in CHCl<sub>3</sub>:toluene (10:90 v/v), were irradiated with LED @ 375 nm, and the absorption spectra were recorded for different irradiation times.

**4.2.4.2. Laser Flash Photolysis (LFP) Experiments.** Nanosecond laser flash photolysis (LFP) experiments were carried out using a Q-switched nanosecond Nd/YAG laser ( $\lambda_{\text{exc}} = 355$  nm, 9 ns pulses; energy reduced down to 10 mJ; minilite Continuum) and the analyzing system (for absorption measurements) consisted of a ceramic xenon lamp, a monochromator, a fast photomultiplier and a transient digitizer (Luzchem LFP 212) [219].

**4.2.4.3. ESR Spin Trapping (ESR-ST) Experiments.** The ESR-ST experiments were carried out using an X-band spectrometer (Bruker EMX-plus). The radicals were created under nitrogen at room temperature upon irradiation by LED@420 nm in CHCl<sub>3</sub>:toluene (10:90 v/v) solution in the presence of Iod and trapped by N-tert-butyl- $\alpha$ -2 phenylnitron (PBN) according to a procedure described in the literature [221]. The ESR spectra simulations were carried out with the WINSIM software.

#### 4.2.5. Photopolymerization

The photosensitive formulations were prepared by first mixing the PI (0.5 wt%, with respect to BP moiety) with the monomers (HEMA or HEMA:PEGDA mixture) and then adding Iod or EDB (2 wt%).

**4.2.5.1. Real-Time Fourier Transform Infrared (RT-FTIR) Spectroscopy.** A JASCO 4100 real-time Fourier transform infrared spectrophotometer was used to follow the (meth)acrylate function conversions versus time for polymerizations of 1.4 mm thick samples. Formulations were irradiated by LED@405 nm under air for 10 min at room temperature. The photopolymerizations were monitored by following the near-infrared (meth)acrylate C=C double-bond peak area at 6117- 6223 cm<sup>-1</sup>. The double bond conversion (DBC) was determined using equation (4.1).

$$\text{DBC \%} = \left(1 - \frac{A_t(6117-6223)}{A_0(6117-6223)}\right) \times 100, \quad (4.1)$$

where A<sub>0</sub> and A<sub>t</sub> denote area of the meth/acrylate bands, and the subscripts t and 0 indicate the curing time and the beginning of the curing, respectively. Some of the formulations were also irradiated at 320-500 nm in air and in laminate for 10 min at room temperature. The photopolymerizations were monitored by following the (meth)acrylate C=C double-bond peak height at 1637 cm<sup>-1</sup>.

**4.2.5.2. Photo-DSC.** Photo-DSC analyses were performed on a DSC 250 (TA Instruments) equipped with an OmniCure 2000 lamp (320-500 nm). Visible light filter was used to perform polymerization in the 400-500 nm range. Formulations (3-4 mg) were irradiated for 10 min (UV-vis light) and 10 – 20 min (visible light) at 30 °C and under nitrogen flow of 50

$\text{mL min}^{-1}$ . The heat release during the polymerization reaction was monitored as a function of time. The rates of polymerization reactions were calculated using equation (4.2).

$$\text{Rate} = \frac{(Q/s)M}{n(\Delta H_p)m}, \quad (4.2)$$

where  $Q/s$  is the heat flow per second,  $M$  is the molar mass of the monomer,  $n$  is the number of double bonds per monomer molecule,  $\Delta H_p$  is the heat of reaction evolved and  $m$  is the mass of monomer in the sample. The theoretical heat for the total conversion of methacrylate double bond is 55 kJ/mol.

#### 4.2.6. Computational Procedure

Geometry optimizations [232] were carried out at UB3LYP/LANL2DZ and UB3LYP/6-31G\* levels using the Gaussian 03 software; geometries were frequency checked; the Molecular Orbitals (MOs) involved in the electronic transitions were extracted. The electronic absorption spectra were calculated with the time-dependent density functional theory (DFT) at the MPW1PW91/LANL2DZ level of theory on the relaxed geometries calculated at the UB3LYP/LANL2DZ level of theory.

### 4.3. Results and Discussion

#### 4.3.1. Synthesis and Characterization of Photoinitiators

In this study, a water soluble and biocompatible OAA scaffold was used to prepare novel PIs. Two PIs functionalized with BP or both BP and phosphonate functional groups were synthesized in two steps (Figure 4.1). In the first step, an OAA was synthesized via an aza-Michael addition reaction between MBA and 1,4-diamino butane in 1:1.15 mol ratio to obtain an amine terminated linear oligomer ( $n=4-6$ ,  $M_n=1057-1542$ ) which can be used for further functionalization [162]. In the second step, the oligomer was reacted again through an aza-Michael addition reaction with acrylate functionalized BP or diethyl vinylphosphonate together with acrylate functionalized BP in 1:1 mol ratio. The products, OAA-B and OAA-BP were obtained as viscous liquids in 51–65% yield after purification

by precipitation into diethyl ether. The synthesized PIs have good solubility (around 200 g/L) in water.

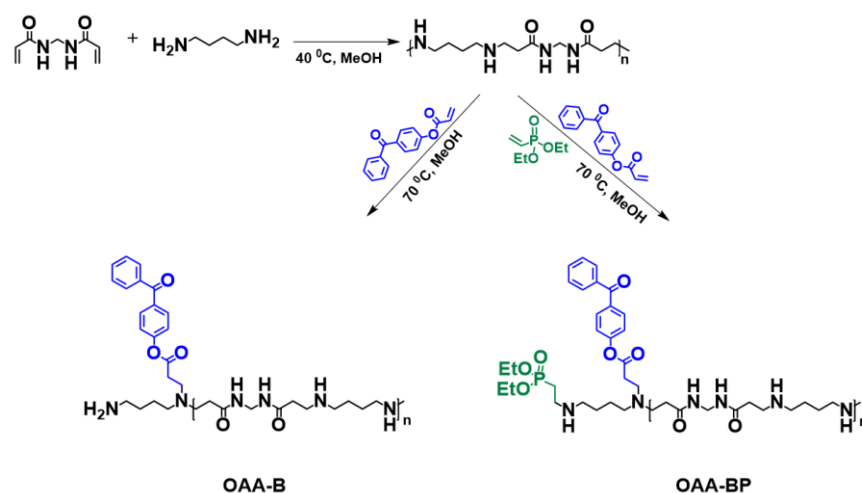


Figure 4.1. The synthesis pathway of PIs.

The structures of the PIs were confirmed by  $^1\text{H}$ ,  $^{13}\text{C}$  NMR and FTIR spectroscopies. In the  $^1\text{H}$  NMR of OAA no peaks corresponding to the double bond protons (5-7 ppm) were observed, indicating that the oligomer is terminated with amine groups (Figure 4.2).  $^1\text{H}$  NMR spectra of the PIs show the aromatic protons of BP between 6.8–7.7 ppm (Figure 4.2 and Figure 4.3). The peaks at 1.5 and 4.5 ppm are ascribed to the methylene protons of the oligomeric backbone. Comparison of the spectra of OAA and PIs reveals that the peak at 3.66 ppm must originate from the tertiary amine groups resulting from the BP addition to the oligomer.

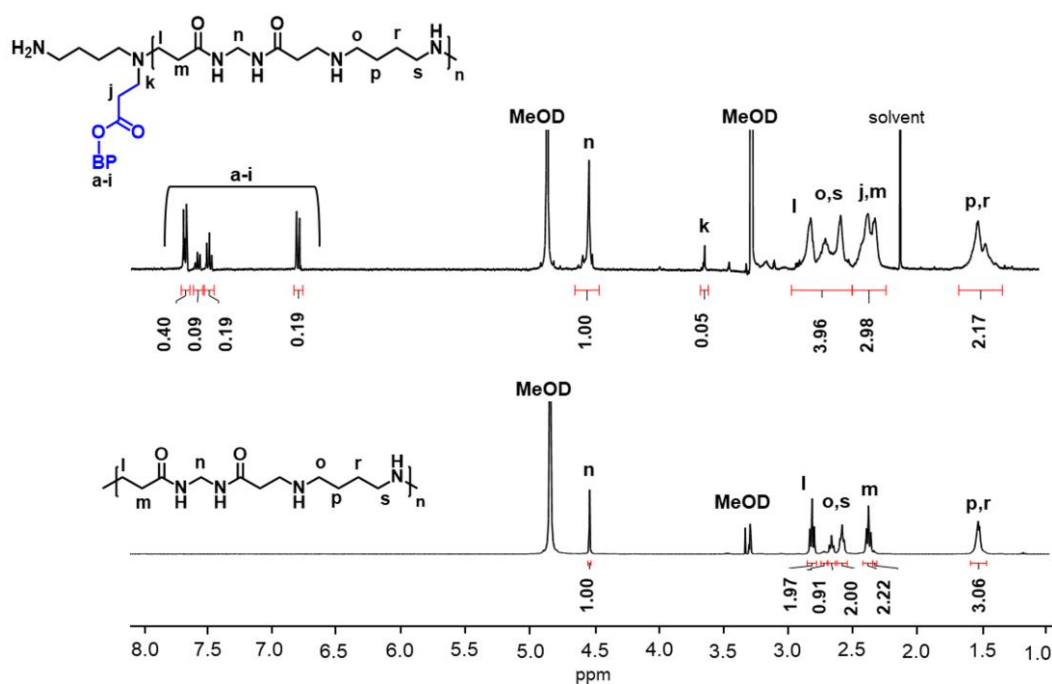


Figure 4.2.  $^1\text{H-NMR}$  spectra of OAA and OAA-B.

In the  $^1\text{H NMR}$  of OAA-BP, the peaks at 1.32 and 4.09 ppm are the characteristic methyl and methylene protons of diethyl phosphonate (Figure 4.3).

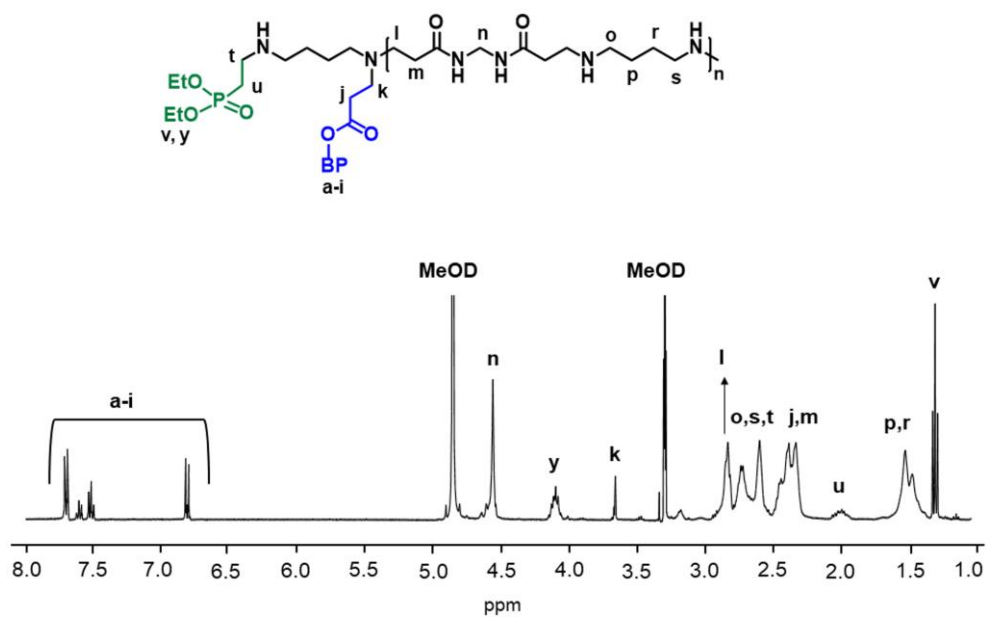


Figure 4.3.  $^1\text{H-NMR}$  spectrum of OAA-BP.

The amounts of BP and phosphonate groups on PIs were calculated by integrating aromatic protons of BP and methyl protons of diethyl phosphonate, respectively, with respect to amido amine protons at 1.5 and 4.5 ppm (Figure 4.2 and Figure 4.3). The amount of BP units in OAA-B and OAA-BP were determined as 9–14 wt%, one BP and one phosphonate functionality/chain on the average. The  $^{13}\text{C}$  NMR spectrum of OAA-BP showed methyl and methylene carbons of phosphonate groups at 16 and 62 ppm, aromatic carbons between 110 and 150 ppm and carbonyl carbons of benzophenone, ester and two different amides (due to their proximity to BP functionality) at around 195, 173, 166 and 173 ppm (Figure 4.4). The mass spectroscopy analysis of OAA-B showed a molecular mass distribution between 1000 and 1500.

The FTIR spectra of PIs show strong peaks at  $1640\text{ cm}^{-1}$  (amide C=O of OAA and ketone C=O of BP),  $3300$  and  $1532\text{ cm}^{-1}$  (N-H). A small peak at  $1730\text{ cm}^{-1}$  is due to the ester C=O of BP functionality. In addition, OAA-BP spectrum shows peaks at  $1215$  (P=O),  $1025$  and  $962\text{ cm}^{-1}$  corresponding to phosphonate functionalities (Figure 4.5).

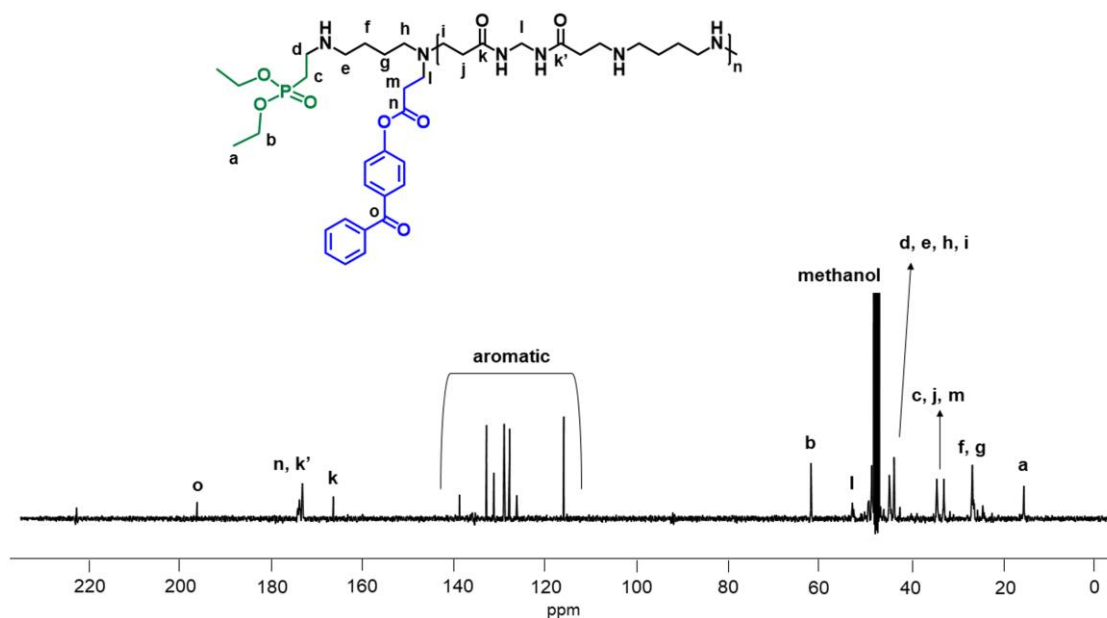


Figure 4.4.  $^{13}\text{C}$ -NMR spectrum of OAA-BP.

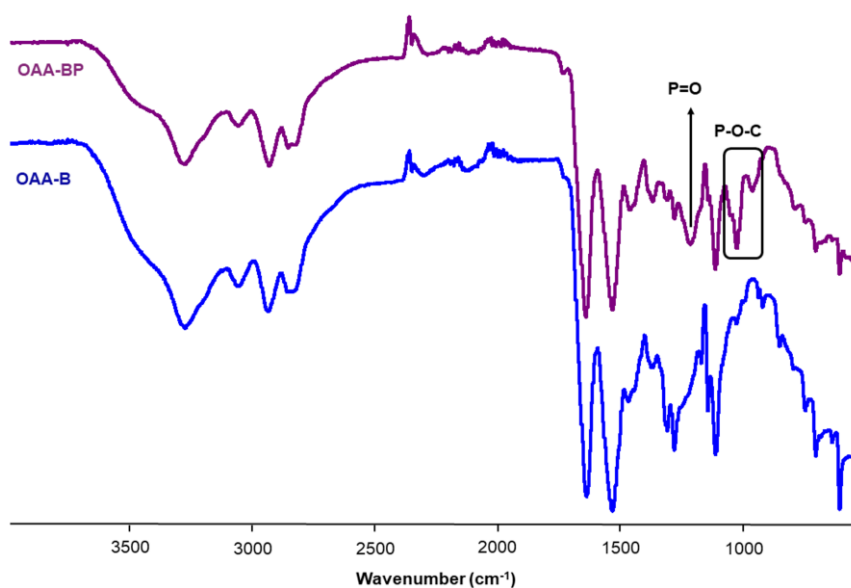


Figure 4.5. FTIR spectra of the synthesized PIs.

### 4.3.2. Light Absorption and Emission Properties

The UV-visible absorption spectra of the synthesized PIs in methanol and water are presented in Figure 4.6a. They showed similar maximum absorption peaks ( $\lambda_{\max}$ ) at 290 nm ( $\pi$ - $\pi^*$  transition) and 344 nm ( $n$ - $\pi^*$  transition) in methanol, bathochromic shift of 40 nm and 14 nm respectively compared to the reference BP (250 nm and 330 nm) (Figure 4.6a and Figure 4.6b). However in water, the peak at 294 nm shifted to 248 nm (blue shift) and hyperchromic shift was observed for the peak at 344 nm for both of the PIs. These shifts can be caused by the polarity differences between solvents, and also more effective hydrogen bonding ability of water than methanol. The molar absorptivity values of PIs are shown in Table 4.1. The molar absorptivity of BP in methanol can also be used to verify the BP amount in PIs, giving that PIs contain 6–11 wt% BP, similar to the values calculated from the NMR data (9–14 wt%).

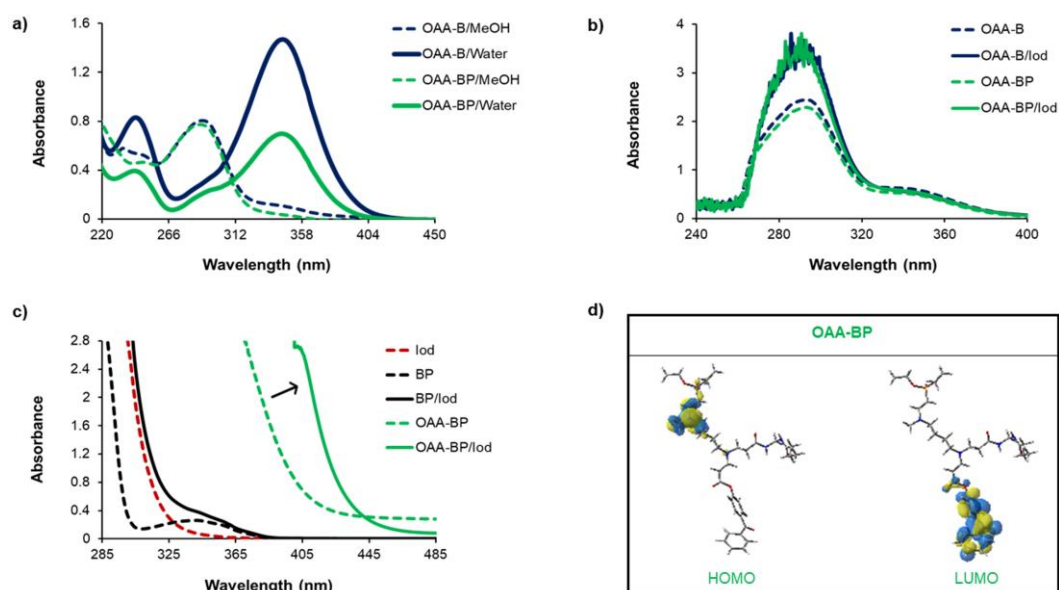


Figure 4.6. UV-vis absorption spectra of (a) OAA-B and OAA-BP ( $0.6 \times 10^{-4}$  M) in MeOH and H<sub>2</sub>O, (b) OAA-B and OAA-BP ( $2.1 \times 10^{-4}$  M) with and without Iod ( $4 \times 10^{-3}$  M) in MeOH, (c) Iod ( $3.5 \times 10^{-3}$  M), BP and OAA-BP ( $1.7 \times 10^{-3}$  M) with and without Iod ( $3.5 \times 10^{-3}$  M) in CHCl<sub>3</sub>:toluene (10:90 v/v), (d) Frontier orbitals (HOMO-LUMO) calculated at the UB3LYP/6-31G\* level for OAA-BP.

Table 4.1. Absorption characteristics of PIs in methanol and water.

PI	Solvent	$\lambda_{\max}$ (nm)	$\epsilon$ ( $M^{-1} \text{ cm}^{-1}$ )
OAA-B	MeOH	290	14181
OAA-B	H <sub>2</sub> O	344	22656
OAA-BP	MeOH	290	11578
OAA-BP	H <sub>2</sub> O	344	14019
BP	MeOH	250	17542

We also studied the formation of CTC between electron-rich OAA-B and OAA-BP and electron-poor Iod. It is known that CTCs absorb light in near-UV or visible range. However, in this case no new peak or shift of the absorption band or other change was observed, indicating that CTCs do not form in methanol (Figure 4.6b). This may be due to

the polar nature of the solvent. To test this hypothesis, UV-visible analysis was also performed in a solvent mixture with a low polarity ( $\text{CHCl}_3$ : toluene 10:90 v/v). As shown in Figure 4.6c, a shift was not observed when Iod was combined with BP. However, a strongly absorbing complex is observed confirming interaction between the amines in OAA-BP and Iod. OAA-B showed the same behavior (Figure 4.7). The optimized geometries and also the frontier orbital (highest occupied molecular orbital (HOMO) and lowest unoccupied molecular orbital (LUMO)) calculations were carried out by DFT calculations on the simplified form of OAA-BP (Figure 4.6d). It can be observed that partial charge transfer transitions are expected with HOMO and LUMO localized on different moieties of their structure, resulting a bathochromic shift.

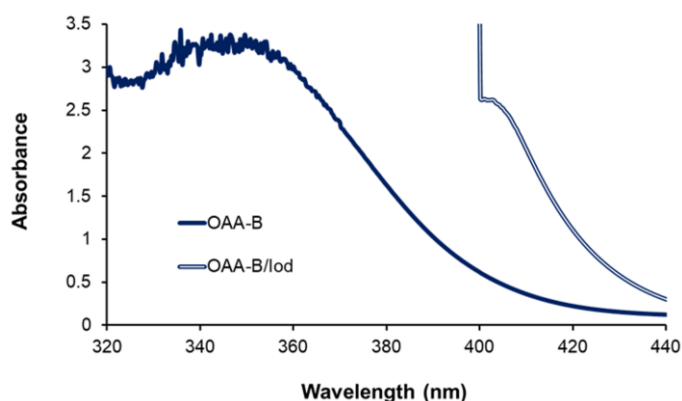


Figure 4.7. UV-vis absorption spectra of OAA-B with and without Iod in  $\text{CHCl}_3$ :toluene (10:90 v/v). OAA-B ( $1.7 \times 10^{-3}$  M) and Iod ( $3.5 \times 10^{-3}$  M).

### 4.3.3. Photochemical Mechanisms

The photochemical mechanisms of the synthesized PIs were investigated by LFP, steady-state photolysis and ESR experiments. LFP analysis was performed to analyze the electronically excited states of the synthesized PIs. In general, amines are hydrogen donors (coinitiators) and quench the excited triplet state of PIs. However, Figure 4.8 indicates that both of the PIs have singlet states only, indicating that the amines are not effective as coinitiators.

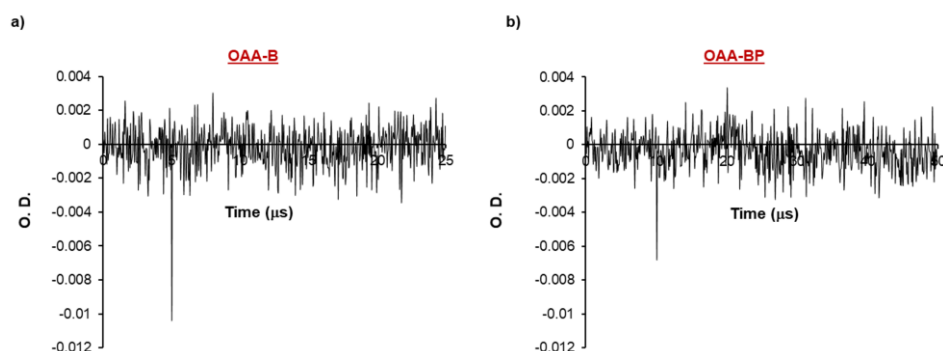


Figure 4.8. LFP results of (a) OAA-B and (b) OAA-BP,  $[PI] = 1.5 \times 10^{-4}$  M in MeOH.

Steady state photolysis of PI/Iod in  $CHCl_3$ :toluene upon irradiation by the LED@375 nm was investigated. We can observe two different radical generation mechanisms: (i) Type II photoinitiation by photoreduction of BP with amines (OAA in the structure and EDB) and (ii) photooxidative reaction between BP/Iod and OAA/Iod (CTC) separately. The first mechanism (i) was not realizing as observed later in the photopolymerization experiments. These PIs work through mechanism (ii).

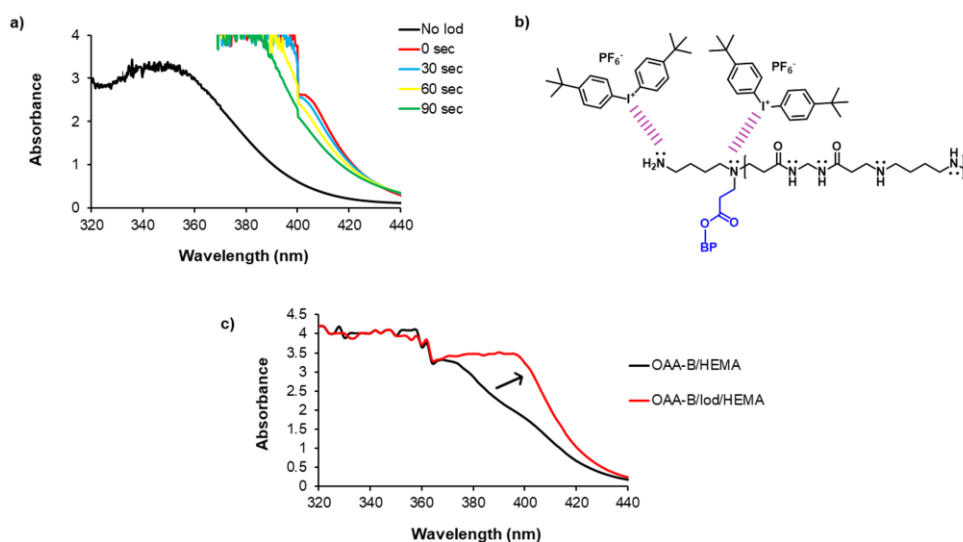


Figure 4.9. Photolysis of (a) OAA-B/Iod mixture by LED at 375 nm, OAA-B ( $1.9 \times 10^{-3}$  M) and Iod ( $3.6 \times 10^{-3}$  M) in  $CHCl_3$ :toluene (10:90 v/v) (b) CTC formation between OAA-B and Iod (c) UV-vis absorption spectra of OAA-B and OAA-B/Iod in HEMA (OAA-B=0.12 wt% wrt BP moiety, Iod=0.48 wt%).

The photolysis in the presence of Iod by CTC formation between amines in PIs and Iod and structure of CTC were shown in Figure 4.9a and 4.9b: The CTC peak at 404 nm is seen to photobleach very fast in  $\text{CHCl}_3$ :toluene mixture (Figure 4.9a for OAA-B, Figure 4.10a for OAA-BP). To observe CTC formation in monomers, analysis was performed with HEMA. When Iod was added to OAA-B/HEMA mixture, a bathochromic shift consistent with CTC formation was observed (Figure 4.9c).

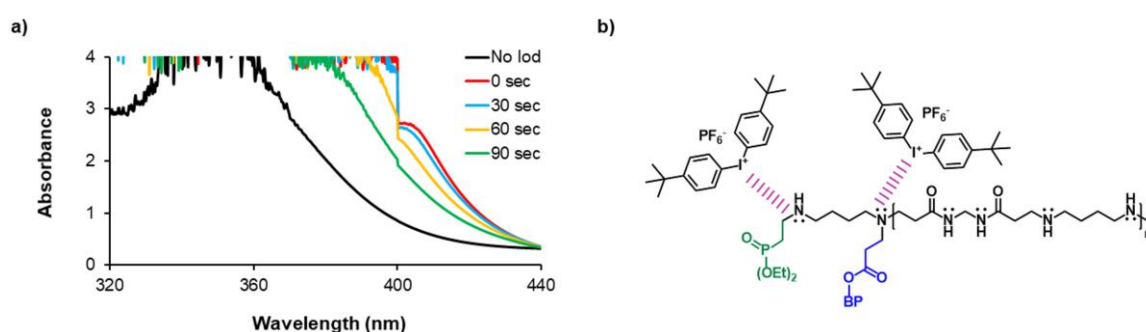


Figure 4.10. (a) Photolysis of OAA-BP ( $1.7 \times 10^{-3}$  M) and Iod ( $3.5 \times 10^{-3}$  M) in  $\text{CHCl}_3$ :toluene (10:90 v/v), (b) CTC formation between OAA-BP and Iod.

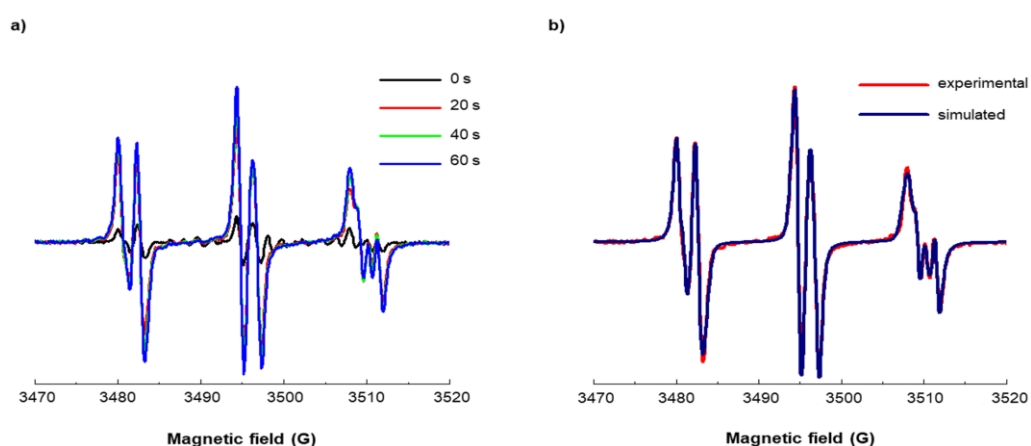


Figure 4.11. ESR-spin trapping spectra of OAA-B/Iod under nitrogen in the presence of PBN (as a spin trap) (a) spectra at different times by LED at 420 nm and (b) experimental and simulated spectra after 60 s irradiation by LED at 420 nm.

ESR-ST measurements were performed for OAA-B/Iod and OAA-BP/Iod mixtures in  $\text{CHCl}_3$ :toluene (10:90 v/v) under nitrogen and in the presence of a spin-trap agent, PBN (Figure 4.11). The intensity of the ESR signals increased with time under 420 nm LED irradiation (Figure 4.11a) and formation of two types of radical/PBN adducts were detected:  $\text{Ar}^*/\text{PBN}$  and  $-\text{NCH}^*/\text{PBN}$ . The corresponding spectra were simulated with the hyperfine coupling constants  $hfc$  ( $a_{\text{N}}=13.7$  G;  $a_{\text{H}}=1.8$  G for OAA-B,  $a_{\text{N}}=13.8$  G;  $a_{\text{H}}=1.8$  G for OAA-BP) for the first and ( $a_{\text{N}}=14.4$  G;  $a_{\text{H}}=2.3$  G for OAA-B and  $a_{\text{N}}=14.5$  G;  $a_{\text{H}}=2.4$  G for OAA-BP) for the second adducts (Figure 4.11b, Figure 4.12) [68].

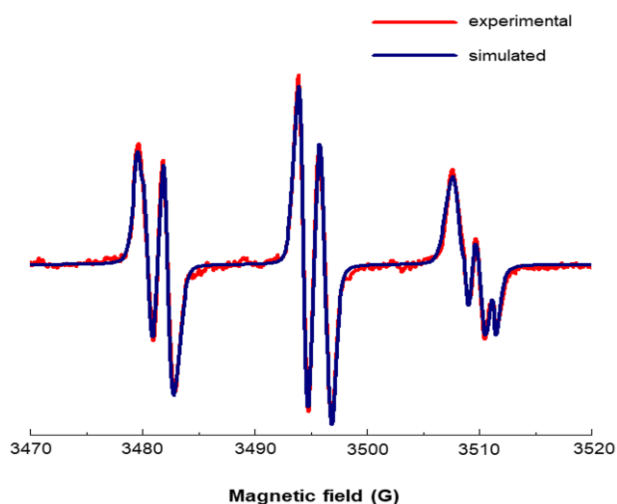


Figure 4.12. Experimental and simulated ESR-spin trapping spectra of OAA-BP/Iod under nitrogen in the presence of PBN (as a spin trap) after 60 s irradiation by LED at 420 nm.

#### 4.3.4. Polymerization Results

The photoinitiation abilities of the synthesized PIs were investigated using HEMA or HEMA:PEGDA ( $M_n=575$  g/mol) mixture by real-time FTIR and photo-DSC. For FTIR studies some of the formulations (Table 4.2) in thick films (thickness about 1.4 mm) were prepared and irradiated by LED@405 nm under air at room temperature.

As shown in Figure 4.13a, BP/Iod did not initiate photopolymerization under irradiation with this LED due to lack of absorbance at this wavelength. Similarly, the

synthesized PIs did not induce photopolymerization when Iod was absent (formulations 1, 2, 2-P) because of their very low absorptivity at 405 nm. However, when Iod was added, excellent photopolymerization efficiencies were observed with final (meth)acrylate conversions around 100%, even though these PIs do not have absorbance at 405 nm, just as BP does not. This behavior can be explained as due to shift of absorbance towards higher wavelengths as a result of CTCs formed between PIs and Iod. High double bond conversions can stem from combination of two types of photoinitiation mechanisms: oxidative interaction between BP in PIs and Iod, and CTC between amines in PIs and Iod.

Table 4.2. Photopolymerization formulations. PI = 0.5 wt% with respect to BP moiety and EDB, Iod = 2 wt% in the formulation. [a] OAA = 3 wt%, [b] OAA = 3 wt%, BP = 0.5 wt%, [c] BP = 1 wt%.

<b>Formulations</b>	<b>PI</b>	<b>Coinitiator</b>	<b>HEMA (wt%)</b>	<b>PEGDA (wt%)</b>
<b>1</b>	OAA-B	-	100	-
<b>2</b>	OAA-B	EDB	60	40
<b>3</b>	OAA-B	Iod	100	-
<b>4</b>	OAA-B	Iod	60	40
<b>5<sup>[a]</sup></b>	OAA	Iod	100	-
<b>6<sup>[b]</sup></b>	OAA + BP	Iod	100	-
<b>7<sup>[b]</sup></b>	OAA + BP	-	100	-
<b>2-P</b>	OAA-BP	EDB	60	40
<b>3-P</b>	OAA-BP	Iod	100	-
<b>4-P</b>	OAA-BP	Iod	60	40
<b>5-P</b>	OAA-BP	-	60	40
<b>BP-1</b>	BP	Iod	100	-
<b>BP-2</b>	BP	Iod	60	40

Photopolymerization studies were also performed under 320–500 nm irradiation by real time FTIR in air and in laminate for formulation 4 and 4-P. As indicated in Figure 4.14, slower polymerization was observed with OAA-B under air compared to OAA-BP but high conversions were achieved in all cases. More rapid polymerization was observed under laminated conditions for both of the PIs.

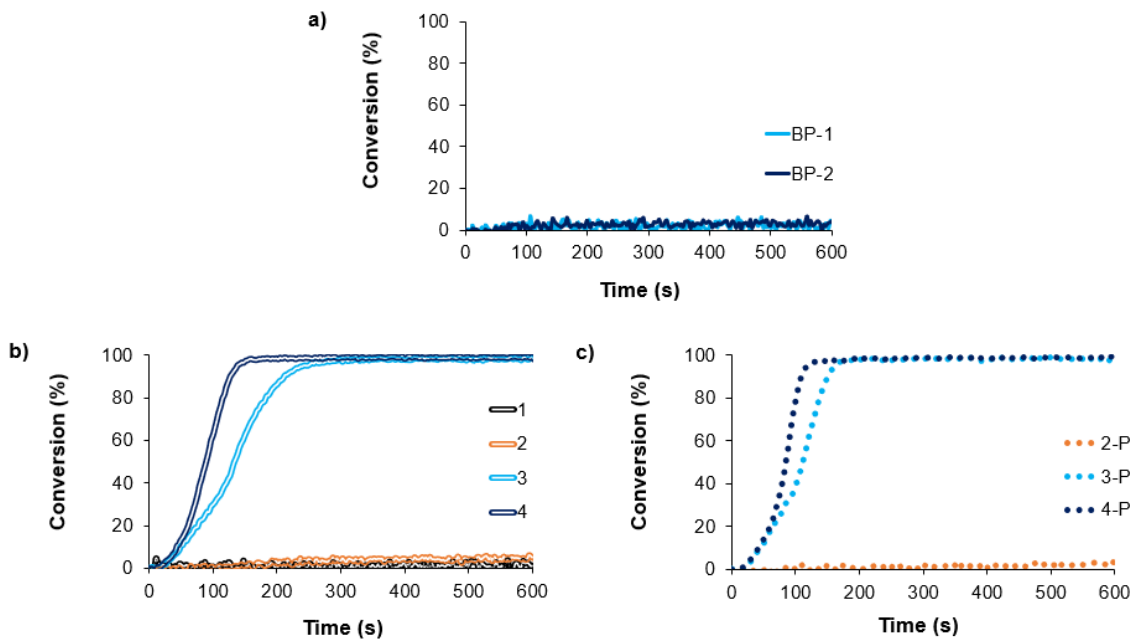


Figure 4.13. (Meth)acrylate conversions (from FTIR experiments) of formulations under air at room temperature upon exposure to LED@405 nm; thickness=1.4 mm: (a) formulation BP-1 and BP-2, (b) formulation 1–4 and (c) formulation 2-P–4-P. Light was turned on at 10 s.

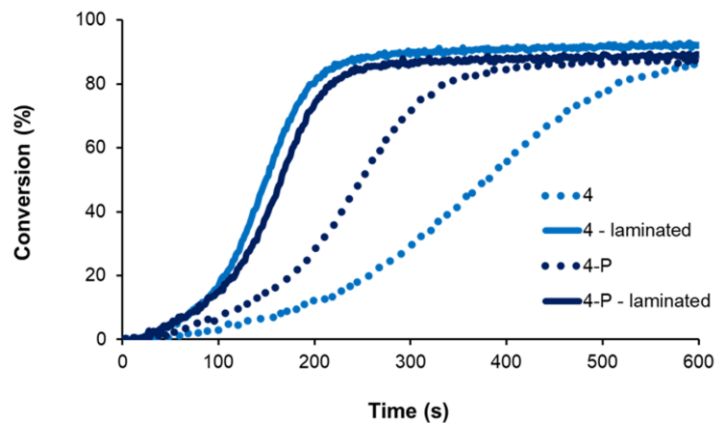


Figure 4.14. (Meth)acrylate conversions (from FTIR experiments) of formulations 4 and 4-P in air and in laminate at room temperature upon exposure to 320 - 500 nm; Light was turned on at 10 s.

Photo-DSC studies were carried out to analyze the photoinitiation efficiencies of the OAA backbone and the BP functionality separately; and then that of their combination in OAA-BP and OAA-B. These studies were performed under two different irradiation conditions: 320–500 nm and 400–500 nm (Figure 4.15, Figure 4.16). To observe the effect of the backbone structure, first OAA/Iod system (formulation 5) which contained 3 wt% OAA (since approximately 3 wt% of the formulations of the synthesized PIs is OAA) was prepared. As shown in Figure 14, the OAA/ Iod system is not very effective in initiating FRP of HEMA at visible wavelength range, but quite effective under 320– 500 nm irradiation; indicating more efficient complex formation in UV region. The curves showed characteristics of HEMA polymerization, diffusion-controlled polymerization due to gel effect observed at low conversion. In order to investigate coinitiator ability of OAA, the OAA/BP mixture (formulation 7) was prepared. This formulation contains 3 wt% OAA and 0.5 wt % of BP, same concentrations as in OAA-B or OAA-BP containing formulations. It was observed that OAA/BP can initiate polymerization of HEMA very slowly at 320–500 nm irradiation, however it is not effective under 400–500 nm (Figure 4.15). As a result, OAA may not be an efficient coinitiator for Type II photopolymerization because it does not contain tertiary amines; but very reactive in formation of CTC in combination with Iod. Slow polymerization can stem from the steric hindrance of the oligomeric radical. HEMA was also polymerized using OAA/BP/Iod system (formulation 6). The results indicate that, like the OAA/Iod system, the OAA/BP/Iod system is not efficient at visible wavelength range; only a decrease in  $t_{max}$  was observed. In UV region, the presence of BP leads to Type II photoinitiation with Iod, in addition to CTC between OAA/Iod, which results in faster polymerization than formulation 5.

Pis where BP is incorporated on OAA backbone, OAA-B and OAA-BP alone (e.g. formulation 5-P) are not effective in FRP at both wavelength ranges (Figure 4.16), although OAA/BP system (formulation 7) is quite reactive in UV range. This can probably be understood by OAA-BP having a singlet excited state whereas the BP in the OAA/BP formulation has a triplet excited state and interacts with amines. OAA-B/Iod and OAA-BP/Iod systems, formulations 3, 3-P and 4-P, were found to be very efficient for FRP under both UV and visible region (Figure 4.15, Figure 4.16). The conversions reached for 3, 3-P, 4-P, 5 and 6 were found to range between 72–100%. We are unable to explain our observation that covalent bonding of BP to the macromolecular backbone leads to much

more efficient polymerization under visible light than when OAA and BP are separately mixed (again, both cases in the presence of Iod). We hypothesize that additional Iod interaction with the tertiary amines formed by the attachment of BP and phosphonate functionalities to the backbone may increase the visible light activity.

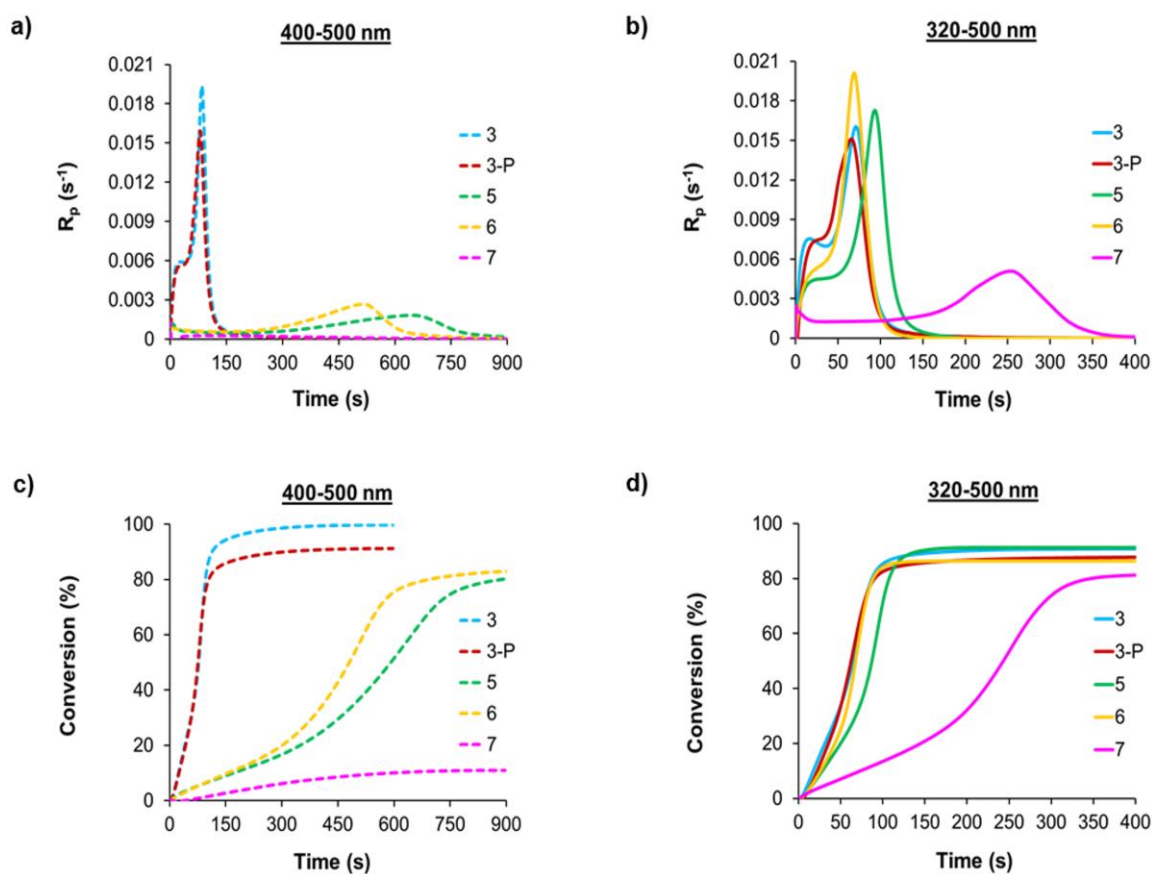


Figure 4.15. Rate of polymerization vs. time and conversion vs. time plots for the photopolymerization of formulations 3, 3-P, 5, 6 and 7 under nitrogen at 30 °C upon exposure to light at (a), (c) 400–500 nm and (b), (d) 320–500 nm.

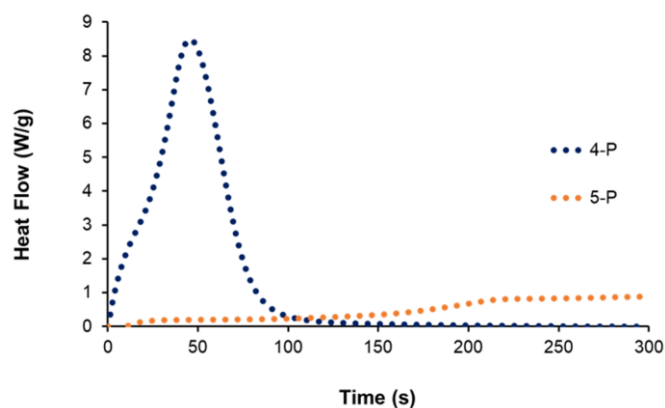
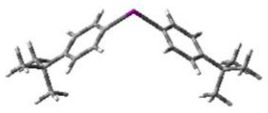
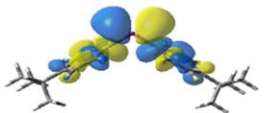
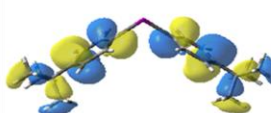
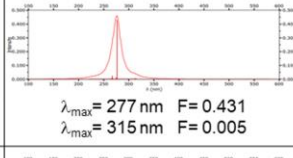
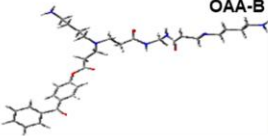
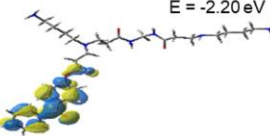
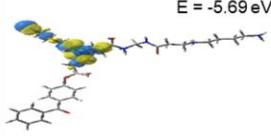
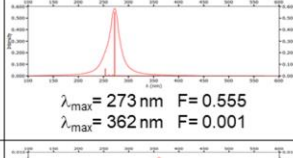
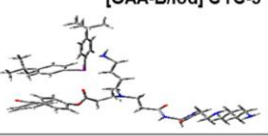
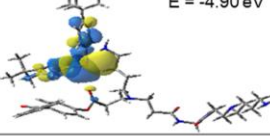
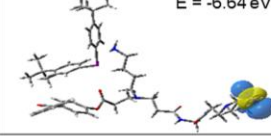
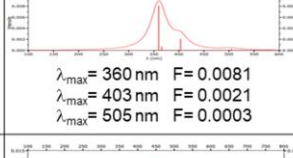
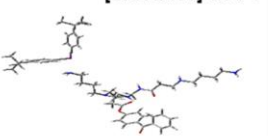
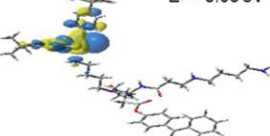
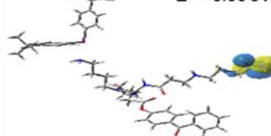
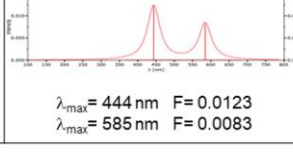


Figure 4.16. Photopolymerization heat flow curves of formulations 4-P (with Iod) and 5-P (no additives) under nitrogen at 30 °C upon exposure to light at 320-500 nm.

#### 4.3.5. Molecular Modeling Studies

OAA, OAA-B and OAA-BP showed efficient initiating ability in combination with Iod by forming CTC. To understand the interaction between them, molecular modeling studies were performed by using DFT calculations. The (frontier) molecular orbitals (MOs) and computed absorption (UV-vis) spectra for Iod alone, OAA-B alone, [OAA-B/Iod] CTC 1° and [OAA-B/Iod] CTC 3° (Figure 4.9b) are shown in Table 4.3. The PIs contain 1°, 2°, and 3° amines, indicating more than one possibility for CTC formation. For both [OAA-B/Iod] CTC 1° and [OAA-B/Iod] CTC 3°, the LUMO is located on the Iod (electron acceptor), whereas the HOMO is located on the oligomeric backbone (electron donor). The energy difference between the LUMO and the HOMO in CTCs is reduced, it is much less than that of OAA-B or Iod alone. [OAA-B/Iod] CTC 1° has more reduced gap (1.50 eV difference) compared to [OAA-B/Iod] CTC 3° (1.74 eV difference). The BP functionality is bonded to OAA by the carbonyl moiety which is an electron withdrawing group. Therefore electrons on the 3° amine on [OAA-B/Iod] CTC 3° might be withdrawn to BP via carbonyl which can lead to increased gap between HOMO and LUMO. As a result, PIs form efficient CTCs with different amines in their structures resulting in excellent photoinitiating ability under visible light. The calculated UV-visible spectra indicate that CTCs have absorption in visible range, which is compatible with experimental UV-visible and photopolymerization results.

Table 4.3. Frontier molecular orbital properties of Iod, OAA-B and the CTC optimized structure ([OAA-B-Iod]CTC) and their respective calculated UV-vis spectra (F = oscillator strength).

Optimized Structures	LUMO	HOMO	Calculated UV-Vis absorption
 <p>Iodonium</p>	 <p>E = -5.71 eV</p>	 <p>E = -10.29 eV</p>	 <p><math>\lambda_{\text{max}} = 277 \text{ nm}</math> F = 0.431  <math>\lambda_{\text{max}} = 315 \text{ nm}</math> F = 0.005</p>
 <p>OAA-B</p>	 <p>E = -2.20 eV</p>	 <p>E = -5.69 eV</p>	 <p><math>\lambda_{\text{max}} = 273 \text{ nm}</math> F = 0.555  <math>\lambda_{\text{max}} = 362 \text{ nm}</math> F = 0.001</p>
 <p>[OAA-B/Iod] CTC-3°</p>	 <p>E = -4.90 eV</p>	 <p>E = -6.64 eV</p>	 <p><math>\lambda_{\text{max}} = 360 \text{ nm}</math> F = 0.0081  <math>\lambda_{\text{max}} = 403 \text{ nm}</math> F = 0.0021  <math>\lambda_{\text{max}} = 505 \text{ nm}</math> F = 0.0003</p>
 <p>[OAA-B/Iod] CTC-1°</p>	 <p>E = -5.03 eV</p>	 <p>E = -6.53 eV</p>	 <p><math>\lambda_{\text{max}} = 444 \text{ nm}</math> F = 0.0123  <math>\lambda_{\text{max}} = 585 \text{ nm}</math> F = 0.0083</p>

#### 4.3.6. Radical Formation Mechanism

The proposed mechanism for the photoinitiation of (meth)acrylates are presented in Figure 4.17. Irradiation of the PIs transforms them from ground state to excited state. The interaction between PIs and Iod through an oxidative pathway leads to the generation of aryl radicals ( $\text{Ar}\cdot$ ) capable of initiating the free-radical polymerization of (meth)acrylates. Also, the formation of a CTC between the amine groups of the PIs and Iod generate aryl radicals through radical cation intermediate to initiate FRP. According to the ESR results, aminoalkyl radical ( $-\text{NCH}^*$ ) is also generated, possibly through electron transfer between radical cation and the PI itself. Formulations without Iod do not polymerize under visible light, indicating that aminoalkyl radical is not produced (or is produced in a negligible amount).

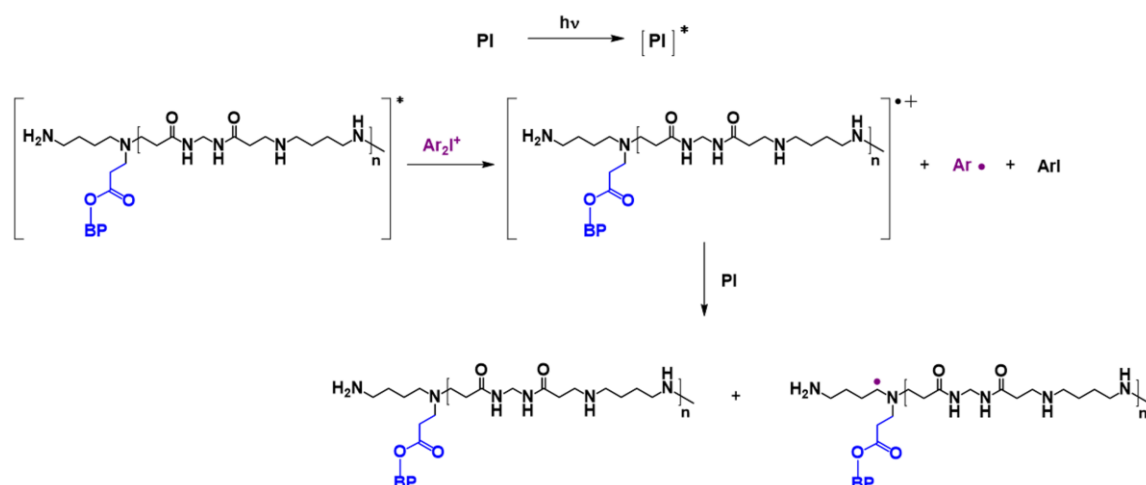


Figure 4.17. Proposed mechanism for the photoinitiation.

#### 4.4. Conclusion

Two BP-substituted oligo(amido amine)s were successfully synthesized and characterized by  $^1H$ ,  $^{13}C$  NMR and FTIR spectroscopy. The synthesis method facilitates many possible functionalizations on the OAA backbone for various purposes, such as tailoring properties of the cured films; in this work we attached a phosphonate group as an example, to increase biocompatibility. These compounds, when combined with Iod, can be used as photoinitiators for visible-light initiated FRP of (meth)acrylates in the presence of air. The excellent initiating abilities of these PIs are due to combination of BP/Iod interaction and CTC formation between amine groups on OAA backbone and Iod, confirmed by DFT studies. The proposed photoinitiation mechanism involves aryl radicals from CTC and oxidative interaction of BP, and aminoalkyl radicals from OAA backbone.

## **5. A WATER SOLUBLE, LOW MIGRATION, AND VISIBLE LIGHT PHOTOINITIATOR BY THIOXANTHONE-FUNCTIONALIZATION OF POLY(ETHYLENE GLYCOL)-CONTAINING POLY( $\beta$ -AMINO ESTER)**

This chapter is published as: Gencoglu, T., T.N. Eren, J. Lalevée, and D. Avci, “A Water Soluble, Low Migration, and Visible Light Photoinitiator by Thioxanthone-Functionalization of Poly (ethylene glycol)-Containing Poly ( $\beta$ -amino ester)”, *Macromolecular Chemistry and Physics*, p. 2100450, 2022. This copyrighted article was reproduced with permission from John Wiley and Sons (Figure A.19).

### **5.1. Introduction**

In this chapter, a novel photoinitiator (PI) is described here for low ecological impact, p(PEGDA575-TX): It is water soluble, polymerizable, thioxanthone (TX) functional, and is a one-component poly(ethylene glycol)-based poly( $\beta$ -amino ester). Our choice of PEGDA as a diacrylate for poly( $\beta$ -amino ester) (PBAE) synthesis was to increase the water solubility of the PI, and TX-functional amine brings visible-light activation. The PEG and aminoalkyl groups in the backbone may act as hydrogen donors for the TX group, possibly enabling one-component use. The synthesized photoinitiator contains thioxanthone and tertiary amine in each repeating unit which leads to an increase in the concentration of these functionalities. With this increase, the photosensitization ability of the PI, its oxygen inhibition ability and cointiation performance are improved. The diacrylate end groups of the synthesized PI lead to incorporation into the network which contributes to migration stability. This PI is expected to be non-toxic due to PEG-containing PBAE structure. It is also soluble in a variety of monomers such as 2-hydroxy ethyl methacrylate (HEMA), triethyleneglycol dimethacrylate (TEGDMA), PEGDA and trimethylolpropane triacrylate (TMPTA), which may lead to utilization in different areas. The reactivity of the novel photoinitiator was studied under UV and visible light irradiation during polymerization of said monomers by differential scanning photocalorimetry (photo-DSC), real time Fourier transform infrared (FTIR) and a

photoreactor. The solubility, UV-visible absorption, steady-state and laser flash photolysis and migration properties were investigated.

## 5.2. Experimental Section

### 5.2.1. Materials

2-Hydroxy-9H-thioxanthen-9-one and 2-(2-aminoethoxy)-9H-thioxanthen-9-one (TXOCH<sub>2</sub>CH<sub>2</sub>NH<sub>2</sub>) were synthesized according to the literature procedures [120], [233,234]. Boc-2-bromoethylamine, trifluoroacetic acid (TFA), 1,8-diazabicyclo[5.4.0]undec-7-ene (DBU), acrylamide (AAm), potassium carbonate, potassium iodide, sodium bicarbonate, ethyl 4-(dimethylamino)benzoate (EDB), poly(ethylene glycol) diacrylate (PEGDA, M<sub>n</sub> = 575 D) and the other reagents and solvents were purchased from Sigma-Aldrich and used as received without further purification. Bis-(4-tert-butylphenyl)-iodonium hexafluorophosphate (SpeedCure938 or Iod) was obtained from Lambson Ltd.

### 5.2.2. Characterization

<sup>1</sup>H-NMR spectra were recorded on a Varian Gemini (400 MHz) spectrometer with deuterated chloroform (CDCl<sub>3</sub>) as solvent and tetramethylsilane as an internal standard. A Nicolet 6700 FTIR spectrophotometer was used for recording IR spectra. GPC analysis was performed in THF using polystyrene standards with Malvern – OmniSEC at Middle East Technical University (METU) Central Laboratory, Ankara, Turkey.

### 5.2.3. Synthesis of p(PEGDA575-TX)

2-(2-Aminoethoxy)-9H-thioxanthen-9-one (58 mg, 0.213 mmol), PEGDA (135 mg, 0.235 mmol) and DBU (16.3 mg, 0.107 mmol) were dissolved in DMF (1.88 mL), and stirred for 2 d at 70 °C. After removal of DMF under reduced pressure the residue was dissolved in dichloromethane and precipitated into diethyl ether (150 mL) to remove unreacted PEGDA and amine, and dried under reduced pressure. p(PEGDA575-TX) macromer was obtained as a yellow viscous liquid in 25% yield.

$^1\text{H-NMR}$  ( $\text{CDCl}_3$ , 400 MHz,  $\delta$ ): 2.47 (4 H,  $\text{O}=\text{C}-\text{CH}_2$ ), 2.87 (6 H,  $\text{CH}_2-\text{N}$ ), 3.62 (32 H,  $\text{O}-\text{CH}_2-\text{CH}_2-\text{O}$ ), 4.1–4.3 (10 H,  $\text{CH}_2-\text{O}-\text{C}=\text{O}$ ,  $\text{O}-\text{CH}_2-\text{CH}_2-\text{N}$ ), 5.77, 6.36 (4 H,  $\text{CH}_2=\text{CH}$ ), 6.09 (2 H,  $\text{CH}=\text{CH}_2$ ), 7.2–8.6 (7 H, aromatic hydrogens) ppm.

FTIR (attenuated total reflectance, ATR): 1100 ( $\text{C}-\text{O}-\text{C}$ ), 1591 ( $\text{C}=\text{C}$ ), 1633 & 1728 ( $\text{C}=\text{O}$ ), 2866 ( $\text{C}-\text{H}$ )  $\text{cm}^{-1}$ .

#### 5.2.4. Photochemical Analysis

5.2.4.1. UV-vis Spectroscopy Experiments. UV-vis measurements were carried out by Carry 3 UV-vis spectrophotometer from Varian. Chloroform solutions of the PI with or without the additives (EDB, Iod) were irradiated with LED@385 nm for steady state photolysis and UV-vis spectra were recorded at different irradiation times. Molar extinction coefficient values were calculated by Beer-Lambert formula  $A = \epsilon c b$ . Here the concentration of the polymer was calculated using weight of the polymer and its number-average molecular weight [ $M_n = (\text{formula weight of end groups}) + (\text{formula weight of repeating unit})(n)$ ]. The number of repeating unit ( $n$ ) was estimated using  $^1\text{H NMR}$ .

5.2.4.2. LFP Experiments. A Q-switched nanosecond Neodymium-doped yttrium aluminum garnet (Nd/YAG) laser ( $\lambda_{\text{exc}} = 355$  nm, 9 ns pulse width; energy reduced down to 10 mJ) by Continuum and an analyzing system consisting of a ceramic xenon lamp, a monochromator, a fast photomultiplier and a transient digitizer (Luzchem LFP 212) were used to carry out nanosecond LFP experiments [219].

#### 5.2.5. Photopolymerization

The photosensitive formulations were prepared by first mixing the PI (0.8 wt%, with respect to TX moiety) with the monomers (HEMA, TEGDMA, PEGDA or TMPTA) and then adding Iod or EDB (2 wt%).

5.2.5.1. RT-FTIR Spectroscopy. Nicolet 6700 real-time Fourier transform infrared spectrometer was used to follow the (meth)acrylate function conversions versus time for polymerizations. Formulations (PI/Iod/HEMA, PI/Iod/TEGDMA, TX/Iod/HEMA,

TX/Iod/TEGDMA) were irradiated by a mercury arc lamp (Omniscure s1000–100 W, 320–500 nm) at 30 °C in aerated medium. The photopolymerizations were monitored by following the infrared (meth)acrylate C=C double-bond peak area at 1610–1650 cm<sup>-1</sup>. The conversion of functional groups was determined using

$$\text{(Meth)acrylate conversion (\%)} = \left(1 - \frac{A_t(1610-1650)}{A_0(1610-1650)}\right) \times 100, \quad (5.1)$$

where  $A_0$  and  $A_t$  denote area of the meth/acrylate bands, and the subscripts  $t$  and  $0$  indicate the curing time and the beginning of the curing.

**5.2.5.2. Photo-DSC.** Photo-DSC analyses were conducted on a DSC 250 (TA Instruments) equipped with a UV–vis light source, Omniscure 2000 with dual-quartz light guide. A visible light filter was used to perform polymerization in the 400–500 nm range. Formulations (3–4 mg) were irradiated for 5 – 20 min at 30 °C and under nitrogen flow of 50 mL min<sup>-1</sup>. The heat flow of the polymerization reaction was monitored as a function of time. The cure speed of polymerization reactions were calculated by using equation (5.2) [235]

$$\text{Rate} = \frac{(Q/s)M}{n(\Delta H_p)m}, \quad (5.2)$$

where  $Q/s$  is the heat flow per second,  $M$  is the molar mass of the monomer,  $n$  is the number of double bonds per monomer molecule,  $\Delta H_p$  is the heat of reaction evolved and  $m$  is the mass of monomer in the sample. The theoretical heats for the total conversion of an acrylate and methacrylate double bond are 86 and 55 kJ mol<sup>-1</sup>, respectively.

**5.2.5.3. Photoreactor.** p(PEGDA575-TX) ( $2.5 \times 10^{-3}$  M) and AAm (4 M) in deionized (DI) water was placed into a pyrex tube and irradiated in a photoreactor containing 12 Philips TL 8W BLB lamps, exposing it to UV light (365 nm) for 30 min.

### 5.2.6. Migration Study

TMPTA in the presence of p(PEGDA575-TX) (0.8 wt%)/EDB (2 wt%) and TX (0.8 wt%)/EDB (2 wt%) was photopolymerized (365 nm) for 90 min in glass vials in the photoreactor described above. The crosslinked polymers were soaked in chloroform for 60 h. The amount of extracted PI was determined by UV–vis spectroscopy [141].

### 5.3. Results and Discussion

#### 5.3.1. Synthesis and Characterization of Photoinitiator

The novel PI was obtained from TXOCH<sub>2</sub>CH<sub>2</sub>NH<sub>2</sub> which was synthesized in two steps [120] according to a general method in reference [233] with an overall yield of 60% (Figure 5.1). First, tert-butyl (3-((9-oxo-9H-thioxanthen-2-yl)oxy)ethyl)carbamate was obtained by a Williamson etherification between 2-hydroxy-9H thioxanthen-9-one and boc-2-bromoethylamine, following a deprotection of the amine group in the presence of TFA. Finally, aza-Michael addition reaction between PEGDA (M<sub>n</sub> = 575 D) and TXOCH<sub>2</sub>CH<sub>2</sub>NH<sub>2</sub> was achieved in dimethyl formamide in the presence of DBU which led to our macromolecular PI, p(PEGDA575-TX). DBU was used as a promoter for aza-Michael reaction to increase the yield [236]. PEGDA was used in excess (acrylate:amine mol ratio = 1.1:1–1.3:1) to obtain a polymerizable PI. The product was purified by precipitation into diethyl ether in which the starting materials are soluble. p(PEGDA575-TX) is a viscous liquid, soluble in water (6–8 g L<sup>-1</sup>), dimethyl formamide (DMF), MeOH, CHCl<sub>3</sub> and tetrahydrofuran (THF).

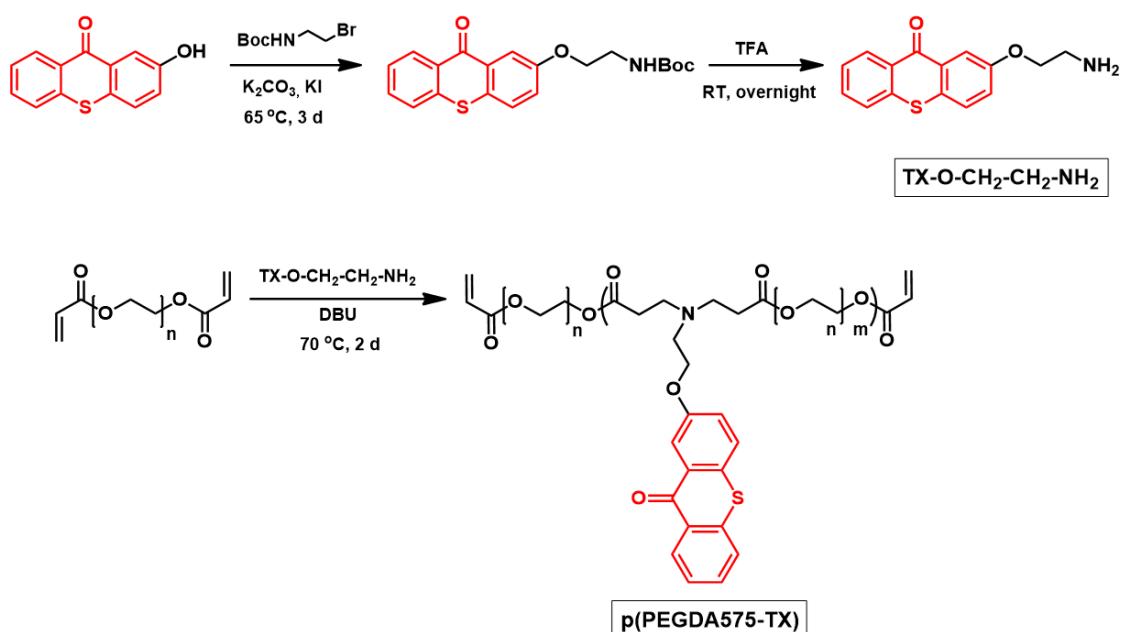


Figure 5.1. Synthesis of TXOCH<sub>2</sub>CH<sub>2</sub>NH<sub>2</sub> and p(PEGDA575-TX).

The structure of p(PEGDA575-TX) was confirmed by  $^1\text{H}$  NMR and FTIR spectroscopies.  $^1\text{H}$  NMR spectrum of the PI shows the aromatic protons of TX between 7.2–8.6 ppm (Figure 5.2). The peak at 3.62 ppm is ascribed to the characteristic methylene protons of the PEG backbone. The peaks between 5.77 and 6.36 ppm show the double bond protons proving the successful synthesis of the polymerizable PI. The average number of repeating units ( $n$ ) was calculated by integrating acrylate protons (assuming that all end groups are acrylates) with respect to methylenes attached to  $\text{C}=\text{O}$  (2.5 ppm) and nitrogen ( $\approx 3$  ppm) and also aromatic protons. The  $n$  values were found to change between 3 and 8, corresponding to  $M_n$  values between 3100 and 7350. p(PEGDA575-TX) contains 20 – 23 wt% TX. Gel permeation chromatography (GPC) analysis was carried out to determine the molecular weight of one of the macromers.  $M_n$ ,  $M_w$  and polydispersity index (PDI) values were found to be 4400, 5100 and 1.16.

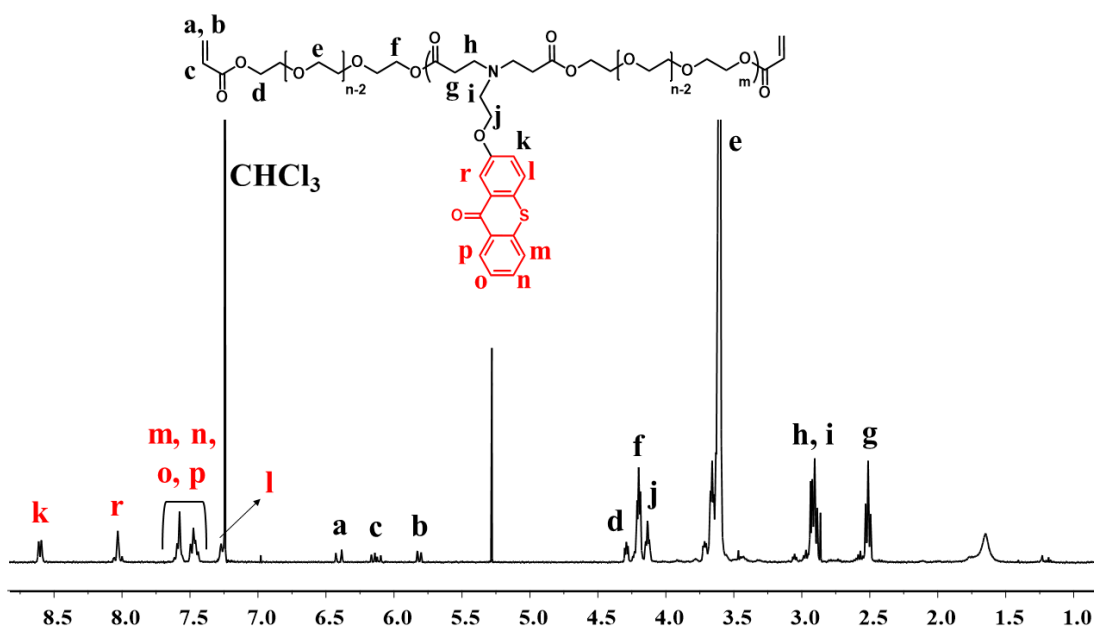


Figure 5.2.  $^1\text{H}$ -NMR spectrum of p(PEGDA575-TX).

To better understand the effect of the catalyst DBU, the synthesis was also performed in its absence. However, no product remained after precipitation into diethyl ether, which shows solubility of the products in that medium. The  $^1\text{H}$  NMR spectrum of the product mixture before precipitation (Figure 5.3), which probably includes monoadducts, shows

multiple peaks between 2.4–3.1 ppm in contrast to two clean peaks in this region for p(PEGDA575-TX). The monoadducts and other products mentioned above probably are formed also in the presence of DBU, however they are removed during the purification step.

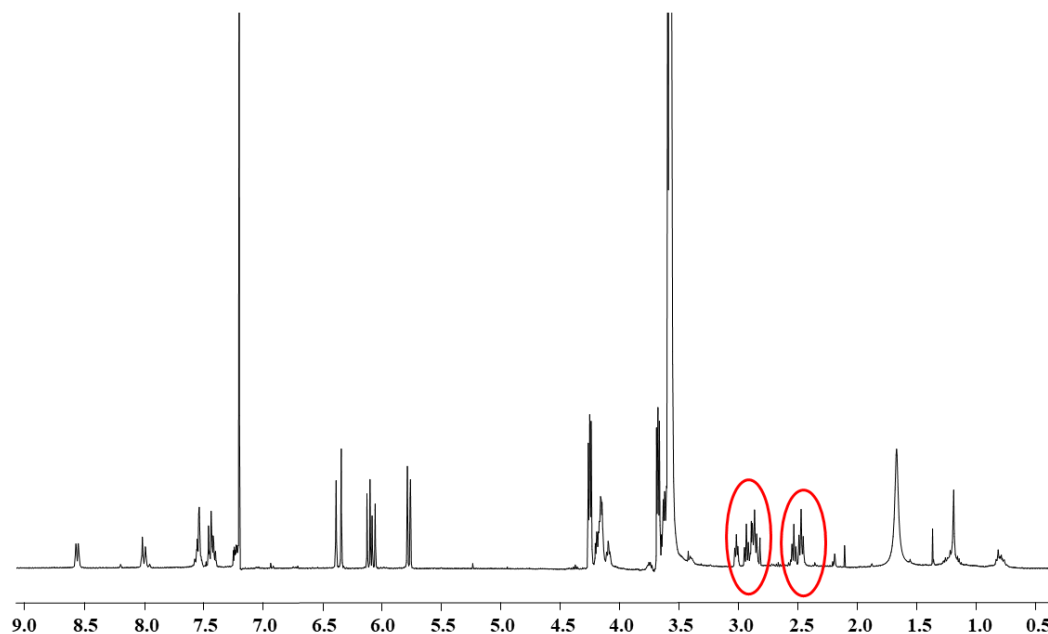


Figure 5.3.  $^1\text{H}$  NMR spectrum of p(PEGDA575-TX) synthesized in the absence of DBU.

The FTIR spectrum of p(PEGDA575-TX) showed strong peaks at 1728 and 1633  $\text{cm}^{-1}$  due to ester and ketone carbonyl stretchings (Figure 5.4).

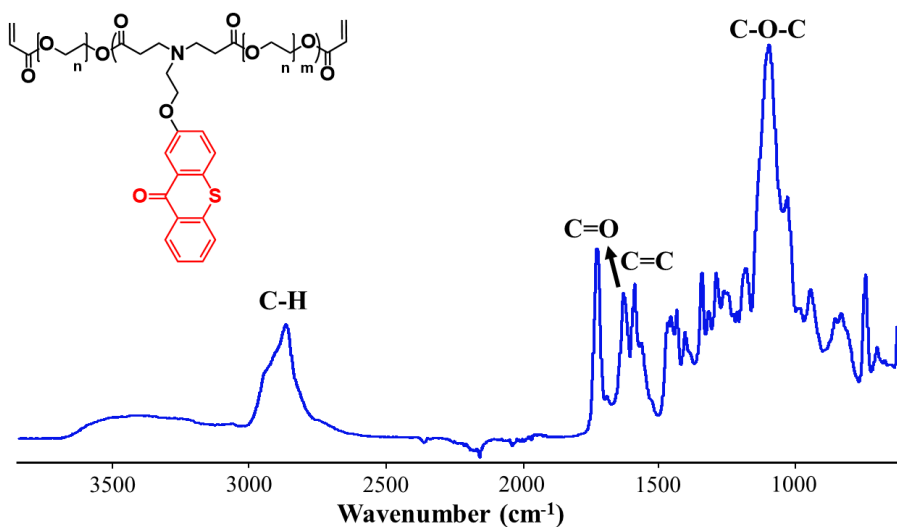


Figure 5.4. FTIR spectrum of p(PEGDA575-TX).

### 5.3.2. Light Absorption Properties

The absorption characteristics of p(PEGDA575-TX) ( $n = 8$ ) were determined by UV–vis spectroscopy in methanol, water and chloroform at room temperature and compared with the reference TX (Figure 5.5). p(PEGDA575-TX) showed three absorption maxima ( $\lambda_{\text{max}}$ ) whereas parent TX has two  $\lambda_{\text{max}}$  (Table 5.1). TX's peak around 250 nm splits into two peaks in p(PEGDA575-TX). Also, a strong bathochromic shift of 20 nm compared to TX was observed for p(PEGDA575-TX) in the 300–400 nm region, which can be explained by the introduction of oxygen atoms attached to the aromatic ring. It can be concluded that p(PEGDA575-TX) is suitable for photopolymerization under visible light. Although the TX concentration used is eight times more than p(PEGDA575-TX), the peaks have similar intensities, confirming higher concentration of TX groups in the PI due to the number of repeating units. The extinction coefficient values listed in Table 5.1 are six to eight times higher than parent TX, again consistent with the  $n$  number. Based on the range of the number of repeating units found, the extinction coefficients are between 14 000 and 47 000.

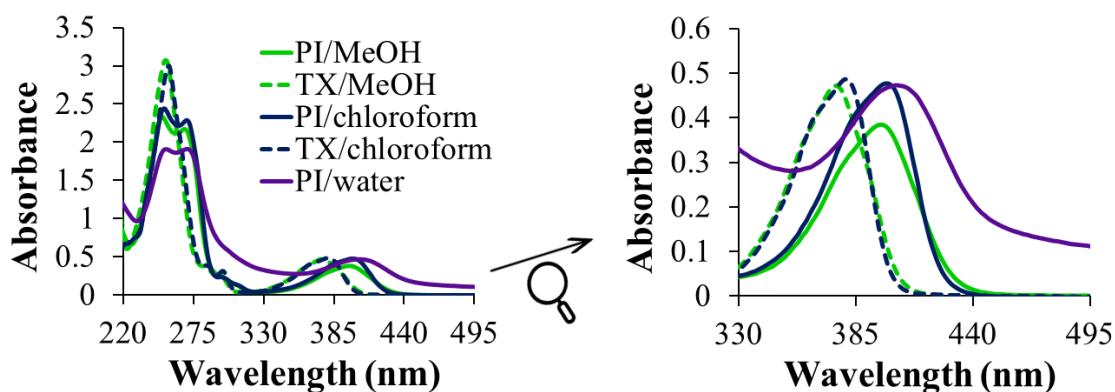


Figure 5.5. UV-vis absorption of p(PEGDA575-TX) ( $n = 8$ ) and TX in methanol, chloroform and water [ $p(\text{PEGDA575-TX})$ ] =  $1 \times 10^{-5}$  M, [ $\text{TX}$ ] =  $8 \times 10^{-5}$  M.

Table 5.1. Absorption characteristics of p(PEGDA575-TX) and TX in different solvents.

PI	$\lambda_{\text{max}}$ [nm]	$\epsilon$ [ $\text{M}^{-1} \text{cm}^{-1}$ ]
p(PEGDA575-TX)	254, 270, 404 (water)	44309 (404 nm)
	252, 268, 398 (methanol)	35168 (398 nm)
	252, 272, 400 (chloroform)	47217 (400 nm)
TX	254, 376 (methanol)	6183 (376 nm)
	256, 380 (chloroform)	6404 (380 nm)

### 5.3.3. Photochemical Mechanisms

Thioxanthone derivatives usually react from their triplet states. In order to probe the associated photochemical reactivity of the novel PI, laser flash photolysis (LFP) experiments were carried out to follow its triplet excited state in real time. Markedly, it is shown that p(PEGDA575-TX) has a rather similar triplet state lifetime to TX, i.e., 5–10  $\mu\text{s}$  (Figure 5.6). When coinitiators are added at increasing concentrations, the triplet state lifetime (and the peak intensity) decreases indicating that the PI undergoes H-abstraction (EDB) and photooxidation (Iod) via the triplet state (Figure 5.6b and Figure 5.6c).

Steady state photolysis studies were performed to investigate the efficiency of p(PEGDA575-TX) alone and in the presence of additives such as EDB and Iod. The photolysis of p(PEGDA575-TX) alone resulted in a decrease of the absorbance upon exposure to light-emitting diode (LED) @385 nm for 45 min, which can be explained with the hydrogen abstraction from the amino or PEG groups in the PI (Figure 5.7). The new peak observed around 330 nm with time may be due to coupling products of radicals such as ketyl radical and aminoalkyl radical (Figure 5.7b) [7], [237]. This result indicates that p(PEGDA575-TX) may be used as one-component polymerizable visible light photoinitiator. A similar photolysis rate was observed for the p(PEGDA575-TX)/EDB system (Figure 5.7c). The addition of Iod results in rapid photobleaching (Figure 5.7d), indicating a strong interaction between p(PEGDA575-TX) and Iod. These results show that p(PEGDA575-TX) favors photooxidation processes by Iod in comparison to photoreduction by EDB, PEG and amines in its structure.

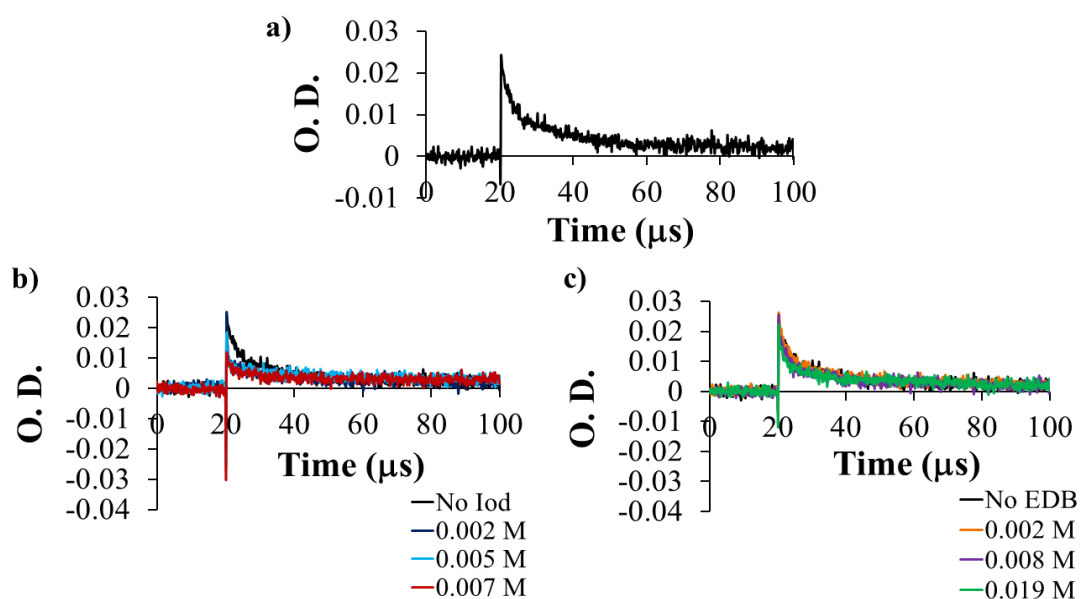


Figure 5.6. Triplet state decay traces observed after laser excitation of p(PEGDA575-TX) ( $n=4$ ) in chloroform at 355 nm, kinetic traces recorded at 600 nm under  $N_2$ : (a) without coinitiator, (b) with Iod, (c) with EDB.

### 5.3.4. Photopolymerization Results

In order to investigate the initiation ability of p(PEGDA575-TX), the free radical polymerizations of HEMA, TEGDMA, TMPTA and PEGDA were performed by photo-DSC using visible radiation (400–500 nm) at 30 °C under nitrogen and compared to TX as reference. The typical  $R_{pmax}$ -time and conversion–time profiles are given in Figures 5.8 and Figure 5.9. First, the one-component nature of p(PEGDA575-TX) was investigated in the absence of an additional coinitiator (Figure 5.8). It can be seen that p(PEGDA575-TX) alone induced efficient free radical photopolymerization of TMPTA (Figure 5.8a). The TMPTA/p(PEGDA575-TX) system polymerized faster ( $R_{pmax} = 0.0224 \text{ s}^{-1}$ ,  $t_{max} = 0.06 \text{ min}$ , conversion = 40%) than the TMPTA/TX system ( $R_{pmax} = 0.0075 \text{ s}^{-1}$ ,  $t_{max} = 0.35 \text{ min}$ , conversion = 38%). However, the novel PI is not able to initiate polymerization of HEMA efficiently but shows slightly better performance during polymerization of TEGDMA, both monomers are methacrylates but TEGDMA is difunctional (Figure 5.8b). For another comparison, we considered the water soluble PEG based TX derivative synthesized by Akat et al. and used in photopolymerization of HEMA (light source: 320–500 nm) [157]; the conversion of the p(PEGDA575-TX)/HEMA formulation (light source: 400–500 nm) was found to be higher than reported by Akat et al.

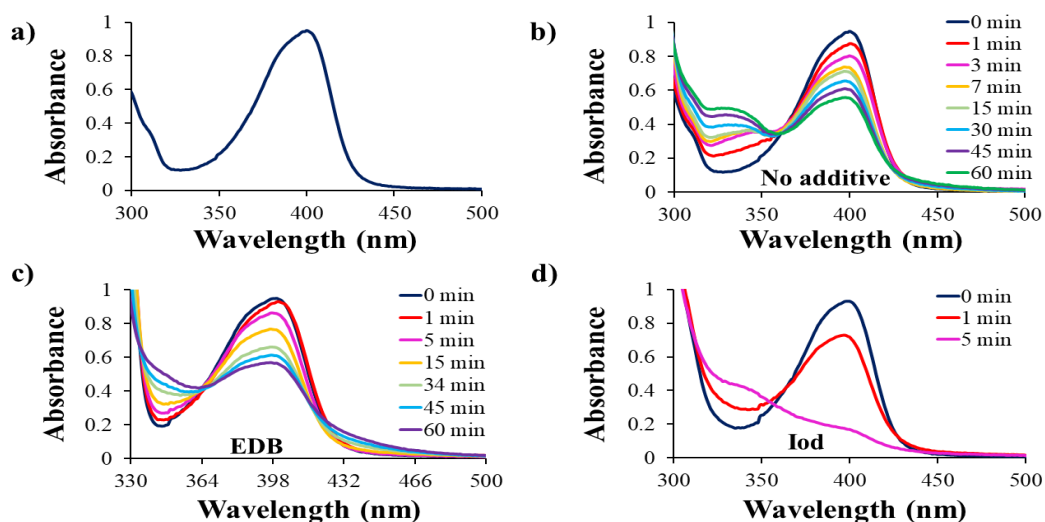


Figure 5.7. (a) UV–vis absorption spectrum of p(PEGDA575-TX) ( $n = 4$ ), photolysis of p(PEGDA575-TX) alone (b), in the presence of (c) EDB ( $1 \times 10^{-3} \text{ M}$ ) and (d) Iod ( $1 \times 10^{-3} \text{ M}$ ) using a 385 nm LED. Solvent: chloroform, [PI]:  $4 \times 10^{-5} \text{ M}$ .

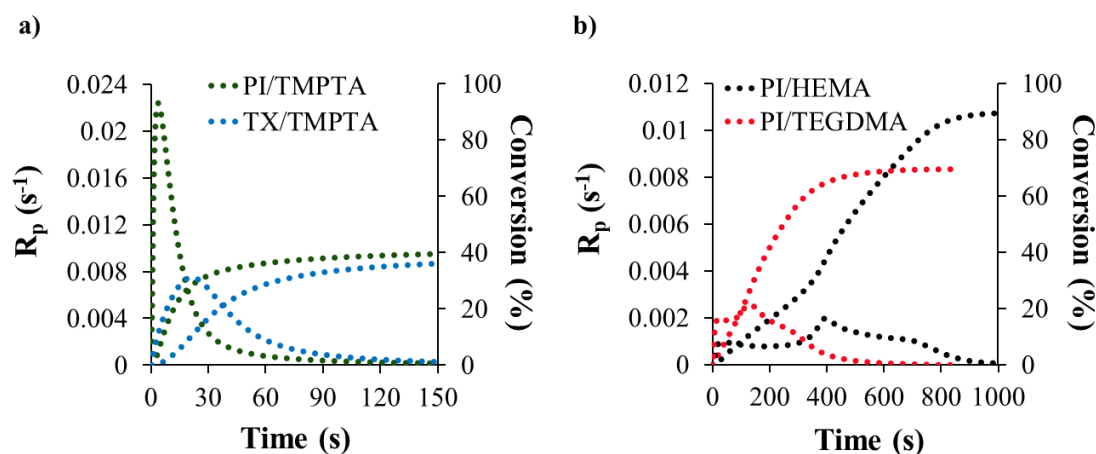


Figure 5.8. Rate of polymerization and double bond conversion graphs of (a) TMPTA and (b) HEMA and TEGDMA in the absence of coinitiators at 30 °C under nitrogen irradiated by 400–500 nm. PI = 0.8 wt% wrt TX moiety.

The photopolymerization ability of p(PEGDA575-TX) was also investigated in the presence of coinitiators such as Iod and EDB (Figure 5.9). It was observed that addition of EDB or Iod leads to both higher  $R_{pmax}$  and similar or higher conversions for TEGDMA and TMPTA. For example, TEGDMA/p(PEGDA575-TX)/EDB, TEGDMA/p(PEGDA575-TX)/Iod systems showed enhanced rates ( $R_{pmax} = 0.0199$  and  $0.0422 s^{-1}$ ),  $t_{max}$  (25.8 and 13.2 s) and conversions (83% and 80%) compared to TEGDMA/p(PEGDA575-TX) alone ( $R_{pmax} = 0.0025 s^{-1}$  and conversion 69%). Also, enhanced  $R_p$  and shorter induction time were observed for p(PEGDA575-TX)/Iod system compared to p(PEGDA575-TX)/EDB system. This result is consistent with the results obtained from photolysis experiments, indicating very fast photolysis of p(PEGDA575-TX)/Iod system. Similar to TEGDMA, TMPTA photopolymerizes more rapidly with Iod in comparison to EDB (Figure 5.9). The commercial photoinitiator TX shows slower photopolymerization kinetics compared to p(PEGDA575-TX) in the presence of both Iod or EDB. One reason can be the better visible light absorption properties (bathochromic shift of 20 nm compared to TX and higher extinction coefficient) of p(PEGDA575-TX) compared to TX. Another reason can be the presence of tertiary amines (donor) on the PI which may form charge transfer complexes with iodonium salts (acceptor) and also contribute to radical generation under near UV or visible light irradiation.

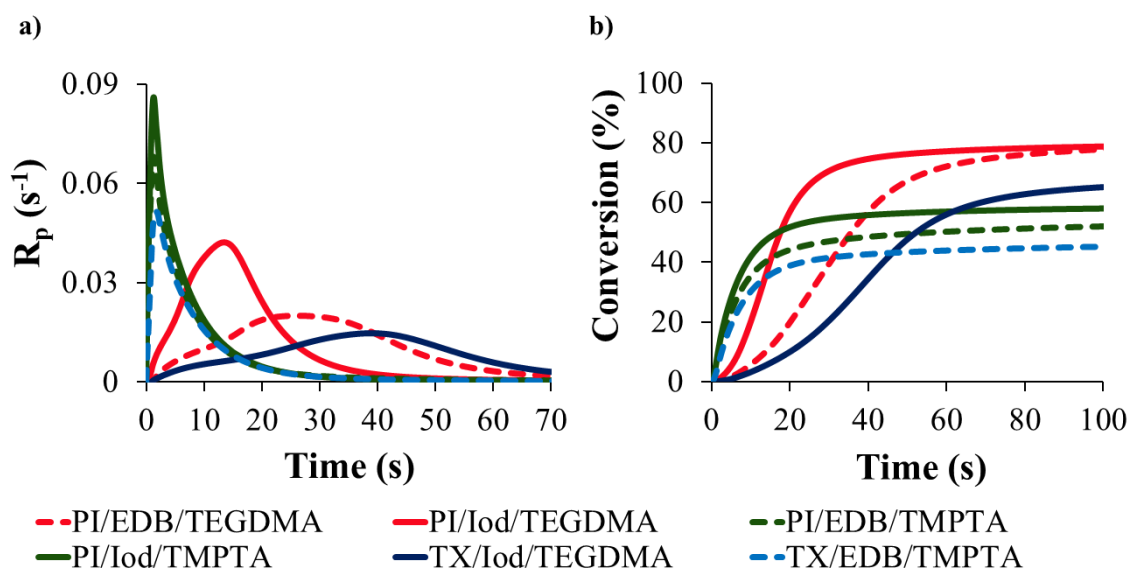


Figure 5.9. (a) Rate of polymerization and (b) double bond conversion graphs of TEGDMA and TMPTA in the presence of coiniciators at 30 °C under nitrogen irradiated by visible light (400–500 nm). PI = 0.8 wt% wrt TX moiety, Iod and EDB = 2 wt%.

It is known that low-molecular weight tertiary amines are effective for reducing the effects of oxygen inhibition. They react with unreactive peroxy radicals formed by the reaction of growing radical chains and oxygen, to convert them to reactive alkylamino radicals. However, small free amines are toxic and have migration problems. Since p(PEGDA575-TX) contains tertiary amines in its structure it can also reduce oxygen inhibition during photopolymerization in air. Therefore, the efficiency of the synthesized PI in air has been also investigated using real-time (RT)-FTIR during photopolymerization of HEMA and TEGDMA upon irradiation with light at 320–500 nm and compared to that of TX. As shown in Figure 5.10, TX/Iod system did not polymerize HEMA and TEGDMA under air. In contrast, formulations containing p(PEGDA575-TX)/Iod were efficiently polymerized, indicating the effect of amines on oxygen inhibition.

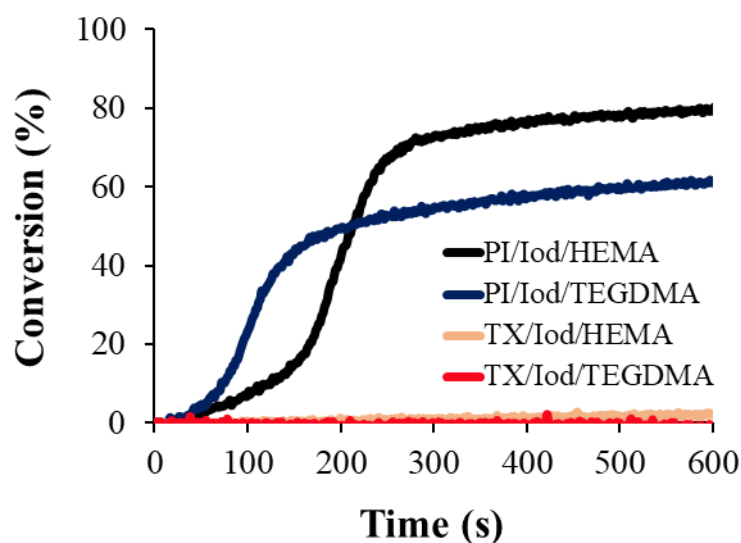


Figure 5.10. Methacrylate conversions of PI/Iod/HEMA and PI/Iod/TEGDMA formulations at 30 °C under nonlaminated conditions irradiated by UV–vis light (320–500 nm). PI = 0.8 wt% wrt TX moiety, Iod = 2 wt%. Irradiation starts at  $t = 10$  s.

The photopolymerization performance of p(PEGDA575-TX)/Iod using visible radiation (400–500 nm) at 30 °C under nitrogen including an aqueous environment was also tested in the polymerization of HEMA and PEGDA using photo-DSC (Figure 5.11).  $R_{pmax}$ ,  $t_{max}$  and conversion values for both monomers with and without water were similar. The photoinitiating efficiency of p(PEGDA575-TX) was also investigated for the photopolymerization of acrylamide (AAm) in aqueous solution in a photoreactor under UV light (365 nm). A crosslinked polymer was obtained, attributed to the macromeric structure of the photoinitiator.

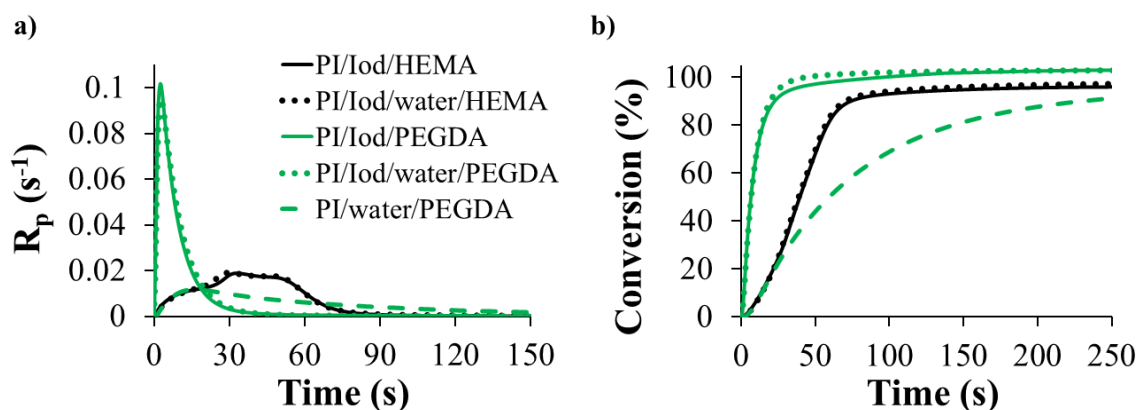


Figure 5.11. (a) Rate of polymerization and (b) double bond conversion graphs of HEMA and PEGDA in the absence and presence of Iod (2 wt%) with (10 wt%) and without water at 30 °C under nitrogen irradiated by 400–500 nm. PI: 0.8 wt% wrt TX moiety.

### 5.3.5. Radical Formation Mechanism

The proposed radical formation mechanisms are presented in Figure 5.12. Upon irradiation, p(PEGDA575-TX) absorbs light and goes to its excited state. The excited state can react with Iod via photooxidation to generate aryl radicals or with EDB by the transfer of the electron from the ketone, followed by the proton abstraction via photoreduction to generate aminoalkyl radicals. In the absence of the additives, p(PEGDA575-TX) can undergo intra- or intermolecular photoreduction by tertiary amines or ethers on its structure. As a result, two types of radicals can be formed: aminoalkyl radicals and radicals on the PEG unit.

### 5.3.6. Migration Stability

The migration stability of p(PEGDA575-TX) was determined by measuring the residual PI of cured TMPTA samples and compared to those of TX. The UV–vis absorption spectra of p(PEGDA575-TX) and TX in chloroform solution were shown in Figure 5.13. The extracted PI was found to be 13% for the synthesized PI ( $n = 3$ ) and 66% for TX. Hence, it can be concluded that p(PEGDA575-TX) has a much higher migration stability compared to TX because of its incorporation into the polymer structure through its double bonds.

Radicals can form on the PI due to amine content which can be an integration point to crosslinked polymer network.

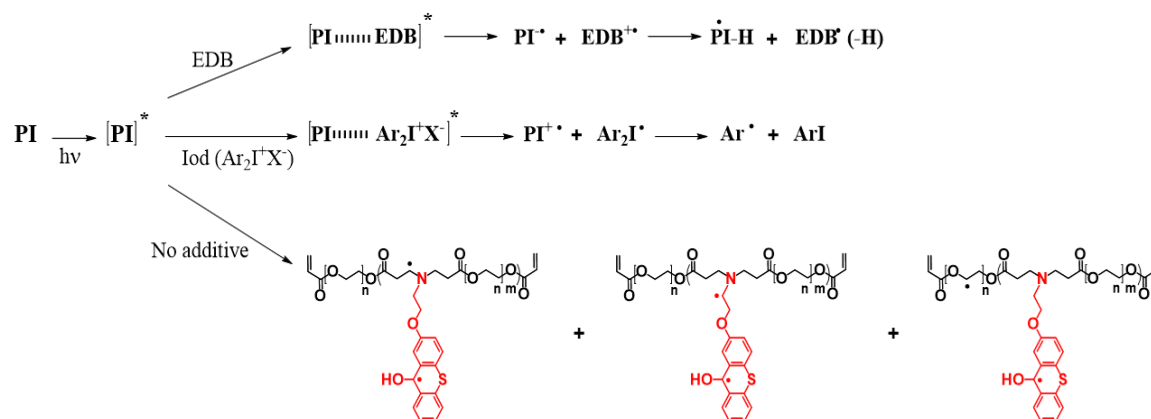


Figure 5.12. Proposed radical formation mechanism.

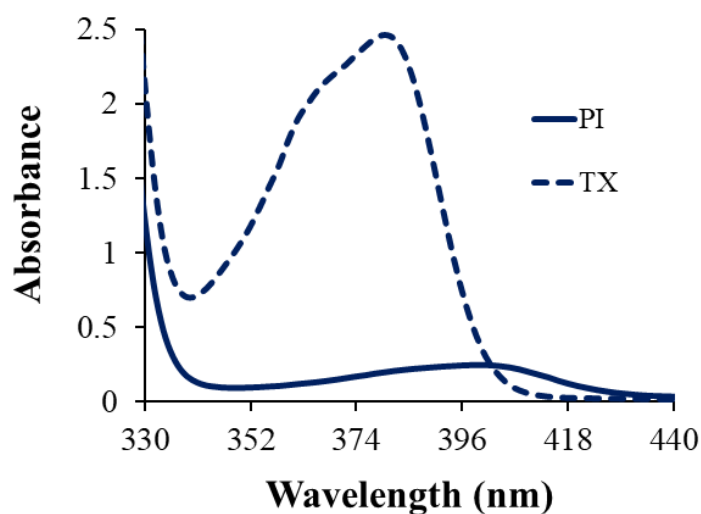


Figure 5.13. UV-vis absorption spectra of TX and p(PEGDA575-TX) extracted with chloroform from the TX/EDB/TMPTA and p(PEGDA575-TX)/EDB/TMPTA (0.8–2–100 wt%) formulations.

#### 5.4. Conclusion

In this study, a novel water soluble, visible light activated and polymerizable PI based on poly(ethylene glycol)-containing poly( $\beta$ -amino ester) with pendant TX groups was successfully prepared and characterized. PI/Iod and PI/EDB systems as well as PI itself undergo steady state photolysis, indicating both photooxidative and photoreductive mechanisms are effective; however, PI/Iod system with the highest photolysis rate signifies that the PI forms radicals more efficiently by a photooxidation mechanism. Therefore, although this PI can work as one-component PI, Iod and EDB synergists increase photopolymerization efficiency by increasing rate of polymerization and decreasing  $t_{\max}$  during photopolymerizations of HEMA, TEGDMA and TMPTA. The synthesized PI showed faster photopolymerization kinetics compared to the commercial photoinitiator TX with or without Iod or EDB. The tertiary amine function of the PI provided both an active hydrogen donor to produce aminoalkyl radicals to initiate polymerization and also reduced oxygen inhibition. Also, due to the polymerizable structure of the PI, the cured material had a fairly good migration stability, leading to reduction of the environmental problems.

## 6. CYCLOPOLYMERIZABLE AND POLY-CYCLIC IRGACURE 2959 DERIVATIVES

### 6.1. Introduction

In this study, two irgacure 2959 (I2959) derivatives were synthesized: cyclopolymerizable and bifunctional I2959 (CTI); and polymeric I2959 (P-CTI) derivatives. CTI is a small molecule PI which is a di(*tert*-butyl) 2,2'-[oxybis(methylene)]bis(2-propenoate) (TBEED) derivative, so it comprises diacrylate functionality which can cyclopolymerize by itself and can be a part of polymerization process as a monomer/crosslinker in the presence of other monomers. On the other hand, P-CTI is a polymeric PI obtained by cyclo-co-polymerization of TBEED and CTI, thus owning cyclic units. Cyclopolymerization is a method to obtain linear polymers with cyclic structures. The linear polymers are synthesized from difunctional monomers which form cyclic units instead of crosslinked polymers. Cyclic structures enhance rigidity on polymers which is beneficial to have high glass transition temperatures [238,239]. They also diminish volumetric shrinkage during polymerization [240,241]. Volumetric shrinkage is observed in polymerization reactions, because monomers come closer to form a new bond which results in shrinkage [242]. Cyclization process can decrease volumetric shrinkage by introducing cyclic units which has larger free volume, and/or via preorientation of monomers which may be unlikely at higher polymerization temperatures [243,244].

Reactivity of CTI as a PI and as a monomer was investigated with variety of monomers such as 2-hydroxyethyl methacrylate (HEMA), triethyleneglycol dimethacrylate (TEGDMA), trimethylolpropane triacrylate (TMPTA) and TBEED under UV-visible light irradiation by differential scanning photocalorimetry (photo-DSC). CTI contains two I2959 moieties, which enables us to use it in lower concentration to achieve a similar reactivity with I2959. Cyclopolymerization ability of CTI was investigated by thermal polymerization. UV-visible absorption and migration properties were investigated.

## 6.2. Experimental Section

### 6.2.1. Materials

TBEED and its carboxylic acid derivative (2,2'-(oxybis(methylene))diacrylic acid (TBEED-COOH)) were synthesized according to the literature procedures [245]. 1,4-diazabicyclo[2.2.2]octane (DABCO), tert-butanol, paraformaldehyde, trifluoroacetic acid (TFA), 2-hydroxy-4'-(2-hydroxyethoxy)-2-methylpropiophenone (I2959), methanesulfonic acid, 4-methoxyphenol and the other reagents and solvents were purchased from Sigma-Aldrich and used as received without further purification.

### 6.2.2. Characterization

$^1\text{H-NMR}$  and  $^{13}\text{C-NMR}$  spectra were recorded on a Varian Gemini (400 MHz) spectrometer with deuterated chloroform ( $\text{CDCl}_3$ ) and deuterated methanol (MeOD) as solvents, and tetramethylsilane as an internal standard. A Nicolet 6700 FT-IR spectrophotometer was used for recording IR spectra.

### 6.2.3. Synthesis of the Photoinitiators

**6.2.3.1. Synthesis of CTI.** It was synthesized based on the literature [246]. TBEED-COOH (0.53 mmol, 99.3 mg), I2959 (1.17 mmol, 263.2 mg) and 4-methoxyphenol (0.40 mg, 0.4 wt% wrt acid) were mixed in three-neck round bottom flask with a water segregator, 1.1 mL toluene was added. The mixture was stirred in an oil bath which was pre-heated to 100 °C, methanesulfonic acid (7.25 mg, 2 wt% wrt reactants) was added. It was stirred for 6 hours at 100 °C under reflux and nitrogen flow. Toluene was evaporated under vacuum. The crude product was dissolved in 3.5 mL ethyl acetate, extracted with 10 wt% NaOH solution (5.9 mL x 3) and distilled water/brine mixture (12 mL/1.2 mL x 4). The solution was dried over anhydrous  $\text{Na}_2\text{SO}_4$ , ethyl acetate was removed under vacuum. The product was obtained as light yellow viscous liquid in 39% yield.

$^1\text{H-NMR}$  (MeOD): 1.47 (12 H,  $\text{CH}_3\text{-C-C=O}$ ), 4.18 (4 H,  $\text{C-CH}_2\text{-O}$ ), 4.27 (4 H,  $\text{C-O-CH}_2$ ), 4.48 (4 H,  $\text{CH}_2\text{-O-C=O}$ ), 5.86, 6.23 (4 H,  $\text{CH}_2\text{=C}$ ), 6.96, 8.17 (8 H, aromatic protons) ppm.

$^{13}\text{C}$ -NMR ( $\text{CDCl}_3$ ): 28.6 ( $\text{CH}_3\text{-C-O}$ ), 62.8 ( $\text{O=C-O-CH}_2$ ), 65.9 ( $\text{O-CH}_2\text{-CH}_2\text{-O}$ ), 68.8 ( $\text{O-CH}_2\text{-C=CH}_2$ ), 75.9 ( $\text{HO-C-(CH}_3)_2$ ), 114.2 ( $\text{CH=C-C=O}$ ), 126.6 ( $\text{CH}_2\text{=C-C=O}$ ), 127.3 ( $\text{CH=C-C=O}$ ), 132.4 ( $\text{CH-CH-C-O}$ ), 136.6 ( $\text{CH}_2\text{=C-C=O}$ ), 162.2 ( $\text{O-C=CH-CH}$ ), 165.5 ( $\text{O=C-O}$ ), 202.5 ( $\text{O=C-C-(CH}_3)_2$ ) ppm.

FTIR: 1158 (C-O), 1573, 1599 (aromatic ring, C=C-C), 1668 (ketone C=O, C=C), 1716 (ester C=O), 3478 (OH)  $\text{cm}^{-1}$ .

**6.2.3.2. Synthesis of P-CTI.** Cyclic PI was obtained by cyclo-co-polymerization of CTI/TBEED (10/90 mol%, 0.8 molar) with AIBN (0.009 molar) in DMF under  $\text{N}_2$  flow. The mixture was purged with nitrogen throughout the polymerization. Polymerization was carried out at 80 °C for 30 minutes. Polymer was purified by precipitation into MeOH/water (5/1 v/v), and obtained as white solid in 25 % yield.

$^1\text{H}$ -NMR ( $\text{CDCl}_3$ ): 1.57 (30 H,  $\text{CH}_3\text{-C-C=O}$ ), 2.02 (8 H,  $\text{C-CH}_2\text{-C}$ ), 2.5 – 4.7 (12 H,  $\text{C-CH}_2\text{-O}$ ,  $\text{O-CH}_2\text{-CH}_2\text{-O}$ ), 6.97, 7.50, 8.01 (8 H, aromatic protons) ppm.

FTIR: 1144 (C-O), 1573, 1601 (aromatic ring, C=C-C), 1679 (ketone C=O), 1722 (ester C=O)  $\text{cm}^{-1}$ .

#### 6.2.4. UV-vis Spectroscopy Experiments

UV-vis measurements were carried out in methanol (MeOH) and chloroform ( $\text{CHCl}_3$ ) by Carry 3 UV/vis spectrophotometer from Varian. Molar extinction coefficient values were calculated by Beer-Lambert formula  $A = \epsilon c b$ . Chloroform solutions of the PI was irradiated with 320-500 nm for steady state photolysis and UV-vis spectra were recorded at different irradiation times. For steady-state photolysis experiment, solutions of CTI in  $\text{CHCl}_3$  was irradiated by a mercury arc lamp (Omnicure s1000–100 W, 320–500 nm), and the absorption spectra were recorded for different irradiation times.

#### 6.2.5. Photopolymerization

The photosensitive formulations were prepared by mixing PIs (0.3 wt%, 0.5 wt%, 1 wt%, 10 wt%, 20 wt%) with the monomers (HEMA, TEGDMA, TBEED and TMPTA). Photo-DSC analyses were conducted on a DSC 250 (TA Instruments) equipped with a UV-

vis light source, Omnicure 2000 with dual-quartz light guide. CTI and P-CTI containing formulations were irradiated by 320-500 nm. Formulations (3-4 mg) were irradiated for 5 minutes at 30 °C under nitrogen flow of 50 mL min<sup>-1</sup>. The heat flow of the polymerization reaction was monitored as a function of time. The cure speed of polymerization reactions were calculated by using equation (6.1).

$$\text{Rate} = \frac{(Q/s)M}{n(\Delta H_p)m}, \quad (6.1)$$

where Q/s is the heat flow per second, M is the molar mass of the monomer, n is the number of double bonds per monomer molecule,  $\Delta H_p$  is the heat of reaction evolved and m is the mass of monomer in the sample. The theoretical heats for the total conversion of an acrylate and methacrylate double bond are 86 kJ/mol and 55 kJ/mol, respectively.

#### 6.2.6. Migration Study

PI/TEGDMA (0.3/99.7 wt%) formulations were photopolymerized (365 nm) for 60 minutes in glass vials. The crosslinked polymers were soaked in chloroform for 60 hours. The amount of extracted PI was determined by UV-vis spectroscopy.

### 6.3. Results and Discussion

#### 6.3.1. Synthesis and Characterization of Photoinitiators

The novel monomeric PI (CTI) was obtained from TBEED-COOH which was synthesized in two steps (Figure 6.1) [245]. In the first step, the Baylis-Hillman reaction of paraformaldehyde with tert-butyl acrylate in the presence of DABCO as catalyst provided TBEED. Then, the tert-butyl groups of TBEED were deprotected by TFA to give TBEED-COOH. The esterification reaction of TBEED-COOH with I2959 was performed using methanesulfonic acid catalyst in toluene to give the corresponding ester in 39 % yield. Methanesulfonic acid also facilitates the solubility of the acid during reaction.

I2959 possesses two reactive hydroxyl groups either of which can undergo esterification. As a result, we also obtain minor products from tert-alcohol group in addition

to the major product [247] (Figure 6.1). These minor products do not reduce the photopolymerization efficiency of CTI because they also contain photoreactive functionalities (I2959 and methacrylate).

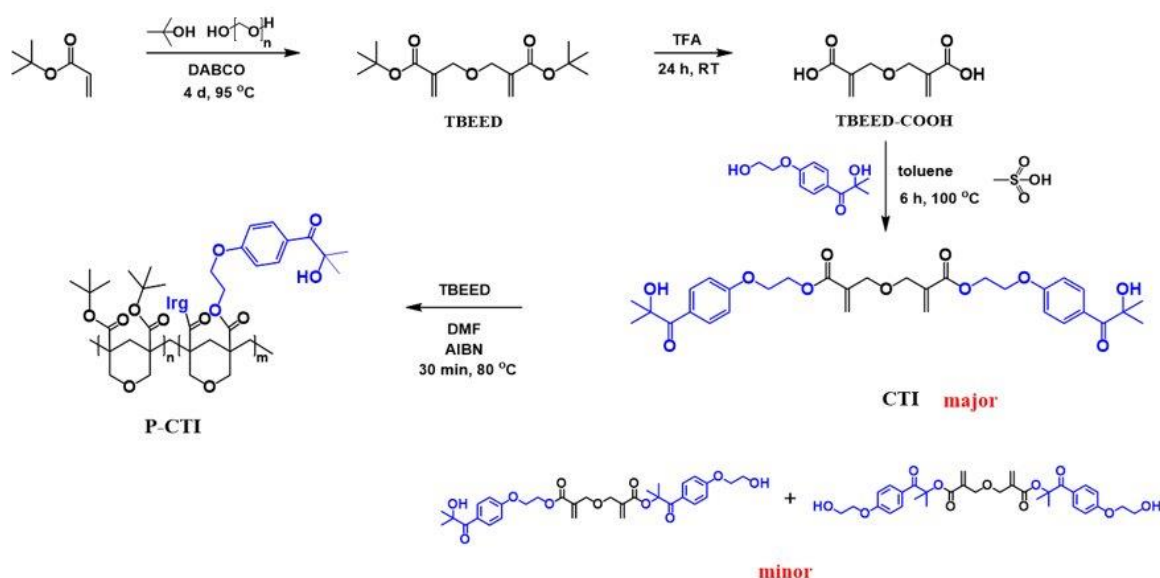


Figure 6.1. Synthesis of TBEED, TBEED-COOH, CTI, P-CTI and minor products.

TBEED is an ether dimer of tert-butyl  $\alpha$ -(hydroxymethyl)acrylate, which is a type of cyclopolymerizable monomer [248-252]. The synthesized PI is a TBEED derivative, so it is highly probable that CTI is also cyclopolymerizable monomer. To attain cyclic units in the PIs structure, poly-cyclic PI (P-CTI) was synthesized by thermal polymerization of CTI/TBEED (10/90 mol%) formulation (Figure 6.1).

The structure of CTI was confirmed by  $^1\text{H-NMR}$ ,  $^{13}\text{C-NMR}$  and FTIR spectroscopies. The  $^1\text{H-NMR}$  spectrum in MeOD shows methyl protons at 1.47 and 1.63 ppm, methylene protons between 4.2 – 4.5 ppm, double bond protons at 5.86 and 6.23 ppm and aromatic hydrogens between 6.96 and 8.17 ppm (Figure 6.2). The small peaks observed around 3.9, 4.1 and 7.5 ppm assigned to the minor products. These peaks are close to the CTI peaks which stems from the similarity between the structures of major and minor products.

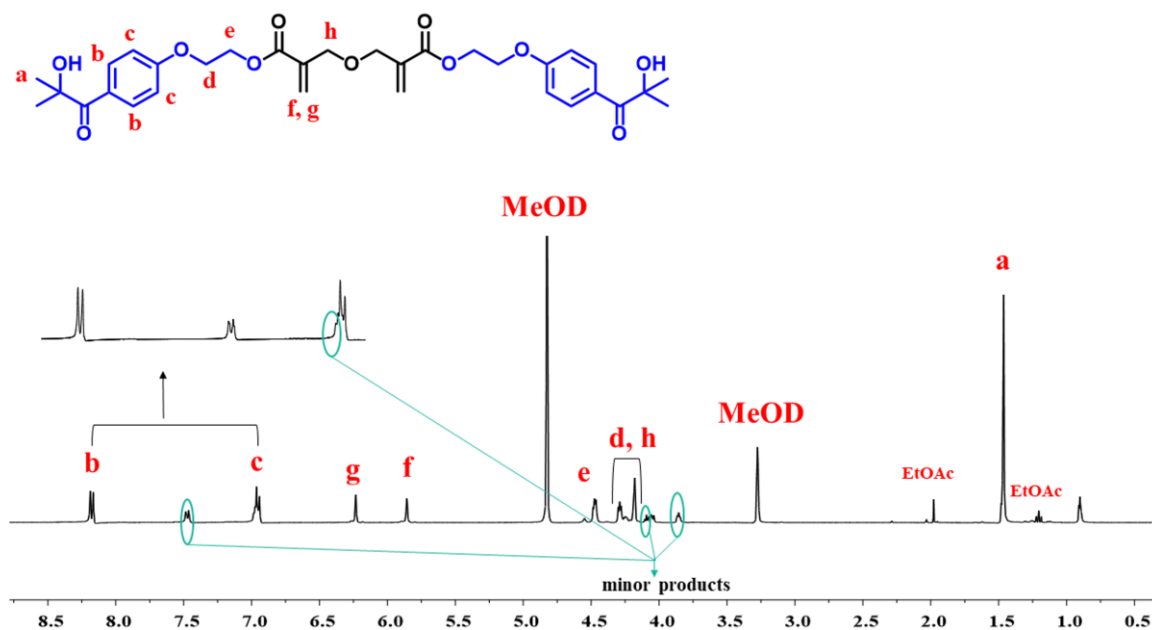


Figure 6.2.  $^1\text{H}$ -NMR spectrum of CTI in MeOD.

$^{13}\text{C}$ -NMR spectrum of CTI shows the peaks at 165.5 and 202.5 ppm which are ascribed to carbons in ester and ketone carbonyls, respectively (Figure 6.3). Aromatic carbons are observed between 125 – 133 ppm except one carbon which appears at 162.2 ppm, more downfield region compared to other aromatic carbons, due to being attached to oxygen. One of the double bond carbons is observed at 126.6 ppm, the other one neighboring ester carbonyl is observed at 136.6 ppm. Similar to  $^1\text{H}$ -NMR,  $^{13}\text{C}$ -NMR spectrum also shows small peaks near the peaks of CTI, confirming the presence of minor products.

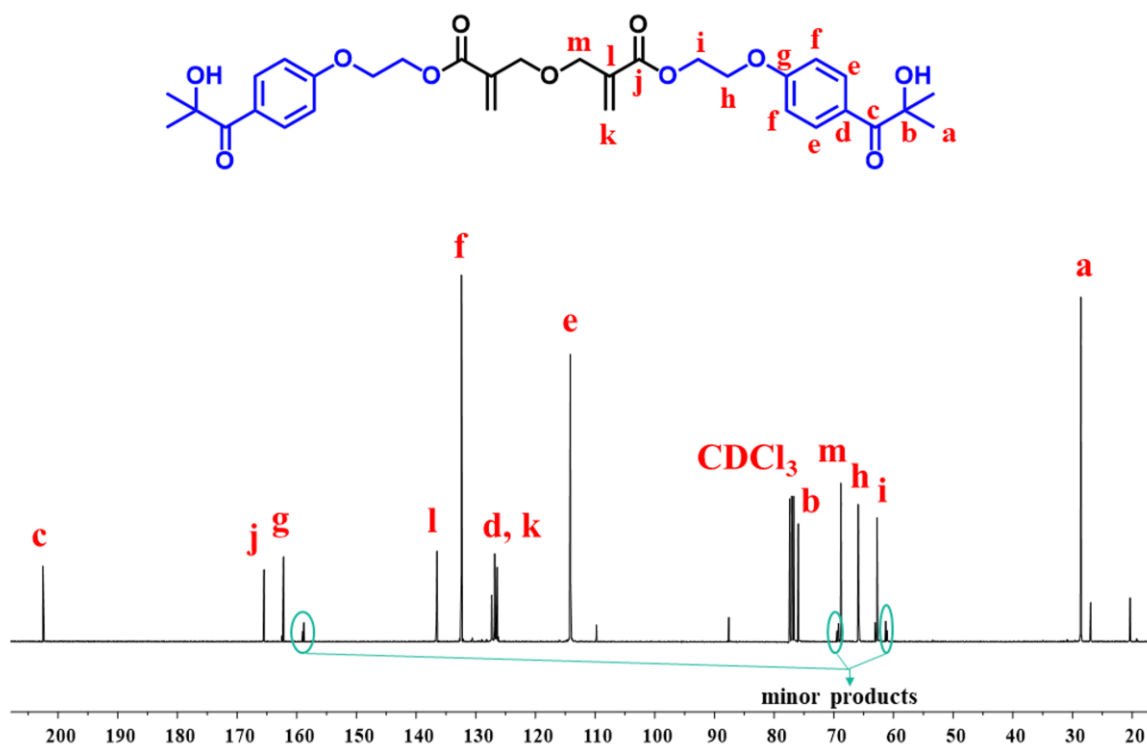


Figure 6.3.  $^{13}\text{C}$ -NMR spectrum of CTI.

The structure of P-CTI was confirmed by  $^1\text{H}$  NMR and FTIR spectroscopies. Methyl protons of tert-butyl groups in TBEED and methyl protons of CTI are observed at 1.57 ppm in  $^1\text{H}$ -NMR (Figure 6.4). The peak at 2.02 ppm indicates the hydrogens at polymeric backbone. The broad peak between 2.5 – 4.7 ppm belongs to protons neighboring oxygens in I2959 and to protons in cyclic backbone. Broad nature of the peak is the indication of polymeric structure. Aromatic hydrogens in CTI appear between 6.8 – 8.2 proving the successful cyclocopolymerization of CTI with TBEED. CTI ratio in the polymer was calculated by integrating aromatic protons to methyl protons and found to be 10 wt %.

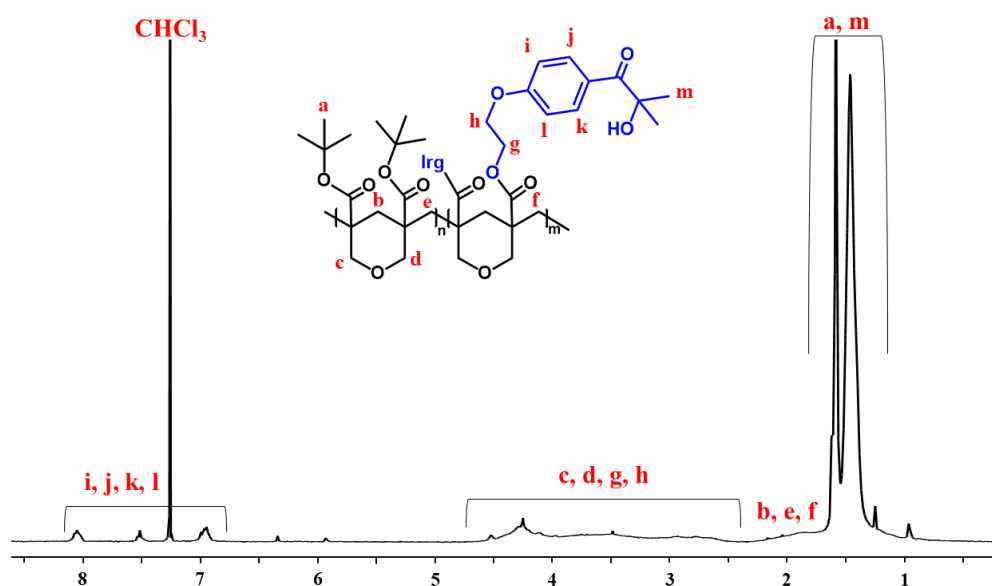


Figure 6.4.  $^1\text{H-NMR}$  spectrum of P-CTI.

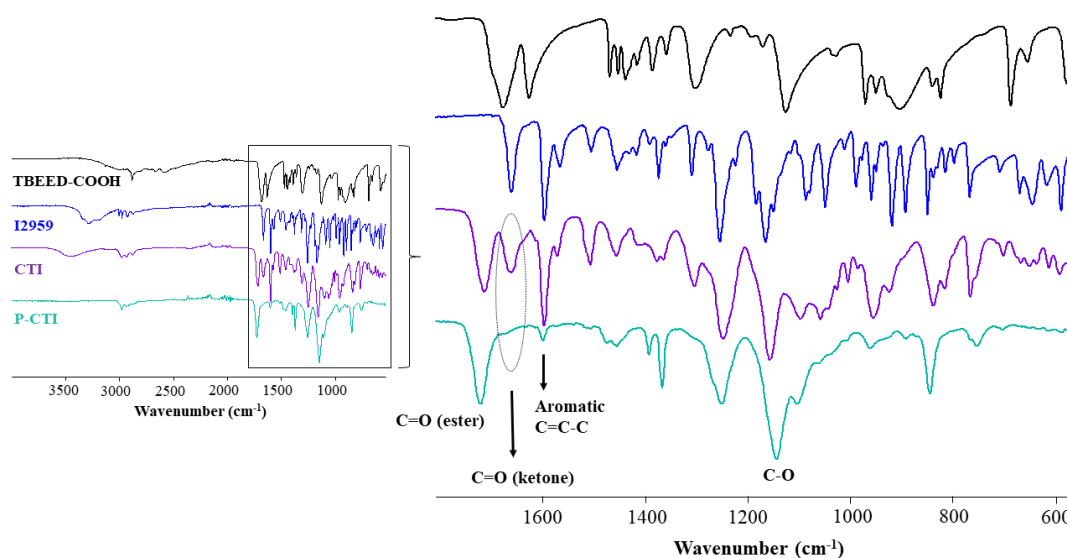


Figure 6.5. FTIR spectra of TBEED-COOH (black spectrum), I2959 (blue spectrum), CTI (purple spectrum) and P-CTI (green spectrum).

The FTIR spectrum of CTI is compared to those of the starting materials (TBEED and I2959). The peaks at  $1668$  and  $1716\text{ cm}^{-1}$  are assigned to the ketone and ester carbonyl stretching vibrations of CTI, respectively (Figure 6.5). The shift in the carbonyl peak of the

acid ( $1678\text{ cm}^{-1}$ ) and the presence of the ketone carbonyl ( $1662\text{ cm}^{-1}$ ) of I2959 also verify the desired product formation. P-CTI has a peak at  $1601\text{ cm}^{-1}$  indicating the aromatic carbon-carbon stretching, verifying the cyclopolymerization of CTI with TBEED.

### 6.3.2. Light Absorption Properties

The absorption characteristics of CTI and P-CTI were analyzed and compared to I2959 by UV-vis spectroscopy in chloroform and methanol. As demonstrated in Figure 6.6, PIs have similar absorption behavior. Absorption maximas ( $\lambda_{\text{max}}$ ) of CTI are at 270 and 276 nm in MeOH and chloroform respectively, and that of P-CTI is at 277 nm in chloroform. These maximas state the  $\pi$ - $\pi^*$  transition for both of the synthesized initiators. Extinction coefficient value ( $\epsilon$ ) of CTI is higher than that of I2959 which stems from the bifunctional character (Table 6.1). Because it contains two I2959 functionalities, nearly doubled extinction coefficient value is anticipated. However it is not observed because two chromophores are not isolated, rather they can interact with each other through partial charge transfer [253,254]. The molar absorptivity of CTI in chloroform is also used to verify the CTI amount in P-CTI, PI contains approximately 13 wt% CTI, similar to the value calculated from the NMR data (10 wt%).

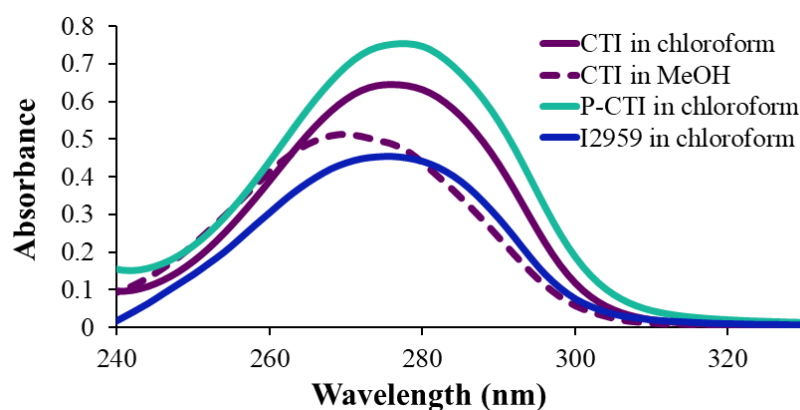


Figure 6.6. UV-vis absorption spectra of CTI, P-CTI and I2959 in  $\text{CHCl}_3$  and MeOH.

$[\text{CTI}]$ ,  $[\text{I2959}] = 2.6 \times 10^{-5}\text{ M}$ ,  $[\text{P-CTI}] = 3.2 \times 10^{-5}\text{ M}$  wrt CTI moiety.

Table 6.1. Absorption characteristics of CTI and I2959.

PI	$\lambda_{\max}$ [nm]	$\epsilon$ [ $M^{-1} \text{ cm}^{-1}$ ]
CTI	270 (MeOH)	20882
	276 ( $\text{CHCl}_3$ )	23912
I2959	276 ( $\text{CHCl}_3$ )	17110

The UV spectral changes of CTI and P-CTI upon photolysis are depicted in Figure 6.7. The absorbance at 276 nm decreased and the absorbance maxima shifted from 276 nm to 270 nm as the photolysis progressed for CTI, and the shift was from 277 nm to 266 nm for P-CTI. It can be concluded that poly-cyclic PI photodegrades faster than small molecule PI based on the higher shift in P-CTI (11 nm) compared to CTI (6 nm). As a result, both PIs decomposed under light irradiation.

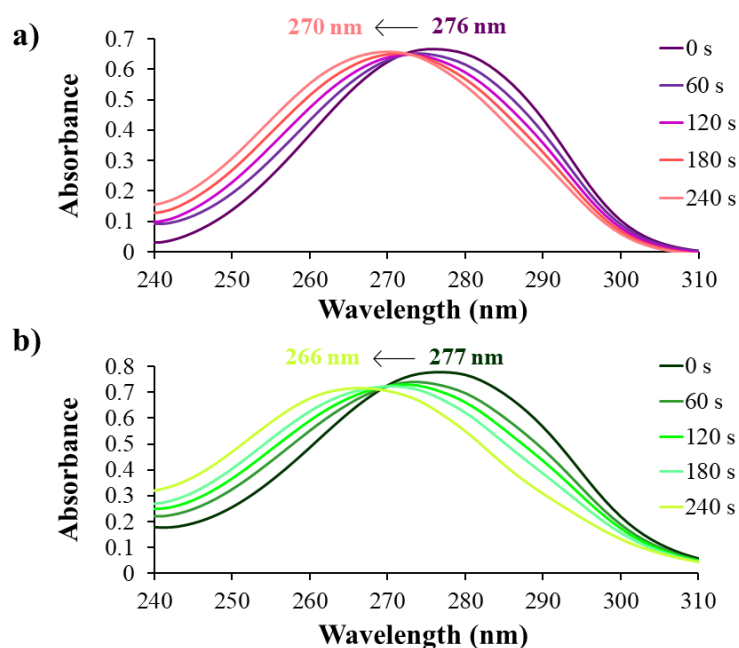


Figure 6.7. Photolysis of (a) CTI ( $2.5 \times 10^{-5} \text{ M}$ ) and (b) P-CTI ( $3.2 \times 10^{-5} \text{ M}$  wrt CTI moiety) under 320-500 nm light illumination.

### 6.3.3. Photopolymerization Results

Photopolymerization ability of CTI as a photoinitiator and as a monomer was analyzed with photo-DSC under irradiation of 320-500 nm at 30 °C. As listed in Table 6.2, polymerization of HEMA and TMPTA containing 0.5, 1, 10 and 20 wt% CTI formulations were monitored.

Table 6.2. Formulation contents,  $R_{pmax}$ ,  $t_{max}$  and conversion values.

PI	Monomer	$R_{pmax}$ ( $s^{-1}$ )	$t_{max}$ (s)	Conversion (%)
CTI (0.5 wt%)	HEMA (99.5 wt%)	0.0193	82.8	95.2
CTI (1 wt%)	HEMA (99 wt%)	0.0230	67.8	89.7
I2959 (1 wt%)	HEMA (99 wt%)	0.0189	71.4	92.2
CTI (10 wt%)	HEMA (90 wt%)	0.0226	42.6	87.7
CTI (20 wt%)	HEMA (20 wt%)	0.0282	33.6	82.0
CTI (1 wt%)	TMPTA (99 wt%)	0.0577	1.8	51.7
I2959 (1 wt%)	TMPTA (99 wt%)	0.0718	1.2	55.6
CTI (20 wt%)	TMPTA (80 wt%)	0.0809	1.8	57.1
P-CTI (0.3 wt%)	TEGDMA (99.7 wt%)	0.0440	19.8	85.4
CTI (0.3 wt%)	TEGDMA (99.7 wt%)	0.0280	28.8	81.5
CTI (1 wt%)	TEGDMA (99 wt%)	0.0450	20.4	83.0
I2959 (1 wt%)	TEGDMA (99 wt%)	0.0529	19.8	78.4
CTI (10 wt%)	TEGDMA (90 wt%)	0.0441	15.6	80.5
I2959 (1 wt%)	TBEED (99 wt%)	0.0438	18.6	74.7
CTI (1 wt%)	TBEED (99 wt%)	0.0345	23.4	78.4
CTI (10 wt%)	TBEED (90 wt%)	0.0553	10.8	87.6
CTI	CTI (100 wt%)	0.0665	4.8	77.6

In order to investigate the efficiency of CTI as a photoinitiator, 0.5 and 1 wt% CTI containing formulations were analyzed and compared to parent I2959 (Figure 6.8a and Figure 6.8b). CTI-HEMA (0.5-99.5 wt%) and CTI-HEMA (1-99 wt%) formulations have a very similar maximum rate of polymerization ( $R_{pmax}$ ) and conversion values, but latter reaches  $t_{max}$  approximately 11 s faster (Table 2). This results may be related to concentrations of PIs. Although it seems like I2959 concentrations are the same due to bifunctional nature of CTI, it is not the case. I2959 is  $4.8 \times 10^{-2}$  M in I2959-HEMA (1-99 wt%) and CTI is  $0.9 \times 10^{-2}$  M in CTI-HEMA (0.5-99.5 wt%), but it can be considered as  $1.8 \times 10^{-2}$  M in terms of I2959 due to bifunctional nature. The I2959 concentration in the former formulation is 2.7 times higher, but both of the formulations have similar  $R_{pmax}$  and  $t_{max}$  values. CTI-HEMA (1-99 wt%) formulation contains  $1.8 \times 10^{-2}$  M PI, and polymerizes faster than the aforementioned formulations. These results show that CTI is a reactive photoinitiator, more so at higher concentrations and more efficient than I2959 in HEMA. As opposed to HEMA, TMPTA polymerizes more rapidly with 1 wt% I2959 compared to 1 wt% CTI.

The photopolymerization ability of CTI as a monomer/PI was also analyzed with increasing concentration of CTI from 1 wt% to 10-20 wt% in HEMA and TMPTA. It was observed that, increasing concentration of CTI makes the photopolymerization induction time shorter for HEMA, but not for TMPTA. It is evident that decrease in the  $t_{max}$  value was higher for slow polymerizing systems (HEMA) compared to those of fast systems (TMPTA). The  $R_{pmax}$  values increased with increasing concentration of CTI, while conversion remains almost constant. This results can be explained by the rise in the crosslinking density due to dimethacrylate nature of CTI. These outcomes indicates that CTI is a polymerizable monomer and a reactive initiator even at raised concentrations.

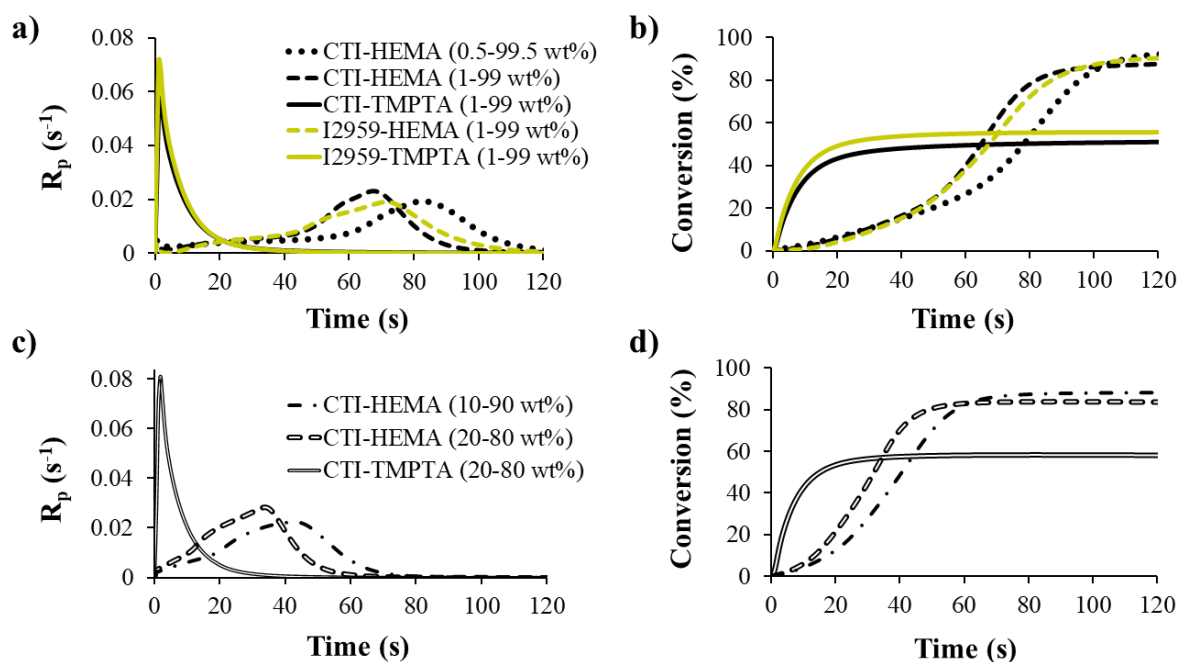


Figure 6.8. Rate of polymerization (a, c) and double bond conversion graphs (b, d) of HEMA and TMPTA in the presence of CTI or I2959 at 30 °C under nitrogen irradiated by 320-500 nm.

Photopolymerization experiments were also conducted with only CTI (100 wt%), and also with TEGDMA and TBEED containing 1 and 10 wt% CTI and I2959 (Figure 6.9). As depicted in Figure 6.9a and 6.9b, 1 wt% CTI and I2959 have similar photoinitiation reactivity and double bond conversions in TEGDMA and TBEED. Even though the concentration of CTI is 2.7 times lower than I2959, the initiation efficiency of CTI is comparable to I2959. Polymerization results depict that CTI is a quiet reactive, self-polymerizable monomer. Similar to HEMA and TMPTA,  $t_{max}$  is shortened as CTI amount increases for both of the monomers (Table 6.2).  $R_{pmax}$  values are approximate in CTI-TEGDMA (1-99 wt%) and CTI-TEGDMA (10-90 wt%). In contrast, rate is raised in TBEED as CTI amount increases from 1 wt% to 10 wt%. It can be explained by the reactivity differences between monomers. This results demonstrates that CTI is efficient PI and reactive monomer.

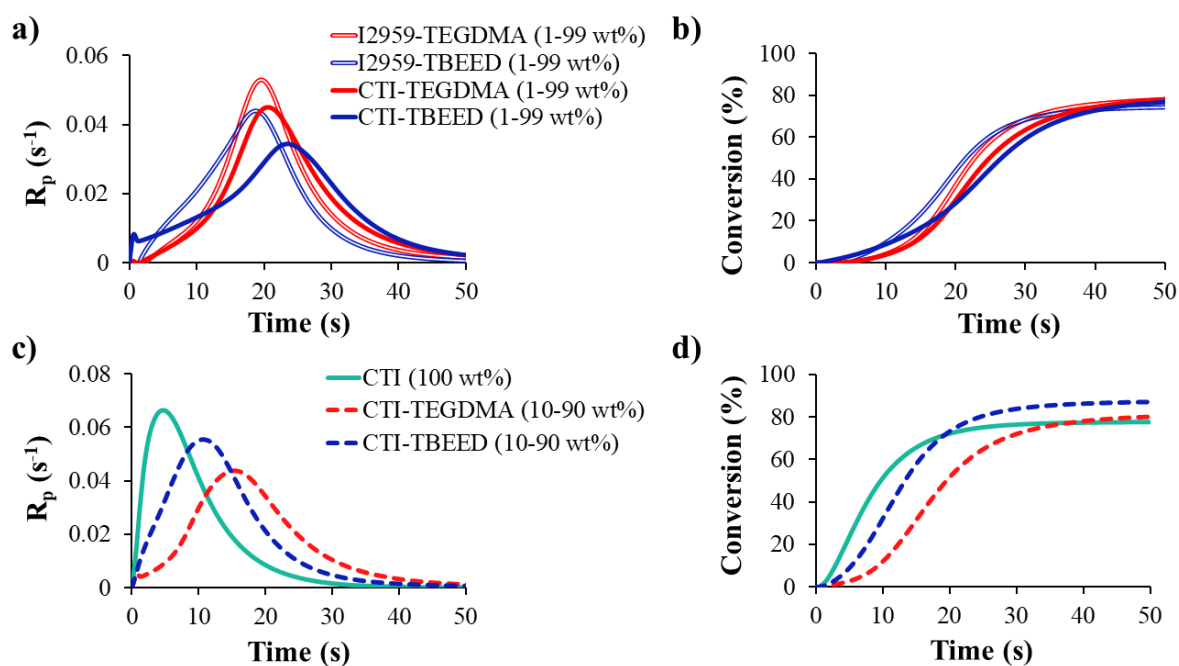


Figure 6.9. (a) Rate of polymerization and (b) double bond conversion graphs of CTI alone (100 wt%), TEGDMA and TBEED in the presence of CTI at 30 °C under nitrogen irradiated by 320-500 nm.

Photopolymerization reactivity of P-CTI was analyzed and compared to CTI in TEGDMA (Figure 6.10). Poly-cyclic PI induces more rapid polymerization than CTI (Table 6.2, Figure 6.10a), stemming from the higher initiation efficiency of P-CTI which is consistent with photolysis results. Higher efficiency can be result of better light-harvesting ability and greater quantum yield of P-CTI compared to CTI. Another reason can arise from the polymeric structure. CTI groups on the polymeric PI may not be consecutively aligned, but rather be separated from each other by the cyclic TBEED units in the backbone. The separation between CTI units diminishes the possibility of combination of two radicals leading to faster curing.

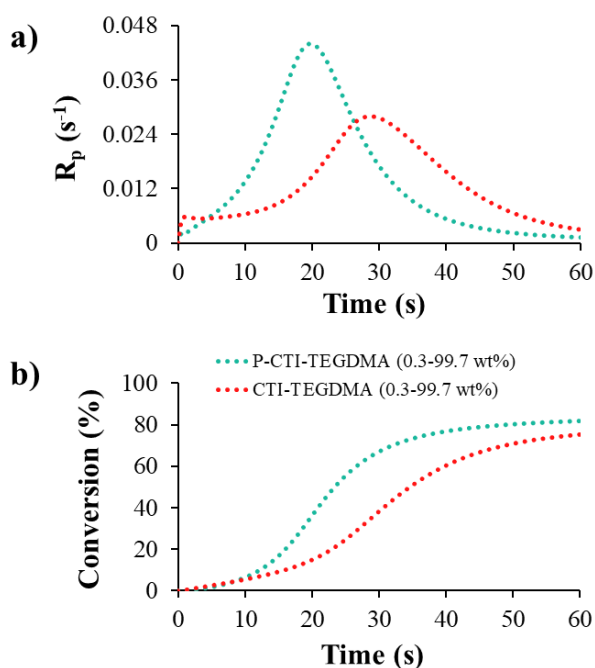


Figure 6.10. (a) Rate of polymerization and (b) double bond conversion graphs of TEGDMA in the presence of CTI and P-CTI (0.3 wt% wrt CTI moiety) at 30 °C under nitrogen irradiated by 320-500 nm.

#### 6.3.4. Migration Results

The migration stability of synthesized CTI was determined by measuring the residual PI of cured TEGDMA samples and compared to those of I2959. The UV-vis absorption spectra of CTI and I2959 in chloroform solution were shown in Figure 6.11. The extracted PI was found to be less than 1% for CTI, and 13% for I2959. Therefore, it can be deduced that CTI has greater leaching stability compared to I2959 because of its incorporation into the polymer structure through its double bonds.

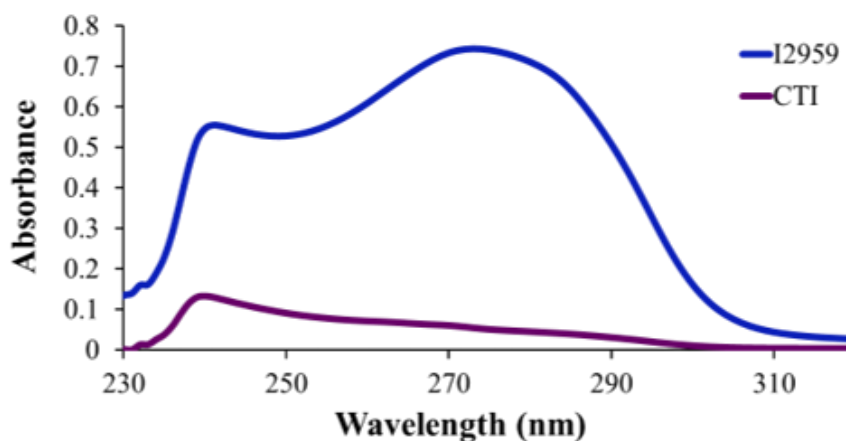


Figure 6.11. UV–vis absorption spectra of I2959 and CTI extracted with chloroform from the PI/TEGDMA (0.3–99.7 wt%) formulations.

#### 6.4. Conclusion

In this study, two novel polymerizable and polymeric PIs were successfully synthesized and characterized. CTI is a bifunctional and cyclopolymerizable PI/monomer derived from I2959/cyclopolymerizable monomer (TBEED). P-CTI is a poly-cyclic PI obtained from the thermal polymerization of CTI-TBEED mixture. Both of the PIs undergo steady state photolysis but P-CTI photodegrades faster than CTI indicating that the polymeric PI generates radicals more effectively. CTI is a self-polymerizable monomer resulting from combining I2959 and polymerizable double bond, and it is compatible with variety of monomers such as HEMA, TEGDMA, TMPTA and TBEED. Because of its bifunctional nature, it can initiate light curing at lower concentrations than parent I2959. CTI raises the  $R_{pmax}$  and shortens  $t_{max}$  at an increasing PI concentration without causing any delay or termination during photopolymerization due to light shielding and high radical amounts. These drawbacks are probably overcome by its highly reactive monomeric nature towards polymerization. Faster radiation curing kinetics are obtained with P-CTI compared to CTI in TEGDMA. Due to CTI's cyclopolymerization tendency and P-CTI's poly-cyclic structure, the synthesized PIs can enhance the mechanical properties of cured material. Also, because of the polymerizable nature of CTI, the obtained polymer has better migration stability than I2959, leading to decrease in the environmental problems.

## 7. CONCLUDING REMARKS

To contribute to the ongoing effort of making polymerization processes more environmentally friendly, multiple functionalizations were used to endow photoinitiators at various degrees with properties of water solubility, migration stability, oxygen inhibition, high reactivity, visible light absorption and biocompatibility.

Four poly(ethylene imine) based PIs with controllable amount of thioxanthone and (bis)phosphonate functionalities (PBT-2, PBT-5, PDT-2 and PDT-5) were synthesized. They have visible light absorption, and they are also fluorescent. These PIs are able to undergo aza-Michael addition reaction with acrylates and free radical polymerization with (meth)acrylates in one-step or dual curing processes leading to formation of interpenetrating network. They form CTCs with iodonium salt through amines in their structures which leads to radical generation and polymerization without irradiation. Besides CTC, presence of amines inhibit oxygen during polymerization. Polymerization is achieved through CTCs and also TX/Iod interaction by visible light illumination (LED@405 nm) under air. Remarkable photoinitiating abilities and high final conversions are found for both one-step and dual curing processes. These novel PIs can act as a photoinitiator and a monomer in dual curing systems, delivering custom-tailored products for various industrial applications.

Two water soluble benzophenone functionalized substituted oligo(amido amine)s (OAA-B and OAA-BP) were produced. Phosphonate group was incorporated onto oligo(amido amine) to realize the versatility of the synthesis method and to increase biocompatibility. In combination with Iod, the PIs possess high photoreactivity under visible light and air. The excellent curing capacities of these PIs are due to combination of type II photoinitiation (BP/Iod interaction) and CTC formation between amine groups on the oligomeric backbone and Iod. Macromolecular structure of the PIs would lead to reduced migration, thus enhanced final polymer properties.

A polymeric, polymerizable, water soluble and visible light activated photoinitiator derived from poly(ethylene glycol) and thioxanthone was successfully prepared. Although the PI is one-component, photopolymerization is more rapid in the presence of coinitiators

such as Iod and EDB. The PI is compatible with various monomers such as HEMA, TEGDMA, PEGDA and TMPTA, and it displays faster photopolymerization kinetics compared to the commercial photoinitiator TX with or without Iod or EDB. The amines in PI makes it capable of inhibiting oxygen and inducing efficient light curing under air. The polymerizable structure of the PI results in quite good migration stability, leading to reduction of the environmental problems.

Two novel polymerizable (CTI) and polymeric (P-CTI) PIs based on I2959 were developed. CTI contains two I2959 moieties (bifunctional) and it is a cyclopolymerizable PI acquired from I2959/cyclopolymerizable monomer. P-CTI is a polymeric PI with cyclic units. CTI is able to photopolymerize itself due to having I2959 and polymerizable double bond, so it can act as both PI and monomer. It efficiently photoinitiates the polymerization of HEMA, TEGDMA, TMPTA and TBEED at lower concentrations than parent I2959 because of its bifunctional nature. Both of the synthesized PIs have improved leaching properties thanks to their polymerizable and polymeric structures. They can also reinforce the mechanical properties of final polymers due to CTI's cyclopolymerization affinity and P-CTI's poly-cyclic structure.

In conclusion, the purpose of this research was to advance the characteristics of commercial photoinitiators by chemical modifications to have desired features such as visible light operation, more efficient radiation curing for various monomers, anti-oxygen inhibition property, improved water solubility, biocompatibility and decreased leaching of PIs. According to the data we have gathered, it is possible to say that appropriate modifications have been achieved to reasonably tailor these desired properties for PIs and properties of final products. Furthermore, the synthetic approach is quite flexible, suitable for a wide range of functionalizations.

## REFERENCES

- [1] Glusac, K., “What Has Light Ever Done for Chemistry?”, *Nature Chemistry*, Vol. 8, No. 8, pp. 734-735, 2016.
- [2] Mai, S., and L. González, “Molecular Photochemistry: Recent Developments in Theory”, *Angewandte Chemie International Edition*, Vol. 59, No. 39, pp. 16832-16846, 2020.
- [3] Paa, W., J.P. Yang, and S. Rentsch, “Intersystem Crossing in Oligothiophenes Studied by fs Time-Resolved Spectroscopy”, *Applied Physics B*, Vol. 71, No. 3, pp. 443-449, 2000.
- [4] Penfold, T.J., E. Gindensperger, C. Daniel, and C.M. Marian, “Spin-Vibronic Mechanism for Intersystem Crossing”, *Chemical Reviews*, Vol. 118, Vol. 15, pp. 6975-7025, 2018.
- [5] Sidman, J.W., “Electronic Transitions due to Nonbonding Electrons Carbonyl, Aza-Aromatic, and Other Compounds”, *Chemical Reviews*, Vol. 58, No. 4, pp. 689-713, 1958.
- [6] Leermakers, P.A. and G.F. Vesley, “Organic Photochemistry and the Excited State”, *Journal of Chemical Education*, Vol. 41, No. 10, p. 535, 1964.
- [7] Fouassier, J.P., and J. Lalevée, *Photoinitiators for Polymer Synthesis: Scope, Reactivity, and Efficiency*, John Wiley & Sons, Germany, 2012.
- [8] Corrigan, N., J. Yeow, P. Judzewitsch, J. Xu, and C. Boyer, “Seeing the Light: Advancing Materials Chemistry Through Photopolymerization”, *Angewandte Chemie International Edition*, Vol. 58, No. 16, pp. 5170-5189, 2019.
- [9] Frank, H.A., J.A. Bautista, J. Josue, Z. Pendon, R.G. Hiller, F.P. Sharples, D. Gosztola, and M.R. Wasielewski, “Effect of the Solvent Environment on the Spectroscopic Properties and Dynamics of the Lowest Excited States of Carotenoids”, *The Journal of Physical Chemistry B*, Vol. 104, No. 18, pp. 4569-4577, 2000.
- [10] Mannekutla, J.R., B.G. Mulimani, and S.R. Inamdar, “Solvent Effect on Absorption and Fluorescence Spectra of Coumarin Laser Dyes: Evaluation of Ground and Excited State Dipole Moments”, *Spectrochimica Acta Part A: Molecular and Biomolecular Spectroscopy*, Vol. 69, No. 2, pp. 419-426, 2008.

- [11] Kaur, M., and A.K. Srivastava, "Photopolymerization: A Review", *Journal of Macromolecular Science, Part C: Polymer Reviews*, Vol. 42, No. 4, pp. 481-512, 2002.
- [12] Chatani, S., C.J. Kloxin, and C.N. Bowman, "The power of Light in Polymer Science: Photochemical Processes to Manipulate Polymer Formation, Structure, and Properties", *Polymer Chemistry*, Vol. 5, No. 7, pp. 2187-2201, 2014.
- [13] Harke, B., P. Bianchini, F. Brandi, and A. Diaspro, "Photopolymerization Inhibition Dynamics for Sub-Diffraction Direct Laser Writing Lithography", *ChemPhysChem*, Vol. 13, No. 6, pp. 1429-1434, 2012.
- [14] Shi, J., M.B. Chan-Park, C. Gong, H. Yang, Y. Gan, and C.M. Li, "Spatially Controlled Oxygen Inhibition of Acrylate Photopolymerization as a New Lithography method for High-Performance Organic Thin-Film Transistors", *Chemistry of Materials*, Vol. 22, No. 7, pp. 2341-2346, 2010.
- [15] Sangermano, M., S. Marchi, L. Valentini, S.B. Bon, and P. Fabbri, "Transparent and Conductive Graphene Oxide/Poly (ethylene glycol) Diacrylate Coatings Obtained by Photopolymerization", *Macromolecular Materials and Engineering*, Vol. 296, No. 5, pp. 401-407, 2011.
- [16] Tang, R., A. Muhammad, J. Yang, and J. Nie, "Preparation of Antifog and Antibacterial Coatings by Photopolymerization", *Polymers for Advanced Technologies*, Vol. 25, No. 6, pp. 651-656, 2014.
- [17] Ye, Q., P. Spencer, Y. Wang, and A. Misra, "Relationship of Solvent to the Photopolymerization Process, Properties, and Structure in Model Dentin Adhesives", *Journal of Biomedical Materials Research Part A*, Vol. 80, No. 2, pp. 342-350, 2007.
- [18] Ye, Q., Y. Wang, K. Williams, and P. Spencer, "Characterization of Photopolymerization of Dentin Adhesives as a Function of Light Source and Irradiance", *Journal of Biomedical Materials Research Part B: Applied Biomaterials*, Vol. 80, No. 2, pp. 440-446, 2007.
- [19] Woods, E.F., A.J. Berl, and J.A. Kalow, "Advances in the Synthesis of  $\pi$ -Conjugated Polymers by Photopolymerization", *ChemPhotoChem*, Vol. 5, No. 1, pp. 4-11, 2021.

- [20] Xu, X., A. Awad, P. Robles-Martinez, S. Gaisford, A. Goyanes, and A.W. Basit, "Vat Photopolymerization 3D Printing for Advanced Drug Delivery and Medical Device Applications", *Journal of Controlled Release*, Vol. 329, pp. 743-757, 2021.
- [21] Bella, F., E.D. Ozzello, S. Bianco, and R. Bongiovanni, "Photo-polymerization of Acrylic/Methacrylic Gel-Polymer Electrolyte Membranes for Dye-Sensitized Solar Cells", *Chemical Engineering Journal*, Vol. 225, pp. 873-879, 2013.
- [22] Dietlin, C., S. Schweizer, P. Xiao, J. Zhang, F. Morlet-Savary, B. Graff, J.P. Fouassier, and J. Lalevée, "Photopolymerization upon LEDs: New Photoinitiating Systems and Strategies", *Polymer Chemistry*, Vol. 6, No. 21, pp. 3895-3912, 2015.
- [23] Yagci, Y., S. Jockusch, and N.J. Turro, "Photoinitiated Polymerization: Advances, Challenges, and Opportunities", *Macromolecules*, Vol. 43, No. 15, pp. 6245-6260, 2010.
- [24] Monroe, B.M., and G.C. Weed, "Photoinitiators for Free-Radical-Initiated Photoimaging Systems", *Chemical Reviews*, Vol. 93, No. 1, pp. 435-448, 1993.
- [25] Decker, C., "Kinetic Study and New Applications of UV Radiation Curing", *Macromolecular Rapid Communications*, Vol. 23, No. 18, pp. 1067-1093, 2002.
- [26] Pan, X., M.A. Tasdelen, J. Laun, T. Junkers, Y. Yagci, and K. Matyjaszewski, "Photomediated Controlled Radical Polymerization", *Progress in Polymer Science*, Vol. 62, pp. 73-125, 2016.
- [27] Zhou, J., X. Allonas, A. Ibrahim, and X. Liu, "Progress in the Development of Polymeric and Multifunctional Photoinitiators", *Progress in Polymer Science*, Vol. 99, p. 101165, 2019.
- [28] Fouassier, J.P., X. Allonas, J. Lalevée, and C. Dietlin, *Photochemistry and Photophysics of Polymer Materials*, John Wiley & Sons, Hoboken, NJ, USA, 2010.
- [29] Dietliker, K., T. Jung, J. Benkhoff, H. Kura, A. Matsumoto, H. Oka, D. Hristova, G. Gescheidt, and G. Rist, "New Developments in Photoinitiators", *Macromolecular Symposia*, Vol. 217, No. 1, pp. 77-98, 2004.
- [30] Rutsch, W., K. Dietliker, D. Leppard, M. Köhler, L. Misev, U. Kolczak, and G. Rist, "Recent Developments in Photoinitiators", *Progress in Organic Coatings*, Vol. 27, No. 1-4, pp. 227-239, 1996.

- [31] Dadashi-Silab, S., C. Aydogan, and Y. Yagci, "Shining a Light on an Adaptable Photoinitiator: Advances in Photopolymerizations Initiated by Thioxanthenes", *Polymer Chemistry*, Vol. 6, No. 37, pp. 6595-6615, 2015.
- [32] Anderson, D.G., R.S. Davidson, and J.J. Elvery, "Thioxanthenes: Their Fate When Used as Photoinitiators", *Polymer*, Vol. 37, No. 12, pp. 2477-2484, 1996.
- [33] Selvaraju, C., A. Sivakumar, and P. Ramamurthy, "Excited State Reactions of Acridinedione Dyes with Onium Salts: Mechanistic Details", *Journal of Photochemistry and Photobiology A: Chemistry*, Vol. 138, No. 3, pp. 213-226, 2001.
- [34] Allen, N. S., "Photoinitiators for UV and Visible Curing of Coatings: Mechanisms and Properties", *Journal of Photochemistry and Photobiology A: Chemistry*, Vol. 100, No. 1-3, pp. 101-107, 1996.
- [35] Tomal, W., and J. Ortyl, "Water-Soluble Photoinitiators in Biomedical Applications", *Polymers*, Vol. 12, No. 5, p. 1073, 2020.
- [36] Radebner, J., A. Eibel, M. Leybold, N. Jungwirth, T. Pickl, A. Torvisco, R. Fischer, U.K. Fischer, N. Moszner, G. Gescheidt, H. Stueger, and M. Haas, "Tetraacylstannanes as Long-Wavelength Visible-Light Photoinitiators with Intriguing Low Toxicity", *Chemistry—A European Journal*, Vol. 24, No. 33, pp. 8281-8285, 2018.
- [37] Moszner, N., F. Zeuner, I. Lamparth, and U.K. Fischer, "Benzoylgermanium Derivatives as Novel Visible-Light Photoinitiators for Dental Composites", *Macromolecular Materials and Engineering*, Vol. 294, No. 12, pp. 877-886, 2009.
- [38] Moszner, N., U.K. Fischer, B. Ganster, R. Liska, and V. Rheinberger, "Benzoyl Germanium Derivatives as Novel Visible Light Photoinitiators for Dental Materials", *Dental Materials*, Vol. 24, No. 7, pp. 901-907, 2008.
- [39] Püschmann, S.D., P. Frühwirt, M. Pillinger, A. Knoechl, M. Mikusch, J. Radebner, A. Torvisco, R.C. Fischer, N. Moszner, G. Gescheidt, and M. Haas, "Synthesis of Mixed-Functionalized Tetraacylgermanes", *Chemistry—A European Journal*, Vol. 27, No. 10, pp. 3338-3347, 2021.
- [40] Püschmann, S.D., P. Frühwirt, S.M. Müller, S.H. Wagner, A. Torvisco, R.C. Fischer, A.M. Kelterer, T. Griesser, G. Gescheidt, and M. Haas, "Synthesis and Characterization of

Diacylgermanes: Persistent Derivatives with Superior Photoreactivity”, *Dalton Transactions*, Vol. 50, No. 34, pp. 11965-11974, 2021.

[41] Rees, M.T.L., G.T. Russell, M.D. Zammit, and T.P. Davis, “Visible Light Pulsed-OPO-Laser Polymerization at 450 nm Employing a Bis (acylphosphine oxide) Photoinitiator”, *Macromolecules*, Vol. 31, No. 6, pp. 1763-1772, 1998.

[42] Xie, C., Z. Wang, Y. Liu, L. Song, L. Liu, Z. Wang, and Q. Yu, “A Novel Acyl Phosphine Compound as Difunctional Photoinitiator for Free Radical Polymerization”, *Progress in Organic Coatings*, Vol. 135, pp. 34-40, 2019.

[43] Wu, Y., R. Li, J. Ke, X. Cheng, R. Tang, Y. Situ, and H. Huang, “Study on Bifunctional Acyldiphenylphosphine Oxides Photoinitiator for Free Radical Polymerization”, *European Polymer Journal*, Vol. 168, p. 111093, 2022.

[44] Dietlin, C., T.T. Trinh, S. Schweizer, B. Graff, F. Morlet-Savary, P.A. Noirot, and J. Lalevée, “Rational Design of Acyldiphenylphosphine Oxides as Photoinitiators of Radical Polymerization”, *Macromolecules*, Vol. 52, No. 20, pp. 7886-7893, 2019.

[45] Liu, Y., T. Wang, C. Xie, X. Tian, L. Song, L. Liu, Z. Wang, and Q. Yu, “Naphthyl-Based Acylphosphine Oxide Photoinitiators with High Efficiency and Low Migration”, *Progress in Organic Coatings*, Vol. 142, p. 105603, 2020.

[46] Duan, H., K. Leng, X. Xu, Q. Li, D. Liu, Y. Han, J. Gao, Q. Yu, and Z. Wang, “Monoacylphosphine Oxides with Substituents in the Phosphonyl Moiety as Norrish I Photoinitiators: Synthesis, Photoinitiation Properties and Mechanism”, *Journal of Photochemistry and Photobiology A: Chemistry*, Vol. 421, p. 113517, 2021.

[47] He, X., Y. Gao, J. Nie, and F. Sun, “Methyl Benzoylformate Derivative Norrish Type I Photoinitiators for Deep-Layer Photocuring Under Near-UV or Visible LED”, *Macromolecules*, Vol. 54, No. 8, pp. 3854-3864, 2021.

[48] Kamoun, E.A., A. Winkel, M. Eisenburger, and H. Menzel, “Carboxylated Camphorquinone as Visible-Light Photoinitiator for Biomedical Application: Synthesis, Characterization, and Application”, *Arabian Journal of Chemistry*, Vol. 9, No. 5, pp. 745-754, 2016.

- [49] Jakubiak, J., X. Allonas, J.P. Fouassier, A. Sionkowska, E. Andrzejewska, L.Å. Lindèn, and J.F. Rabek, “Camphorquinone–Amines Photoinitiating Systems for the Initiation of Free Radical Polymerization”, *Polymer*, Vol. 44, No. 18, pp. 5219-5226, 2003.
- [50] Ikemura, K., K. Ichizawa, Y. Jogetsu, and T. Endo, “Synthesis of a Novel Camphorquinone Derivative Having Acylphosphine Oxide Group, Characterization by UV-VIS Spectroscopy and Evaluation of Photopolymerization Performance”, *Dental Materials Journal*, Vol. 29, No. 2, pp. 122-131, 2010.
- [51] Kamoun, E.A., M.A. Abu-Saied, A.S. Doma, H. Menzel, and X. Chen, “Influence of Degree of Substitution and Folic Acid Cointiator on Pullulan-HEMA Hydrogel Properties Crosslinked Under Visible-Light Initiating System”, *International Journal of Biological Macromolecules*, Vol. 116, pp. 1175-1185, 2018.
- [52] Rahal, M., B. Graff, J. Toufaily, T. Hamieh, M. Ibrahim-Ouali, F. Dumur, and J. Lalevée, “Naphthyl-Naphthalimides as High-Performance Visible Light Photoinitiators for 3D Printing and Photocomposites Synthesis”, *Catalysts*, Vol. 11, No. 11, p. 1269, 2021.
- [53] Zhang, J., N. Zivic, F. Dumur, P. Xiao, B. Graff, J.P. Fouassier, D. Gigmes, and J. Lalevée, “N-[2-(Dimethylamino) ethyl]-1, 8-Naphthalimide Derivatives as Photoinitiators Under LEDs”, *Polymer Chemistry*, Vol. 9, No. 8, pp. 994-1003, 2018.
- [54] Rahal, M., H. Mokbel, B. Graff, V. Pertici, D. Gigmes, J. Toufaily, T. Hamieh, F. Dumur, and J. Lalevée, “Naphthalimide-Based Dyes as Photoinitiators Under Visible Light Irradiation and Their Applications: Photocomposite Synthesis, 3D Printing and Polymerization in Water”, *ChemPhotoChem*, Vol. 5, No. 5, pp. 476-490, 2021.
- [55] Bonardi, A.H., S. Zahouily, C. Dietlin, B. Graff, F. Morlet-Savary, M. Ibrahim-Ouali, D. Gigmes, N. Hoffmann, F. Dumur, and J. Lalevee, “New 1, 8-Naphthalimide Derivatives as Photoinitiators for Free-Radical Polymerization upon Visible Light”, *Catalysts*, Vol. 9, No. 8, p. 637, 2019.
- [56] Abdallah, M., D. Magaldi, A. Hijazi, B. Graff, F. Dumur, J.P. Fouassier, T.T. Bui, F. Goubard, and J. Lalevée, “Development of New High-Performance Visible Light Photoinitiators Based on Carbazole Scaffold and Their Applications in 3D Printing and Photocomposite Synthesis”, *Journal of Polymer Science Part A: Polymer Chemistry*, Vol. 57, No. 20, pp. 2081-2092, 2019.

- [57] Zhou, R., X. Sun, R. Mhanna, J.P. Malval, M. Jin, H. Pan, D. Wan, F. Morlet-Savary, H. Chaumeil, and C. Joyeux, “Wavelength-Dependent, Large-Amplitude Photoinitiating Reactivity within a Carbazole-Coumarin Fused Oxime Esters Series”, *ACS Applied Polymer Materials*, Vol. 2, No. 5, pp. 2077-2085, 2020.
- [58] Dumur, F., “Recent Advances on Carbazole-Based Photoinitiators of Polymerization”, *European Polymer Journal*, Vol. 125, p. 109503, 2020.
- [59] Rahal, M., M. Abdallah, T.T. Bui, F. Goubard, B. Graff, F. Dumur, J. Toufaily, T. Hamieh, and J. Lalevée, “Design of New Phenothiazine Derivatives as Visible Light Photoinitiators”, *Polymer Chemistry*, Vol. 11, Vol. 19, pp. 3349-3359, 2020.
- [60] Ma, X., R. Gu, L. Yu, W. Han, J. Li, X. Li, and T. Wang, “Conjugated Phenothiazine Oxime Esters as Free Radical Photoinitiators”, *Polymer Chemistry*, Vol. 8, No. 39, pp. 6134-6142, 2017.
- [61] Zhu, Y., D. Xu, Y. Zhang, Y. Zhou, Y. Yagci, and R. Liu, “Phenacyl Phenothiazinium Salt as a New Broad-Wavelength-Absorbing Photoinitiator for Cationic and Free Radical Polymerizations”, *Angewandte Chemie International Edition*, Vol. 60, No. 31, pp. 16917-16921, 2021.
- [62] Yilmaz, G., B. Aydogan, G. Temel, N. Arsu, N. Moszner, and Y. Yagci, “Thioxanthone–Fluorenes as Visible Light Photoinitiators for Free Radical Polymerization”, *Macromolecules*, Vol. 43, No. 10, pp. 4520-4526, 2010.
- [63] Tunc, D., and Y. Yagci, “Thioxanthone-Ethylcarbazole as a Soluble Visible Light Photoinitiator for Free Radical and Free Radical Promoted Cationic Polymerizations”, *Polymer Chemistry*, Vol. 2, No. 11, pp. 2557-2563, 2011.
- [64] Balta, D.K., G. Temel, G. Goksu, N. Ocal, and N. Arsu, “Thioxanthone–Diphenyl Anthracene: Visible Light Photoinitiator”, *Macromolecules*, Vol. 45, No. 1, pp. 119-125, 2012.
- [65] Wu, X., M. Jin, J.P. Malval, D. Wan, and H. Pu, “Visible Light-Emitting Diode-Sensitive Thioxanthone Derivatives Used in Versatile Photoinitiating Systems for Photopolymerizations”, *Journal of Polymer Science Part A: Polymer Chemistry*, Vol. 55, No. 24, pp. 4037-4045, 2017.

- [66] Tar, H., D. Sevinc Esen, M. Aydin, C. Ley, N. Arsu, and X. Allonas, "Panchromatic Type II Photoinitiator for Free Radical Polymerization Based on Thioxanthone Derivative", *Macromolecules*, Vol. 46, No. 9, pp. 3266-3272, 2013.
- [67] Hola, E., M. Pilch, and J. Ortyl, "Thioxanthone Derivatives as a New Class of Organic Photocatalysts for Photopolymerisation Processes and the 3D Printing of Photocurable Resins under visible light", *Catalysts*, Vol. 10, No. 8, p. 903, 2020.
- [68] Wu, Q., Y. Xiong, Q. Liang, and H. Tang, "Developing Thioxanthone Based Visible Photoinitiators for Radical Polymerization", *Rsc Advances*, Vol. 4, No. 94, pp. 52324-52331, 2014.
- [69] Yilmaz, G., A. Tuzun, and Y. Yagci, "Thioxanthone–Carbazole as a Visible Light Photoinitiator for Free Radical Polymerization", *Journal of Polymer Science Part A: Polymer Chemistry*, Vol. 48, No. 22, pp. 5120-5125, 2010.
- [70] Qin, X., G. Ding, Y. Gong, C. Jing, G. Peng, S. Liu, L. Niu, S. Zhang, Z. Luo, H. Li, and F. Gao, "Stilbene-Benzophenone Dyads for Free Radical Initiating Polymerization of Methyl Methacrylate Under Visible Light Irradiation", *Dyes and Pigments*, Vol. 132, pp. 27-40, 2016.
- [71] Xue, T., Y. Li, X. Zhao, J. Nie, and X. Zhu, "A Facile Synthesized Benzophenone Schiff-Base Ligand as Efficient Type II Visible Light Photoinitiator", *Progress in Organic Coatings*, Vol. 157, p. 106329, 2021.
- [72] Xiao, P., F. Dumur, B. Graff, D. Gigmes, J.P. Fouassier, and J. Lalevée, "Variations on the Benzophenone Skeleton: Novel High Performance Blue Light Sensitive Photoinitiating Systems", *Macromolecules*, Vol. 46, No. 19, pp. 7661-7667, 2013.
- [73] Zhang, J., N. Zivic, F. Dumur, P. Xiao, B. Graff, D. Gigmes, J.P. Fouassier, and J. Lalevée, "A Benzophenone-Naphthalimide Derivative as Versatile Photoinitiator of Polymerization Under Near UV and Visible Lights", *Journal of Polymer Science Part A: Polymer Chemistry*, Vol. 53, No. 3, pp. 445-451, 2015.
- [74] Huang, T.L., Y.H. Li, and Y.C. Chen, "Benzophenone Derivatives as Novel Organosoluble Visible Light Type II Photoinitiators for UV and LED Photoinitiating Systems", *Journal of Polymer Science*, Vol. 58, No. 20, pp. 2914-2925, 2020.

- [75] Wang, G., K. Zhang, Y. Wang, C. Zhao, B. He, Y. Ma, and W. Yang, “Decorating an Individual Living Cell with a Shell of Controllable Thickness by Cytocompatible Surface Initiated Graft Polymerization”, *Chemical Communications*, Vol. 54, No. 37, pp. 4677-4680, 2018.
- [76] Bender, C.J., “Theoretical Models of Charge-Transfer Complexes”, *Chemical Society Reviews*, Vol. 15, No. 4, pp. 475-502, 1986.
- [77] Kaya, K., J. Kreutzer, and Y. Yagci, “A Charge-Transfer Complex of Thioxanthonephenacyl Sulfonium Salt as a Visible-Light Photoinitiator for Free Radical and cationic polymerizations”, *ChemPhotoChem*, Vol. 3, No. 11, pp. 1187-1192, 2019.
- [78] Li, J., X. Zhang, J. Nie, and X. Zhu, “Visible Light and Water-Soluble Photoinitiating System Based on the Charge Transfer Complex for Free Radical Photopolymerization”, *Journal of Photochemistry and Photobiology A: Chemistry*, Vol. 402, p. 112803, 2020.
- [79] Xu, D., X. Zou, Y. Zhu, Z. Yu, M. Jin, and R. Liu, “Phenothiazine-Based Charge-Transfer Complexes as Visible-Light Photoinitiating Systems for Acrylate and Thiol-Ene Photopolymerization”, *Progress in Organic Coatings*, Vol. 166, p. 106772, 2022.
- [80] Wang, D., P. Garra, J.P. Fouassier, B. Graff, Y. Yagci, and J. Lalevée, “Indole-Based Charge Transfer Complexes as Versatile Dual Thermal and Photochemical Polymerization Initiators for 3D Printing and Composites”, *Polymer Chemistry*, Vol. 10, No. 36, pp. 4991-5000, 2019.
- [81] Wang, D., P. Garra, S. Lakhdar, B. Graff, J.P. Fouassier, H. Mokbel, M. Abdallah, and J. Lalevée, “Charge Transfer Complexes as Dual Thermal and Photochemical Polymerization Initiators for 3D Printing and Composites Synthesis”, *ACS Applied Polymer Materials*, Vol. 1, No. 3, pp. 561-570, 2019.
- [82] Garra, P., B. Graff, F. Morlet-Savary, C. Dietlin, J.M. Becht, J.P. Fouassier, and J. Lalevée, “Charge Transfer Complexes as Pan-Scaled Photoinitiating Systems: From 50  $\mu\text{m}$  3D Printed Polymers at 405 nm to Extremely Deep Photopolymerization (31 cm)”, *Macromolecules*, Vol. 51, No. 1, pp. 57-70, 2018.
- [83] Garra, P., A. Caron, A. Al Mousawi, B. Graff, F. Morlet-Savary, C. Dietlin, Y. Yagci, J.P. Fouassier, and J. Lalevée, “Photochemical, Thermal Free Radical, and Cationic

Polymerizations Promoted by Charge Transfer Complexes: Simple Strategy for the Fabrication of Thick Composites”, *Macromolecules*, Vol. 51, No. 19, pp. 7872-7880, 2018.

[84] Wang, D., K. Kaya, P. Garra, J.P. Fouassier, B. Graff, Y. Yagci, and J. Lalevée, “Sulfonium Salt Based Charge Transfer Complexes as Dual Thermal and Photochemical Polymerization Initiators for Composites and 3D Printing”, *Polymer Chemistry*, Vol. 10, No. 34, pp. 4690-4698, 2019.

[85] Garra, P., F. Morlet-Savary, C. Dietlin, J.P. Fouassier, and J. Lalevée, “On-Demand Visible Light Activated Amine/Benzoyl Peroxide Redox Initiating Systems: A unique Tool to Overcome the Shadow Areas in Photopolymerization Processes”, *Macromolecules*, Vol. 49, No. 24, pp. 9371-9381, 2016.

[86] Tasdelen, M.A., B. Karagoz, N. Bicak, and Y. Yagci, “Phenacylpyridinium Oxalate as a Novel Water-Soluble Photoinitiator for Free Radical Polymerization”, *Polymer Bulletin*, Vol. 59, No. 6, pp. 759-766, 2008.

[87] Lin, H., D. Zhang, P.G. Alexander, G. Yang, J. Tan, A.W.M. Cheng, and R.S. Tuan, “Application of Visible Light-Based Projection Stereolithography for Live Cell-Scaffold Fabrication with Designed Architecture”, *Biomaterials*, Vol. 34, No. 2, pp. 331-339, 2013.

[88] Sun, G., Y. Huang, J. Ma, D. Li, Q. Fan, Y. Li, and J. Shao, “Photoinitiation Mechanisms and Photogelation Kinetics of Blue Light Induced Polymerization of Acrylamide with Bicomponent Photoinitiators”, *Journal of Polymer Science*, Vol. 59, No. 7, pp. 567-577, 2021.

[89] Figg, C.A., J.D. Hickman, G.M. Scheutz, S. Shanmugam, R.N. Carmean, B.S. Tucker, C. Boyer, and B.S. Sumerlin, “Color-Coding Visible Light Polymerizations to Elucidate the Activation of Trithiocarbonates Using Eosin Y”, *Macromolecules*, Vol. 51, No. 4, pp. 1370-1376, 2018.

[90] Peng, Y., Z. Wang, J. Peña, Z. Guo, and J. Xing, “Effect of TEOA on the Process of Photopolymerization at 532 nm and Properties of Nanogels”, *Photochemistry and Photobiology*, Vol. 98, No. 1, pp. 132-140, 2022.

[91] Li, J., Y. Peng, J. Peña, and J. Xing, “An Initiating System with High Efficiency for PEGDA Photopolymerization at 532 nm”, *Journal of Photochemistry and Photobiology A: Chemistry*, Vol. 411, p. 113216, 2021.

- [92] Encinas, M.V., A.M. Rufs, S.G. Bertolotti, and C.M. Previtali, "Xanthene Dyes/Amine as Photoinitiators of Radical Polymerization: A Comparative and Photochemical Study in Aqueous Medium", *Polymer*, Vol. 50, No. 13, pp. 2762-2767, 2009.
- [93] Qi, Y., M.R. Gleeson, J. Guo, S. Gallego, and J.T. Sheridan, "Quantitative Comparison of Five Different Photosensitizers for Use in a Photopolymer", *Physics Research International*, Vol. 2012, pp. 1-11, 2012.
- [94] Orellana, B., A.M. Rufs, M.V. Encinas, C.M. Previtali, and S. Bertolotti, "The Photoinitiation Mechanism of Vinyl Polymerization by Riboflavin/Triethanolamine in Aqueous Medium", *Macromolecules*, Vol. 32, No. 20, pp. 6570-6573, 1999.
- [95] Ahmad, I., K. Iqbal, M.A. Sheraz, S. Ahmed, S.A. Ali, S.H. Kazi, T. Mirza, R. Bano, and M. Aminuddin, "Solvent Effect on Photoinitiator Reactivity in the Polymerization of 2-Hydroxyethyl Methacrylate", *Advances in Physical Chemistry*, Vol. 2013, pp. 1-6, 2013.
- [96] Ahmad, I., K. Iqbal, M.A. Sheraz, S. Ahmed, T. Mirza, S.H. Kazi, and M. Aminuddin, "Photoinitiated Polymerization of 2-Hydroxyethyl Methacrylate by Riboflavin/Triethanolamine in Aqueous Solution: A Kinetic Study", *International Scholarly Research Notices*, Vol. 2013, pp. 1-7, 2013.
- [97] Michel, S. S.E., A. Kilner, J.C. Eloi, S.E. Rogers, W.H. Briscoe, and M.C. Galan, "Norbornene-Functionalized Chitosan Hydrogels and Microgels via Unprecedented Photoinitiated Self-Assembly for Potential Biomedical Applications", *ACS Applied Bio Materials*, Vol. 3, No. 8, pp. 5253-5262, 2020.
- [98] Kamoun, E.A., A.M. Omer, M.M. Abu-Serie, S.N. Khattab, H.M. Ahmed, and A.A. Elbardan, "Photopolymerized PVA-g-GMA Hydrogels for Biomedical Applications: Factors Affecting Hydrogel Formation and Bioevaluation Tests", *Arabian Journal for Science and Engineering*, Vol. 43, No. 7, pp. 3565-3575, 2018.
- [99] Billiet, T., E. Gevaert, T. De Schryver, M. Cornelissen, and P. Dubruel, "The 3D Printing of Gelatin Methacrylamide Cell-Laden Tissue-Engineered Constructs with High Cell Viability", *Biomaterials*, Vol. 35, No. 1, pp. 49-62, 2014.
- [100] Lin, C.H., K.F. Lin, K. Mar, S.Y. Lee, and Y.M. Lin, "Antioxidant N-Acetylcysteine and Glutathione Increase the Viability and Proliferation of MG63 Cells Encapsulated in the

Gelatin Methacrylate/VA-086/Blue Light Hydrogel System”, *Tissue Engineering Part C: Methods*, Vol. 22, No. 8, pp. 792-800, 2016.

[101] Rouillard, A.D., C.M. Berglund, J.Y. Lee, W.J. Polacheck, Y. Tsui, L.J. Bonassar, and B.J. Kirby, “Methods for Photocrosslinking Alginate Hydrogel Scaffolds with High Cell Viability”, *Tissue Engineering Part C: Methods*, Vol. 17, No. 2, pp. 173-179, 2011.

[102] Chandler, E.M., C.M. Berglund, J.S. Lee, W.J. Polacheck, J.P. Gleghorn, B.J. Kirby, and C. Fischbach, “Stiffness of Photocrosslinked RGD-Alginate Gels Regulates Adipose Progenitor Cell Behavior”, *Biotechnology and Bioengineering*, Vol. 108, No. 7, pp. 1683-1692, 2011.

[103] Occhetta, P., N. Sadr, F. Piraino, A. Redaelli, M. Moretti, and M. Rasponi, “Fabrication of 3D Cell-Laden Hydrogel Microstructures Through Photo-Mold Patterning”, *Biofabrication*, Vol. 5, No. 3, p. 035002, 2013.

[104] Lima, A.C., C.A. Custódio, C. Alvarez-Lorenzo, and J.F. Mano, “Biomimetic Methodology to Produce Polymeric Multilayered Particles for Biotechnological and Biomedical Applications”, *Small*, Vol. 9, No. 15, pp. 2487-2492, 2013.

[105] Fairbanks, B.D., M.P. Schwartz, C.N. Bowman, and K.S. Anseth, “Photoinitiated Polymerization of PEG-Diacrylate with Lithium Phenyl-2, 4, 6-Trimethylbenzoylphosphinate: Polymerization Rate and Cytocompatibility”, *Biomaterials*, Vol. 30, No. 35, pp. 6702-6707, 2009.

[106] Benedikt, S., J. Wang, M. Markovic, N. Moszner, K. Dietliker, A. Ovsianikov, H. Grützmacher, and R. Liska, “Highly Efficient Water-Soluble Visible Light Photoinitiators”, *Journal of Polymer Science Part A: Polymer Chemistry*, Vol. 54, No. 4, pp. 473-479, 2016.

[107] Majima, T., W. Schnabel, and W. Weber, “Phenyl-2, 4, 6-Trimethylbenzoylphosphinates as Water-Soluble Photoinitiators. Generation and Reactivity of  $O=P(C_6H_5)(O^-)$  Radical Anions”, *Die Makromolekulare Chemie: Macromolecular Chemistry and Physics*, Vol. 192, No. 10, pp. 2307-2315, 1991.

[108] Wang, H., B. Zhang, J. Zhang, X. He, F. Liu, J. Cui, Z. Lu, G. Hu, J. Yang, Z. Zhou, and R. Wang, “General One-Pot Method for Preparing Highly Water-Soluble and Biocompatible Photoinitiators for Digital Light Processing-Based 3D Printing of Hydrogels”, *ACS Applied Materials & Interfaces*, Vol. 13, No. 46, pp. 55507-55516, 2021.

- [109] Balta, D.K., G. Temel, M. Aydin, and N. Arsu, "Thioxanthone Based Water-Soluble Photoinitiators for Acrylamide Photopolymerization", *European Polymer Journal*, Vol. 46, No. 6, pp. 1374-1379, 2010.
- [110] Chen, H., L. Pieuchot, P. Xiao, F. Dumur, and J. Lalevée, "Water-Soluble/Visible-Light-Sensitive Naphthalimide Derivative-Based Photoinitiating Systems: 3D Printing of Antibacterial Hydrogels", *Polymer Chemistry*, Vol. 13, No. 20, pp. 2918-2932, 2022.
- [111] Jiang, X., and J. Yin, "Water-Soluble Polymeric Thioxanthone Photoinitiator Containing Glucamine as Coinitiator", *Macromolecular Chemistry and Physics*, Vol. 209, No. 15, pp. 1593-1600, 2008.
- [112] Allen, N.S., E.M. Howells, E. Lam, F. Catalina, P.N. Green, W.A. Green, and W. Chen, "Photopolymerisation and Flash Photolysis of a Water Soluble Benzophenone Photoinitiator: Influence of Tertiary Amine", *European Polymer Journal*, Vol. 24, No. 6, pp. 591-593, 1988.
- [113] Aubry, B., F. Dumur, M. Lansalot, E. Bourgeat-Lami, E. Lacote, and J. Lalevée, "Development of Water-Soluble Type I Photoinitiators for Hydrogel Synthesis", *Macromol*, Vol. 2, No. 1, pp. 131-140, 2022.
- [114] Le, C.M.Q., T. Petitory, X. Wu, A. Spangenberg, J. Ortyl, M. Galek, L. Infante, H. Thérien-Aubin, and A. Chemtob, "Water-Soluble Photoinitiators from Dimethylamino-Substituted Monoacylphosphine Oxide for Hydrogel and Latex Preparation", *Macromolecular Chemistry and Physics*, Vol. 222, No. 19, p. 2100217, 2021.
- [115] Temel, G., and N. Arsu, "One-Pot Synthesis of Water-Soluble Polymeric Photoinitiator via Thioxanthonation and Sulfonation Process", *Journal of Photochemistry and Photobiology A: Chemistry*, Vol. 202, No. 1, pp. 63-66, 2009.
- [116] Kojima, K., M. Ito, H. Morishita, and N. Hayashi, "A Novel Water-Soluble Photoinitiator for the Acrylic Photopolymerization Type Resist System", *Chemistry of Materials*, Vol. 10, No. 11, pp. 3429-3433, 1998.
- [117] Abdallah, M., A. Hijazi, B. Graff, J.P. Fouassier, G. Rodeghiero, A. Gualandi, F. Dumur, P.G. Cozzi, and J. Lalevée, "Coumarin Derivatives as Versatile Photoinitiators for 3D Printing, Polymerization in Water and Photocomposite Synthesis", *Polymer Chemistry*, Vol. 10, No. 7, pp. 872-884, 2019.

- [118] Müller, G., M. Zalibera, G. Gescheidt, A. Rosenthal, G. Santiso-Quinones, K. Dietliker, and H. Grützmacher, “Simple One-Pot Syntheses of Water-Soluble Bis (acyl) Phosphane Oxide Photoinitiators and Their Application in Surfactant-Free Emulsion Polymerization”, *Macromolecular Rapid Communications*, Vol. 36, No. 6, pp. 553-557, 2015.
- [119] Qiu, J., and J. Wei, “Water-Soluble and Polymerizable Thioxanthone Photoinitiator Containing Imidazole”, *Journal of Applied Polymer Science*, Vol. 131, No. 16, p. 40659, 2014.
- [120] Eren, T.N., T. Gencoglu, M. Abdallah, J. Lalevee, and D. Avci, “A Water Soluble and Highly Reactive Bisphosphonate Functionalized Thioxanthone-Based Photoinitiator”, *European Polymer Journal*, Vol. 135, p. 109906, 2020.
- [121] Karasu, F., D.K. Balta, R. Liska, and N. Arsu, “Photoinitiated Polymerization of  $\beta$ -Cyclodextrin/Methyl Methacrylate Host/Guest Complex in the Presence of Water Soluble Photoinitiator, Thioxanthone-Catechol-O,O'-Diacetic Acid”, *Journal of Inclusion Phenomena and Macrocyclic Chemistry*, Vol. 68, No. 1, pp. 147-153, 2010.
- [122] Eren, T.N., J. Lalevee, and D. Avci, “Bisphosphonic Acid-Functionalized Water-Soluble Photoinitiators”, *Macromolecular Chemistry and Physics*, Vol. 220, No. 19, p. 1900268, 2019.
- [123] Liska, R., S. Knaus, H. Gruber, and J. Wendrinsky, “Carbohydrate Modified Photoinitiators”, *Surface Coatings International*, Vol. 83, No. 6, pp. 297-303, 2000.
- [124] Wang, Y., X. Jiang, and J. Yin, “A Water-Soluble Supramolecular-Structured Photoinitiator Between Methylated  $\beta$ -Cyclodextrin and 2, 2-dimethoxy-2-phenylacetophenone”, *Journal of Applied Polymer Science*, Vol. 105, No. 6, pp. 3819-3823, 2007.
- [125] Zhang, J., F. Dumur, P. Xiao, B. Graff, D. Bardelang, D. Gigmes, J.P. Fouassier, and J. Lalevée, “Structure Design of Naphthalimide Derivatives: Toward Versatile Photoinitiators for near-UV/Visible LEDs, 3D Printing, and Water-Soluble Photoinitiating Systems”, *Macromolecules*, Vol. 48, No. 7, pp. 2054-2063, 2015.

- [126] Zhang, J., P. Xiao, S. Shi, and J. Nie, "Preparation and Characterization of a Water Soluble Methylated  $\beta$ -Cyclodextrin/Camphorquinone Complex", *Polymers for Advanced Technologies*, Vol. 20, No. 9, pp. 723-728, 2009.
- [127] Li, T., Z. Su, H. Xu, X. Ma, J. Yin, and X. Jiang, "A Supramolecular Polymeric Photoinitiator with Enhanced Dispersion in Photo-Curing Systems", *Polymer Chemistry*, Vol. 11, No. 11, pp. 1885-1893, 2020.
- [128] Aparicio, J.L., and M. Elizalde, "Migration of Photoinitiators in Food Packaging: A Review", *Packaging Technology and Science*, Vol. 28, No. 3, pp. 181-203, 2015.
- [129] Wu, Y., R. Li, J. Wang, Y. Situ, and H. Huang, "A New Carbazolyl-Based acylphosphine Oxide Photoinitiator with High Performance and Low Migration", *Journal of Polymer Science*, Vol. 60, No. 1, pp. 52-61, 2022.
- [130] Breloy, L., R. Losantos, D. Sampedro, M. Marazzi, J.P. Malval, Y. Heo, J. Akimoto, Y. Ito, V. Brezová, and D.L. Versace, "Allyl Amino-Thioxanthone Derivatives as Highly Efficient Visible Light H-Donors and Co-Polymerizable Photoinitiators", *Polymer Chemistry*, Vol. 11, No. 26, pp. 4297-4312, 2020.
- [131] Wei, J., and B. Wang, "A Highly Efficient Polymerizable Photoinitiator Comprising Benzophenone, Thio Moieties, and N-Arylmaleimide", *Macromolecular Chemistry and Physics*, Vol. 212, No. 1, pp. 88-95, 2011.
- [132] Qiu, J., and J. Wei, "Thioxanthone Photoinitiator Containing Polymerizable N-Aromatic Maleimide for Photopolymerization", *Journal of Polymer Research*, Vol. 21, No. 9, pp. 1-7, 2014.
- [133] Wang, H., Y. Shi, J. Wei, X. Jiang, and J. Yin, "ESR and Kinetic Study of a Novel Polymerizable Photoinitiator Comprising the Structure of N-Phenylmaleimide and Benzophenone for Photopolymerization", *Journal of Applied Polymer Science*, Vol. 101, No. 4, pp. 2347-2354, 2006.
- [134] Wang, H., J. Wei, X. Jiang, and J. Yin, "Novel Chemical-Bonded Polymerizable Sulfur-Containing Photoinitiators Comprising the Structure of Planar N-Phenylmaleimide and benzophenone for photopolymerization", *Polymer*, Vol. 47, No. 17, pp. 4967-4975, 2006.

- [135] Jiang, B., T. Zhang, L. Zhao, Z. Xu, and Y. Huang, "Effect of Polymerizable Photoinitiators on the UV-Polymerization Behaviors of Photosensitive Polysiloxane", *Journal of Polymer Science Part A: Polymer Chemistry*, Vol. 55, No. 1, pp. 1696-1705, 2017.
- [136] Wang, H., J. Wei, X. Jiang, and J. Yin, "Novel Polymerizable Sulfur-Containing Benzophenones as Free-Radical Photoinitiators for Photopolymerization", *Macromolecular Chemistry and Physics*, Vol. 207, No. 12, pp. 1080-1086, 2006.
- [137] Ren, X., W. Liu, Q. Yao, S. Wang, W. Liu, H. Gu, D. Wang, J. Fan, and X. Peng, "A UV-LED Excited Photoinitiator with Low Toxicity and Low Migration for Photocurable Inks", *Dyes and Pigments*, Vol. 200, p. 110133, 2022.
- [138] Wu, Q., X. Wang, Y. Xiong, J. Yang, and H. Tang, "Thioxanthone Based One-Component Polymerizable Visible Light Photoinitiator for Free radical Polymerization", *RSC advances*, Vol. 6, No. 70, pp. 66098-66107, 2016.
- [139] Qiu, W., J. Zhu, K. Dietliker, and Z. Li, "Polymerizable Oxime Esters: An Efficient Photoinitiator with Low Migration Ability for 3D Printing to Fabricate Luminescent Devices", *ChemPhotoChem*, Vol. 4, No. 11, pp. 5296-5303, 2020.
- [140] Liang, S., Y.D. Yang, H.Y. Zhou, Y.Q. Li, and J.X. Wang, "Novel Polymerizable HMPP-Type Photoinitiator with Carbamate: Synthesis and Photoinitiating Behaviors", *Progress in Organic Coatings*, Vol. 110, pp. 128-133, 2017.
- [141] Yang, J., R. Tang, S. Shi, and J. Nie, "Synthesis and Characterization of Polymerizable One-Component Photoinitiator Based on Sesamol", *Photochemical & Photobiological Sciences*, Vol. 12, No. 5, pp. 923-929, 2013.
- [142] Hou, G., S. Shi, S. Liu, and J. Nie, "Synthesis and Evaluation of 4-Benzophenone Methoxyl Methacrylate as a Polymerizable Photoinitiator", *Polymer Journal*, Vol. 40, No. 3, pp. 228-232, 2008.
- [143] Wu, Q., Y. Mo, Y. Zhang, F. Li, and M. Deng, "Photophysical/Photochemical, Kinetic, and Migration Stability Studies of One-Component Polymerizable Thioxanthone-Based Photoinitiators", *Macromolecular Chemistry and Physics*, Vol. 222, No. 20, p. 2100221, 2021.

- [144] Yao, M., S. Liu, C. Huang, J. Nie, and Y. He, "Significantly Improve the Photoinitiation Ability of Hydroxyalkyl-Derived Polymerizable  $\alpha$ -Hydroxyalkylacetophenone Photoinitiators by Blocking Hyperconjugation", *Journal of Photochemistry and Photobiology A: Chemistry*, Vol. 419, p. 113451, 2021.
- [145] Wu, Q., K. Tang, Y. Xiong, X. Wang, J. Yang, and H. Tang, "High-Performance and Low Migration One-Component Thioxanthone Visible Light Photoinitiators", *Macromolecular Chemistry and Physics*, Vol. 218, No. 6, p. 1600484, 2017.
- [146] Chen, W., X. Liu, L. Wang, J. Zhao, and G. Zhao, "Synthesis and Preliminary Photopolymerization Evaluation of Photopolymerizable Type II Photoinitiators BRA and TXRA", *Progress in Organic Coatings*, Vol. 133, pp. 191-197, 2019.
- [147] Yang, J., W. Liao, Y. Xiong, Q. Wu, X. Wang, Z. Li, and H. Tang, "Naphthalimide Dyes: Polymerizable One-Component Visible Light Initiators", *Dyes and Pigments*, Vol. 148, pp. 16-24, 2018.
- [148] Eren, T.N., B. Graff, J. Lalevee, and D. Avci, "Thioxanthone-Functionalized 1, 6-Heptadiene as Monomeric Photoinitiator", *Progress in Organic Coatings*, Vol. 128, pp. 148-156, 2019.
- [149] Xue, T., H. Lu, H. Yuan, Y. He, J. Nie, and X. Zhu, "A Bis-Acrylate Functionalized Enone as Photoinitiator and Crosslinker in Photopolymerization", *Progress in Organic Coatings*, Vol. 162, p. 106587, 2022.
- [150] Karahan, Ö., D.K. Balta, N. Arsu, and D. Avci, "Synthesis and Evaluations of Novel Photoinitiators with Side-Chain Benzophenone, Derived from Alkyl  $\alpha$ -Hydroxymethacrylates", *Journal of Photochemistry and Photobiology A: Chemistry*, Vol. 274, pp. 43-49, 2014.
- [151] Cesur, B., O. Karahan, S. Agopcan, T.N. Eren, N. Okte, and D. Avci, "Difunctional Monomeric and Polymeric Photoinitiators: Synthesis and Photoinitiating Behaviors", *Progress in Organic Coatings*, Vol. 86, pp. 71-78, 2015.
- [152] Balta, D.K., Ö. Karahan, D. Avci, and N. Arsu, "Synthesis, Photophysical and Photochemical Studies of Benzophenone Based Novel Monomeric and Polymeric Photoinitiators", *Progress in Organic Coatings*, Vol. 78, pp. 200-207, 2015.

- [153] Oesterreicher, A., M. Roth, D. Hennen, F.H. Mostegel, M. Edler, S. Kappaun, and T. Griesser, “Low Migration Type I Photoinitiators for Biocompatible Thiol-Ene Formulations”, *European Polymer Journal*, Vol. 88, pp. 393-402, 2017.
- [154] Roth, M., D. Hennen, A. Oesterreicher, F.H. Mostegel, S. Kappaun, M. Edler, and T. Griesser, “Exploring Functionalized Benzophenones as Low-Migration Photoinitiators for Vinyl Carbonate/Thiol Formulations”, *European Polymer Journal*, Vol. 88, pp. 403-411, 2017.
- [155] Wang, J., S. Stanic, A.A. Altun, M. Schwentenwein, K. Dietliker, L. Jin, J. Stampfl, S. Baudis, R. Liska, and H. Grützmacher, “A Highly Efficient Waterborne Photoinitiator for Visible-Light-Induced Three-Dimensional Printing of Hydrogels”, *Chemical Communications*, Vol. 54, No. 8, pp. 920-923, 2018.
- [156] Wang, K., Y. Lu, P. Chen, J. Shi, H. Wang, and Q. Yu, “Novel One-Component Polymeric Benzophenone Photoinitiator Containing Poly (ethylene glycol) as Hydrogen donor”, *Materials Chemistry and Physics*, Vol. 143, No. 3, pp. 1391-1395, 2014.
- [157] Akat, H., B. Gacal, D.K. Balta, N. Arsu, and Y. Yagci, “Poly (ethylene glycol)-Thioxanthone Prepared by Diels–Alder Click Chemistry as One-Component Polymeric Photoinitiator for Aqueous Free-Radical Polymerization”, *Journal of Polymer Science Part A: Polymer Chemistry*, Vol. 48, No. 10, pp. 2109-2114, 2010.
- [158] Wen, Y., X. Jiang, and J. Yin, “Polymeric Michler's Ketone Photoinitiators: The Effect of Chain Flexibility”, *Progress in Organic Coatings*, Vol. 66, No. 1, pp. 65-72, 2009.
- [159] Kreutzer, J., K. Kaya, and Y. Yagci, “Poly (propylene oxide)-Thioxanthone as One-Component Type II Polymeric Photoinitiator for Free Radical Polymerization with Low Migration BEhavior”, *European Polymer Journal*, Vol. 95, pp. 71-81, 2017.
- [160] Wu, Y., X. Zhang, D. Chen, Y. Ma, Q. Wang, J. Wang, and W. Yang, “Synthesis and Characterization of a Novel Kind of Water-Soluble Macromolecular Photoinitiators and Their Application for the Preparation of Water-Soluble Branched Polymers”, *Industrial & Engineering Chemistry Research*, Vol. 60, No. 21, pp. 7755-7763, 2021.
- [161] Temel, G., B. Aydogan, N. Arsu, and Y. Yagci, “Synthesis and Characterization of One-Component Polymeric Photoinitiator by Simultaneous Double Click Reactions and Its

Use in Photoinduced Free Radical Polymerization”, *Macromolecules*, Vol. 42, No. 16, pp. 6098-6106, 2009.

[162] Eren, T.N., J. Lalevee, and D. Avci, “Water Soluble Polymeric Photoinitiator for Dual-Curing of Acrylates and Methacrylates”, *Journal of Photochemistry and Photobiology A: Chemistry*, Vol. 389, p. 112288, 2020.

[163] Kork, S., G. Yilmaz, and Y. Yagci, “Poly (vinyl alcohol)–Thioxanthone as One-Component Type II Photoinitiator for Free Radical Polymerization in Organic and Aqueous Media”, *Macromolecular Rapid Communications*, Vol. 36, No. 10, pp. 923-928, 2015.

[164] Liu, Y., X. Huang, K. Han, Y. Dai, X. Zhang, and Y. Zhao, “High-Performance Lignin-Based Water-Soluble Macromolecular Photoinitiator for the Fabrication of Hybrid Hydrogel”, *ACS Sustainable Chemistry & Engineering*, Vol. 7, No. 4, pp. 4004-4011, 2019.

[165] Huang, X., Y. Zhang, F. Li, J. Zhang, Y. Dai, M. Shi, and Y. Zhao, “Highly Efficient Alginate-Based Macromolecular Photoinitiator for Crosslinking and Toughening Gelatin Hydrogels”, *Journal of Polymer Science*, Vol. 58, No. 10, pp. 1439-1449, 2020.

[166] Li, T., Z. Su, H. Xu, X. Jiang, X. Ma, and J. Yin, “Hyperbranched Poly (ether amine)(hPEA) as Novel Backbone for Amphiphilic One-Component Type-II Polymeric Photoinitiators”, *Chinese Chemical Letters*, Vol. 29, No. 3, pp. 451-455, 2018.

[167] Wen, Y., X. Jiang, R. Liu, and J. Yin, “Amphipathic Hyperbranched Polymeric Thioxanthone Photoinitiators (AHPTXs): Synthesis, Characterization and Photoinitiated Polymerization”, *Polymer*, Vol. 50, No. 16, pp. 3917-3923, 2009.

[168] Jiang, X., and J. Yin, “Dendritic Macrophotoinitiator Containing Thioxanthone and Cointiator Amine”, *Macromolecules*, Vol. 37, No. 21, pp. 7850-7853, 2004.

[169] Jiang, X., W. Wang, H. Xu, and J. Yin, “Water-Compatible Dendritic Macrophotoinitiator Containing Thioxanthone”, *Journal of Photochemistry and Photobiology A: Chemistry*, Vol. 181, No. 2-3, pp. 233-237, 2006.

[170] Chen, Y., J. Loccufier, L. Vanmaele, E. Barriau, and H. Frey, “Novel Multifunctional Polymeric Photoinitiators and Photo-Coinitiators Derived from Hyperbranched Polyglycerol”, *Macromolecular Chemistry and Physics*, Vol. 208, No. 15, pp. 1694-1706, 2007.

- [171] Chen, Y., J. Loccufier, L. Vanmaele, and H. Frey, "Novel Multifunctional Hyperbranched Polymeric Photoinitiators with Built-in Amine Coinitiators for UV Curing", *Journal of Materials Chemistry*, Vol. 17, No. 32, pp. 3389-3392, 2007.
- [172] Wu, Y., X. Zhang, D. Chen, Y. Ma, Q. Wang, J. Wang, and W. Yang, "Water-Soluble Branched Polyacrylamides Prepared by UV-Initiated Polymerization Using a Novel Kind of Water-Soluble Macromolecular Photoinitiator", *Industrial & Engineering Chemistry Research*, Vol. 60, No. 33, pp. 12166-12174, 2021.
- [173] Corrales, T., F. Catalina, N.S. Allen, and C. Peinado, "Novel Water Soluble Copolymers Based on Thioxanthone: Photochemistry and Photoinitiation Activity", *Journal of Photochemistry and Photobiology A: Chemistry*, Vol. 169, No. 1, pp. 95-100, 2005.
- [174] Yang, J., W. Liao, Y. Xiong, X. Wang, Z. Li, and H. Tang, "A Multifunctionalized Macromolecular Silicone-Naphthalimide Visible Photoinitiator for Free Radical Polymerization", *Progress in Organic Coatings*, Vol. 115, pp. 151-158, 2018.
- [175] Wang, H., J. Wei, X. Jiang, and J. Yin, "Highly Efficient Sulfur-Containing Polymeric Photoinitiators Bearing Side-Chain Benzophenone and Coinitiator Amine for Photopolymerization", *Journal of Photochemistry and Photobiology A: Chemistry*, Vol. 186, No. 1, pp. 106-114, 2007.
- [176] Wei, J., R. Lu, and F. Liu, "Novel, Highly Efficient Polymeric Benzophenone Photoinitiator Containing Coinitiator Moieties for Photopolymerization", *Polymers for Advanced Technologies*, Vol. 21, No. 9, pp. 656-662, 2010.
- [177] Angiolini, L., D. Caretti, S. Rossetti, E. Salatelli, and M. Scoconi, "Radical Polymeric Photoinitiators Bearing Side-Chain Camphorquinone Moieties Linked to the Main Chain Through a Flexible Spacer", *Journal of Polymer Science Part A: Polymer Chemistry*, Vol. 43, No. 23, pp. 5879-5888, 2005.
- [178] Eren, T.N., N. Okte, F. Morlet-Savary, J.P. Fouassier, J. Lalevee, and D. Avci, "One-Component Thioxanthone-Based Polymeric Photoinitiators", *Journal of Polymer Science Part A: Polymer Chemistry*, Vol. 54, No. 20, pp. 3370-3378, 2016.
- [179] Xiao, P., Y. Wang, M. Dai, S. Shi, G. Wu, and J. Nie, "Synthesis and Photopolymerization Kinetics of Polymeric One-Component Type II Photoinitiator

Containing Benzophenone Moiety and Tertiary Amine”, *Polymer Engineering & Science*, Vol. 48, No. 5, pp. 884-888, 2008.

[180] Jiang, X., and J. Yin, “Polymeric Photoinitiator Containing In-Chain Thioxanthone and Coinitiator Amines”, *Macromolecular Rapid Communications*, Vol. 25, No. 6, pp. 748-752, 2004.

[181] Sun, F., Y. Li, N. Zhang, and J. Nie, “Initiating Gradient Photopolymerization and Migration of a Novel Polymerizable Polysiloxane  $\alpha$ -Hydroxy Alkylphenones Photoinitiator”, *Polymer*, Vol. 55, No. 16, pp. 3656-3665, 2014.

[182] Hu, L., A. Asif, J. Xie, and W. Shi, “Synthesis and Photoinitiating Behavior of Hyperbranched Polymeric Photoinitiators Bearing Coinitiator Amine”, *Polymers for Advanced Technologies*, Vol. 22, No. 12, pp. 1673-1680, 2011.

[183] Qi, Y., X. Zhang, X. Huang, Y. Zhang, M. Shi, and Y. Zhao, “High-Efficient Lignin-Based Polymerizable Macromolecular Photoinitiator with UV-Blocking Property for Visible light polymerization”, *International Journal of Biological Macromolecules*, Vol. 204, pp. 234-244, 2022.

[184] Zhang, X., S. Keck, Y. Qi, S. Baudis, and Y. Zhao, “Study on Modified Dealkaline Lignin as Visible Light Macromolecular Photoinitiator for 3D Printing”, *ACS Sustainable Chemistry & Engineering*, Vol. 8, No. 29, pp. 10959-10970, 2020.

[185] Song, Q., K. Shang, T. Xue, Z. Wang, D. Pei, S. Zhao, J. Nie, and Y. Chang, “Macrocyclic Photoinitiator Based on Prism [5] Arene Matching LEDs Light with Low Migration”, *Macromolecular Rapid Communications*, Vol. 42, No. 17, p. 2100299, 2021.

[186] Gou, L., B. Opheim, C.N. Coretsopoulos, and A.B. Scranton, “Consumption of the Molecular Oxygen in Polymerization Systems Using Photosensitized Oxidation of Dimethylantracene”, *Chemical Engineering Communications*, Vol. 193, No. 5, pp. 620-627, 2006.

[187] Shenoy, R., and C.N. Bowman, “Mechanism and Implementation of Oxygen Inhibition Suppression in Photopolymerizations by Competitive Photoactivation of a Singlet Oxygen Sensitizer”, *Macromolecules*, Vol. 43, No. 19, pp. 7964-7970, 2010.

- [188] O'Brien, A.K., and C.N. Bowman, "Impact of Oxygen on Photopolymerization Kinetics and Polymer Structure", *Macromolecules*, Vol. 39, No. 7, pp. 2501-2506, 2006.
- [189] Studer, K., C. Decker, E. Beck, and R. Schwalm, "Overcoming Oxygen Inhibition in UV-Curing of Acrylate Coatings by Carbon Dioxide Inerting: Part II", *Progress in Organic Coatings*, Vol. 48, No. 1, pp. 101-111, 2003.
- [190] El-Roz, M., J. Lalevée, X. Allonas, and J.P. Fouassier, "Mechanistic Investigation of the Silane, Germane, and Stannane Behavior When Incorporated in Type I and Type II Photoinitiators of Polymerization in Aerated Media", *Macromolecules*, Vol. 42, No. 22, pp. 8725-8732, 2009.
- [191] Bouzrati-Zerelli, M., M. Maier, C.P. Fik, C. Dietlin, F. Morlet-Savary, J.P. Fouassier, J. E. Klee, and J. Lalevée, "A Low Migration Phosphine to Overcome the Oxygen Inhibition in New High Performance Photoinitiating Systems for Photocurable Dental Type Resins", *Polymer International*, Vol. 66, No. 4, pp. 504-511, 2017.
- [192] Husár, B., S.C. Ligon, H. Wutzel, H. Hoffmann, and R. Liska, "The Formulator's Guide to Anti-Oxygen Inhibition Additives", *Progress in Organic Coatings*, Vol. 77, No. 11, pp. 1789-1798, 2014.
- [193] Xu, F., J.L. Yang, Y.S. Gong, G.P. Ma, and J. Nie, "A Fluorinated Photoinitiator for Surface Oxygen Inhibition Resistance", *Macromolecules*, Vol. 45, No. 3, pp. 1158-1164, 2012.
- [194] Xie, G., Z. Shuai, Y. Huang, M. Yu, Z. Zeng, and J. Yang, "Use of Floating Acylphosphine Oxide-Based Photoinitiators to Reduce Surface Oxygen Inhibition of UV-LED photopolymerization", *Progress in Organic Coatings*, Vol. 147, p. 105716, 2020.
- [195] Hou, H., Y. Gan, J. Yin, and X. Jiang, "Multifunctional POSS-Based Nano-Photo-Initiator for Overcoming the Oxygen Inhibition of Photo-Polymerization and for Creating Self-Wrinkled Patterns", *Advanced Materials Interfaces*, Vol. 1, No. 9, p. 1400385, 2014.
- [196] Yang, J., C. Xu, Y. Xiong, X. Wang, Y. Xie, Z. Li, and H. Tang, "A Green and Highly Efficient Naphthalimide Visible Photoinitiator with an Ability Initiating Free Radical Polymerization Under Air", *Macromolecular Chemistry and Physics*, Vol. 219, No. 24, p. 1800256, 2018.

- [197] Zhang, Y., Y. He, J. Yang, X. Zhang, R. Bongiovanni, and J. Nie, "A Fluorinated Compound Used as Migrated Photoinitiator in the Presence of Air", *Polymer*, Vol. 71, pp. 93-101, 2015.
- [198] Chen, W., L. Wang, X. Liu, B. Chen, and G. Zhao, "Synthesis and Preliminary Photopolymerization Evaluation of Novel Photoinitiators Containing Phototrigger to Overcome Oxygen Inhibition in the UV-Curing System", *Journal of Photochemistry and Photobiology A: Chemistry*, Vol. 388, p. 112187, 2020.
- [199] Yang, J., C. Xu, W. Liao, Y. Xiong, X. Wang, and H. Tang, "Visible Macrophotoinitiators with Si-H: High Efficient Anti-Oxygen Inhibition and Modified Cured Polymer Materials", *Progress in Organic Coatings*, Vol. 138, p. 105410, 2020.
- [200] Chen, Y.C., T.Y. Liu, and Y.H. Li, "Photoreactivity Study of Photoinitiated Free Radical Polymerization Using Type II Photoinitiator Containing Thioxanthone Initiator as a Hydrogen Acceptor and Various Amine-type Co-initiators as Hydrogen Donors", *Journal of Coatings Technology and Research*, Vol. 18, No. 1, pp. 99-106, 2021.
- [201] Green, G.E., B.P. Stark, and S.A. Zahir, "Photocross-Linkable Resin Systems", *Journal of Macromolecular Science, Part C: Polymer Reviews*, Vol. 21, No. 2, pp. 187-273, 1981.
- [202] Andrzejewska, E., "Photopolymerization Kinetics of Multifunctional Monomers", *Progress in Polymer Science*, Vol. 26, No. 4, pp. 605-665, 2001.
- [203] Marcinkowska, A., and E. Andrzejewska, "Viscosity Effects in the Photopolymerization of Two-Monomer Systems", *Journal of Applied Polymer Science*, Vol. 116, No. 1, pp. 280-287, 2010.
- [204] Topa, M., and J. Ortyl, "Moving Towards a Finer Way of Light-Cured Resin-Based Restorative Dental Materials: Recent Advances in Photoinitiating Systems Based on Iodonium Salts", *Materials*, Vol. 13, No. 18, p. 4093, 2020.
- [205] Anastasio, R., W. Peerbooms, R. Cardinaels, and L.C.A. Van Breemen, "Characterization of Ultraviolet-Cured Methacrylate Networks: From Photopolymerization to Ultimate Mechanical Properties", *Macromolecules*, Vol. 52 No. 23, pp. 9220-9231, 2019.

- [206] Guit, J., M.B.L. Tavares, J. Hul, C. Ye, K. Loos, J. Jager, R. Folkersma, and V.S.D. Voet, "Photopolymer Resins with Biobased Methacrylates Based on Soybean Oil for Stereolithography", *ACS Applied Polymer Materials*, Vol. 2, No. 2, pp. 949-957, 2020.
- [207] Zwinkels, J., "Light, Electromagnetic Spectrum", *Encyclopedia of Color Science and Technology*, Vol. 8071, pp. 1-8, 2015.
- [208] Blyth, J., and A.W. Hofmann, "Ueber das Styrol und Einige Seiner Zersetzungsproducte", *Justus Liebigs Annalen der Chemie*, Vol. 53, No. 3, pp. 289-329, 1845.
- [209] Tehfe, M.A., F. Louradour, J. Lalevée, and J.P. Fouassier, "Photopolymerization Reactions: On the Way to a Green and Sustainable Chemistry", *Applied Sciences*, Vol. 3, No. 2, pp. 490-514, 2013.
- [210] Konuray, A.O., X. Fernández-Francos, À. Serra, and X. Ramis, "Sequential Curing of Amine-Acrylate-Methacrylate Mixtures Based on Selective Aza-Michael Addition Followed by Radical Photopolymerization", *European Polymer Journal*, Vol. 84, pp. 256-267, 2016.
- [211] González, G., X. Fernández-Francos, À. Serra, M. Sangermano, and X. Ramis, "Environmentally-Friendly Processing of Thermosets by Two-Stage Sequential Aza-Michael Addition and Free-Radical Polymerization of Amine-Acrylate Mixtures", *Polymer Chemistry*, Vol. 6, No. 39, pp. 6987-6997, 2015.
- [212] Retailleau, M., A. Ibrahim, C. Croutxé-Barghorn, X. Allonas, C. Ley, and D. Le Nouen, "One-Pot Three-Step Polymerization System Using Double Click Michael Addition And Radical Photopolymerization", *ACS Macro Letters*, Vol. 4, No. 12, pp. 1327-1331, 2015.
- [213] Nair, D.P., N.B. Cramer, J.C. Gaipa, M.K. McBride, E.M. Matherly, R.R. McLeod, R. Shandas, and C.N. Bowman, "Two-Stage Reactive Polymer Network Forming Systems", *Advanced Functional Materials*, Vol. 22, No. 7, pp. 1502-1510, 2012.
- [214] Konuray, O., X. Fernández-Francos, X. Ramis, and À. Serra, "State of the Art in Dual-Curing Acrylate Systems", *Polymers*, Vol. 10, No. 2, p. 178, 2018.

- [215] Guo, Q., *Thermosets: Structure, Properties, And Applications*, Woodhead Publishing, Cambridge, United Kingdom, 2017.
- [216] Catalina, F., C. Peinado, E.L. Madruga, R. Sastre, J.L. Mateo, and N.S. Allen, “Radical Copolymerization of 2-Acryloyl Thioxanthone with Methyl Methacrylate”, *Journal of Polymer Science Part A: Polymer Chemistry*, Vol. 28, No. 5, pp. 967-972, 1990.
- [217] Degenhardt, C.R., and D.C. Burdsall, “Synthesis of Ethenylidenebis (Phosphonic Acid) And Its Tetraalkyl Esters”, *The Journal of Organic Chemistry*, Vol. 51, No. 18, pp. 3488-3490, 1986.
- [218] Atkins, P., and J. De Paula, *Elements of Physical Chemistry*, Oxford University Press, Oxford, 2013.
- [219] Lalevée, J., N. Blanchard, M. El-Roz, B. Graff, X. Allonas, and J.P. Fouassier, “New Photoinitiators Based on the Silyl Radical Chemistry: Polymerization Ability, ESR Spin Trapping, and Laser Flash Photolysis Investigation”, *Macromolecules*, Vol. 41, No. 12, pp. 4180-4186, 2008.
- [220] Tordo, P., “Spin-Trapping: Recent Developments and Applications”, *Electron Paramagnetic Resonance*, Royal Society of Chemistry, Cambridge, United Kingdom, 1998.
- [221] Duling, D.R., “Simulation of Multiple Isotropic Spin-Trap EPR Spectra”, *Journal of Magnetic Resonance Series B*, Vol. 104, No. 2, pp. 105-110, 1994.
- [222] Genest, A., D. Portinha, E. Fleury, and F. Ganachaud, “The Aza-Michael Reaction as an Alternative Strategy to Generate Advanced Silicon-Based (macro) Molecules and Materials”, *Progress in Polymer Science*, Vol. 72, pp. 61-110, 2017.
- [223] Al Mousawi, A., P. Garra, M. Schmitt, J. Toufaily, T. Hamieh, B. Graff, J. P. Fouassier, F. Dumur, and J. Lalevée, “3-Hydroxyflavone and N-phenylglycine in High Performance Photoinitiating Systems for 3D Printing and Photocomposites Synthesis”, *Macromolecules*, Vol. 51, No. 12, pp. 4633-4641, 2018.
- [224] Retaillieu, M., J. Pierrel, A. Ibrahim, C. Croutxé-Barghorn, and X. Allonas, “Sequenced Click Chemistry and Photopolymerization: A New Approach Toward Semi-Interpenetrating Polymer Networks”, *Polymers for Advanced Technologies*, Vol. 28, No. 4, pp. 491-495, 2017.

- [225] Karasu, F., C. Rocco, Y. Zhang, C. Croutxé-Barghorn, X. Allonas, L.G.J. van der Ven, R.A.T.M. van Benthem, and A.C.C. Esteves, “LED-cured Self-Replenishing Hydrophobic Coatings Based on Interpenetrating Polymer Networks (IPNs)”, *RSC Advances*, Vol. 6, No. 40, pp. 33971-33982, 2016.
- [226] Kalakkunnath, S., D.S. Kalika, H. Lin, and B.D. Freeman, “Segmental Relaxation Characteristics of Cross-Linked Poly (ethylene oxide) Copolymer Networks”, *Macromolecules*, Vol. 38, No. 23, pp. 9679-9687, 2005.
- [227] Vargün, E., M. Sankir, B. Aran, N.D. Sankir, and A. Usanmaz, “Synthesis and Characterization of 2-Hydroxyethyl Methacrylate (HEMA) and Methyl Methacrylate (MMA) Copolymer Used as Biomaterial”, *Journal of Macromolecular Science Part A: Pure and Applied Chemistry*, Vol. 47, No. 3, pp. 235-240, 2010.
- [228] Park, J., Q. Ye, E.M. Topp, A. Misra, S.L. Kieweg, and P. Spencer, “Effect of Photoinitiator System and Water Content on Dynamic Mechanical Properties of a Light-Cured BisGMA/HEMA Dental Resin”, *Journal of Biomedical Materials Research Part A*, Vol. 93, No. 4, pp. 1245-1251, 2010.
- [229] Mauro, N., F. Chiellini, C. Bartoli, M. Gazzarri, M. Laus, D. Antonioli, P. Griffiths, A. Manfredi, E. Ranucci, and P. Ferruti, “RGD-mimic Polyamidoamine–Montmorillonite Composites with Tunable Stiffness as Scaffolds for Bone Tissue-Engineering Applications”, *Journal of Tissue Engineering and Regenerative Medicine*, Vol. 11, No. 7, pp. 2164-2175, 2017.
- [230] Elzes, M.R., N. Akeroyd, J.F.J. Engbersen, and J.M.J. Paulusse, “Disulfide-functional Poly (amido amine)s with Tunable Degradability for Gene Delivery”, *Journal of Controlled Release*, Vol. 244, pp. 357-365, 2016.
- [231] Temel, G., B. Enginol, M. Aydin, D.K. Balta, and N. Arsu, “Photopolymerization and Photophysical Properties of Amine Linked Benzophenone Photoinitiator for Free Radical Polymerization”, *Journal of Photochemistry and Photobiology A: Chemistry*, Vol. 219, No. 1, pp. 26-31, 2011.
- [232] Foresman, J., and E. Frish, *Exploring Chemistry*, Gaussian Inc., Pittsburg, USA, 1996.
- [233] Garofalo, A., A. Parat, C. Bordeianu, C. Ghobril, M. Kueny-Stotz, A. Walter, J. Jouhannaud, S. Begin-Colin, and D. Felder-Flesch, “Efficient Synthesis of Small-Sized

Phosphonated Dendrons: Potential Organic Coatings of Iron Oxide Nanoparticles”, *New Journal of Chemistry*, Vol. 38, No. 11, pp. 5226-5239, 2014.

[234] Korkut, S. E., G. Temel, D.K. Balta, N. Arsu, and M.K. Şener, “Type II Photoinitiator Substituted Zinc Phthalocyanine: Synthesis, Photophysical and Photopolymerization Studies”, *Journal of Luminescence*, Vol. 136, pp. 389-394, 2013.

[235] Smith, T.J., B.S. Shemper, J.S. Nobles, A.M. Casanova, C. Ott, and L.J. Mathias, “Crosslinking Kinetics of Methyl and Ethyl ( $\alpha$ -hydroxymethyl) Acrylates: Effect of Crosslinker Type and Functionality”, *Polymer*, Vol. 44, No. 20, pp. 6211-6216, 2003.

[236] Yeom, C.E., M.J. Kim, and B.M. Kim, “1, 8-Diazabicyclo [5.4.0] undec-7-ene (DBU)-Promoted Efficient and Versatile Aza-Michael Addition”, *Tetrahedron*, Vol. 63, No. 4, pp. 904-909, 2007.

[237] Balta, D.K., E. Bagdatli, N. Arsu, N. Ocal, and Y. Yagci, “Chemical Incorporation of Thioxanthone into  $\beta$ -cyclodextrin and Its Use in Aqueous Photopolymerization of Methyl Methacrylate”, *Journal of Photochemistry and Photobiology A: Chemistry*, Vol. 196, No. 1, pp. 33-37, 2008.

[238] Morita, K., T. Hashimoto, M. Urushisaki, and T. Sakaguchi, “Cationic Cyclopolymerization of Divinyl Ethers with Norbornane-, Norbornene-, or Adamantane-Containing Substituents: Synthesis of Cyclopoly (divinyl ether) s with Bulky Rigid Side Chains Leading to High Glass Transition Temperature”, *Journal of Polymer Science Part A: Polymer Chemistry*, Vol. 51, No. 11, pp. 2445-2454, 2013.

[239] Hashimoto, T., H. Takagi, Y. Hasegawa, H. Matsui, M. Urushisaki, and T. Sakaguchi, “Living/Controlled Cationic Cyclopolymerization of Divinyl Ether with a Cyclic Acetal Moiety: Synthesis of Poly (vinyl ether) s with High Glass Transition Temperature Based on Incorporation of Cyclized Main Chain and Cyclic Side Chains”, *Journal of Polymer Science Part A: Polymer Chemistry*, Vol. 48, No. 4, pp. 952-958, 2010.

[240] Peer, G., M. Kury, C. Gorsche, Y. Catel, P. Frühwirt, G. Gescheidt, N. Moszner, and R. Liska, “Revival of Cyclopolymerizable Monomers as Low-Shrinkage Cross-Linkers”, *Macromolecules*, Vol. 53, No. 19, pp. 8374-8381, 2020.

- [241] Ruppitsch, L.A., G. Peer, K. Ehrmann, T. Koch, and R. Liska, "Photopolymerization of Difunctional Cyclopolymerizable Monomers with Low Shrinkage Behavior", *Journal of Polymer Science*, Vol. 59, No. 6, pp. 519-531, 2021.
- [242] Braga, R.R., R.Y. Ballester, and J.L. Ferracane, "Factors Involved in the Development of Polymerization Shrinkage Stress in Resin-Composites: A Systematic Review", *Dental Materials*, Vol. 21, No. 10, pp. 962-970, 2005.
- [243] Gray Jr, T.F., and G.B. Butler, "The Fundamental Basis for Cyclopolymerization. X. A Systematic Study of the Cyclopolymerization of Methacrylic Anhydride", *Journal of Macromolecular Science—Chemistry*, Vol. 9, No. 1, pp. 45-82, 1975.
- [244] Stansbury, J.W, "Cyclopolymerizable Monomers for Use in Dental Resin Composites", *Journal of Dental Research*, Vol. 69, No. 3, pp. 844-848, 1990.
- [245] Tsuda, T., and L.J. Mathias, "Cyclopolymerization of Ether Dimers of  $\alpha$ -(hydroxymethyl) Acrylic Acid and Its Alkyl Esters: Substituent Effect on Cyclization Efficiency and Microstructures", *Polymer*, Vol. 35, No. 15, pp. 3317-3328, 1994.
- [246] Ma, Z., X. Niu, Z. Xu, and J. Guo, "Synthesis of Novel Macrophotoinitiator for the Photopolymerization of Acrylate", *Journal of Applied Polymer Science*, Vol. 131, No. 11, 2014.
- [247] Selen, F., V. Can, and G. Temel, "Preparation of Photodegradable Polyacrylamide Hydrogels via Micellar Copolymerization and Determination of Their Phototunable Elasticity and Swelling Behaviors", *RSC Advances*, Vol. 6, No. 38, pp. 31692-31697, 2016.
- [248] Tsuda, T., and L.J. Mathias, "Cyclopolymerization of Ether Dimers of  $\alpha$ -(hydroxymethyl) Acrylic Acid and Its Alkyl Esters: Substituent Effect on Cyclization Efficiency and Microstructures", *Polymer*, Vol. 35, No. 15, pp. 3317-3328, 1994.
- [249] Mathias, L.J., S.H. Kusefoglul, and J.E. Ingram, "Cyclopolymerization of the Ether of Methyl. Alpha.-(hydroxymethyl) Acrylate", *Macromolecules*, Vol. 21, No. 2, pp. 545-546, 1988.
- [250] Erkoc, S., and A.E. Acar, "Controlled/Living Cyclopolymerization of Tert-butyl  $\alpha$ -(hydroxymethyl) Acrylate Ether Dimer via Reversible Addition Fragmentation Chain Transfer Polymerization", *Macromolecules*, Vol. 41, No. 23, pp. 9019-9024, 2008.

[251] Erkoc, S., L.J. Mathias, and A.E. Acar, "Cyclopolymerization of Tert-Butyl  $\alpha$ -(Hydroxymethyl) Acrylate (TBHMA) Ether Dimer via Atom Transfer Radical Polymerization (ATRP)", *Macromolecules*, Vol. 39, No. 26, pp. 8936-8942, 2006.

[252] Albayrak, A.Z., and D. Avci, "Novel Phosphorus-Containing Cyclopolymers from Ether Dimer of Tert-butyl  $\alpha$ -Hydroxymethyl Acrylate", *Designed Monomers and Polymers*, Vol. 7, No. 3, pp. 291-300, 2004.

[253] Roth, M., D. Hennen, A. Oesterreicher, F. Mostegel, A. Samusjew, M. Edler, E. Maier, and T. Griesser, "Highly Water-Soluble Alpha-Hydroxyalkylphenone Based Photoinitiator for Low-Migration Applications", *Macromolecular Chemistry and Physics*, Vol. 218, No. 14, p. 1700022, 2017.

[254] Dietlin, C., J. Lalevee, X. Allonas, J.P. Fouassier, M. Visconti, G. Li Bassi, and G. Norcini, "Reactivity and Efficiency of Difunctional Radical Photoinitiators", *Journal of Applied Polymer Science*, Vol. 107, No. 1, pp. 246-252, 2008.

## APPENDIX A: COPYRIGHT LICENCES

### License Details

This Agreement between Turkan Gencoglu ("You") and John Wiley and Sons ("John Wiley and Sons") consists of your license details and the terms and conditions provided by John Wiley and Sons and Copyright Clearance Center.

Print

Copy

License Number	5436990292015
License date	Nov 27, 2022
Licensed Content Publisher	John Wiley and Sons
Licensed Content Publication	Wiley Books
Licensed Content Title	Photoinitiators for Polymer Synthesis: Scope, Reactivity, and Efficiency
Licensed Content Author	Jacques Lalevée Jean-Pierre Fouassier
Licensed Content Date	Aug 1, 2012
Licensed Content Pages	1
Type of Use	Dissertation/Thesis
Requestor type	University/Academic
Format	Print and electronic
Portion	Figure/table
Number of figures/tables	1
Will you be translating?	No
Title	MULTIFUNCTIONAL MONOMERIC AND POLYMERIC PHOTODINITIATORS FOR FREE RADICAL PHOTOPOLYMERIZATION
Institution name	Bogazici University
Expected presentation date	Dec 2022
Order reference number	1
Portions	Figure 8.1
Requestor Location	Turkan Gencoglu Bogazici University

Figure A.1. Permission from [7] John Wiley and Sons, Copyright (2012).

The screenshot shows the RightsLink interface. At the top, there is a navigation bar with the CCC RightsLink logo and user options: Home, Help, Email Support, and Turkan Gencoglu. The main content area displays the following information:

**Photoinitiated Polymerization: Advances, Challenges, and Opportunities**  
 Author: Yusuf Yagci, Steffen Jockusch, Nicholas J. Turro  
 Publication: Macromolecules  
 Publisher: American Chemical Society  
 Date: Aug 1, 2010  
 Copyright © 2010, American Chemical Society

**PERMISSION/LICENSE IS GRANTED FOR YOUR ORDER AT NO CHARGE**

This type of permission/license, instead of the standard Terms and Conditions, is sent to you because no fee is being charged for your order. Please note the following:

- Permission is granted for your request in both print and electronic formats, and translations.
- If figures and/or tables were requested, they may be adapted or used in part.
- Please print this page for your records and send a copy of it to your publisher/graduate school.
- Appropriate credit for the requested material should be given as follows: "Reprinted (adapted) with permission from {COMPLETE REFERENCE CITATION}. Copyright {YEAR} American Chemical Society." Insert appropriate information in place of the capitalized words.
- One-time permission is granted only for the use specified in your RightsLink request. No additional uses are granted (such as derivative works or other editions). For any uses, please submit a new request.

If credit is given to another source for the material you requested from RightsLink, permission must be obtained from that source.

At the bottom, there are two buttons: "BACK" and "CLOSE WINDOW".

Figure A.2. Permission from [23] American Chemical Society, Copyright (2010).

## License Details

This Agreement between Turkan Gencoglu ("You") and Elsevier ("Elsevier") consists of your license details and the terms and conditions provided by Elsevier and Copyright Clearance Center.

[Print](#) [Copy](#)

License Number	5437260692139
License date	Nov 27, 2022
Licensed Content Publisher	Elsevier
Licensed Content Publication	Progress in Polymer Science
Licensed Content Title	Photomediated controlled radical polymerization
Licensed Content Author	Xiangcheng Pan, Mehmet Atilla Tasdelen, Joachim Laun, Thomas Junkers, Yusuf Yagci, Krzysztof Matyjaszewski
Licensed Content Date	Nov 1, 2016
Licensed Content Volume	62
Licensed Content Issue	n/a
Licensed Content Pages	53
Type of Use	reuse in a thesis/dissertation
Portion	figures/tables/illustrations
Number of figures/tables/illustrations	1
Format	both print and electronic
Are you the author of this Elsevier article?	No
Will you be translating?	No
Title	MULTIFUNCTIONAL MONOMERIC AND POLYMERIC PHOTOINITIATORS FOR FREE RADICAL PHOTOPOLYMERIZATION
Institution name	Bogazici University
Expected presentation date	Dec 2022
Order reference number	3
Portions	Table 1
Requestor Location	Turkan Gencoglu Bogazici University

Figure A.3. Permission from [26] Elsevier, Copyright (2016).

## License Details

This Agreement between Turkan Gencoglu ("You") and Elsevier ("Elsevier") consists of your license details and the terms and conditions provided by Elsevier and Copyright Clearance Center.

[Print](#) [Copy](#)

License Number	5437251482998
License date	Nov 27, 2022
Licensed Content Publisher	Elsevier
Licensed Content Publication	Progress in Polymer Science
Licensed Content Title	Progress in the development of polymeric and multifunctional photoinitiators
Licensed Content Author	Junyi Zhou, Xavier Allonas, Ahmad Ibrahim, Xiaoxuan Liu
Licensed Content Date	Dec 1, 2019
Licensed Content Volume	99
Licensed Content Issue	n/a
Licensed Content Pages	1
Type of Use	reuse in a thesis/dissertation
Portion	figures/tables/illustrations
Number of figures/tables/illustrations	1
Format	both print and electronic
Are you the author of this Elsevier article?	No
Will you be translating?	No
Title	MULTIFUNCTIONAL MONOMERIC AND POLYMERIC PHOTOINITIATORS FOR FREE RADICAL PHOTOPOLYMERIZATION
Institution name	Bogazici University
Expected presentation date	Dec 2022
Order reference number	2
Portions	Scheme 2
Requestor Location	Turkan Gencoglu Bogazici University

Figure A.4. Permission from [27] Elsevier, Copyright (2019).

1. Polymer Chemistry 

0.00 USD

Article: Shining a light on an adaptable photoinitiator: advances in photopolymerizations initiated by thioxanthenes

ISSN	1759-9954	Publisher Portion	Royal Society of Chemistry
Type of Use	Republish in a thesis/dissertation		Chart/graph/table/figure

[Hide Details](#)

## LICENSED CONTENT

Publication Title	Polymer Chemistry	Rightsholder	Royal Society of Chemistry
Article Title	Shining a light on an adaptable photoinitiator: advances in photopolymerizations initiated by thioxanthenes	Publication Type	Journal
		Start Page	6595
		End Page	6615
Author/Editor	Royal Society of Chemistry (Great Britain)	Issue	37
		Volume	6
Date	01/01/2010		
Language	English		
Country	United Kingdom of Great Britain and Northern Ireland		

## REQUEST DETAILS

Portion Type	Chart/graph/table/figure	Distribution	Worldwide
Number of Charts / Graphs / Tables / Figures Requested	1	Translation	Original language of publication
Format (select all that apply)	Print, Electronic	Copies for the Disabled?	No
Who Will Republish the Content?	Academic Institution	Minor Editing Privileges?	No
Duration of Use	Life of current edition	Incidental Promotional Use?	No
Lifetime Unit Quantity	Up to 499	Currency	USD
Rights Requested	Main product		

## NEW WORK DETAILS

Title	MULTIFUNCTIONAL MONOMERIC AND POLYMERIC PHOTOINITIATORS FOR FREE RADICAL PHOTOPOLYMERIZATION	Institution Name	Bogazici University
		Expected Presentation Date	2022-12-20
Instructor Name	Turkan Gencoglu		

## ADDITIONAL DETAILS

Order Reference Number	N/A	The Requesting Person/Organization to Appear on the License	Turkan Gencoglu
------------------------	-----	---	-----------------

## REUSE CONTENT DETAILS

Title, Description or Numeric Reference of the Portion(s)	Scheme 5	Title of the Article/Chapter the Portion Is From	Shining a light on an adaptable photoinitiator: advances in photopolymerizations initiated by thioxanthenes
Editor of Portion(s)	Dadashi-Silab, Sajjad; Aydogan, Cansu; Yagci, Yusuf	Author of Portion(s)	Dadashi-Silab, Sajjad; Aydogan, Cansu; Yagci, Yusuf
Volume of Serial or Monograph	6	Issue, if Republishing an Article From a Serial	37
Page or Page Range of Portion	6595-6615	Publication Date of Portion	2015-01-01

[Remove](#)

Figure A.5. Permission from [31] Royal Society of Chemistry, Copyright (2015).

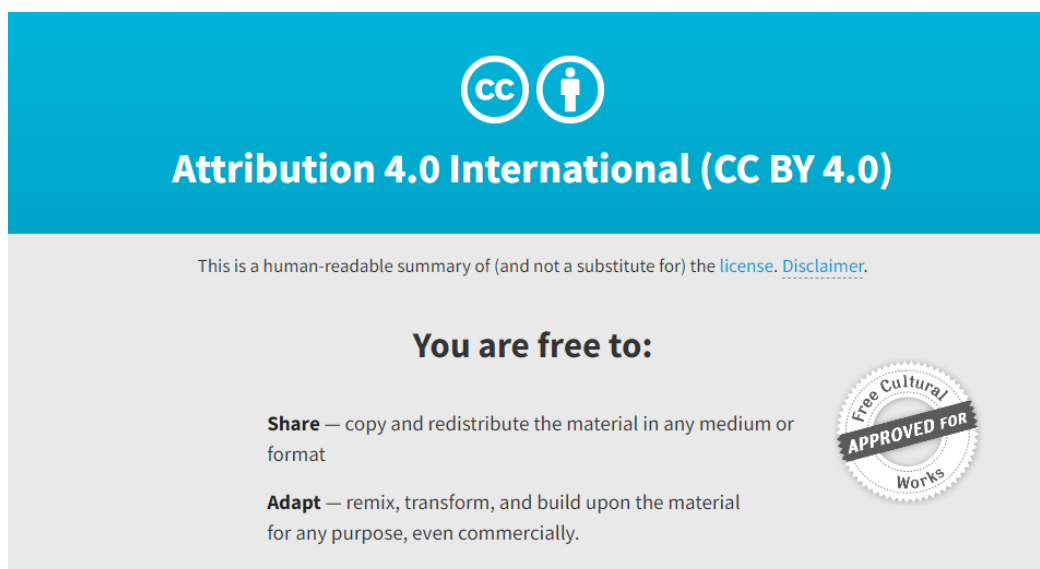
## License Details

This Agreement between Turkan Gencoglu ("You") and Elsevier ("Elsevier") consists of your license details and the terms and conditions provided by Elsevier and Copyright Clearance Center.

[Print](#) [Copy](#)

License Number	5437280326810
License date	Nov 27, 2022
Licensed Content Publisher	Elsevier
Licensed Content Publication	Journal of Photochemistry and Photobiology A: Chemistry
Licensed Content Title	Excited state reactions of acridinedione dyes with onium salts: mechanistic details
Licensed Content Author	C Selvaraju,A Sivakumar,P Ramamurthy
Licensed Content Date	Jan 31, 2001
Licensed Content Volume	138
Licensed Content Issue	3
Licensed Content Pages	14
Type of Use	reuse in a thesis/dissertation
Portion	figures/tables/illustrations
Number of figures/tables/illustrations	1
Format	both print and electronic
Are you the author of this Elsevier article?	No
Will you be translating?	No
Title	MULTIFUNCTIONAL MONOMERIC AND POLYMERIC PHOTOINITIATORS FOR FREE RADICAL PHOTOPOLYMERIZATION
Institution name	Bogazici University
Expected presentation date	Dec 2022
Order reference number	4
Portions	Scheme 1
Requestor Location	Turkan Gencoglu Bogazici University

Figure A.6. Permission from [33] Elsevier, Copyright (2001).



The image shows a Creative Commons Attribution 4.0 International (CC BY 4.0) license banner. At the top, there are two icons: a person in a circle and the letters 'CC' in a circle. Below the icons, the text reads 'Attribution 4.0 International (CC BY 4.0)'. Underneath, it states 'This is a human-readable summary of (and not a substitute for) the license. [Disclaimer.](#)'. The main body of the banner is light gray and contains the heading 'You are free to:' followed by two bullet points: 'Share — copy and redistribute the material in any medium or format' and 'Adapt — remix, transform, and build upon the material for any purpose, even commercially.' To the right of the text is a circular seal that says 'Free Cultural Works' around the perimeter and 'APPROVED FOR' across the center.

Figure A.7. Permission from [35]

(<https://www.ncbi.nlm.nih.gov/pmc/articles/PMC7285382/>), licensed under CC BY 4.0

(<https://creativecommons.org/licenses/by/4.0/>).



[Home](#)
[Help](#)
[Live Chat](#)
Turkan Gencoglu

---

**On-Demand Visible Light Activated Amine/Benzoyl Peroxide Redox Initiating Systems: A Unique Tool To Overcome the Shadow Areas in Photopolymerization Processes**



**Author:** P. Garra, F. Morlet-Savary, C. Dietlin, et al  
**Publication:** Macromolecules  
**Publisher:** American Chemical Society  
**Date:** Dec 1, 2016  
Copyright © 2016, American Chemical Society

---

**PERMISSION/LICENSE IS GRANTED FOR YOUR ORDER AT NO CHARGE**

This type of permission/license, instead of the standard Terms and Conditions, is sent to you because no fee is being charged for your order. Please note the following:

- Permission is granted for your request in both print and electronic formats, and translations.
- If figures and/or tables were requested, they may be adapted or used in part.
- Please print this page for your records and send a copy of it to your publisher/graduate school.
- Appropriate credit for the requested material should be given as follows: "Reprinted (adapted) with permission from {COMPLETE REFERENCE CITATION}. Copyright {YEAR} American Chemical Society." Insert appropriate information in place of the capitalized words.
- One-time permission is granted only for the use specified in your RightsLink request. No additional uses are granted (such as derivative works or other editions). For any uses, please submit a new request.

If credit is given to another source for the material you requested from RightsLink, permission must be obtained from that source.

BACK
CLOSE WINDOW

Figure A.8. Permission from [85] American Chemical Society, Copyright (2016).

### License Details

This Agreement between Turkan Gencoglu ("You") and Elsevier ("Elsevier") consists of your license details and the terms and conditions provided by Elsevier and Copyright Clearance Center.

[Print](#) [Copy](#)

License Number	5438190298214
License date	Nov 29, 2022
Licensed Content Publisher	Elsevier
Licensed Content Publication	Biomaterials
Licensed Content Title	Photoinitiated polymerization of PEG-diacrylate with lithium phenyl-2,4,6-trimethylbenzoylphosphinate: polymerization rate and cytocompatibility
Licensed Content Author	Benjamin D. Fairbanks, Michael P. Schwartz, Christopher N. Bowman, Kristi S. Anseth
Licensed Content Date	Dec 1, 2009
Licensed Content Volume	30
Licensed Content Issue	35
Licensed Content Pages	6
Type of Use	reuse in a thesis/dissertation
Portion	figures/tables/illustrations
Number of figures/tables/illustrations	1
Format	both print and electronic
Are you the author of this Elsevier article?	No
Will you be translating?	No
Title	MULTIFUNCTIONAL MONOMERIC AND POLYMERIC PHOTOINITIATORS FOR FREE RADICAL PHOTOPOLYMERIZATION
Institution name	Bogazici University
Expected presentation date	Dec 2022
Order reference number	5
Portions	Figure 1
Requestor Location	Turkan Gencoglu Bogazici University

Figure A.9. Permission from [105] Elsevier, Copyright (2009).

### License Details

This Agreement between Turkan Gencoglu ("You") and Springer Nature ("Springer Nature") consists of your license details and the terms and conditions provided by Springer Nature and Copyright Clearance Center.

[Print](#) [Copy](#)

License Number	5438191053027
License date	Nov 29, 2022
Licensed Content Publisher	Springer Nature
Licensed Content Publication	Journal of Inclusion Phenomena
Licensed Content Title	Photoinitiated polymerization of $\beta$ -cyclodextrin/methyl methacrylate host/guest complex in the presence of water soluble photoinitiator, thioxanthone-catechol-O,O'-diacetic acid
Licensed Content Author	Feyza Karasu et al
Licensed Content Date	Mar 4, 2010
Type of Use	Thesis/Dissertation
Requestor type	academic/university or research institute
Format	print and electronic
Portion	figures/tables/illustrations
Number of figures/tables/illustrations	1
Will you be translating?	no
Circulation/distribution	30 - 99
Author of this Springer Nature content	no
Title	MULTIFUNCTIONAL MONOMERIC AND POLYMERIC PHOTOINITIATORS FOR FREE RADICAL PHOTOPOLYMERIZATION
Institution name	Bogazici University
Expected presentation date	Dec 2022
Order reference number	6
Portions	Scheme 3
Requestor Location	Turkan Gencoglu Bogazici University

Figure A.10. Permission from [121] Springer Nature, Copyright (2010).

### License Details

This Agreement between Turkan Gencoglu ("You") and Elsevier ("Elsevier") consists of your license details and the terms and conditions provided by Elsevier and Copyright Clearance Center.

[Print](#) [Copy](#)

License Number	5438200157520
License date	Nov 29, 2022
Licensed Content Publisher	Elsevier
Licensed Content Publication	European Polymer Journal
Licensed Content Title	Exploring functionalized benzophenones as low-migration photoinitiators for vinyl carbonate/thiol formulations
Licensed Content Author	Meinhart Roth, Daniel Hennen, Andreas Oesterreicher, Florian H. Mostegel, Stefan Kappaun, Matthias Edler, Thomas Griesser
Licensed Content Date	Mar 1, 2017
Licensed Content Volume	88
Licensed Content Issue	n/a
Licensed Content Pages	9
Type of Use	reuse in a thesis/dissertation
Portion	figures/tables/illustrations
Number of figures/tables/illustrations	1
Format	both print and electronic
Are you the author of this Elsevier article?	No
Will you be translating?	No
Title	MULTIFUNCTIONAL MONOMERIC AND POLYMERIC PHOTOINITIATORS FOR FREE RADICAL PHOTOPOLYMERIZATION
Institution name	Bogazici University
Expected presentation date	Dec 2022
Order reference number	7
Portions	Figure 3
Requestor Location	Turkan Gencoglu Bogazici University

Figure A.11. Permission from [154] Elsevier, Copyright (2017).

## License Details

This Agreement between Turkan Gencoglu ("You") and Elsevier ("Elsevier") consists of your license details and the terms and conditions provided by Elsevier and Copyright Clearance Center.

[Print](#) [Copy](#)

License Number	5438201385007
License date	Nov 29, 2022
Licensed Content Publisher	Elsevier
Licensed Content Publication	Progress in Organic Coatings
Licensed Content Title	A bis-acrylate functionalized enone as photoinitiator and crosslinker in photopolymerization
Licensed Content Author	Tanlong Xue,Hongwei Lu,Hengda Yuan,Yuxuan He,Jun Nie,Xiaoqun Zhu
Licensed Content Date	Jan 1, 2022
Licensed Content Volume	162
Licensed Content Issue	n/a
Licensed Content Pages	1
Type of Use	reuse in a thesis/dissertation
Portion	figures/tables/illustrations
Number of figures/tables/illustrations	1
Format	both print and electronic
Are you the author of this Elsevier article?	No
Will you be translating?	No
Title	MULTIFUNCTIONAL MONOMERIC AND POLYMERIC PHOTOINITIATORS FOR FREE RADICAL PHOTOPOLYMERIZATION
Institution name	Bogazici University
Expected presentation date	Dec 2022
Order reference number	8
Portions	Figure 7
Requestor Location	Turkan Gencoglu Bogazici University

Figure A.12. Permission from [149] Elsevier, Copyright (2022).

## License Details

This Agreement between Turkan Gencoglu ("You") and John Wiley and Sons ("John Wiley and Sons") consists of your license details and the terms and conditions provided by John Wiley and Sons and Copyright Clearance Center.

[Print](#) [Copy](#)

License Number	5438211382372
License date	Nov 29, 2022
Licensed Content Publisher	John Wiley and Sons
Licensed Content Publication	Macromolecular Rapid Communications
Licensed Content Title	Poly(vinyl alcohol)-Thioxanthone as One-Component Type II Photoinitiator for Free Radical Polymerization in Organic and Aqueous Media
Licensed Content Author	Yusuf Yagci, Gorkem Yilmaz, Senem Kork
Licensed Content Date	Apr 8, 2015
Licensed Content Volume	36
Licensed Content Issue	10
Licensed Content Pages	6
Type of Use	Dissertation/Thesis
Requestor type	University/Academic
Format	Print and electronic
Portion	Figure/table
Number of figures/tables	1
Will you be translating?	No
Title	MULTIFUNCTIONAL MONOMERIC AND POLYMERIC PHOTOINITIATORS FOR FREE RADICAL PHOTOPOLYMERIZATION
Institution name	Bogazici University
Expected presentation date	Dec 2022
Order reference number	9
Portions	Scheme 2
Requestor Location	Turkan Gencoglu Bogazici University

Figure A.13. Permission from [163] John Wiley and Sons, Copyright (2015).

## License Details

This Agreement between Turkan Gencoglu ("You") and John Wiley and Sons ("John Wiley and Sons") consists of your license details and the terms and conditions provided by John Wiley and Sons and Copyright Clearance Center.

[Print](#) [Copy](#)

License Number	5438220632361
License date	Nov 29, 2022
Licensed Content Publisher	John Wiley and Sons
Licensed Content Publication	Macromolecular Rapid Communications
Licensed Content Title	Macrocyclic Photoinitiator Based on Prism[5]arene Matching LEDs Light with Low Migration
Licensed Content Author	Yincheng Chang, Jun Nie, Shuai Zhao, et al
Licensed Content Date	Jun 25, 2021
Licensed Content Volume	42
Licensed Content Issue	17
Licensed Content Pages	7
Type of Use	Dissertation/Thesis
Requestor type	University/Academic
Format	Print and electronic
Portion	Figure/table
Number of figures/tables	1
Will you be translating?	No
Title	MULTIFUNCTIONAL MONOMERIC AND POLYMERIC PHOTOINITIATORS FOR FREE RADICAL PHOTOPOLYMERIZATION
Institution name	Bogazici University
Expected presentation date	Dec 2022
Order reference number	10
Portions	Figure 2
Requestor Location	Turkan Gencoglu Bogazici University

Figure A.14. Permission from [185] John Wiley and Sons, Copyright (2021).

## License Details

This Agreement between Turkan Gencoglu ("You") and Elsevier ("Elsevier") consists of your license details and the terms and conditions provided by Elsevier and Copyright Clearance Center.

[Print](#) [Copy](#)

License Number	5438221430989
License date	Nov 29, 2022
Licensed Content Publisher	Elsevier
Licensed Content Publication	Progress in Organic Coatings
Licensed Content Title	The formulator's guide to anti-oxygen inhibition additives
Licensed Content Author	Branislav Husár, Samuel Clark Ligon, Harald Wutzel, Helmut Hoffmann, Robert Liska
Licensed Content Date	Nov 1, 2014
Licensed Content Volume	77
Licensed Content Issue	11
Licensed Content Pages	10
Type of Use	reuse in a thesis/dissertation
Portion	figures/tables/illustrations
Number of figures/tables/illustrations	1
Format	both print and electronic
Are you the author of this Elsevier article?	No
Will you be translating?	No
Title	MULTIFUNCTIONAL MONOMERIC AND POLYMERIC PHOTOINITIATORS FOR FREE RADICAL PHOTOPOLYMERIZATION
Institution name	Bogazici University
Expected presentation date	Dec 2022
Order reference number	11
Portions	Scheme 2
Requestor Location	Turkan Gencoglu Bogazici University

Figure A.15. Permission from [192] Elsevier, Copyright (2014).

## License Details

This Agreement between Turkan Gencoglu ("You") and Springer Nature ("Springer Nature") consists of your license details and the terms and conditions provided by Springer Nature and Copyright Clearance Center.

[Print](#) [Copy](#)

License Number	5438230662689
License date	Nov 29, 2022
Licensed Content Publisher	Springer Nature
Licensed Content Publication	Journal of Coatings Technology and Research
Licensed Content Title	Photoreactivity study of photoinitiated free radical polymerization using Type II photoinitiator containing thioxanthone initiator as a hydrogen acceptor and various amine-type co-initiators as hydrogen donors
Licensed Content Author	Yung-Chung Chen et al
Licensed Content Date	Sep 29, 2020
Type of Use	Thesis/Dissertation
Requestor type	academic/university or research institute
Format	print and electronic
Portion	figures/tables/illustrations
Number of figures/tables/illustrations	1
Will you be translating?	no
Circulation/distribution	1 - 29
Author of this Springer Nature content	no
Title	MULTIFUNCTIONAL MONOMERIC AND POLYMERIC PHOTOINITIATORS FOR FREE RADICAL PHOTOPOLYMERIZATION
Institution name	Bogazici University
Expected presentation date	Dec 2022
Order reference number	12
Portions	Figure 6
Requestor Location	Turkan Gencoglu Bogazici University

Figure A.16. Permission from [200] Springer Nature, Copyright (2020).

## License Details

This Agreement between Turkan Gencoglu ("You") and John Wiley and Sons ("John Wiley and Sons") consists of your license details and the terms and conditions provided by John Wiley and Sons and Copyright Clearance Center.

[Print](#) [Copy](#)

License Number	5438231268485
License date	Nov 29, 2022
Licensed Content Publisher	John Wiley and Sons
Licensed Content Publication	Macromolecular Chemistry and Physics
Licensed Content Title	A Green and Highly Efficient Naphthalimide Visible Photoinitiator with an Ability Initiating Free Radical Polymerization under Air
Licensed Content Author	Jianjing Yang, Can Xu, Ying Xiong, et al
Licensed Content Date	Nov 9, 2018
Licensed Content Volume	219
Licensed Content Issue	24
Licensed Content Pages	8
Type of Use	Dissertation/Thesis
Requestor type	University/Academic
Format	Print and electronic
Portion	Figure/table
Number of figures/tables	1
Will you be translating?	No
Title	MULTIFUNCTIONAL MONOMERIC AND POLYMERIC PHOTOINITIATORS FOR FREE RADICAL PHOTOPOLYMERIZATION
Institution name	Bogazici University
Expected presentation date	Dec 2022
Order reference number	13
Portions	Figure 4
Requestor Location	Turkan Gencoglu Bogazici University

Figure A.17. Permission from [196] John Wiley and Sons, Copyright (2018).

### License Details

This Agreement between Turkan Gencoglu ("You") and John Wiley and Sons ("John Wiley and Sons") consists of your license details and the terms and conditions provided by John Wiley and Sons and Copyright Clearance Center.

[Print](#)
[Copy](#)

License Number	5438251368467
License date	Nov 29, 2022
Licensed Content Publisher	John Wiley and Sons
Licensed Content Publication	ChemistrySelect
Licensed Content Title	Benzophenone-Functionalized Oligo(Amido Amine)/Iodonium Salt Systems as Visible Light Photoinitiators
Licensed Content Author	Duygu Avci, Jacques Lalevée, Fabrice Morlet-Savary, et al
Licensed Content Date	Jun 16, 2021
Licensed Content Volume	6
Licensed Content Issue	23
Licensed Content Pages	9
Type of Use	Dissertation/Thesis
Requestor type	Author of this Wiley article
Format	Print and electronic
Portion	Full article
Will you be translating?	No
Title	MULTIFUNCTIONAL MONOMERIC AND POLYMERIC PHOTOINITIATORS FOR FREE RADICAL PHOTOPOLYMERIZATION
Institution name	Bogazici University
Expected presentation date	Dec 2022
Order reference number	14
Requestor Location	Turkan Gencoglu Bogazici University

Figure A.18. Permission from “Benzophenone-Functionalized Oligo(Amido Amine)/Iodonium Salt Systems as Visible Light Photoinitiators”, John Wiley and Sons, Copyright (2021).

### License Details

This Agreement between Turkan Gencoglu ("You") and John Wiley and Sons ("John Wiley and Sons") consists of your license details and the terms and conditions provided by John Wiley and Sons and Copyright Clearance Center.

[Print](#)
[Copy](#)

License Number	5438260574550
License date	Nov 29, 2022
Licensed Content Publisher	John Wiley and Sons
Licensed Content Publication	Macromolecular Chemistry and Physics
Licensed Content Title	A Water Soluble, Low Migration, and Visible Light Photoinitiator by Thioxanthone-Functionalization of Poly(ethylene glycol)-Containing Poly( $\beta$ -amino ester)
Licensed Content Author	Turkan Gencoglu, Tugce Nur Eren, Jacques Lalevée, et al
Licensed Content Date	Mar 25, 2022
Licensed Content Volume	223
Licensed Content Issue	13
Licensed Content Pages	9
Type of Use	Dissertation/Thesis
Requestor type	Author of this Wiley article
Format	Print and electronic
Portion	Full article
Will you be translating?	No
Title	MULTIFUNCTIONAL MONOMERIC AND POLYMERIC PHOTOINITIATORS FOR FREE RADICAL PHOTOPOLYMERIZATION
Institution name	Bogazici University
Expected presentation date	Dec 2022
Order reference number	15
Requestor Location	Turkan Gencoglu Bogazici University

Figure A.19. Permission from “A Water Soluble, Low Migration, and Visible Light Photoinitiator by Thioxanthone-Functionalization of Poly(ethylene glycol)-Containing Poly( $\beta$ -amino ester)”, John Wiley and Sons, Copyright (2022).